THE UNIVERSITY *of* EDINBURGH

Metal-Mediated Molecular Machines

David Howgego

Degree of Doctor of Philosophy

School of Chemistry

The University of Edinburgh

August 2012

"Science, my lad, is built upon many mistakes; but they are errors which it is good to fall into, for they lead little by little to the truth."

- Jules Verne

Table of Contents

Abstract and Layout of Thesis

Nature abounds with ingenious nanoscopic machines employed to carry out all of the requisite tasks that collectively contribute to the molecular basis of life. This thesis focuses primarily on a sub-set known as "molecular walkers" which can perambulate along intracellular molecular motorways carrying out such essential tasks as vesicle transport and muscle contraction. A summary of these incredible natural motors is presented in Chapter I along with a review of the artificial small-molecule mimics reported to date. When elucidating a set of design principles for synthetic analogues, inspiration is taken from the mechanism of the biological bipedal motor protein kinesin with a focus on potential strategies to enable directional walking.

Transition metal-ligand chemistry is utilised as one such strategy in Chapter II through the governance of walker-track interactions in the design, synthesis and operation of a bimetallic molecular biped. A palladium(II) moiety is selectively and intramolecularly stepped between pyridine-derivative binding sites in the track using a thermal stimulus in the presence of a coordinating solvent. Acid-base manipulations facilitate directional stepping by means of an energy ratchet mechanism allowing the track to do work on the biped unit and ultimately drive it away from equilibrium.

The potential of malleable transition metal binding-event energetics is explored further in Chapter III with the design and synthesis of a platinum(II)-complexed [2]rotaxane. Thermodynamic and kinetic stimuli are investigated as means to mediate selective shuttling of a Pt-complexed macrocycle between two ligand binding sites in the thread. The substitution pattern of the ligands and the kinetic stability of the metal-ligand bonds afford exceptional metastability to the co-conformers of the molecule in the absence of an external stimulus providing the possibility for long-term information storage.

In Chapter IV, a novel macrocycle is used to demonstrate the chemical orthogonality of acid-mediated hydrazone exchange with respect to the palladium(II) stepping mechanism described in Chapter II and show that two such motifs can be independently addressed within a single molecule. These linkages are then utilised as mutually exclusive chemo-selective switches to individually operate opposing feet in an unprecedented first-generation small-molecule walker-track system.

Declaration

The scientific work presented in this thesis was carried out in the School of Chemistry at the University of Edinburgh between September 2009 and August 2012. Unless otherwise stated, it is the work of the author and has not been submitted in whole or in part for any other degree or professional qualification at this or any other university or institute of learning.

Signed

Date

Acknowledgments

Firstly, I would like to thank my supervisor Professor David Leigh for giving me the opportunity to work in an incredible research environment over the past three years with a truly liberating degree of faith and freedom. All members of the Leigh group, past and present, have contributed to a unique learning and living experience and I would particularly like to acknowledge Dr Victor Blanco for his relentless patience during our bumpy ride together through the world of molecular walkers. Dr Jon Beves is also acknowledged for his support and camaraderie during the tough times and for sharing a mutual disposition for sarcasm and cynicism as invaluable tools in such spots.

Johnny Lloyd is gratefully acknowledged as a fountain of questionable advice and moral guidance in times of need whilst Jimmy Page is naturally recognised along with John, Paul, George and Ringo for invaluable contributions when whiling away weekends in the laboratory. My thanks go to Andy Bell and the Festibelly team for relaxing summer sabbaticals over the past three years and I extend my utmost gratitude to Tribes for giving me the opportunity to intersperse the writing of this thesis with casual performances at monstrous rock events around the country fulfilling every young boy's dream of combining life in research science with a rock'n'roll alter ego.

Robert and Mark Howgego are respectfully recognised as noble competitors within an on-going social experiment in which this document will form but a small chapter.

Dr Katherine Josephs is wholeheartedly commended for suffering the author's company for much of the duration of this degree, a feat for which I will be forever grateful.

Finally, I would like to thank my mother and father for their unquestioning love, support and understanding over the past three years, and indeed throughout my entire life; this thesis is dedicated to you.

List of Abbreviations

δ	chemical shift
aq.	aqueous
ATP	adenosine triphosphate
calcd.	calculated
cat.	catalytic amount
CuAAc	copper(I)-catalysed azide alkyne cycloaddition
dec.	decomposes
DIAD	diisopropylazodicarboxylate
DIPEA	diisopropylethylamine
DMAP	4-dimethylaminopyridine
DMSO	dimethylsulfoxide
DMF	*N,N'*-dimethylformamide
DNA	deoxyribonucleic acid
equiv	equivalent(s)
ESI	electrospray ionisation
ET	electron transfer
Et_2O	diethylether
EtOAc	ethyl acetate
Et_3N	triethylamine
FAB	fast atom bombardment
h	hour(s)
HPLC	high performance liquid chromatography
HOMO	highest occupied molecular orbital
HRMS	high resolution mass spectrometry
Hz, MHz	hertz, megahertz
IPA	isopropyl alcohol (2-propanol)
IR	infrared
ISC	inter-system crossing
J	coupling constant
LCMS	liquid chromatography mass spectrometry
LRMS	low resolution mass spectrometry
LUMO	lowest unoccupied molecular orbital

MeCN	acetonitrile
MeOH	methanol
min	minute(s)
m.p.	melting point
MS	mass spectrometry
m/z	mass-to-charge ratio
NMR	nuclear magnetic resonance
$Pd(PPh_3)_4$	tetrakis(triphenylphosphine)palladium(0)
$Pd(PPh_3)_2Cl_2$	Bis(triphenylphosphine)palladium dichloride
PFP	pentafluorophenol
ppm	part per million
quant.	quantitative
RT	room temperature
SUMO	singly occupied molecular orbital
TFA	trifluoroacetic acid
THF	tetrahydrofuran
TLC	thin layer chromatography
TsOH	4-*para*-toluenesulfonic acid
UV	ultraviolet (light)
VT	variable temperature

Note: conventional abbreviations for units and physical quantities are not included.

General Remarks on Experimental Data

Unless otherwise stated, all reagents were purchased from commercial sources and used without further purification. Dry CH_2Cl_2, $CHCl_3$ and THF were obtained by passing the solvent (HPLC grade) through an activated alumina column on a PureSolv™ solvent purification system (InnovativeTechnologies, Inc., MA). Dry DMF and MeOH were purchased from Sigma-Aldrich. Flash column chromatography was carried out using Kieselgel C60 (Merck, Germany) as the stationary phase. Analytical TLC was performed on pre-coated silica gel plates (0.25 mm thick, 60F254, Merck, Germany) and observed under UV light. All ^{1}H and ^{13}C NMR spectra were recorded on Bruker AVA 400, AVA 500 (cryoprobe), or AVA 600 instruments, at a constant temperature of 298 K unless stated otherwise. Chemical shifts are reported in parts per million and referenced to residual solvent. Coupling constants (*J*) are reported in Hertz (Hz). Standard abbreviations indicating multiplicity were used as follows: m = multiplet, quint. = quintet, q = quartet, t = triplet, d = doublet, s = singlet, b = broad. Assignment of the ^{1}H NMR signals was accomplished by two-dimensional NMR spectroscopy (COSY, NOESY, HSQC, HMBC). All melting points were determined using a Sanyo Gallenkamp apparatus and are uncorrected. Mass spectrometric analysis was carried out by the mass spectrometry services at the University of Edinburgh and by the EPSRC National Centre at the University of Wales, Swansea. Microwave experiments were carried out using a Biotage Initiator microwave reactor and a Lot Oriel Gruppe150W Xe lamp was used for irradiation in all photochemical studies.

Chapter I

Molecular Walkers

"Any intelligent fool can make things bigger and more complex. It takes a touch of genius - and a lot of courage - to move in the opposite direction."

- Albert Einstein

1.1 Synopsis

At the dawn of the twenty first century, man stands in awe of Nature's phenomenal achievements in moulding the world around us. Its intangible complexities have provided myth and mystery to our forebears with each successive generation of philosophers offering their own theories and solutions in the gradual evolution of our knowledge and understanding. As awareness of the molecular basis of life has grown over the last fifty years, the exquisite intricacies of Nature's methods have become evermore apparent and one conclusion has been prevalent throughout: the control of molecular-level motion is fundamentally essential to life.

Nature employs a host of hugely varied and sophisticated molecular machines and motors to instigate controlled movement at the molecular level; each individually suited to its environment and specifically designed to carry out essential tasks such as vesicle transport, sensory transduction and muscle contraction. Kinesins are a particularly impressive superfamily of linear motor protein that act as "molecular walkers" capable of transporting cargoes along cellular motorways to predefined locations. The primary obstacle to designing artificial analogues of these systems is the incorporation of appropriate interactions between the "feet" of the walker unit and the track upon which it walks. DNA base-pair interactions and dynamic covalent chemistry have both been used successfully in the past but the advancement of the field depends upon developing improved levels of control over stepping mechanisms and the potential to customise systems for specific environments. In this thesis, transition metal-ligand motifs are developed as the molecular sub-components for one such mechanism and the first example of metal mediated stepping in a synthetic molecular biped is described.

1.2 Introduction

The science of substances in the seventeenth century was dominated, as it had been for many years prior, by those with an aim of transmuting lead into gold and the quest for the ever-illusive Philosopher's Stone. As the century drew to a close, however, the threads of Aristotle's four element theory were beginning to come loose and, with the publication of *The Sceptical Chymist*[1] in 1661, Robert Boyle effectively sounded the death knell on alchemy and implored its ambassadors to lay down their quills in favour of the test tube and rigorous calculated experiment; for, to his mind, only with the accompaniment of concurrent results from such experiments could their theories ever be unequivocally proven fact. This radical idea shook the very foundations of science and set in motion a revolution that would eventually herald him as one of the founding fathers of modern chemistry.

A veritable explosion of scientific research and discovery soon followed fuelling an exponential growth in mankind's understanding of the fundamentals of life on Earth, matched only by his will to control them. However, with this increasing wealth of knowledge came an awakening sense of awe at the disparity between Nature and humankind's respective capacities to constructively wield the forces of the world, most notably at the molecular level. This realisation was famously laid out by Richard Feynman in a speech to the California Institute of Technology[2] in 1959 when he proposed that scientists would one day be able to manufacture active molecular species that function and carry out useful tasks on a nanoscopic scale, in much the same way that Nature manipulates molecular-level movement to perform the vast majority of its key operations. The rise of the field of synthetic molecular machines has been instrumental in meeting some of the challenges thrown down by Feynman and examples now exist of fully functional synthetic molecular motors[3] that consume fuel and do mechanical work at the molecular level. Most of these systems are designed to achieve rotary motion[4] whilst linear molecular motors have received far less attention.

This chapter will address a particular set of linear motors known as "molecular walkers", which are motor units that can walk down molecular tracks. A general set of principles for the design of such systems is outlined and the progression of the field to date is critically reviewed.

1.3 Molecular Machines

Molecular motors and machines are ubiquitous throughout biology as the shepherds of chemical systems at the molecular level. They are capable of controlling nano- and micrometre scale movements on account of their inherent ability to drive said systems away from equilibrium, thereby enabling specific tasks to be performed and work to be done.[3,5] Thus far however, scientists have struggled to synthetically replicate anything close to such control, primarily due to the fact that the macroscopic mechanical engineering that has been developed and mastered over the years is governed by fundamental physics inapplicable at the molecular level.[6]

Molecules and their constituent parts do not subscribe to the Newtonian laws of momentum. Instead they are incredibly susceptible to temperature variation and exist in a constant state of flux, moving incessantly and in a random, chaotic manner known as Brownian motion. The effect of gravity on these systems is negligible and, when in solution, movement is dominated by the frictional forces of their extremely viscous surroundings.[7] Consequently, any attempt at controlled, inertia-induced displacement is rendered ineffectual by the overpowering effects of the environment's background motion. R. D. Astumian deemed Brownian machines' remarkable proficiency to overcome these ordeals equivalent to man being able to "*swim in molasses and walk in a hurricane*".[8] They accomplish this feat, not by attempting to counteract and overpower the adverse forces, but rather by harnessing them in order to meet their own ends. This is often achieved through the use of mechanical bonds that can incur restrictions upon the degrees of freedom available to a machine's component parts with respect to one another, whilst still retaining the potential for large amplitude displacement along certain desired vectors. By using a stimulus that can affect the nature of these mechanical bonds, it is possible to drive the systems away from their equilibrated states, which can subsequently result in overall controlled, directional molecular motion. It should be noted, however, that this capacity alone does not warrant a system to be termed a "molecular machine", as the other prerequisite for such an accolade is the ability to carry out constructive work.

It is pertinent at this juncture to more rigorously define the term and hereafter molecular machines will be considered as: "*a subset of molecular devices in which some*

stimulus triggers the controlled, large amplitude mechanical motion of one component relative to another which results in a net task being performed".[3]

One area in which Nature truly displays a *tour de force* in terms of manipulating molecular motion is in biology's wide array of motor proteins. These fall into the two broad classes of rotary and linear motors.

1.4 Motor Proteins

Nature employs an army of incredibly diverse motor proteins throughout biology with a huge range of different molecular architectures and cellular roles, but all of them commonly operate by converting an energy input into mechanical or chemical work. This is how DNA and RNA polymerases[9] are able to convert monomeric nucleotides into incredibly sequence-specific polymers; how translocation pores[10] are able to selectively transport proteins through membranes against concentration gradients; how the remarkable rotary motor of bacterial flagellar[11] propels bacteria at speeds of hundreds of micrometres per second; how the rotating motor F_0F_1-ATPase[12] uses a proton gradient to produce the ubiquitous cellular fuel adenosine triphosphate (ATP); and how the hoards of different molecular walkers walk along molecular cytoskeletal polymer highways within the cell performing such tasks as mitosis, sensory transduction and muscle contraction as well as the imperative act of intracellular cargo transportation. These natural molecular walkers are known as cytoskeletal motor proteins[13] and are of particular importance here as they provide the inspiration for the work carried out in this thesis.

Linear Motor Proteins

As previously mentioned, the crowded cytoplasmic environment within cells is not conducive to efficient cargo conveyance by means of one-off spot forces because inertial terms are heavily outweighed by motion dampening frictional forces in the highly viscous surroundings. Nor can diffusion alone be counted upon to accommodate the many important intracellular reactions at a suitable rate. Nature, therefore, often employs linear motor proteins as cargo carrying molecular walkers to manage these highly specific tasks. These proteins fall into three superfamilies; myosins, dyneins, and kinesins (Figure 1.1) and all function by converting chemical energy into mechanical work by means of ATP hydrolysis.

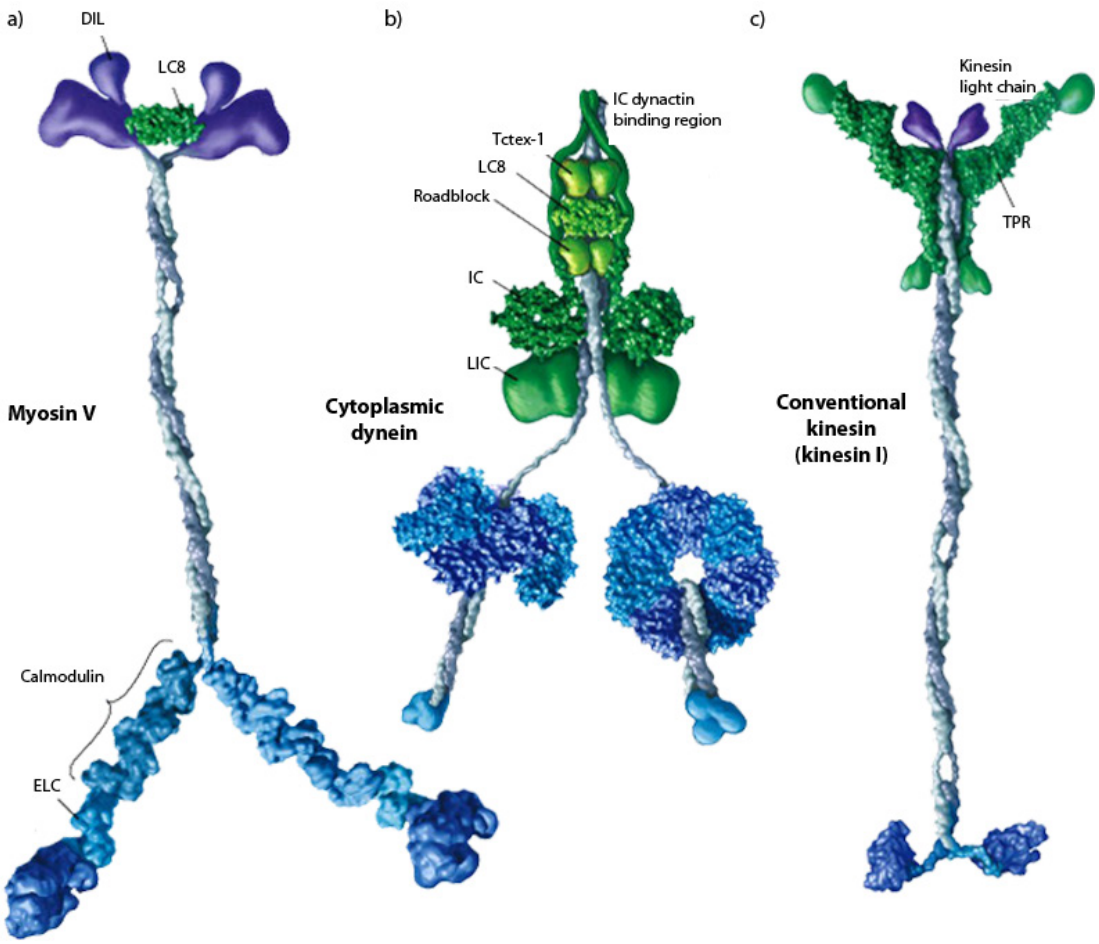

Figure 1.1 *- Comparison of examples from the three superfamilies of Nature's linear proteins: (a) myosin-V; (b) cytoplasmic dynein; (c) kinesin-I. Colour coding: dark blue: motor domains; light blue: mechanical amplifiers; purple: cargo attachment site; green: motor units. Modified with permission (Cell Press).*[13c]

Differential to their rotary analogues, linear motor proteins achieve controlled *translational* motion with the aid of well-defined tracks to which they adhere and along which they can "walk". Myosins,[14] responsible for muscle-contraction in the body and intracellular vesicle transport, bind actin filaments[15] as a track whereas dyneins[16] and kinesins[17] traverse along tightly wound biopolymers known as microtubules.[18] Many of the members of these three superfamilies exhibit different modes of action and are employed simultaneously within the same organism to carry out specific tasks. Although kinesins were the last of the three superfamilies to be discovered,[19] they have since proven susceptible to simple manipulation using the various tools of molecular biology, and a prolific wealth of literature is now devoted to them.[17,20] To date, it has been established that the human body plays host to at least 45 discernable kinesins with variations in overall structure and function but significant sequence homology in

the motor domains throughout the set.[21] The majority of research has predominantly revolved around conventional kinesin (also known as kinesin-1 and hereafter referred to simply as kinesin) due to the ease of its purification from brain homogenates[20d] and it is the mode of action of this species upon which the synthetic systems in this thesis are based.

1.5 Kinesin

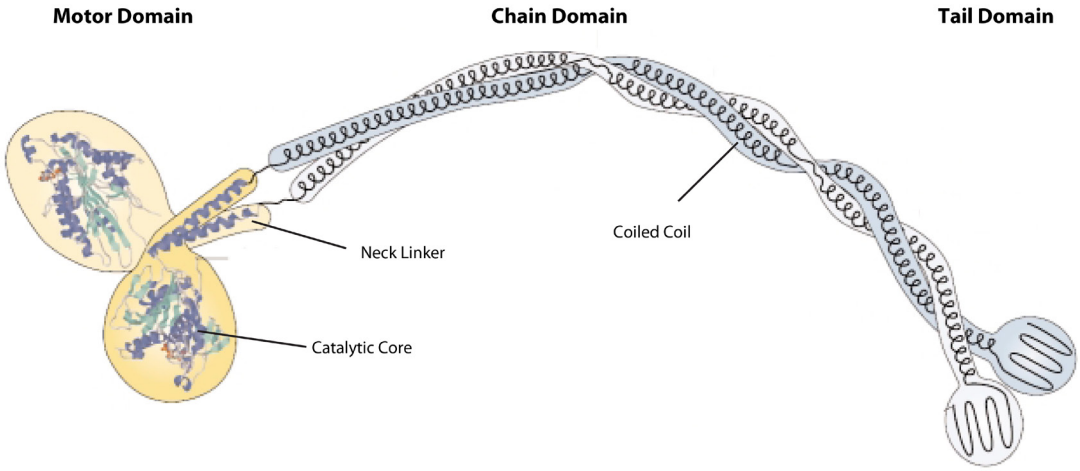

Figure 1.2 *- Conventional Kinesin: illustration based upon the crystal structure of the catalytic core and neck linker and the electron-microscopy images of the chain and tail domains. Modified with permission (Nature Publishing Group).*[24]

Kinesin is a homodimeric species made up of two chains of 120 and 130 kDa each and comprising three distinct domains: motor; chain; and tail as shown in Figure 1.2. The motor domain consists of two identical motor heads or "feet", each containing a catalytic core that binds to tubulin subunits in the microtubule track[22] and controls ATP hydrolysis in the molecule. The feet are connected to the central stalk chain domain *via* adjacent flexible neck linkers, which control their respective orientation and ensure that they are held at the optimum separation of 8 nm;[23] in keeping with the spacing between α/β-tubulin dimers in microtubules and hence kinesin's individual stepping distance. The coiled-coil stalk of the chain domain is in turn bound to the tail domain, which is responsible for both recognition and binding of specific organelles and vesicles.

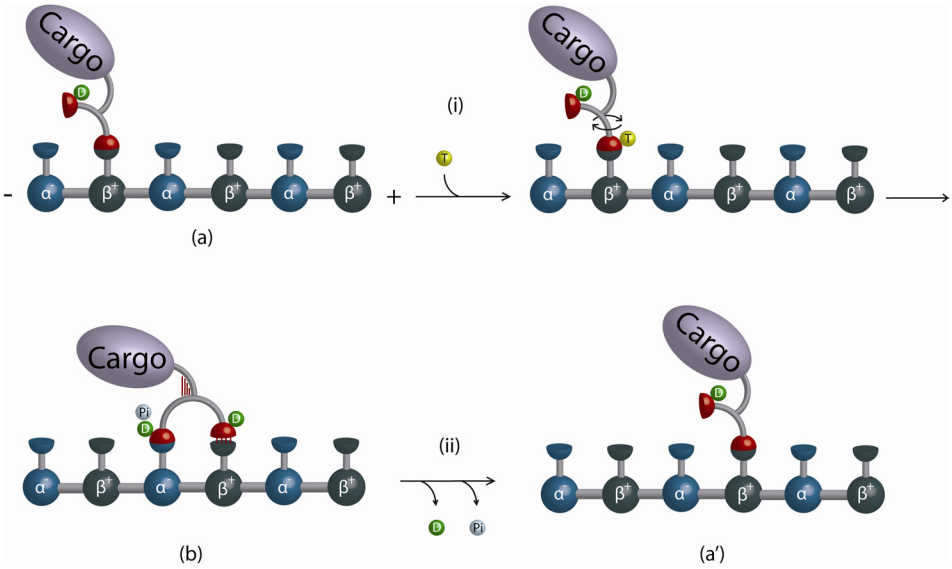

Figure 1.3 *- Kinesin's mode of action: (a) "resting state" with one head strongly bound to the track, the other free to explore binding sites. (i) ATP (T) binds kinetically locked foot; (b) stepping foot forms weekly-bound state with next binding site. (ii) dissociation of phosphate (Pi) and ADP (D); (a') analogous to initial resting state but one tubulin dimer along the track. α and β represent the different tubulin dimers that impose overall polarity on the track.*

The walking action of kinesin is fuelled by the hydrolysis of ATP to adenosine diphosphate (ADP) and an inorganic phosphate (Pi). In a resting state (Figure 1.3a), kinesin is tightly attached to the microtubule track *via* a kinetically locked, nucleotide-free foot. The tethered foot, meanwhile, is not bound to the track but its motor domain is bound to ADP (D), the microtubule-activated release of which is stably inhibited.[20c,25] ATP can selectively bind the locked foot with its vacant motor domain, partially relieving this inhibition whilst simultaneously releasing a significant amount of energy. This release gives rise to docking of the neck linker to the motor domain, which manifests itself in a conformational change that slings the tethered foot towards the plus-end of the microtubule in the so-called power-stroke. The unbound foot is then free to explore the available binding sites, both in front and behind its opposing foot; however, the neck-linker docking enforces a temporary asymmetric energy potential favouring the forward step (Figure 1.3b) and is therefore responsible for the overall directionality of kinesin's movement by means of a Brownian ratchet mechanism[3] (*vide infra*). There is still some debate as to the order in which the following events proceed, but in Block's "consensus model",[17a] ADP is released from the anterior foot leading to tightened binding with the microtubule and increased ring strain which supresses subsequent premature binding of ATP before the posterior foot has hydrolysed its

respective ATP expelling inorganic phosphate.[20c,d,26] This process culminates in an analogous state to the original resting state, only two tubulin units along[23b] (Figure 1.3a') and is tantamount to a single catalytic stepping cycle, the repetition of which constitutes kinesin's complete walking mode of action. This locomotive method is commonly referred to as a "passing-leg" or "hand-over-hand" mechanism and, after years of debate, was independently confirmed for kinesin by both Kaseda *et al.*[27] and Yildiz *et al.*[26b] Optical trapping studies have shown kinesin to be capable of up to 100 ATP turnovers before complete dissociation from its track equating to a walk of ~1 mm in a single direction.[20a,28]

Whereas in day-to-day life the walker decides which route to take, in the case of kinesin, it is in fact the track that ultimately dictates directionality. This comes as a result of anisotropy in the polymeric microtubule where the chains of self-assembled α/β-tubulin dimers create an inherent overall polarity in the track.[29] As previously mentioned, kinesins walk unidirectionally with 42 of the 45 human kinesins known to perambulate from negative to positive, which, in most cells, amounts to anterograde motion where cargo is transported away from the centre to the periphery of the cell.[21]

The primary aim of this project is to use the fundamental principles of molecular walking exhibited by kinesin to investigate potential chemical motifs for use as components in the design of simplified synthetic small molecular analogues.

1.6 Design Principles For Synthetic Walking Molecules

The term "molecular walker" has so far been applied to a class of natural linear motors because they move in a manner reminiscent of man's own mode of perambulation. However, considering the staggering differences between life at the macro- and molecular levels in terms of environments and the laws by which they are governed, it seems prudent to outline a precise set of definitions for use when establishing principles for the design of minimalist artificial analogues. The Oxford English Dictionary defines stepping as, "*An act of bodily motion consisting in raising the foot from the ground and bringing it down again in a fresh position*" and walking as, "*The action of moving or travelling . . . by lifting and setting down each foot in turn so that one of the feet is always touching the ground*". From this it can be said that a walker must have at least two well-defined feet that, as a pair or set, act as the only necessary points of bodily attachment to a surface or track in order to mediate stepping. Furthermore a

prerequisite exists such that one foot must be in contact with the surface or track at all times regardless of the other foot/feet. Such a system will cease to be termed a walker if it begins to translocate its centre of mass without the use of discrete steps (e.g. *rolling* or *tumbling*) or at such a time that no feet remain attached to the track (e.g. *running* or *jumping*). By adopting these provisos the basic principles of walking can be transferred to a synthetic design. However, whereas Nature has had millions of years to evolve, try and test-drive the molecular walkers described in the previous sections, synthetic analogues must be designed, tuned and built for instant effective operation. In a recent critical review of walking molecules, von Delius and Leigh[30] outlined five fundamental characteristics of the dynamic behaviour with respect to the interactions between the walker units and their tracks, which are discussed in detail below.

1.7 Keep Your Feet On The Ground - Processivity

Processivity is the ability of a molecular walker to remain attached to its track during operation. Whereas their macroscopic counterparts enjoy the benefit of gravity to keep their feet securely on the ground, molecular walkers must incorporate additional safeguards to ensure this linkage at all times. Whilst not all of Nature's linear motors operate processively (e.g. conventional myosin), non-processive motors can only do work in large ensembles where multiple walker units are simultaneously attached to the same track. This is a very difficult and complicated feat to achieve synthetically and so this project will focus primarily upon walker units that do not fully detach from their tracks. One factor that can significantly affect a system's processivity is the act of inter-track stepping, but this can be quite easily avoided in artificial systems by operating under dilute reaction conditions or appending the molecular track to a suitable surface.

In a perfectly processive molecular walker, the walker unit is attached to its track by some means at all times. The easiest way to achieve this synthetically is to incorporate two chemically different feet that can be labilised under mutually exclusive conditions so that when one foot is undergoing a stepping process, the other is kinetically locked to the track and acts as an inert pivot. The simplest possible hypothetical walker unit of this kind is outlined in Figure 1.4 and has two feet (*1* and *2*) linked together by an inelastic, non-rigid linker motif that separates them by a fixed distance (*x*). Consider setting this walker unit upon a track with two alternating footholds (*A* and *B*), each foothold also separated by distance x.

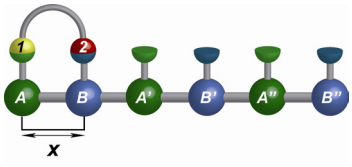

Figure 1.4 *- Generic two-footed walker unit upon an ABABAB track in state [1A, 2B].*[31]

If it is specified that, dependent upon two mutually exclusive external stimuli, *1* and *2* can have binding preferences for either *A* or *B*, then locked generic linkages *1A*, *1B*, *2A*, and *2B* can all be readily formed. The walker's initial position can be described as [*1A*, *2B*], with foot *1* shown in yellow, foot *2* in red and *A* and *B* are green and blue respectively. Applying a stimulus that labilises foot *1* from foothold *A* whilst leaving linkage *2B* unperturbed generates the intermediate [*2B*]*1**, where foot *2* is still strongly bound to foothold *B* but foot *1* is free to explore other binding sites (here indicated by ***) *via* free rotation around the non-rigid linker (Figure 1.5). Upon removal of the stimulus, foot *1* will regain its affinity for foothold *A* and re-form a locked generic *1A* linkage with the closest suitable foothold giving rise to a statistical 1:1 ratio of spatial isomers [*1A*, *2B*] and [*2B*, *1A'*], where *1A'* indicates that this linkage is one *AB* unit away from the origin.

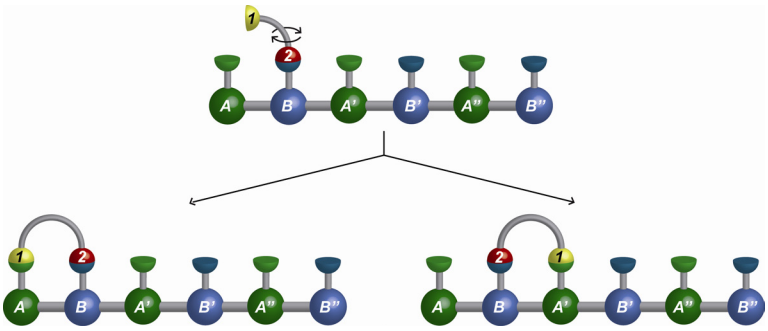

Figure 1.5 *- Mid-step co-conformation of [2B]1* (top) gives rise to equal populations of the two states [1A, 2B] (left) and [2B, 1A'] (right) when the stimulus is applied favouring the formation of generic linkage 1A.*

By applying a second, orthogonal stimulus that labilises foot *2* from foothold *B* whilst leaving linkages *1A* and *1A'* unperturbed, generic states of the type [*1A*]*2** are formed. Free rotation about the non-rigid linker, followed by subsequent removal of the second stimulus, regenerates generic *2B* linkages resulting in three statistically populated translational isomers; [*1A*, *2B*], [*2B*, *1A'*], and [*1A'*, *2B'*] in the ratio 2:1:1 (Figure 1.6). This distribution is the result of the walker units starting from state [*1A*, *2B*] (half of the total number) when the second stimulus is applied being unable to make any progress

down the track due to constraints imposed by the inelastic link to locked foot *1* on foothold *A*, whilst the walker units initially in state [*2B*, *1A'*] can either recover this state, or advance to [*1A'*, *2B'*] upon removal of the stimulus, each outcome having a probability of 0.5.

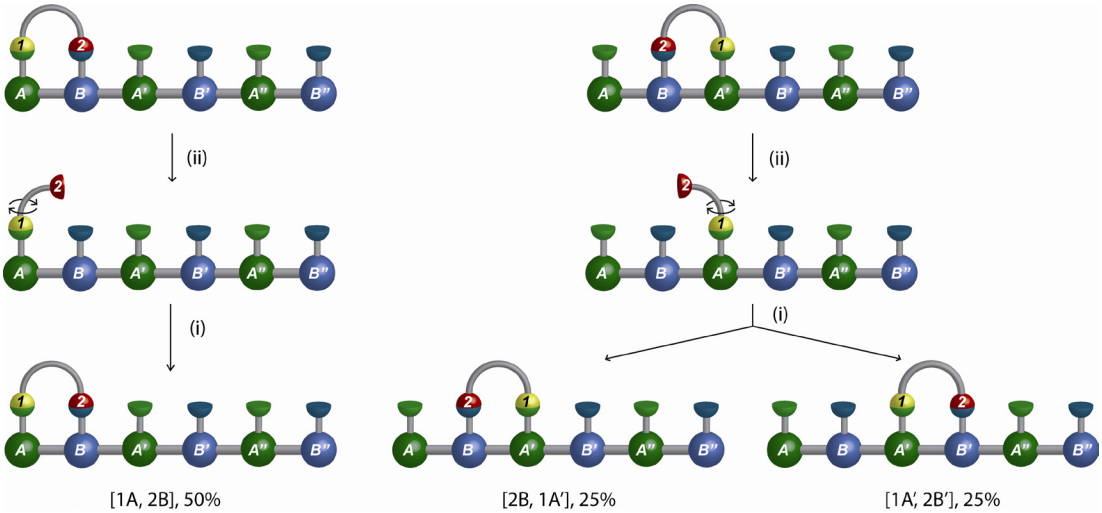

Figure 1.6 *- Three co-conformers possible after the second step of an ABABAB walker.*

Reapplying the first stimulus labilises all generic *1A* linkages generating various different states of [*2B*]*1**, which then give rise to four inequivalent spatial isomers upon removal of the stimulus to the ratio of 3:3:1:1. The second law of thermodynamics states that unidirectional motion can only be achieved in conjunction with energy expenditure.[32] In a system such as this, devoid of chemical fuel and where there is no in-built directional bias, there can be no controlled directed motion and the overall populations of each state are governed purely by statistics. In this sense, Figure 1.6 is slightly misleading because, as drawn, it implies a general migration of walker units from left to right. However, this is only because [*1A*, *2B*] was arbitrarily elected as the starting state. In fact, if the sequence of alternating stimuli were repeated for a suitably long time, the system would reach equilibrium with the populations of each state abiding by a normal distribution about a modal population class in the centre of the track. A molecule such as this, that uses two simple switches as feet and migrates in either direction along a track with equal probability cannot be deemed a motor because it is incapable of performing useful tasks and cannot achieve any net-mechanical work.

1.8 Ratchet Mechanisms - Directionality

For a molecular walker to be directional it must migrate either preferentially, or exclusively to a single end of a molecular track in the same manner as all of Nature's translational molecular motors. The study of non-equilibrium statistical mechanics and thermodynamics has proven to be a very useful tool in elucidating key aspects of achieving directional bias in molecular-level motion. The Principle of Detailed Balance[33] states that, within a system at equilibrium, transitions between any two states take place in either direction at an equal rate.

Eqn 1.1 - $N_i P_{ij} = N_j P_{ji}$

For a system that contains species *i* and *j* in dynamic exchange at equilibrium, the number of transitions from state *i* to state *j* is equal to the number of transitions in the opposite direction as described by Equation 1.1, where N_i is the number of particles in state *i* and P_{ij} is the probability of transition from state *i* to *j* for a given particle.[34]

These terms can help define the key differences between simple molecular switches and genuine molecular motors. A switch can be described as a system that progresses from state *i* to *j* along a reaction pathway and can only be returned to its original state by returning along that same pathway, thereby undoing the task performed in the initial transition. Alternatively, a motor can return to state *i* from *j via* a different, non-reciprocal route to the one already travelled meaning that the completion of a cycle of operation can reset the motor without undoing the mechanical work done on the system. In this way switches are said to influence a system as a function of state, whereas motors influence a system as a function of the trajectory of their components or substrates.[3] Regardless of the molecular device in question, be it a switch or a motor, directionality can only be achieved by disturbing the equilibrium with an energy input (a fuel or external stimulus) that facilitates the breaking of detailed balance. A dynamic switch will re-equilibrate to its thermodynamic minimum upon suspension of the stimulus or fuel input, whereas a molecular motor can harness the work done by invoking impassable kinetic barriers to dynamic exchange between states thus compartmentalising the system.[3] This method is exploited in both biological and synthetic molecular motors[8,35] and can be described according to Brownian ratchet theory,[36] which explains how the thermally driven positional displacement of a substrate can be captured by the imposition of a kinetic barrier to the reversal of the

displacement once the thermodynamic driving force is removed. Although many different theoretical variations exist, they all rely upon three key facets of the theory: the presence of a randomising element (Brownian motion in molecular scale motors); an energy input; and an asymmetric potential of energy or information in the direction of the motion. In this way, a Brownian particle can be transported directionally along a compartmentalised potential energy surface. The instillation of directionality is governed by the nature of the third of these tenets which can be divided into the two general classes of energy ratchets and information ratchets.

Energy Ratchets

In an energy ratchet mechanism, the transport of a particle along a potential energy surface is achieved by periodic perturbation of the thermodynamic minima and kinetic barriers. Cyclic fluctuation of energy maxima and minima can facilitate directional movement irrespective of the position of the particle on the surface.

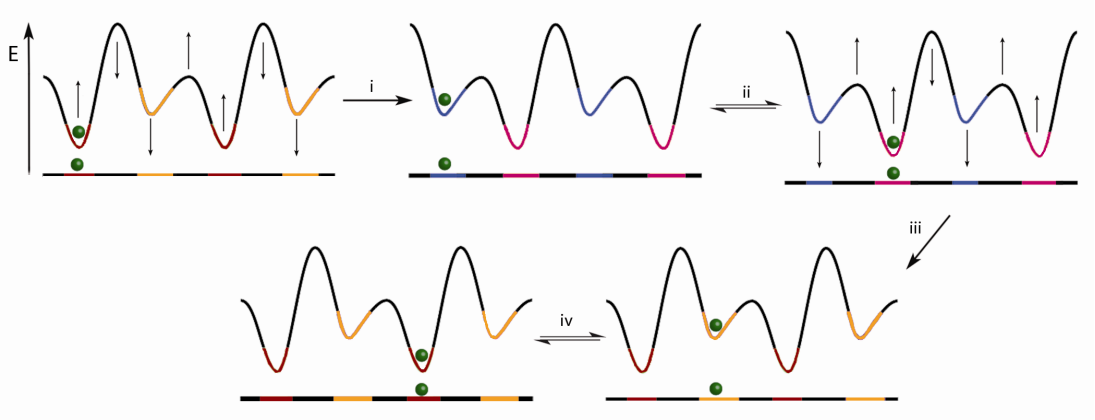

Figure 1.7 *- Brownian energy ratchet mechanism. Sequential fluctuation of the energy maxima and minima induce directional movement of a Brownian particle (green).*

Figure 1.7 shows a Brownian particle (green) at equilibrium upon an asymmetric potential energy surface that incorporates a periodic series of two unique energy maxima and two unique energy minima. The particle can be transferred from left to right by simultaneously or sequentially inverting the relative energies of the thermodynamic minima and the kinetic barriers. Although some transport of the particle from right to left will still occur, the majority of the particles will translocate rightwards because, as drawn, the orange and blue thermodynamic minima always have the greater kinetic barrier to their left. It is clear that the direction of transport can therefore be controlled by manipulation of the relative energies of each state and

several catenane- and rotaxane-based molecular motors and devices have been reported that operate using energy ratchet mechanisms.[4c,d,37]

Information Ratchets

Alternatively, the thermodynamic minima of the potential energy surfaces of information ratchets are fixed and directional motion is achieved by raising and lowering kinetic barriers to translation according to the position of the particle. There is therefore a requirement for information of the particle's position to be communicated to the kinetic barrier.

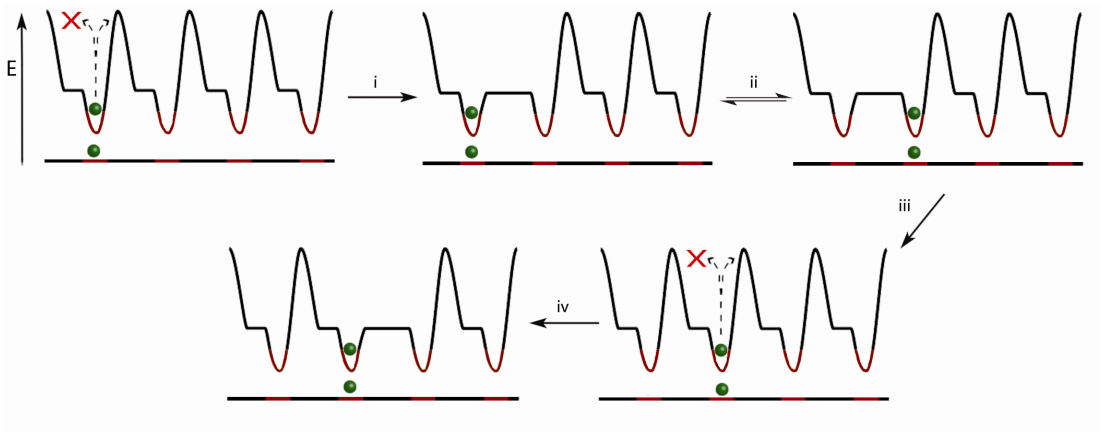

Figure 1.8 *- Brownian Information ratchet mechanism. A Brownian particle (green) is directionally transported along an asymmetric potential energy surface. The relative magnitudes of the kinetic barriers result from an information transfer between the particle and the barrier (dotted arrow).*

In Figure 1.8, a Brownian particle lies at equilibrium upon an asymmetric potential energy surface that incorporates a series of identical potential energy wells, each separated by a kinetic barrier. A stipulation exists such that the particle can only communicate its presence to the kinetic barrier directly to its right. In so doing, the barrier can be lowered establishing a new equilibrium where a 1:1 distribution will form between the first two wells and the barrier is subsequently raised again. Because migration to the left is impossible, the particle can progress directionally despite the unbiased reversibility of step ii. Although reports of rotaxane-based information ratchets have been scarce,[38] a synthetic small molecule capable of directionally walking along a track by means of information ratchet mechanisms has recently been reported[39] and will be discussed in detail in Section 1.11.

1.9 Repetitive, Progressive, Autonomous Operation

The other stipulation for linear molecular motors is that they can be operated in a repetitive and progressive manner. This means that they must be able to repeatedly carry out similar mechanical cycles, and that it is possible to reset the walker-track conjugate after operation without undoing the physical task that was originally performed. This can be readily achieved in non-interlocked molecular walker systems by detachment of the walker unit from the end of the track along which it has walked, and subsequently reattaching it at the original starting position. In terms of ratchet nomenclature, this is known as an "escapement"[37a] where the ratcheted substrate (the walker unit) can be released and the system reset with the overall achievement of net-mechanical work being done. The presence of an escapement defines the difference between a simple ratchet and a genuine motor.

Autonomous operation is certainly a long-term goal for synthetic systems as the vast majority of cytoskeletal motor proteins operate allosterically and autonomously in the constant presence of an ATP fuel. Their feet are coordinated and the systems employ complex structural gates to enforce processivity. Two synthetic examples have been reported recently in which small molecules can walk processively along polyamine tracks through reversible imine formation without the aid of external stimuli,[40] however, both systems are non-directional. It is also difficult to envisage how one might instil an appropriate bias with current synthetic techniques, short of simply introducing a thermodynamic sink at the end of the track to which the walker units would statistically migrate.

An alternative approach is to devise designs that incorporate sequential stepping of feet controlled by external stimuli, which can ultimately allow for greater degrees of control over the direction of movement as well as the rate and distances travelled. The following discussion will therefore exclusively cover sequenced stepping mechanisms, specifically in bipedal systems. These designs rely upon the operator's ability to address each foot-foothold interaction independently of the other. In the design of random walkers based on the simplistic models described in Section 1.7, this requirement is practically realisable through the incorporation of two orthogonal, chemo-selective molecular switches that individually govern the foot-track connectivities and hence the nanoscale motility of each foot. However, in order to

attain the coveted prize of directionality, an asymmetric potential must be sequentially introduced during the stepping process of each foot, in other words, one must substitute simple switches for ratchet motifs.

1.10 Molecular Motion: Switches, Shuttles and Ratchets

Nature's methods of manipulating molecular movement through the control of Brownian motion have been an inspiration to scientists for decades, but it was not until the late twentieth century that synthetic skills reached a suitable level for mimics to be designed and made in the laboratory. In 1994, Stoddart *et al*. reported one of the first examples of a synthetic molecular device capable of harnessing Brownian motion to produce well-defined movement of its constituent parts.[41] The system made use of template-directed rotaxane synthesis to achieve a [2]rotaxane with a tetra-cationic cyclophane macrocycle threaded onto a stoppered two-station track as shown in Figure 1.9. A biphenol and a benzidine unit provide the two π-electron donor stations.

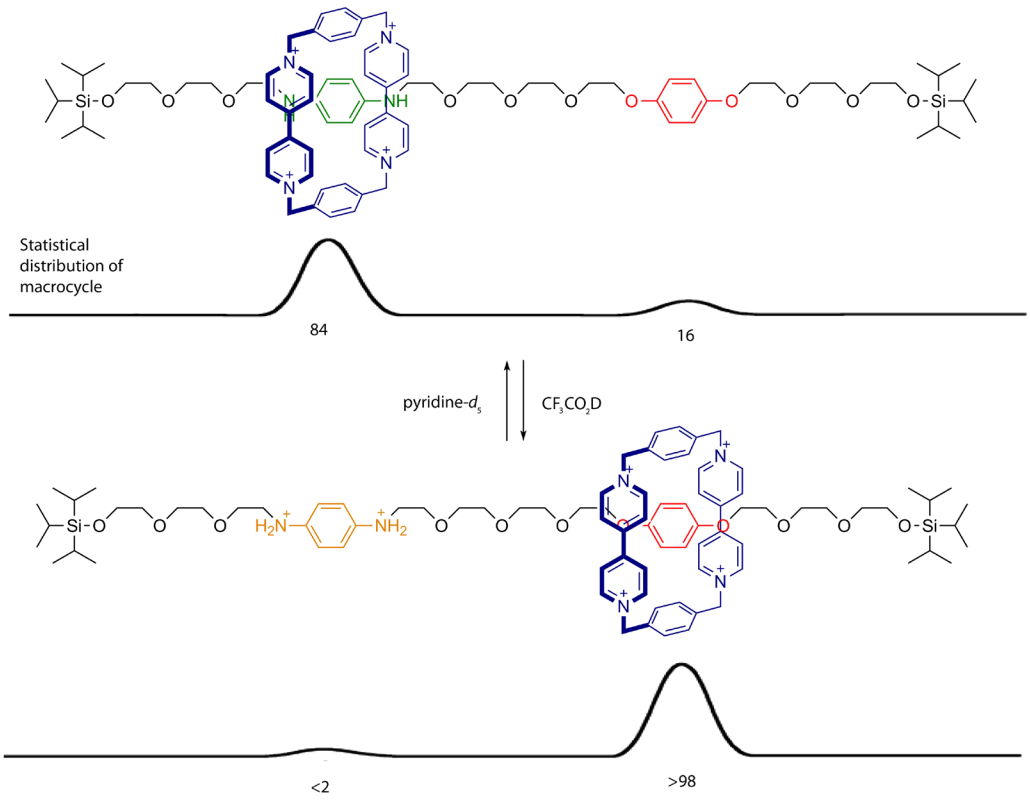

Figure 1.9 *- Switchable molecular shuttle: (top) neutral conditions, the macrocycle preferentially occupies the benzidine station (left); (bottom) protonation of the benzidine moiety results in switching of the macrocycle to preferentially occupy the biphenol station (right).*[41]

At room temperature, the macrocycle shuttles between stations at a rate comparable to the NMR timescale, however, when the system was cooled, ^{1}H NMR and ultraviolet/visible spectroscopy confirmed that the majority of the macrocycles resided on the benzidine station. It was then shown that the average distribution of macrocycles could be shifted to have a majority on the biphenol station by two separate means: either by adding two equivalents of acid and hence protonating the basic nitrogen atoms on the benzidine residue, or alternatively, by the electrochemical oxidation of this station. Both of these methods make use of repulsive electrostatic interactions between the positively charged macrocycle and the post-switching cationic nature of the benzidine station, ultimately resulting in a controlled shuttling process. This system was one of the first examples of what have come to be known as molecular shuttles, a subset of switchable species within the then-emerging field of synthetic molecular machines, and provided precedent for a whirlwind of research that followed which has been comprehensively reviewed.[3,42] An enormous amount of work has since focused upon the goal of achieving unidirectional motion by controlling relative inter-component movement of interlocked molecular devices, both rotational,[4a,b,43] and translational.[44] Catenanes and rotaxanes have proven to be particularly suited to such tasks, as they possess mechanical bonds that can incur significant restrictions upon the degrees of freedom available to the interlocked components whilst simultaneously accommodating large amplitude motion along a desired vector. Molecular shuttles of the type outlined in Figure 1.9 can be described in terms of their individual components where the thread fulfils the role of the "machine" entity and can do work on the macrocycle, which is regarded as a Brownian particle. The vast majority of examples in the literature represent simple rotaxane switches that can be moved between positional states, but each time the position is switched, the work done during the previous positional change is consequently undone. In 2006, Leigh *et al.* reported the first example of a [2]rotaxane that could be locked in an out-of-equilibrium state by means of an energy ratchet mechanism[37a] meaning the thread could be reset after operation without automatically instigating the reverse shuttling of the macrocycle. Only a few examples of such molecular ratchets exist in the literature,[37,38] the most recent of which is described in Figure 1.10.

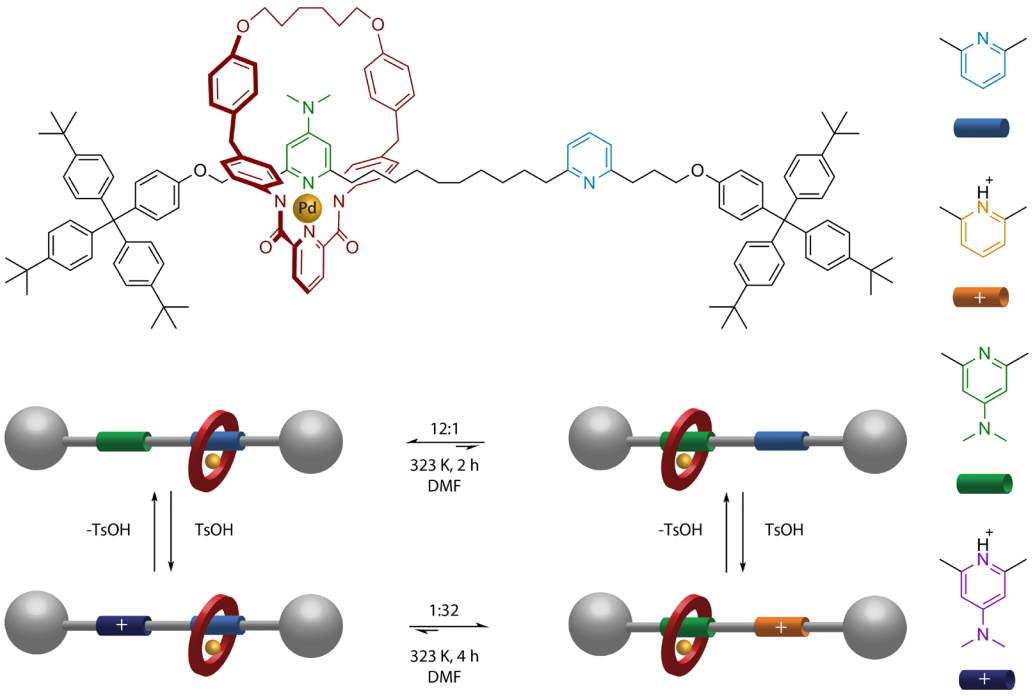

Figure 1.10 *- Operation conditions and positional bias of switchable palladium(II)-complexed molecular shuttle that operates by an energy ratchet mechanism.*[37c]

The system comprises a palladium(II)-complexed macrocycle threaded on a stoppered two-station track. A 4-dimethylaminopyridine (DMAP) and a pyridine group (Py) in the track provide the two ligand-binding sites (stations). The metal remains complexed to the macrocycle at all times and translocation of the ring-complex is dictated by simple ligand exchange. The stimulus for labilising palladium from either of the two monodentate ligands in the thread is elevated temperature in the presence of a coordinating solvent. Re-coordination to a particular station in the track is achieved by allowing the system to cool to room temperature. Whilst the labilising stimulus is being applied, an equilibrium is established to which an asymmetric bias can be induced by addition or removal of protons. Protonation of the more basic binding site determines the position of equilibrium. Importantly, the stability of the Pd-N bond in these complexes ensures that variations in the chemical state of the thread, i.e. degree of protonation, have no effect on the position of the macrocycle without application of the labilising stimulus because of a kinetic barrier to equilibration, thus rendering the system an efficient molecular energy ratchet. Combining the mechanistic principles extrapolated from biology with the expertise and knowledge cultivated through development of rotaxanes as molecular switches and ratchets has led to the first steps in the promising field of synthetic linear molecular motors.

1.11 Synthetic Walking Molecules

Until relatively recently, the only synthetic structures capable of taking multiple, processive steps along a molecular track had been unanimously assembled, at least in part, from DNA building blocks.[45] These DNA walkers represent genuine linear molecular motors where the walker units migrate progressively in a specified direction along molecular tracks and can be operated in a repetitive manner. The systems are highly efficient and can be synthesised in an automated fashion, thus providing valuable inroads to useful and applicable mimics of Nature's packhorse motor proteins. However, whereas high precision analytical techniques such as nuclear magnetic resonance spectroscopy (NMR) and high performance liquid chromatography (HPLC) are largely incompatible with the large chemical structures involved in DNA walkers, they can be readily applied to small-molecule systems facilitating more intricate mechanistic analysis and tunability of components. Although many examples exist of small molecules who's mode of motion is purported as "walking",[40,46] most lack the requisite processivity or directional bias to be deemed verifiable molecular walkers and it was not until 2010 that von Delius *et al*. reported the synthesis and operation of the first highly processive two-legged small molecule translational motor capable of walking up and down a molecular track.[39] Whereas linear motor proteins and synthetic DNA walkers utilise non-covalent interactions to bind the walker to the track, this system made use of dynamic covalent chemistry so that, during the walking process, the different feet form actual covalent bonds with the track that are either labile, or kinetically locked under different sets of conditions.

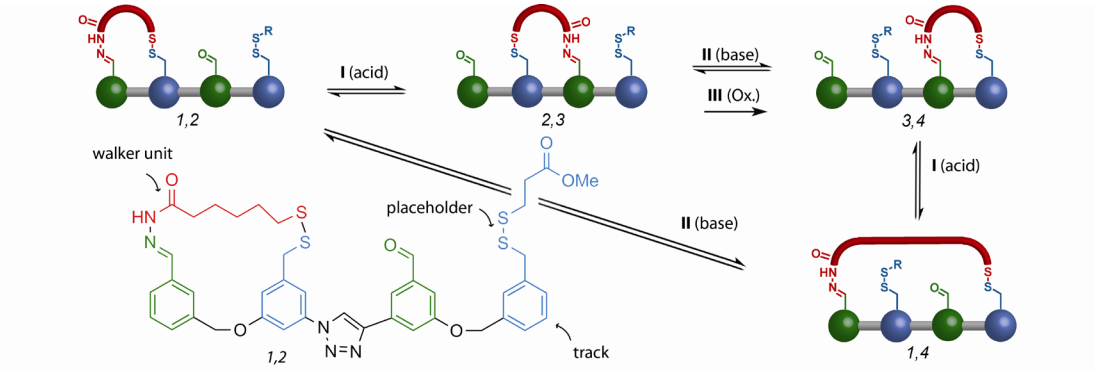

Figure 1.11 *- First non-DNA based small-molecule capable of directional motion along a track: Local equilibria connect the four positional isomers (1,2), (2,3), (3,4), and (1,4) under various conditions. The upper pathway represents the major passing-leg mechanism from (1,2) to (3,4) (through 2,3) and the lower pathway (through 1,4) is a minor double-step mechanism.*[39]

The design outlined in Figure 1.11 incorporates many of the theoretical concepts covered so far. The walker unit functions using a passing-leg gait and has two chemically different feet, one that forms a hydrazone bond with the track, and one that forms a disulphide bond. These feet reversibly bind different footholds of the track depending on the applied stimulus. Under acidic conditions, the disulfide bond between one foot and the track is kinetically locked whilst the hydrazone foot is free to explore other binding sights. In contrast, when basic conditions are applied, the hydrazone foot is locked in place and the disulfide foot is free to sample forward and backward binding sites. When operated in this form by simply alternating the stimuli, this system is directly comparable to the first hypothetical example discussed in Section 1.7. The predicted outcome is confirmed with a steady-state, minimum-energy distribution of walkers around a central point achieved after several stimulant oscillations (results do not match the theoretical model perfectly due to elasticity in the linker). Directional bias was introduced by replacing the base-promoted disulfide exchange reaction with a kinetically controlled redox reaction and hence, leading the system to conform to an information ratchet mechanism. Not only did this provide the first example of a non-DNA based synthetic molecular walker, but the two passing-leg gait steps taken in this system constitute the full repeat cycle necessary for the molecule to walk down a hypothetically infinite polymeric track of alternating benzaldehyde and benzylic disulfide stations, presenting potential for the transport of molecular cargo over relatively long distances.

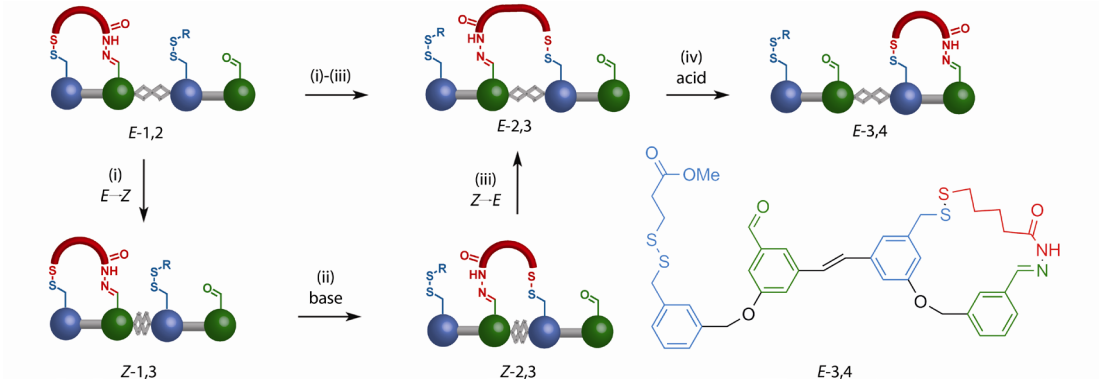

Figure 1.12 *- Operating mechanism of a directional light-driven walker-track conjugate based on adjustable ring strain between the walker (red) and the track in one positional isomer: (i) minimises walker-track ring-strain in the 2,3 position; (ii) labilises the disulfide foot; (iii) maximises walker-track ring-strain in the 2,3 position; (iv) labilises the hydrazone foot. The reaction sequence shown results in transport of the walker from left to right; switching steps (ii) and (iv) would cause the walker to be transported from right to left.*

The same hydrazone and disulfide foot-foothold linkage chemistry was utilised in a more recent, light-driven synthetic walker molecule that could be transported in either direction along a molecular track by means of an energy ratchet mechanism.[47] The design is very similar to the previous example but for the introduction of a stilbene unit between the internal aldehyde and the disulfide foothold of the track (Figure 1.12). Selective photoisomerisation of the stilbene moiety provides the potential for directionality in this system as it can induce significant ring-strain upon the isomer that bridges the stilbene linkage. E→Z isomerisation favours stepping over the central stilbene unit, while subsequent Z→E isomerisation provides a driving force to move away from the central position and allows the operator to choose the direction of motion by electing which foot is labilised next, an element of control not available to natural systems. The variation in ring-strain induced by stilbene isomerisation equates to the manipulation of thermodynamic minima whilst the oscillation of acid and base addition mediates the alteration of kinetic barriers experienced by the walker unit culminating in exceptional control over the directionality of the biped with the maintenance of a high degree of processivity.

1.12 Conclusions and Aims

Life on Earth is the product of billions of years of biological evolution. During this time, Nature has learnt to harness, control and manipulate incessant Brownian motion at the molecular level as a means of regulating intracellular function in all complex living organisms by using a plethora of intricate motor proteins. The incredible results of this progression lie all around and act as vivid inspiration for scientists by illuminating the vast scale of possibilities attainable through chemical engineering and nanotechnology. Whilst the inherent hydrogen-bonding arrays of DNA base pairing have already been utilised in the design of artificial translational molecular motors, the toolbox of synthetic chemistry holds vast potential for alternative, ingenious molecular walkers capable of carrying out tasks on a much smaller scale than that of motor proteins.

The aim of this thesis is to investigate new motifs for use as potential components in synthetic small-molecule walker units capable of processive and directional migration along molecular tracks. Transition metal-ligand interactions were identified as promising foot-foothold connections in this quest on account of their variable thermodynamic and kinetic binding properties, making them amenable for use in

conjunction with Brownian ratchet mechanisms. Experimental research in the pursuit of this goal has led to an effective palladium(II) motif for use in directional stepping along poly-pyridyl tracks (Chapter II), comprehensive investigation into similar platinum(II) moieties to achieve variable dynamics (Chapter III), and finally the orthogonal combination of palladium(II)-ligand interactions with dynamic covalent chemistry in the design and synthesis of an unprecedented first-generation molecular walker.

2.13 References

1. Boyle, R. *The Sceptical Chymist*, Cadwell: London, **1661**.

2. Feynman, R. P. *California Institute of Technology Journal of Engineering and Science* **1960**, *4*, 23-36.

3. Kay, E. R.; Leigh, D. A.; Zerbetto, F. *Angew. Chem., Int. Ed.* **2007**, *46*, 72-191.

4. a) Kelly, T. R.; De Silva, H.; Silva, R. A. *Nature* **1999**, *401*, 150-152;

b) Koumura, N.; Zijlstra, R. W. J.; van Delden, R. A.; Harada, N.; Feringa, B. L. *Nature* **1999**, *401*, 152-155;

c) Leigh, D. A.; Wong, J. K. Y.; Dehez, F.; Zerbetto, F. *Nature* **2003**, *424*, 174-179;

d) Hernández, J. V.; Kay, E. R.; Leigh, D. A. *Science* **2004**, *306*, 1532-1537;

e) Fletcher, S. P.; Dumur, F.; Pollard, M. M.; Feringa, B. L. *Science* **2005**, *310*, 80-82;

f) van Delden, R. A.; ter Wiel, M. K. J.; Pollard, M. M.; Vicario, J.; Koumura, N.; Feringa, B. L. *Nature* **2005**, *437*, 1337-1340;

g) Eelkema, R.; Broer, D. J.; Feringa, B. L. *Nature* **2006**, *465*, 163.

h) Haratyunyan, S. R.; Ernst, K.-H.; Feringa, B. L. *Nature* **2011**, *479*, 208-211;

i) Browne, W. R.; Feringa, B. L.; Meech, S. R. *Nature Chem.* **2012**, *4*, 547-551.

5. Schilwa, M. *Molecular Motors*, Wiley-VCH: Weinheim, **2003**.

6. Purcell, E. M. *Am. J. Phys.* **1977**, *45*, 3-11.

7. a) Brown, R. *The Miscelaneous Botanical Works of Robert Brown*, Ray Society: London, **1886**;

b) Einstein, A. *Annalen Der Physik* **1905**, *17*, 549-560;

c) Haw, M. *Physics World* **2005**, *18*, 19-22.

8. Astumian, R. D. *Phys. Chem. Chem. Phys.* **2007**, *9*, 5067-5083.

9. *For recent review articles on DNA and RNA polymerases, see:*

a) Murakami, K. S.; Darst, S. A. *Curr. Opin. Chem. Biol.* **2003**, *13*, 31-39;

b) Prakash, S.; Johnson, R. E.; Prakash, L. *Annu. Rev. Biochem.* **2005**, *74*, 317-353;

c) Berdis, A. J. *Chem. Rev.* **2009**, *109*, 2862-2879.

10. *For recent review articles on translocation pores, see:*

a) Yoneda, Y. *J. Biochem.* **1997**, *121*, 811-817;

b) Branton, D.; Deamer, D. W.; Marziali, A.; Bayley, H.; Benner, S. A.; Butler, T.; Di Ventra, M.; Garaj, S.; Hibbs, A.; Huang, X.; Jovanovich, S. B.; Krstic, P. S.; Lindsay, S.; Ling, X. S.; Mastrangelo, C. H.; Meller, A.; Oliver, J. S.; Pershin, Y. V.; Ramsey, J. M.; Riehn, R.; Soni, G. V.; Tabard-Cossa, V.; Wanunu, M.; Wiggin, M.; A Schloss, J. A. *Nature Biotechnol.* **2008**, *26*, 1146-1153;

c) Marakov, D. E. *Acc. Chem. Res.* **2009**, *42*, 281-289.

11. *For review articles on the flagellar motor, see:*

a) Meister, M.; Lowe, G.; Berg, H. C. *Cell* **1987**, *49*, 643-650;

b) Berg, H. C. *Annu. Rev. Biochem.* **2003**, *72*, 19-54;

c) Xing, J. H.; Bai, F.; Berry, R.; Oster, G. *Proc. Natl. Acad. Sci. U. S. A.* **2006**, *103*, 1260-1265.

d) Sowa, Y.; Berry, R. M. *Quart. Rev. Biophys.* ***2008***, *41*, 103-106.

12. *For recent review articles on the rotating F_0F_1-ATPase motor, see:*

a) Ueno, H.; Suzuki, T.; Kinosita, K.; Yoshida, M. *Proc. Natl. Acad. Sci. U. S. A.* **2005**, *102*, 1333-1338;

b) Nakamoto, R. K.; Scanlon, J. A. B.; Al-Shawi, M. K. *Arch. Biochem. Biophys.* **2008**, *476*, 43-50;

c) von Ballmoos, C.; Cook, G. M.; Dimroth, P. *Annu. Rev. Biophys.* **2008**, *37*, 43-64.

13. *For review articles covering cytoskeletal motor proteins, see:*

a) Vale, R. D.; Milligan, R. A. *Science* **2000**, *288*, 88-95;

b) Schilwa, M.; Woehlke, G. *Nature* **2003**, *422*, 759-765;

c) Vale, R. D. *Cell* **2003**, *112*, 467-480;

d) Amos, L. A. *Cell Mol. Life Sci.* **2008**, *65*, 509-515.

14. *For recent reviews on members of the myosin superfamily, see:*

a) Sellers, J. R.; Veigel, C. *Curr. Opin. Cell. Biol.* **2006**, *18*, 68-73;

b) Vicente-Manzanares, M.; Ma, X.; Adelstein, R. S.; Horwitz, A. R. *Nature Rev. Mol. Cell Biol.* **2009**, *10*, 778-790;

c) Spudich, J. A.; Sivaramakrishnan, S. *Nature Rev. Mol. Cell Biol.* **2010**, *11*, 128-137.

15. Holmes, K. C.; Popp, D.; Gebhard, W.; Kabsch, W. *Nature* **1990**, *347*, 44-49.

16. *For recent reviews on members of the dynein superfamily, see:*

a) Oiwa, K.; Sakakibara, H. *Curr. Opin. Cell. Biol.* **2005**, *17*, 98-103;

b) Kardon, J. R.; Vale, R. D. *Nature Rev. Mol. Cell Biol.* **2009**, *10*, 854-865;

c) Walter, W. J.; Diez, S. *Nature* **2012**, *482*, 44-45.

17. *For recent reviews on members of the kinesin superfamily, see:*

a) Block, S. M. *Biophys. J.* **2007**, *92*, 2986-2995;

b) Hirokawa, N.; Nitta, R.; Okada, Y. *Nature Rev. Mol. Cell Biol.* **2009**, *10*, 877-883;

c) Verhey, K. J.; Hammond, J. W. *Nature Rev. Mol. Cell Biol.* **2009**, *10*, 765-777.

18. a) Mitchison, T.; Kirschner, M. *Nature* **1984**, *312*, 237-241;

b) Alberts, B. B., D; Lewis, J. *Moleclar Biology of the Cell;* 3 ed.; Garland Publishing Inc.: New York, London, **1994**;

c) Kozielski, F.; Arnal, I.; Wade, R. H. *Curr. Biol.* **1998**, *8*, 191-198;

d) Hirose, K.; Lowe, J.; Alonso, M.; Cross, R. A.; Amos, L. A. *Cell Struct. Funct.* **1999**, *24*, 277-284;

e) Marx, A.; Müller, J.; Mandelkow, E.-M.; Hoenger, A.; Mandelkow, E. *J. Muscle Res. Cell. Motil.* **2006**, *27*, 125-137.

19. Vale, R. D.; Reese, T. S.; Sheetz, M. P. *Cell* **1985**, *42*, 39-50.

20. a) Svoboda, K.; Schmidt, C. F.; Schnapp, B. J.; Block, S. M. *Nature* **1993**, *365*, 721-727;

b) Howard, M. *Motor Proteins and the Cytoskeleton*; Sinauer Associates, Inc.: Sunderland, **2001**;

c) Carter, N. J.; Cross, R. A. *Nature* **2005**, *435*, 308-312;

d) Carter, N. J.; Cross, R. A. *Curr. Opin. Cell Biol.* **2006**, *18*, 61-67.

21. Yildiz, A.; Selvin, P. R. *Trends Cell Biol.* **2005**, *15*, 112-120.

22. Kull, F. J. *Essays in Biochemistry*; Banting, G. H., S. J., Ed.; Portland Press: London, **2000**.

23. a) Schnitzer, M. J.; Block, S. M. *Nature* **1997**, *388*, 286-389;

b) Styer, L. B., J. M.; Tymoczko, J, L, *Biochemistry*; 5 ed.; W. H. Freeman: San Francisco, **2002**.

24. Woehlke, G.; Schliwa, M. *Nature Rev. Mol. Cell Biol.* **2000**, *1*, 50-58.

25. Hackney, D. D. *Proc. Natl Acad. Sci. U. S. A.* **1994**, *91*, 6865-6869.

26. *For discussion on the selctive binding of ATP, see:*

a) Svoboda, K.; Block, S. M. *Cell* **1994**, *77*, 773-784;

b) Yildiz, A.; Tomishige, M.; Vale, R. D.; Selvin, P. R. *Science* **2004**, *303*, 676-678.

27. Kaseda, K.; Higuchi, H.; Hirose, K. *Nature Cell Biol.* **2003**, *5*, 1079-1082.

28. *Selected articles on aspects of the motor mechanism of conventional kinesin:*

a) Howard, J.; Hudspeth, A. J.; Vale, R. D. *Nature* **1989**, *342*, 154-157;

b) Block, S. M.; Goldstein, L. S. B.; Schnapp, B. J. *Nature* **1990**, *348*, 348-352;

c) Hackney, D. D. *Nature* **1995**, *377*, 448-451;

d) Vale, R. D.; Funatusu, T.; Pierce, D. W.; Romberg, L.; Harada, Y.; Yanagida, T. *Nature* **1996**, *380*, 451-454;

e) Case, R. B.; Pierce, D. W.; Hom-Booher, N.; Hart, C. L.; Vale, R. D. *Cell* **1997**, *90*, 959-966;

f) Romberg, L.; Pierce, D. W.; Vale, R. D. *J. Cell. Biol.* **1998**, *140*, 1407-1416;

g) Thorn, K. S.; Ubersax, J. A.; Vale, R. D. *J. Cell. Biol.* **2000**, *151*, 1093-1100;

h) Yajima, J.; Alonso, M. C.; Cross, R. A.; Toyoshima, Y. Y. *Curr. Biol.* **2002**, *12*, 301-306.

29. Wade, R. H.; Hyman, A. A. *Curr. Opin. Cell Biol.* **1997**, *9*, 12-17.

30. von Delius, M.; Leigh, D. A. *Chem. Soc. Rev.* **2011**, *40*, 3656-3676.

31. The left-hand entry within the brackets indicates the leftmost foot on the track as drawn.

32. a) Carnot, S.; Clausius, R.; Thomson, W. *The second law of thermodynamics: memoirs by Carnot, Clausius and Thomson*, Harper & Brothers: New York, **1899**;

b) Davis, A. P. *Angew. Chem., Int. Ed.* **1998**, *37*, 909-910.

33. a) Onsager, L. *Phys. Rev.* **1931**, *37*, 405-426;

b) Onsager, L. *Phys. Rev.* **1931**, *38*, 2265-2279.

34. Morrissey, B. W. *J. Chem. Educ.* **1875**, *52*, 296-298.

35. a) Astumian, R. D. *Science* **1997**, *276*, 917-922;

b) Jülicher, F.; Ajdari, A.; Prost, J. *Rev. Mod. Phys.* **1997**, *69*, 1269-1282;

c) Oster, G.; Wang, H. Y. *Trends Cell Biol.* **2003**, *13*, 114-121;

d) Astumian, R. D. *Biophys. J.* **2010**, *98*, 2401-2409.

36. *Selected articles on Brownian ratchet theory:*

a) Astumian, R. D.; Derényi, I. *Eur. Biophys. J.* **1997**, *27*, 474-489;

b) Mahadevan, L.; Matsudaira, P. *Science* **2000**, *288*, 95-99;

c) Bustamante, C.; Keller, D.; Oster, G. *Acc. Chem. Res.* **2001**, *34*, 412-420;

d) Reimann, P. *Phys. Rep.* **2002**, *361*, 57-265.

37. *For examples of rotaxane-based energy ratchets, see:*

a) Chatterjee, M. N.; Kay, E. R.; Leigh, D. A. *J. Am. Chem. Soc.* **2006**, *128*, 4058-4073;

b) Crowley, J. D.; Leigh, D. A.; Lusby, P. J.; McBurney, R. T.; Perret-Aebi, L.-E.; Petzold, C.; Slawin, A. M. Z.; Symes, M. D. *J. Am. Chem. Soc.* **2007**, *129*, 15085-15090;

c) Leigh, D. A.; Lusby, P. J.; McBurney, R. T.; Symes, M. D. *Chem. Commun.* **2010**, *46*, 2382-2384.

38. *For examples of rotaxane-based information ratchets, see:*

a) Serrelli, V.; Lee, C.-F.; Kay, E. R.; Leigh, D. A. *Nature* **2007**, *445*, 523-527;

b) Alvarez-Perez, M.; Goldup, S. M.; Leigh, D. A.; Slawin, A. M. Z. *J. Am. Chem. Soc.* **2008**, *130*, 1836-1838;

(c) Carlone, A.; Goldup, S. M.; Lebrasseur, N.; Leigh, D. A.; Wilson, A. *J. Am. Chem. Soc.* **2012**, *14*, 8321-8323.

39. a) von Delius, M.; Geertsema, E. M.; Leigh, D. A. *Nature Chem.* **2010**, *2*, 96-101;

b) von Delius, M.; Geertsema, E. R.; Leigh, D. A.; Tang, T. D. *J. Am. Chem. Soc.* **2010**, *132*, 16134-16145.

40. a) Campaña, A. G.; Carlone, A.; Chen, K.; Dryden, D. T. F.; Leigh, D. A.; Lewandowska, U.; Mullen, K. M. *Angew. Chem., Int. Ed.* **2012**, *51*, 5480-5483;

b) Kovaříček, P.; Lehn, J.-M. *J. Am. Chem. Soc.* **2012**, *134*, 9446-9455.

41. Bissell, R. A.; Cordova, E.; Kaifer, A. E.; Stoddart, J. F. *Nature* **1994**, *369*, 133-137.

42. *Selected reviews on the field of molecular machines:*

a) Balzani, V.; Credi, A.; Raymo, F. M.; Stoddart, J. F. *Angew. Chem., Int. Ed.* **2000**, *39*, 3349-3391;

b) Pease, A. R.; Jeppesen, J. O.; Stoddart, J. F.; Luo, Y.; Collier, C. P.; Heath, J. R. *Acc. Chem. Res.* **2001**, *34*, 433-444;

c) Raehm, L.; Sauvage, J.-P. *Molecular machines and motors based on transition metal-containing catenanes and rotaxanes*, vol. 99; Springer-Verlag: Berlin, **2001**;

d) Balzani, V. V., M.; Credi, A. *Molecular Devices and Machines - A Journey into the Nanoworld*, Wiley VCH: Weinheim, **2003**;

e) Bonnet, S.; Collin, J.-P.; Koizumi, M.; Mobian, P.; Sauvage, J.-P. *Adv. Mater.* **2006**, *18*, 1239-1250.

43. *For other examples of rotary molecular motors, see:*
Geertsema, E. M.; van der Molen, S. J.; Martens, M.; Feringa, B. L. *Proc. Natl. Acad. Sci. U. S. A.* **2009**, *106*, 16919-16924 and references therein.

44. *Selected examples of translational motion in interlocked species:*

a) Benniston, A. C.; Harriman, A. *Angew. Chem., Int. Ed.* **1993**, *32*, 1459-1461;

b) Collin, J.-P.; Dietrich-Buchecker, C.; Gaviña, P.; Jimenez-Molero, M. C.; Sauvage, J.-P. *Acc. Chem. Res.* **2001**, *34*, 477-487;

c) Altieri, A.; Bottari, G.; Dehez, F.; Leigh, D. A.; Wong, J. K. Y.; Zerbetto, F. *Angew. Chem., Int. Ed.* **2003**, *42*, 2296-2300;

d) Létinois-Halbes, U.; Hanss, D.; Beierle, J. M.; Collin, J.-P.; Sauvage, J.-P. *Org. Lett.* **2005**, *7*, 5753-5756;

e) Durola, F.; Sauvage, J.-P. *Angew. Chem., Int. Ed.* **2007**, *46*, 3537-3540;

f) Collin, J.-P.; Durola, F.; Lux, J.; Sauvage, J.-P. *Angew. Chem., Int. Ed.* **2009**, *47*, 8532-8535;

g) Tokunaga, Y.; Kawabata, M.; Matsubara, N. *Org. Biomol. Chem.* **2011**, *9*, 4948-4953.

45. a) Shin, J.-S.; Pierce, N. A. *J. Am. Chem. Soc.* **2004**, *126*, 10834-10835;

b) Yin, P.; Yan, H.; Daniell, X. G.; Tuberfield, A. J. *Angew. Chem., Int. Ed.* **2004**, *43*, 4906-4911;

c) Bath, J.; Green, S. J.; Tuberfield, A. J. *Angew. Chem., Int. Ed.* **2005**, *44*, 4358-4361;

d) Kelly, T. R. *Angew. Chem., Int. Ed.* **2005**, *44*, 4124-4127;

e) Tian, Y.; He, Y.; Chen, Y.; Yin, P.; Mao, C. *Angew. Chem., Int. Ed.* **2005**, *44*, 4355-4358;

f) Green, S. J.; Bath, J.; Tuberfield, A. J. *Phys. Rev. Lett.* **2008**, *101*, 238101;

g) Omabegho, T.; Sha, R.; Seeman, N. C. *Science* **2009**, *324*, 67-71;

h) Gu, H.; Chao, J.; Xiao, S.-J.; Seeman, N. C. *Nature* **2010**, *465*, 202-205;

i) Lund, K.; Manzo, A. J.; Dabby, N.; Michelotti, N.; Johnson-Buck, A.; Nangreave, J.; Taylor, S.; Pei, R.; Stojanovic, M. N.; Walter, N. G.; Winfree, E.; Yan, H. *Nature* **2010**, *465*, 206-211;

j) Wang, Z.-G.; Elbaz, J.; Willner, I. *Nano Lett.* **2011**, *11*, 304-309;

k) Wang, C.; Ren, J.; Qu, X. *Chem. Commun.* **2012**, *47*, 1428-1430;

l) You, M. X.; Chen, Y.; Zhang, X.; Liu, H.; Wang, R.; Wang, K.; Williams, K. R.; Tan, W. *Angew. Chem., Int. Ed.* **2012**, *51*, 2457-2460.

46. *Selected examples of synthetic small-molecules capable of "walking", which lack directionality of processivity:*

a) Mitra, S.; Lawton, R. G. *J. Am. Chem. Soc.* **1979**, *101*, 3097-3110;

b) Johnson, L. K.; Killian, C. M.; Brookhart, M. *J. Am. Chem. Soc.* **1995**, *117*, 6414-6415;

c) Kwon, K.-Y.; Wong, K. L.; Pawin, G.; Bartels, L.; Stolbov, S.; Rahman, T. S. *Phys. Rev. Lett.* **2005**, *95*, 166101;

d) Weinmann, D. P.; Winkler, H. D. F.; Falenski, J. A.; Koksch, B.; Schalley, C. A. *Nature Chem.* **2009**, *1*, 573-577;

e) Winkler, H. D. F.; Weinmann, D. P.; Springer, A.; Schalley, C. A. *Angew. Chem., Int. Ed.* **2009**, *48*, 7246-7250;

f) Tkachov, R.; Senkovskyy, V.; Komber, H.; Sommer, J.-U.; Kiriy, A. *J. Am. Chem. Soc.* **2010**, *132*, 7803-7810;

g) Perl, A.; Gomez-Casado, A.; Thompson, D.; Dam, H. H.; Jonkheijm, P.; Reinhoudt, D. N.; Huskens, J. *Nature Chem.* **2011**, *3*, 317-322.

47. von Delius, M.; Barrell, M. J.; Campaña, A. G.; Geertzema, E. M.; Leigh, D. A. *Angew. Chem., Int. Ed.* **2011**, *50*, 285-290.

Chapter II

Controlled Stepping of a Bimetallic Palladium(II)/Platinum(II)-Based Molecular Biped

Acknowledgements

The work presented in this chapter was born out of a larger project on which the author worked with Dr Victor Blanco, Dr Jonathon E. Beves, Dr Barry A Blight, Dr Romen Carrillo, Dr Daniel M. D'Souza and Dr Mark D. Symes, all of whom are gratefully recognised for their efforts. Prof. Alexandra M. Z. Slawin is acknowledged for solving the crystal structures presented herein.

2.1 Synopsis

Building on the generic design principles laid out in Chapter I, novel methods of practically instilling directional stepping mechanisms into chemical walker-track systems were explored. In this chapter the design, synthesis, characterisation, and operation of a bimetallic molecular biped is described. It comprises a three-foothold track upon which a palladium(II) complex can be selectively stepped between 4-dimethylaminopyridine and pyridine ligand sites via reversible protonation whilst remaining attached to the track by means of a kinetically inert platinum(II) complex throughout. The substitution pattern of the three ligand binding sites and the kinetic stability of the metal-ligand coordination bonds afford the two positional isomers a high degree of metastability and mean that altering the chemical state of the track does not automatically instigate stepping in the absence of an additional stimulus (heat in the presence of a coordinating solvent). This enables the track to do work on the biped unit and ultimately drive it away from equilibrium by means of an energy ratchet mechanism.

2.2 Introduction

Although transition metal coordination motifs have been widely employed as molecular switches and devices[1] where redox-,[2] chemical-,[3] or photo-stimulation[4] have been used effectively to direct molecular structure and function, the application of metal-ligand interactions to induce controlled molecular-level motion away from equilibrium[1,5] has been far less widely reported. Apart from the interim use of zinc(II) ions to instigate conformational change in a single stroke of a rotary motor,[3e] examples of genuine molecular ratchets involving metal-ligand bonds have been limited to interlocked stimuli-switchable molecular shuttles[6] in which a thread can be manipulated to translocate a submolecular component energetically uphill and subsequently reset without undoing the task performed.[5] Such a facet grants these systems a higher degree of sophistication than that of simple dynamic switches.[1,7] However, the interlocked nature of the designs confines the molecular motion to a single dimension constraining not only the relative movement of the components, but also the achievable ambitions of the machines. For instance, a moveable macrocycle mechanically linked to a thread cannot select between branches or manoeuvre junctions within that thread without breaking covalent bonds. Whilst an interlocked approach can still yield systems capable of doing work on a substrate,[5] there are only limited examples of *bona fide* molecular motors synthesized in this way[8] as such an accolade requires the potential for repetitive operation. The fulfilment of said requisite depends upon the presence of an escapement (a means of releasing the ratcheted substrate) so that the entire system can be reset and operated again without undoing the previously performed task. Escapement is inherently difficult in interlocked architectures and is usually only achieved when the subject of the operation upon which the work is being done is either part of a separate entity,[9] or in a cyclic system such as a catenane.[8]

In order to match the growing fervour for building molecular machines with greater scope for applications beyond one-dimensional motion, there is a requirement to move away from interlocked species towards designs with more degrees of freedom. Metal-ligand bonding is set to be a powerful tool in this progression as it provides a potential conduit to compartmental control over individual submolecular components. Facile manipulation of binding kinetics may facilitate the transportation pathways of ratcheting and escapement in the design of complex molecular motors, both in the

established rotary field,[3e,8,10] and the relatively new area of linear motors including synthetic molecular walkers.[11]

This chapter chronicles the assembly and operation of a molecular energy ratchet based on a tethered bimetallic transition metal complex where palladium(II) and platinum(II) complexes function as opposing feet on a poly-pyridyl track comprising three distinct ligand binding sites (footholds). The palladium(II) complex can be selectively stepped between vacant footholds by acid-base manipulations using the kinetically inert platinum(II) complex as a pivot. In so doing, this non-interlocked species can be driven energetically uphill and ultimately fixed into a thermodynamically unfavourable positional isomer distribution without permanently altering the state of the footholds, thus constituting the efficient metal-mediated stepping of a molecular biped along a track.

2.3 Complex Design and Selective Addressability

The palladium(II) complex is based upon a motif previously used to organise tridentate pyridine 2,6-dicarboxamide and derivatised monodentate pyridine ligands about a square planar palladium(II) centre in the assembly of catenanes,[12] rotaxanes[13] and molecular shuttles.[6] This *N,N,N*-pincer complex is particularly attractive due to the stability afforded by the chelate effect, ensuring the metal ion remains bound at all times by the tridentate ligand with only one binding site available for monodentate ligand substitution[14] and the maintenance of an overall neutral system throughout. The design shown in Figure 2.1 exploits the preference of this class of palladium(II) and platinum(II) complexes to selectively bind *N*-heterocycles as a function of basicity[6,15] enabling their thermodynamic bias towards different ligands to be controlled by acid-base manipulations. The palladium(II) complex can therefore be stepped back and forth between a 4-dimethylaminopyridine (DMAP) and a pyridine (Py) foothold by means of protonation/deprotonation and thermal activation. Throughout this process the palladium(II) foot remains tethered to the track *via* the opposing platinum(II) complex, which has a considerably higher kinetic stability under the stepping conditions. The substitution pattern of the pyridine derivatives and the kinetic stability of the metal-ligand bonds mean that altering the chemical state of the track by adding or removing protons does not automatically cause a change in the positional isomer distribution in the absence of an additional stimulus (heat in the presence of a coordinating solvent).

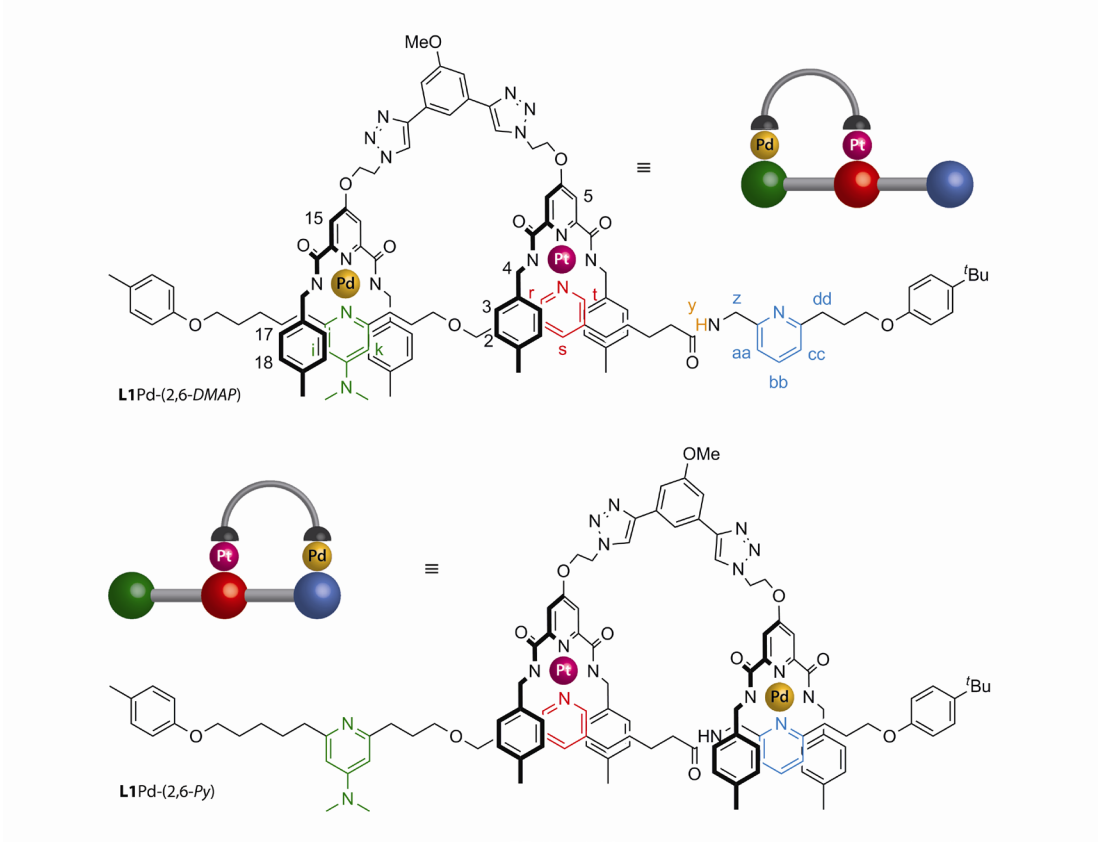

Figure 2.1 *- Two metastable positional isomers of the bimetallic biped:* ***L1****Pd-(2,6-DMAP)*[16] *and* ***L1****Pd-(2,6-Py).*

Operational control over discrete, well-defined stepping mechanisms is a prerequisite in the design of extended molecular walker systems based upon alternating stimuli-induced directional stepping[17] and can be achieved through careful consideration of the thermodynamics and kinetics of each step. For the present design, the effect of varying the substitution patterns of Py and DMAP ligands on the stabilities of their respective metal complexes was investigated.

In simple exchange experiments analogous to previous studies with macrocyclic palladium(II) complexes,[6a] **L2**Pd- could be selectively switched between 2,6-dihexylPy and 2,6-dihexylDMAP ligands by the addition of acid or base in the presence of a coordinating solvent, as shown in Scheme 2.1a and 2.1b. All **L2**Pd-2,6-disubstituted complexes were shown to be stable at both ambient and elevated temperature (338 K) in the non-coordinating solvent $CDCl_3$. Conversely, some exchange of the monodentate ligands was observed in these reactions when carried out in neat CD_3CN at room temperature (See Experimental Section (ES), Figure 2.7), allowing the solvent mixture to be adjusted to manipulate the exchange kinetics.

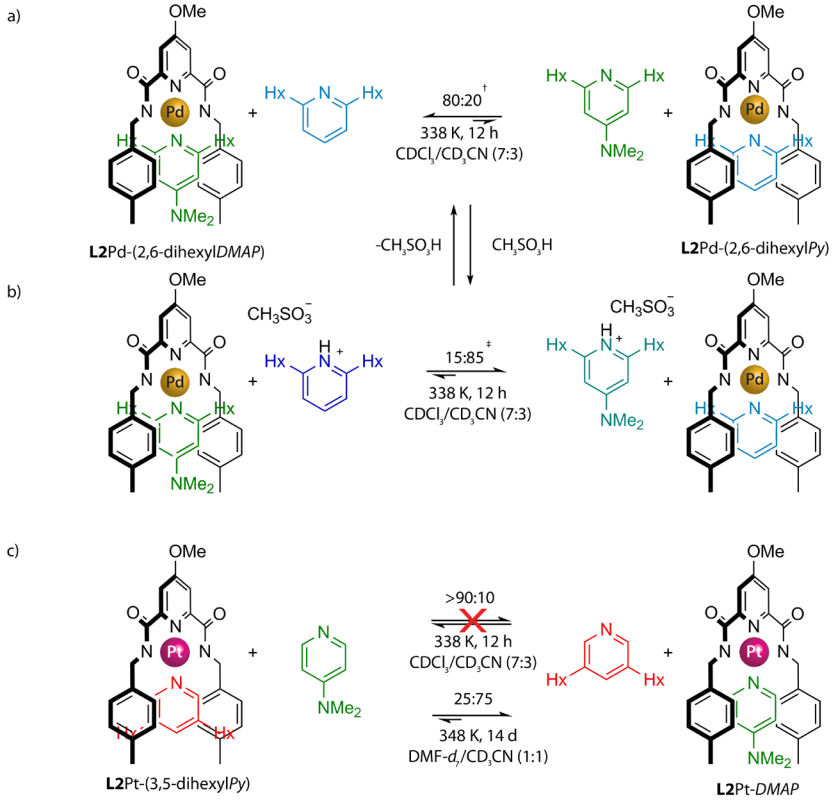

Scheme 2.1 *- Reversible exchange of monodentate ligands[18] in* ***L2****Pd-complexes and the kinetic stability of* ***L2****Pt-complexes in* $CDCl_3/CD_3CN$ *(7:3) at 338 K: (a) neutral conditions; (b) in the presence of* CH_3SO_3H *(1 equiv). Times required to reach equilibrium: † 12 h; ‡ 40 h. No exchange of 2,6-dihexylheterocyclic ligands was observed in* $CDCl_3$ *under neutral conditions or in the presence of* CH_3SO_3H*, even at 338 K for 2 days; (c) did not reach equilibrium after 12 h in which time <10% exchange of 2,6-dihexylPy for DMAP was observed. Equilibrium was reached after 14 days in DMF-*d_7*/*CD_3CN *(1:1) at 348 K.*

Switchable kinetic control is imperative to the proposed ratchet mechanism,[5] and an optimised solvent mixture of $CDCl_3/CD_3CN$ (7:3) was used where all 2,6-disubstituted complexes in Scheme 2.1 were shown to be kinetically inert at ambient temperature (stimulus OFF state). However, upon heating at 338 K (stimulus ON state), 80% of the 2,6-dihexylPy coordinated to **L2**Pd was exchanged for 2,6-dihexylDMAP (Scheme 2.1a) within 12 h on account of the latter's superior binding ability.[19] This process could be reversed (Scheme 2.1b) by adding one equivalent of methanesulfonic acid, where the inverted selectivity is defined by the relative basicities of the two heterocycles.[20] Although palladium(II) complexes of 3,5-disubstituted pyridines were thermodynamically preferred to the 2,6-disubstituted analogues (ES Figure 2.6), their lability in the absence of the external stimuli renders them unsuitable for use as feet in a molecular walker system (ES Figure 2.7).

The analogous platinum(II) complex **L2**Pt-(3,5-dihexyl*Py*) showed a similar superior thermodynamic preference for unsubstituted DMAP over Py (See Chapter III, Figure 3.2), although the kinetic stability of the 3,5-disubstituted pyridine complex in $CDCl_3/CD_3CN$ (7:3) was sufficient for it to be considered relatively inert under the palladium(II) stepping conditions (<10% exchange after 12 h at 338 K) (Scheme 2.1c). Additionally, the steric hindrance of 2,6-dihexylPy was found to prevent any observable coordination to platinum(II) centres, enabling **L2**Pt- complexes to perfectly discriminate between 2,6- and 3,5-disubstituted pyridines.

The results indicated that a tethered palladium(II) complex could be made to step along a track whilst maintaining a high degree of processivity[17] (that is, a constant attachment to the track) through linkage to a fixed opposing foot. In this first example, a platinum(II) complex is employed as an inert foot-foothold pivot motif in a model for a bimetallic molecular walker with the potential for future development of orthogonal stimuli capable of independently operating a second foot.

2.4 Synthesis and Characterisation of Tethered Bimetallic Transition Metal complex L1Pd-(2,6-*DMAP*)

Bimetallic complex **L1**Pd-(2,6-*DMAP*) was achieved by a compartmentalised strategy. The key reactions of the synthetic route for the feet and foothold sub-components are shown in Scheme 2.2 and the final assembly of the complete machine is illustrated in Scheme 2.3. Comprehensive synthetic details are given in Experimental Section 2.8.

Component **18** was prepared in 42% overall yield *via* a series of Sonogashira cross-coupling reactions[21] starting from 2,6-diiodo-4-dimethylaminopyridine (**1**), 3,5-dibromopyridine (**4**) and suitable alkyne building blocks (**2** & **5**), using standard conditions as well as TMS deprotection of **6** with tetrabutylammonium fluoride and subsequent hydrogenation of the alkyne groups with $Pd(OH)_2/C$. The final foothold of the track, compound **9**, was prepared through Boc protection of 6-iodopyridin-2-ylmethylamine (**7**) prior to Sonogashira coupling with alkyne **8**, hydrogenation, and finally Boc-removal using trifluoroacetic acid. Hydrolysis of the methyl ester group of **18** using LiOH, and subsequent PyBroP mediated amide coupling with **9** afforded the free three-foothold track **19** (Scheme 2.3b).

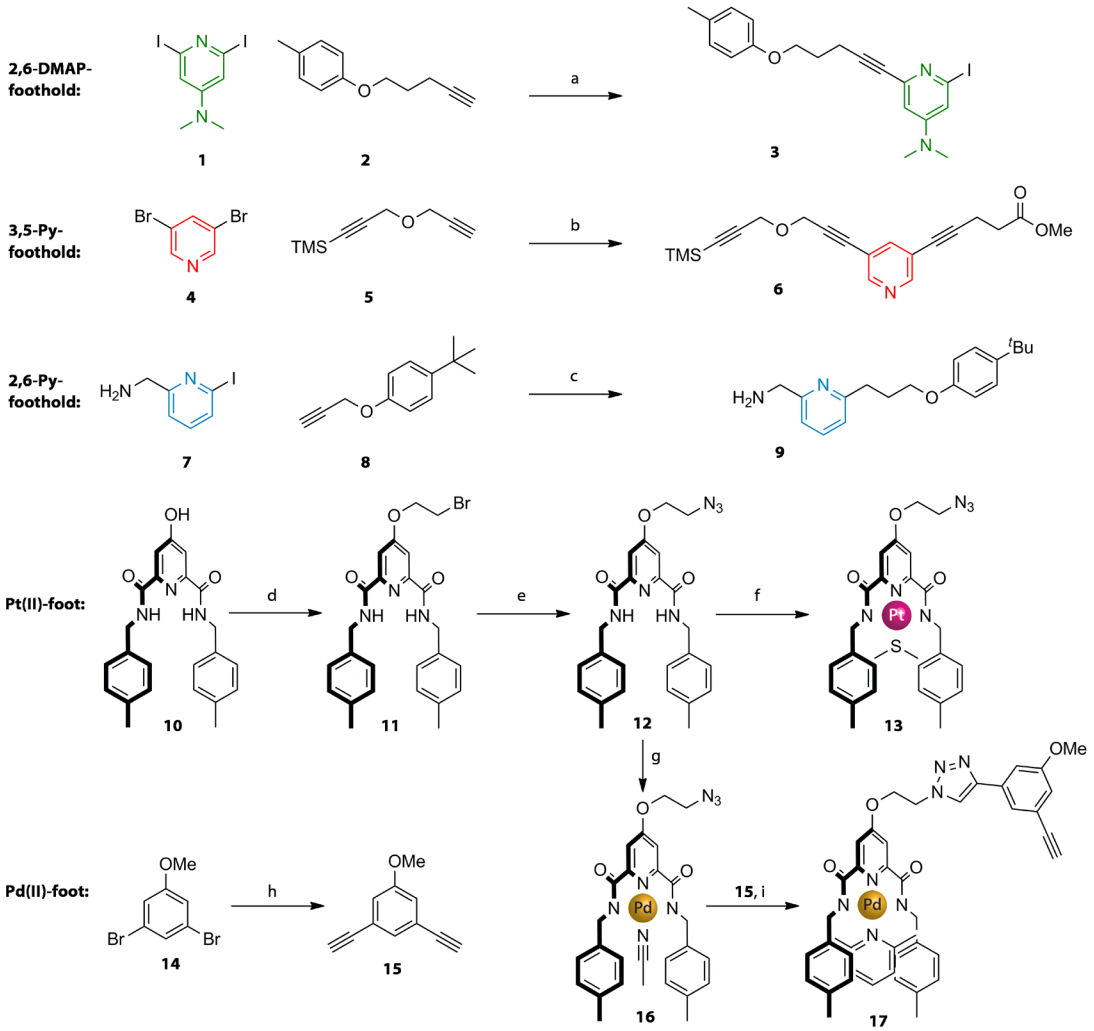

Scheme 2.2 *- Synthesis of subcomponents. Reagents and conditions: (a) $PdCl_2(PPh_3)_2$, CuI, Et_3N/THF, 56%; (b) (i)* ***5****, $PdCl_2(PPh_3)_2$, CuI, Et_3N/THF, 85%, (ii) methyl-4-pentynoate, $PdCl_2(PPh_3)_2$, CuI, Et_3N/THF, 71%; (c) (i)* ***7****, Boc_2O, CH_2Cl_2, 97%, (ii)* ***8****, $Pd(PPh_3)_4$, CuI, Et_3N/THF, 88%, (iii) H_2, $Pd(OH)_2$/C, K_2CO_3, THF, 98%, (iv) CF_3COOH, $CHCl_3$, 96%; (d) 1,2-dibromoethane, K_2CO_3, acetone, 72%; (e) NaN_3, NaI, DMF, 81%; (f) NaH, $PtCl_2(SMe_2)_2$, THF, 64%; (g) $Pd(OAc)_2$, CH_3CN, 84%; (h) i) trimethylsilylacetylene, $PdCl_2(PPh_3)_2$, CuI, THF/Et_3N, (ii) KOH, MeOH, 94%; (i) (i) 2,6-lutidine, CH_2Cl_2 (ii)* ***15****, DIPEA, $Cu(CH_3CN)_4{\cdot}PF_6$, TBTA, 80% (from* ***12****).*

The metal complexes were prepared from the common pyridine-2,6-dicarboxamide unit **12**, obtained in two steps by Williamson etherification and subsequent azide S_N2 displacement from **10** (Schemes 2.2d & 2.2e). The platinum(II) moiety required deprotonation of the amide groups of **12** with NaH in THF and subsequent reaction with $PtCl_2(SMe_2)_2$ to yield the dimethylsulfide-platinum(II) complex **13** (Scheme 2.2f). Selective coordination of this complex to the preferred central foothold on track **19** was achieved by simply stirring an equimolar solution of the two components, exploiting the preference of the Pt(II) complex for the 3,5-substitution pattern (Scheme 2.3c).

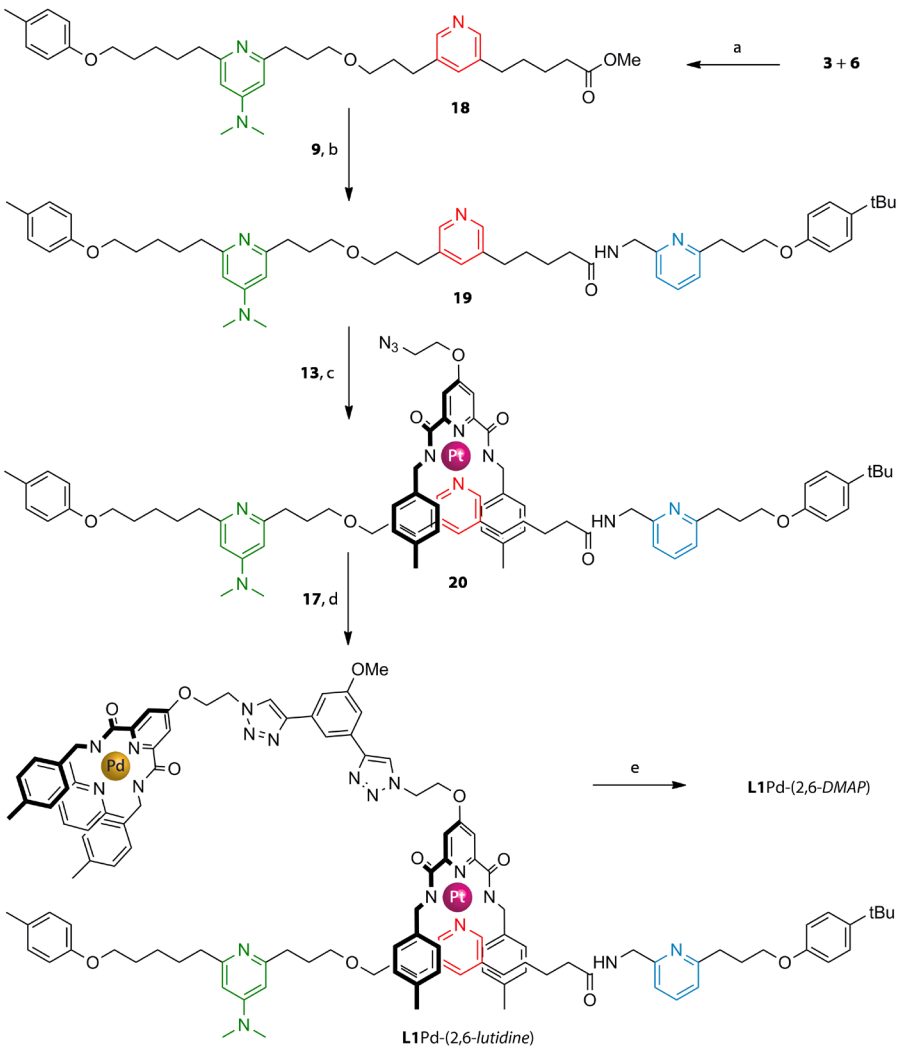

Scheme 2.3 *- Synthesis of Bimetallic Complex* ***L1****Pd-(2,6-DMAP). Reagents and conditions: (a) (i)* ***6****, TBAF, THF/H_2O (9:1), 95%; (ii) $Pd(PPh_3)_4$, CuI, Et_3N/THF, 86%, (iii) H_2, $Pd(OH)_2$/C, K_2CO_3, THF, 78%; (b) (i) LiOH, MeOH/H_2O/THF, 97%. (ii)* ***9****, PyBroP, DIPEA, DMF, 86%; (c)* ***13****, DMF, 62%; (d)* ***17****, DIPEA, $Cu(CH_3CN)_4{\cdot}PF_6$, TBTA, 85%; (e) $CHCl_3/CH_3CN$ (7:3), 76%.*

Palladium(II) complex **16** was prepared through reaction of pyridine-2,6-dicarboxamide **12** with palladium(II) acetate in CH_3CN for 16 h to give the product as a yellow precipitate (Scheme 2.2g), which was converted in one pot to **17** in 80% yield (Scheme 2.2i) by complexation to 2,6-lutidine in CH_2Cl_2 and subsequent copper(I)-catalyzed azide-alkyne Huisgen cycloaddition[22] (CuAAC) using 5 equivalents of dialkyne **15** (*N,N*-diisopropylethylamine (DIPEA), $Cu(CH_3CN)_4{\cdot}PF_6$, *tris*[(1-benzyl-1H-1,2,3-triazol-4-yl)methyl]amine (TBTA), 12 h). This key reaction established the applicability of versatile CuAAC "click" chemistry in the presence of palladium(II) complexes of the type used in this study. The following step was considerably more

demanding as it required the coupling of palladium(II) and platinum(II) precursors (**17**, and **20** respectively) using the established CuAAC "click" reaction in addition to selective intramolecular coordination of the palladium(II) centre to the preferred *N*-heterocycle binding site. To achieve this, an equimolar mixture of **17** and **20** was subjected to adjusted Huisgen cycloaddition conditions to afford bimetallic intermediate **L1**Pd-(2,6-*lutidine*) demonstrating that CuAAC "click" reactions are practical synthetic ligation tools in the presence of transition metal complexes and multiple metal binding sites (Scheme 2.3d), despite the potential for pyridines to bind Cu(I). Adjusting the reaction concentration to favour intramolecular coordination of the 2,6-DMAP foothold, **L1**Pd-(*2,6-lutidine*) was subjected to the optimised conditions used in the model exchange experiments ($CHCl_3$/CH_3CN (7:3), 0.16 mM, 338 K, 14 h, Scheme 2.1a) exploiting both the disparate ligand strengths of the free 2,6-lutidine and the 2,6-DMAP/Py footholds of the track, as well as the kinetic stability of the Pt-(3,5-*Py*) complex, to form bimetallic complex **L1**Pd in a remarkable 76% yield after silica column chromatography purification (Scheme 2.3e). Electrospray mass spectrometry confirmed the isolated product constitution as **L1**Pd with mass peaks at *m/z* = 2225.6 and 2247.9 corresponding to the $[M+H]^+$ and $[M+Na]^+$ ions respectively with isotopic distributions concordant with theoretical predictions.

In order to further explore the potential of this approach in building multi-foothold synthetic molecular walkers, an alternative incremental route was also attempted using bimetallic transition metal complex **21** (Figure 2.2) as a core scaffold for extended systems.[23] Such a convergent strategy would not only allow for compartmental extension of the track, but also provide the basis for branched systems through the addition of a range of different footholds. Ultimately, difficulties in hydrolysis of the methylester in the presence of the palladium(II) complex, along with the demonstrated ease of selective attachment of platinum(II) to the central foothold of track **19** resulted in this route being abandoned for the large scale preparation of the complete machine **L1**Pd-(2,6-*DMAP*).[24] The method did, however, provide invaluable information allowing for unambiguous ^1H NMR assignment that confirmed the bimetallic structure as **L1**Pd-(2,6-*DMAP*) through comparison of spectral data (ES Figure 2.12).

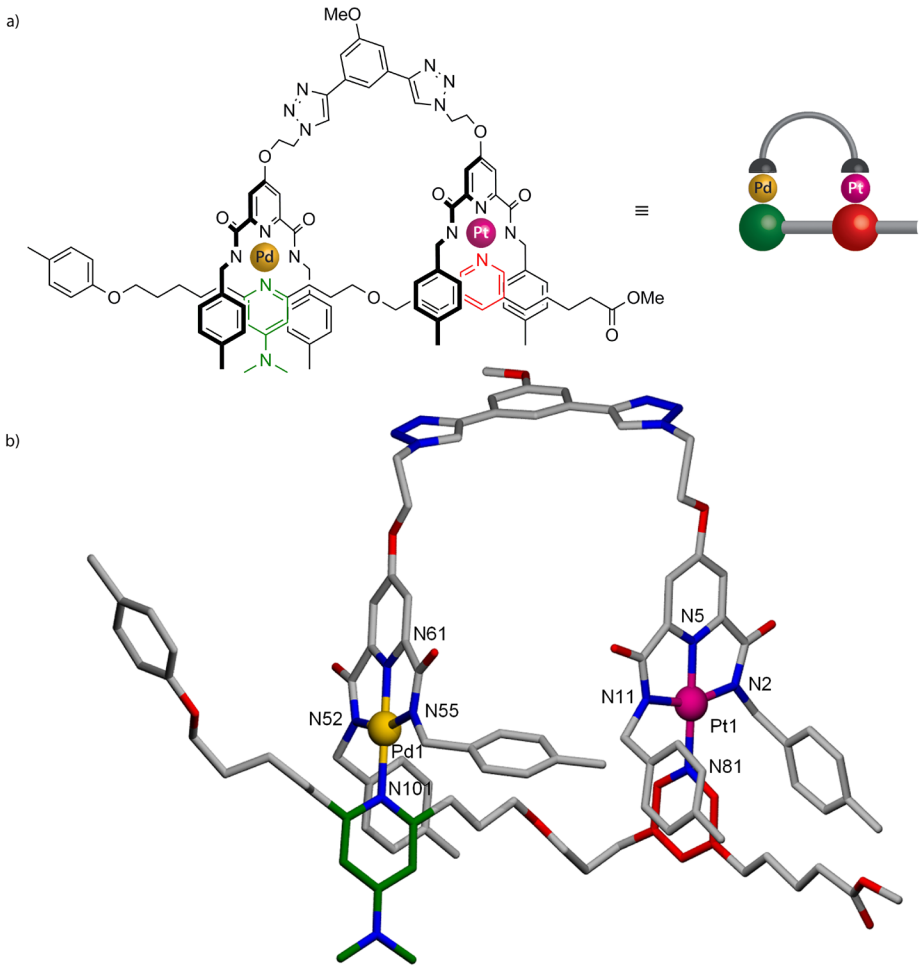

Figure 2.2 *- Graphic representations of bimetallic complex* ***21****. Hydrogen and deuterium atoms are omitted for clarity: (a) chemical structure; (b) X-ray crystal structure. Solvent molecules are omitted for clarity. Nitrogen atoms are shown in blue, oxygen atoms in red, the palladium atom in gold, the platinum atom in pink and carbon atoms in grey (DMAP and pyridine carbon atoms are shown in green and red respectively). Selected bond lengths (Å) and angles (°): Pd1–N52, 2.027; Pd1–N55, 1.939; Pd1–N61, 2.034; Pd1–N101, 2.113; Pt1–N2, 2.021; Pt1–N5, 1.925; Pt1–N11, 2.027; Pt1–N81, 2.043; N52–Pd1–N61, 160.3; N11–Pt1–N2, 160.6; N55–Pd1–N101, 178.1; N5–Pt1–N81, 179.0.*

Slow evaporation of a solution of bimetallic complex **21** in $CHCl_3$/EtOH afforded suitable single crystals for X-ray diffraction analysis.[25] The solid-state structure confirms the coordination of the palladium(II) moiety to the DMAP foothold. All metal-ligand bonds lie within the expected ranges and are similar for both the palladium(II) and the platinum(II) complexes with a distorted square-planar coordination geometry observed for each of the metal centres (Figure 2.2b). The tolyl rings of the dicarboxamide motifs do not participate in π-π-stacking with the DMAP or Py footholds of the track, instead adopting a similar conformation to those observed previously in analogous macrocyclic ligands.[6a,13a] The 3,5-ditriazoloanisole linker unit is almost

coplanar with the three central hydrogen atoms engaged in intermolecular hydrogen-bond interactions with the oxygen atom of a carbonyl group of an adjacent palladium(II)-containing motif ([C–H···O] distances 2.38, 2.39 and 2.39 Å).

^{1}H NMR spectroscopy of the isolated complex **L1**Pd (Figure 2.3b) revealed a single positional isomer with the palladium(II) complex of the biped coordinated solely to the 2,6-DMAP-foothold, analogous to compound **21**. A comparison between the spectra of free track **19** (Figure 2.3a) and **L1**Pd-(2,6-*DMAP*) in CD_2Cl_2 shows the expected upfield shifts of the signals of both the 2,6-DMAP- ($\Delta\delta H_i$ = –0.20 ppm and $\Delta\delta H_k$ = –0.18 ppm), and the 3,5-Py-groups ($\Delta\delta H_r$ = –0.88 ppm, $\Delta\delta H_s$ = –0.29 ppm and $\Delta\delta H_t$ = –0.45 ppm), while the resonances of the 2,6-Py-foothold ($H_{aa\text{-}cc}$), and those relating to the adjacent methylene (H_z) occur at almost identical values in both species.

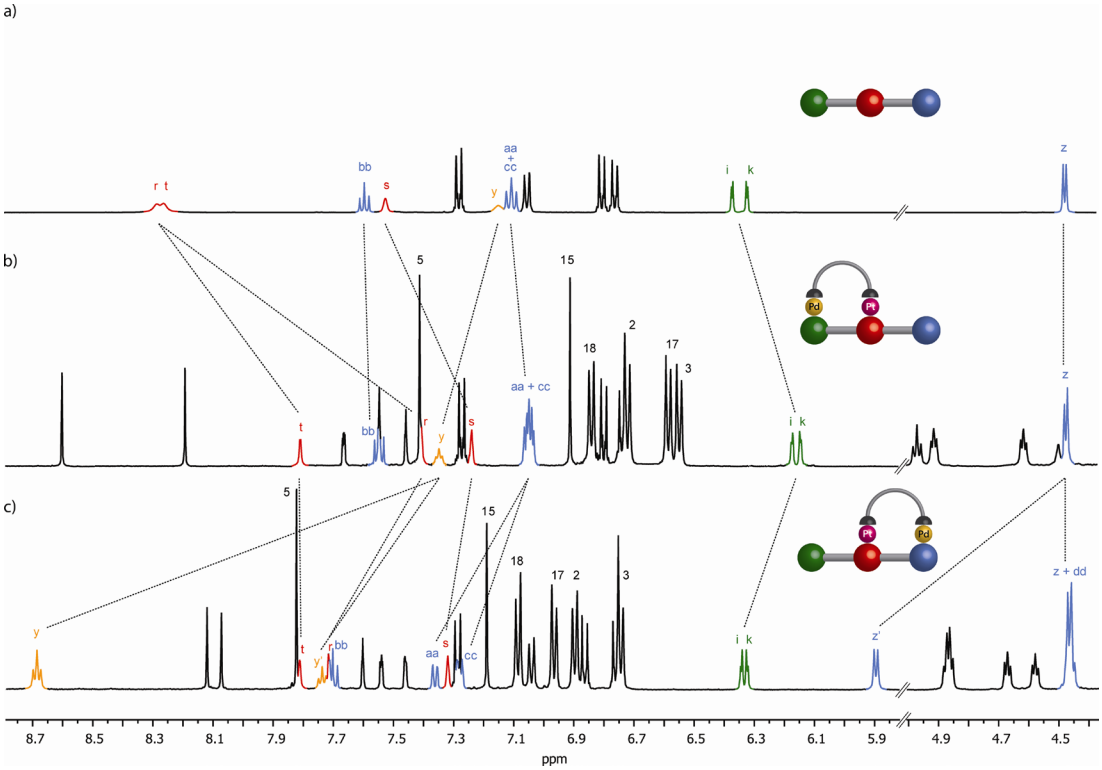

Figure 2.3 *- ^{1}H NMR spectra (500 MHz, CD_2Cl_2, 298K) of the two positional isomers of the bimetallic complex **L1**Pd and the free track for comparison: (a) track **19**; (b) **L1**Pd-(2,6-DMAP); (c) **L1**Pd-(2,6-Py). The lettering in the figure refers to the assignments in Figure 2.1.*

2.5 Protonation-Driven Stepping

In accordance with model studies, in the absence of acid, the palladium(II) complex of **L1**Pd-(2,6-*DMAP*) can be classified as thermodynamically stable when heated in $CDCl_3/CD_3CN$ (7:3) at 338 K.[26] Furthermore, upon addition of 1 equivalent of methanesulfonic acid to a pure sample at room temperature, the ^1H NMR spectrum showed significant broadening in the 2,6-Py resonances ($H_{aa\text{-}cc}$) but no discernable change in either the 2,6-DMAP ($H_{i\text{-}k}$), nor the 3,5-Py signals ($H_{r\text{-}t}$), indicating that protonation of the 2,6-Py foothold had occurred but no positional isomerisation had taken place. No changes were observed after 30 h at room temperature, indicating that the transition metal complexes are kinetically locked in the presence of acid under ambient conditions. In fact, stepping of the palladium(II) complex was only observed at 338 K in the presence of 1 equivalent of acid (Scheme 2.4). The operation was monitored by ^1H NMR spectroscopy and shown to reach equilibrium within 40 h, after which no further exchange was observed, indicating that a thermodynamic minimum had been reached. The reaction mixture was diluted with toluene by a factor of two and the solvents removed gradually under reduced pressure to ensure a consistently low concentration of the machine with respect to the coordinating solvent, CH_3CN.[27] The crude residue was deprotonated (K_2CO_3, CH_2Cl_2, 30 min) and the sample analysed by ^1H NMR and high-performance liquid chromatography (HPLC) to reveal an equilibrium 15:85 distribution of **L1**Pd-(2,6-*DMAP*):(2,6-*Py*) (ES Figure 2.14).

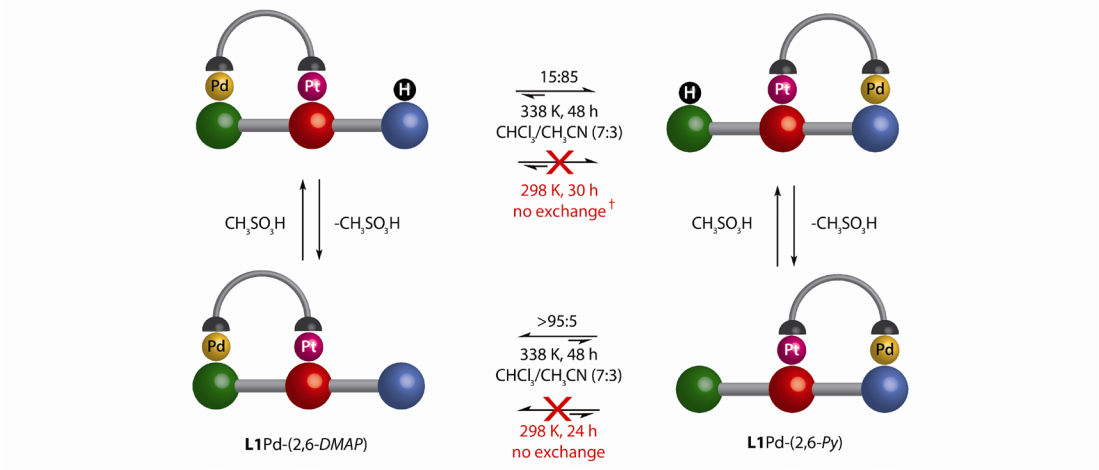

Scheme 2.4 *- Stepping of Pd(II)/Pt(II)-Complexed Molecular Biped. † No exchange after 30 h at 298 K in $CDCl_3/CD_3CN$ (7:3) with CH_3SO_3H (1 equiv), <5% exchange in $CDCl_3/CD_3CN$ after 30 h at 338 K. ‡ No exchange observed after 24 h at 298 K in $CDCl_3/CD_3CN$ (7:3).*

The neutral positional isomers obtained were readily separated by preparative thin layer chromatography to give pure, kinetically stable samples of both **L1**Pd-(2,6-*Py*) (major product) and **L1**Pd-(2,6-*DMAP*) (minor product). The ^{1}H NMR spectrum of the former is shown in Figure 2.3c, while the latter matches that of **L1**Pd-(2,6-*DMAP*) precisely. After operation, the resonances of the 2,6-DMAP-foothold (H_{i+k}) were found to have shifted downfield ($\Delta\delta H_i$ = 0.17 ppm and $\Delta\delta H_k$ = 0.18 ppm) resembling the non-complexed 2,6-DMAP-foothold in free track, **19** (Figure 2.3a). Similarly, the 2,6-Py signals (H_{aa-cc}) show shifts ($\Delta\delta H_{aa}$ = 0.31 ppm, $\Delta\delta H_{bb}$ = 0.16 ppm and $\Delta\delta H_{cc}$ = 0.24 ppm) in accordance with the equivalent resonances in the model exchange experiment (Scheme 2.1b & ES Figure 2.9 for NMR). Interestingly, upon enclosing the amide bond of the track within the macrocycle of **L1**Pd-(2,6-*Py*), two separate signals can be seen for both the amide proton ($H_{y/y'}$), and the adjacent methylene protons ($H_{z/z'}$) as a result of the *cis*/*trans*-amide isomers (H_{y+z}, major isomer, $H_{y'+z'}$, minor isomer). Using variable temperature ^{1}H NMR ($C_2D_2Cl_4$, 378 K), these two pairs of resonances were shown to coalesce. Electrospray mass spectrometry of the product showed identical peaks
(*m/z* = 2226.0 $[M+H]^+$ and 2248.0 $[M+Na]^+$) with matching isotopic distribution to those observed for **L1**Pd-(2,6-*DMAP*), supporting the identity of the new product as the positional isomer **L1**Pd-(2,6-*Py*).

2.6 Deprotonation-Driven Stepping

A sample of the of the neutralised 15:85 crude mixture of **L1**Pd-(2,6-*DMAP*:2,6-*Py*) from the protonation-driven stepping experiment was subjected to exchange conditions (338 K in $CDCl_3$/CD_3CN (7:3)). After 24 h at elevated temperature, the ratio had changed to >95:5 in favour of **L1**Pd-(2,6-*DMAP*), whilst in an identical sample left at room temperature for the same period, no change was observed. The ratio observed at equilibration at 338 K is in accordance with the previous neutral stepping experiment demonstrating an equilibrium distribution almost completely in favour of **L1**Pd-(2,6-*DMAP*) in the absence of acid, and the absolute reversibility of the switching mechanism. These experiments illustrate that the reaction conditions identified in this study allow the system to be locked in a thermodynamically unfavourable positional isomer distribution between the two footholds enabling ratcheting of the biped unit away from its equilibrium state and for work to be done on it by the track.

2.7 Conclusion

Nature boasts a veritable plethora of molecular-level systems in which the thermodynamics and kinetics of binding events can be rapidly and systematically controlled *via* ingenious manipulation of hydrogen bonding and electrostatic interactions to achieve phenomenal control over molecular-level motion. Routes to synthetic mimics of these systems have thus far proven elusive as the mastery of such weak and ephemeral binding events lies at the boundary of modern-day synthetic chemistry. Metal coordination motifs have shown exciting signs as one potential method and have indeed provided examples of controlled molecular-level motion by exploiting the kinetics and thermodynamics of ligand binding events.[6] This chapter has described an acid-base operable ratchet based upon a non-interlocked palladium(II)/platinum(II) bimetallic system in which one of two transition metal complexes can be selectively labilised and stepped either way along an energy gradient between two different binding sites by means of an energy ratchet mechanism, and kinetically relocked with a high degree of positional discrimination. In so doing, a strategy has been developed for synthesising sophisticated tracks with multiple metal ion binding sites using Sonogashira methodology and a means of attaching transition metal units through an orthogonal combination of metal coordination and CuAAC "click" chemistry. Such expertise, coupled with further investigation into the thermodynamics and kinetics of a potential opposing foot moiety should prove useful in the development of switchable, metastable components for advanced molecular machinery, most notably linear molecular motors in the form of synthetic small molecule molecular walkers.

2.8 Experimental Section

General Information

Unless stated otherwise, all reagents and solvents were purchased from Aldrich Chemicals and used without further purification. Compounds **1**,[6a] **4**,[28] $PtCl_2(SMe_2)_2$[29] and *tris*[(1-benzyl-1H-1,2,3-triazol-4-yl)methyl]amine (TBTA)[11a,30] were prepared according to literature procedures.

Synthesis of Model Ligands

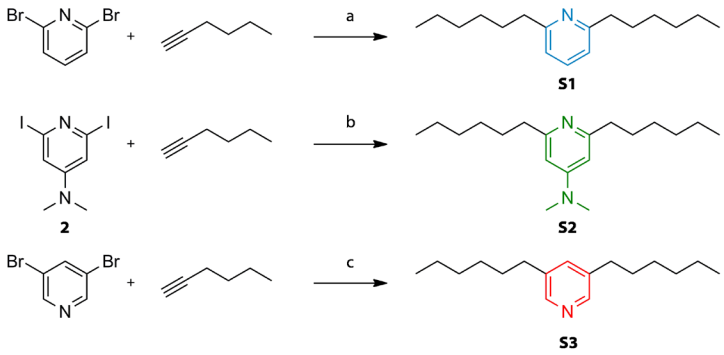

Scheme 2.5 *- Reagents and conditions: (a) (i) CuI, $PdCl_2(PPh_3)_2$, THF/Et_3N, (ii) H_2, $Pd(OH)_2/C$, K_2CO_3, THF, 54%; (b) (i) CuI, $PdCl_2(PPh_3)_2$, THF/Et_3N, (ii) H_2, $Pd(OH)_2/C$, K_2CO_3, THF, 77%; (c) (i) CuI, $PdCl_2(PPh_3)_2$, THF/Et_3N, (ii) H_2, $Pd(OH)_2/C$, K_2CO_3, THF, 54%.*

Synthesis of S1

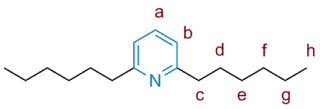

A solution of 2,6-dibromopyridine (540 mg, 2.31 mmol, 1.00 equiv) in THF/Et_3N (1:1, 8 mL) was purged with nitrogen for 20 min. 1-Hexyne (750 mg, 9.07 mmol, 4.00 equiv) was added *via* syringe and the mixture purged for a further 10 min. $PdCl_2(PPh_3)_2$ (95.0 mg, 0.14 mmol, 0.06 equiv) and CuI (12.9 mg, 0.07 mmol, 0.03 equiv) were added and the reaction stirred at 50 °C for 12 h. A precipitate formed, was filtered off and the filtrate was concentrated under reduced pressure. The residue was dissolved in CH_2Cl_2 (20 mL) washed with sat. NH_4Cl (2 × 20 mL) and dried over $MgSO_4$. The crude product was purified by column chromatography (SiO_2, petroleum ether/EtOAc 95:5) to give a pale yellow oil which was immediately dissolved in THF (10 mL). $Pd(OH)_2/C$ (20 wt.% Pd, 100 mg, 30 wt. %) and K_2CO_3 (5.00 equiv) were added and the reaction was stirred under a hydrogen atmosphere at room temperature for 16h. The solution was filtered through a pad of Celite® and the solvent removed under reduced pressure to give **S1** (334 mg, 58%) as a clear, brown oil. ^1H NMR ($CDCl_3$, 400 MHz): δ = 7.48 (t, J = 7.7 Hz, 1H, H_a), 6.94 (d, J = 7.7 Hz, 2H, H_b), 2.79–2.70 (m, 4H, H_c), 1.75–1.58 (m, 4H, H_g), 1.44–1.04 (m, 12H, H_{d+e+f}), 0.87 (t, J = 7.0 Hz, 7H, H_h). ^{13}C NMR (125 MHz, $CDCl_3$): δ = 162.1, 136.5, 119.7, 38.8, 31.9, 30.3, 29.3, 22.7, 14.2. HRMS (NSI$^+$): m/z = 248.2368 $[M+H]^+$ (calcd. 248.2373 for $C_{17}H_{30}N^+$).

Synthesis of S2

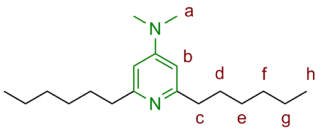

A solution of 2,6-diiodo-4-(*N,N*-dimethylamino)-pyridine (300 mg, 0.80 mmol, 1.00 equiv) in THF/Et_3N (1:1, 15 mL) was purged with nitrogen for 20 min. $PdCl_2(PPh_3)_2$ (56.0 mg, 0.08 mmol, 0.10 equiv) and CuI (7.70 mg, 0.04 mmol, 0.05 equiv) were added and the mixture purged for a further 10 min. 1-Hexyne (750 mg, 9.07 mmol, 4.00 equiv) was added *via* syringe and the reaction stirred at 50 °C for 18 h in the absence of light. The solvent was removed under reduced pressure. The residue was dissolved in EtOAc (50 mL) washed with sat. NH_4Cl (60 mL) and dried over $MgSO_4$. The crude product was purified by column chromatography (SiO_2, petroleum ether/EtOAc 4:1) to give a pale, yellow oil which was immediately dissolved in THF (30 mL). $Pd(OH)_2/C$ (20 wt.% Pd, 150 mg, 30 wt. %) and K_2CO_3 (500 mg, 3.41 mmol, 5.00 equiv) were added and the reaction was stirred under H_2 at room temperature for 16 h. The solution was filtered through a pad of Celite® and the solvent removed under reduced pressure to give **S2** (190 mg, 77%) as a pale yellow oil. ^1H NMR (500 MHz, $CDCl_3$): δ = 6.20 (s, 2H, H_b), 2.95 (s, 6H, H_a), 2.63 (m, 4H, H_c), 1.66 (m, 4H, H_d), 1.41–1.23 (m, 12H, H_{e+f+g}), 0.86 (t, J = 7.1 Hz, 6H, H_h). ^{13}C NMR (125 MHz, $CDCl_3$): δ = 162.1, 155.4, 102.8, 39.3, 39.2, 31.9, 30.5, 29.4, 22.7, 14.2. HRMS (NSI^+): m/z = 291.2792 $[M+H]^+$ (calcd. 291. 2795 for $C_{19}H_{35}N_2^+$).

Synthesis of S3

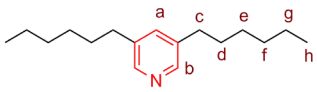

A solution of 3,5-dibromopyridine (540 mg, 2.31 mmol, 1.00 equiv) in THF/Et_3N (1:1, 8 mL) was purged with nitrogen for 20 min. 1-Hexyne (750 mg, 9.07 mmol, 4.00 equiv) was added *via* syringe and the mixture purged for a further 10 min. $PdCl_2(PPh_3)_2$ (95.0 mg, 0.14 mmol, 0.06 equiv) and CuI (13.0 mg, 0.07 mmol, 0.03 equiv) were added and the reaction stirred at 50 °C for 12 h. A precipitate formed, was filtered off and the filtrate concentrated under reduced pressure. The crude residue was dissolved in CH_2Cl_2, washed with sat. NH_4Cl (2 × 20 mL) and dried over $MgSO_4$. The crude product was purified by column chromatography (SiO_2, petroleum ether/EtOAc 95:5) to give a

pale, yellow oil which was immediately dissolved in THF (10 mL) and purged with nitrogen for 10 min. $Pd(OH)_2/C$ (20 wt.% Pd, 100 mg, 30 wt. %) and K_2CO_3 (5.00 equiv) were added and the solution purged with hydrogen for 10 min. The reaction was left to stir under hydrogen at room temperature for 16 h. The solution was filtered through a pad of Celite® and the solvent removed under reduced pressure to give **S3** (330 mg, 58%) as an orange oil. ^{1}H NMR ($CDCl_3$, 400 MHz): δ = 8.25 (s, 2H, H_b), 7.28 (s, 1H, H_a), 2.57 (t, J = 7.7 Hz, 4H, H_c), 1.68–1.51 (m, 4H, H_d), 1.43–1.19 (m, 12H, H_{e+f+g}), 0.88 (t, J = 6.9 Hz, 6H, H_h). ^{13}C NMR (125 MHz, $CDCl_3$): δ = 147.5, 137.6, 135.9, 33.1, 31.8, 31.3, 29.0, 22.7, 14.2. HRMS (NSI$^+$): m/z = 248.2368 $[M+H]^+$ (calcd. 248.2373 for $C_{17}H_{30}N^+$).

Synthesis of Model Complexes

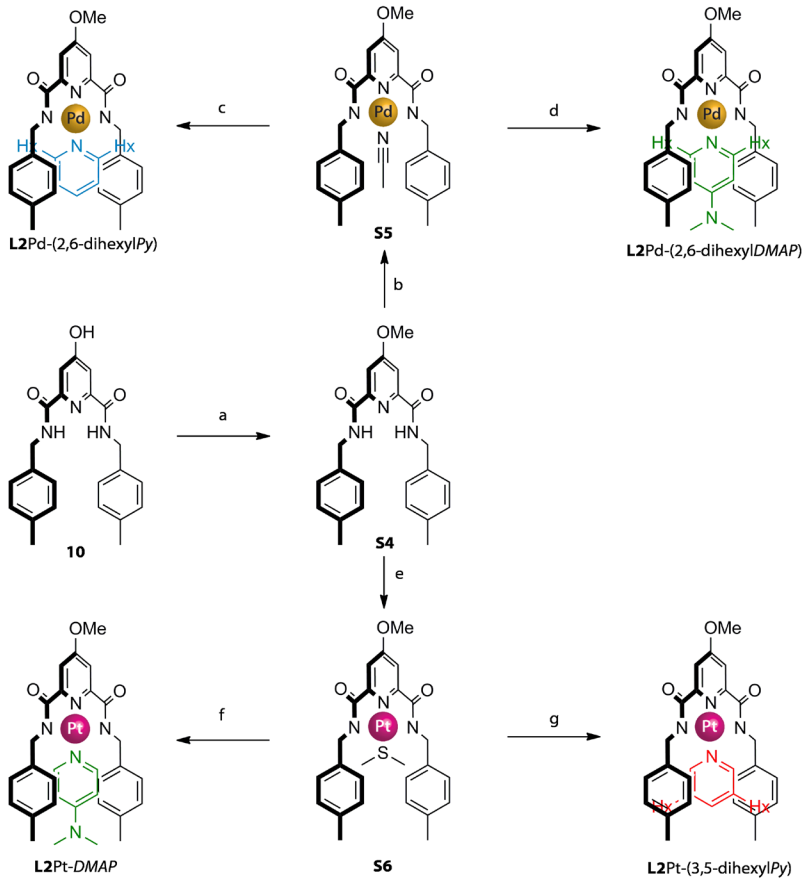

Scheme 2.6 *- Reagents and conditions: (a) MeI, K_2CO_3, DMF, quant.; (b) $Pd(OAc)_2$, CH_3CN, 79%; (c)* ***S1****, CH_2Cl_2, 79%; (d)* ***S2****, $CHCl_3$, 80%; (e) NaH, $PtCl_2(SMe_2)_2$, THF, 74%; (f) 4-dimethylaminopyridine, CH_2Cl_2, 83%; (g)* ***S2****, CH_2Cl_2, 95%.*

Synthesis of 10

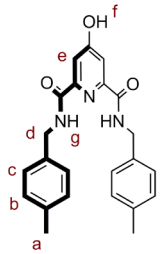

A 250 mL oven dried flask was charged with chelidamic acid monohydrate (2.98 g, 16.2 mmol, 1.00 equiv) and pentafluorophenol (6.13 g, 33.3 mmol, 2.00 equiv). To the solids was added THF (70 mL) and the suspension cooled to 0 °C. Dicyclohexylcarbodiimide (7.70 g, 35.4 mmol, 2.20 equiv) was added and, once dissolved, DMAP (100 mg, 0.05 equiv) was added and the reaction mixture stirred at room temperature for 18 h. A precipitate formed and was filtered off. The filtrate was concentrated under reduced pressure and the residue purified by column chromatography (SiO_2, petroleum ether/EtOAc 3:2) affording a yellow oil which was immediately dissolved in $CHCl_3$ (200 mL) and cooled to 0 °C. 4-methylbenzylamine (5.90 g, 49.0 mmol, 3.00 equiv) and Et_3N (8.22 g, 81.2 mmol, 5.00 equiv) were added dropwise *via* syringe and the reaction mixture stirred at room temperature for 1 h. A precipitate evolved and was filtered off. The solvent was removed under reduced pressure, the residue re-dissolved in CH_2Cl_2 and washed successively with saturated NH_4Cl (2 × 100 mL) and water (2 × 100 mL) and dried over $MgSO_4$. The crude yellow solid was purified by flash column chromatography (SiO_2, CH_2Cl_2/MeOH 95:5) to give **10** (2.20 g, 35%) as an off-white solid. m.p. 162–165 °C. ^{1}H NMR (400 MHz, $CDCl_3$): δ = 8.08 (s, 4H, H_{e+g}), 7.23 (d, J = 7.8 Hz, 4H, H_b), 7.15 (d, J = 7.8 Hz, 4H, H_c), 4.63 (d, J = 6.0 Hz, 4H, H_d), 2.35 (s, 6H, H_a). ^{13}C NMR (125 MHz, $CDCl_3$): δ = 166.0, 163.2, 150.2, 136.1, 135.3, 128.5, 126.9, 111.6, 42.1, 20.2. HRMS (ESI^+): m/z = 390.1815 $[M+H]^+$ (calcd. 390.1812 for $C_{23}H_{24}N_3O_3^+$).

Synthesis of S4

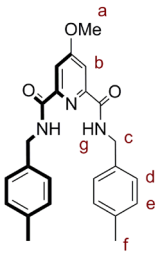

To a solution of **10** (430 mg, 1.10 mmol, 1.00 equiv) in DMF (10 mL) was added CH_3I (190 mg, 1.20 mmol, 1.20 equiv) and K_2CO_3 (750 mg, 5.50 mmol, 5.00 equiv) and the solution stirred at room temperature for 15 h. The solvent was removed under reduced pressure and the residue dissolved in CH_2Cl_2 and washed with H_2O. The organic phase was dried over $MgSO_4$ and the solvent removed under reduced pressure to yield **S4** (440 g, quant.) as an off-white solid. m.p. 130-132 °C. ^{1}H NMR (500 MHz, $CDCl_3$): δ = 7.98 (t, J = 5.8 Hz, 2H, H_g), 7.88 (s, 2H, H_b), 7.21 (d, J = 8.0 Hz, 4H, H_e), 7.12 (d, J = 7.8 Hz, 4H, H_d), 4.61 (d, J = 6.0 Hz, 4H, H_c), 3.96 (s, 3H, H_a), 2.33 (s, 6H, H_f). ^{13}C NMR (125 MHz, $CDCl_3$): δ = 168.6, 163.5, 150.9, 137.4, 135.2, 129.5, 127.9, 111.3, 56.2, 43.4, 21.3. HRMS (ESI$^+$): m/z = 404.1966 $[M+H]^+$ (calcd. 404.1969 for $C_{24}H_{26}N_3O_3^+$).

Synthesis of S5

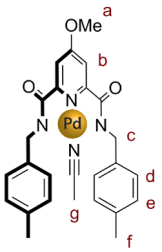

To a solution of **S4** (220 mg, 0.55 mmol, 1.00 equiv) in CH_3CN (15 mL) was added $Pd(OAc)_2$ (150 mg, 0.66 mmol, 1.20 equiv) and the solution stirred at room temperature for 12 h. A precipitate was filtered off, washed with ice-cold CH_3CN and dried under reduced pressure to give **S5** (240 mg, 79%) as an amorphous green/grey solid. ^{1}H NMR (500 MHz, $CDCl_3$): δ = 7.23 (s, 2H, H_b), 7.19 (d, J = 7.9 Hz, 4H, H_e), 7.08 (d, J = 7.9 Hz, 4H, H_d), 4.49 (s, 4H, H_c), 3.97 (s, 3H, H_a), 2.30 (s, 6H, H_f), 2.00 (s, 3H, H_g). ^{13}C NMR (125 MHz, $CDCl_3$): δ = 170.7, 170.2, 154.7, 138.7, 135.9, 129.0, 127.3, 116.5, 110.8, 56.9, 50.1, 21.2, 2.0. HRMS (NSI$^+$): m/z = 508.0844 $[M–CH_3CN+H]^+$ (calcd. 508.0848 for $C_{24}H_{24}N_3O_3Pd^+$).

Synthesis of S6

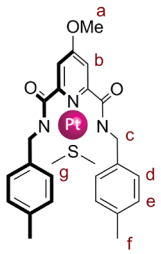

A solution of **S4** (300 mg, 0.74 mmol, 1.00 equiv) in THF (25 mL) was purged with N_2 for 1 h. NaH (50.0 mg, 2.10 mmol, 2.80 equiv) was added in THF *via* syringe and the mixture stirred at room temperature for 5 h. The clear yellow solution formed was wrapped in foil and cooled to 0 °C. $PtCl_2(SMe_2)_2$ (340 mg, 0.89 mmol, 1.20 equiv) was added and the solution allowed to warm to room temperature while stirring for 16 h. The solvent was removed under reduced pressure and the crude residue purified by flash column chromatography (SiO_2, CH_2Cl_2/MeOH 99:1) to yield **S6** (360 mg, 74%) as an orange solid. m.p. 200 °C (dec.). ^{1}H NMR (500 MHz, $CDCl_3$): δ = 7.38 (s, 2H, H_b), 7.16 (d, J = 7.9 Hz, 4H, H_e), 7.06 (d, J = 7.9 Hz, 4H, H_d), 4.77 (s, 4H, H_c), 4.01 (s, 3H, H_a), 2.27 (s, 6H, H_f), 1.82 (s, 6H, H_g). ^{13}C NMR (125 MHz, $CDCl_3$): δ = 172.4, 170.5, 152.0, 137.0, 136.1, 129.2, 126.6, 110.9, 57.0, 50.2, 22.1, 21.2. HRMS (NSI$^+$): m/z = 659.1650 $[M+H]^+$ (calcd. 659.1652 for $C_{26}H_{30}N_3O_3PtS^+$).

Synthesis of L2Pd-(2,6-dihexyl*Py*)

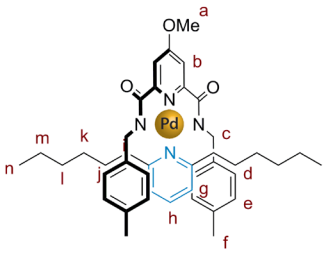

A solution of **S5** (30.0 mg, 0.06 mmol, 1.00 equiv) and **S1** (17.0 mg, 0.06 mmol, 1.00 equiv) in CH_2Cl_2 (1.5 mL) was stirred at room temperature for 12 h. The solvent was removed under reduced pressure and the crude product purified by flash column chromatography (SiO_2, CH_2Cl_2/MeOH 98:2) to give **L2**Pd-(2,6-dihexyl*Py*) (35.0 mg, 79%) as an orange crystalline solid. m.p. 240 °C (dec.). ^{1}H NMR (500 MHz, $CDCl_3$): δ = 7.74 (t, J = 7.8 Hz, 1H, H_h), 7.37 (s, 2H, H_b), 6.99 (d, J = 7.8 Hz, 2H, H_g), 6.81 (d, J = 7.8 Hz, 4H, H_e), 6.48 (d, J = 7.9 Hz, 4H, H_d), 4.01 (s, 3H, H_a), 3.96 (s, 4H, H_c), 2.92 – 2.84 (m, 4H,

H_i), 2.22 (s, 6H, H_f), 1.40 – 1.12 (m, 16H, $H_{j+k+l+m}$), 0.87 (t, *J* = 7.1 Hz, 6H, H_n). ^{13}C NMR (125 MHz, $CDCl_3$): δ = 171.3, 169.9, 164.1, 154.5, 138.7, 138.3, 135.8, 128.8, 127.5, 120.8, 110.7, 56.8, 49.6, 38.8, 31.9, 29.3, 27.7, 22.7, 21.1, 14.2. HRMS (NSI$^+$): *m/z* = 755.3142 $[M+H]^+$ (calcd. 755.3152 for $C_{41}H_{53}N_4O_3Pd^+$); 777.2959 $[M+Na]^+$ (777.2972 for $C_{41}H_{52}N_4NaO_3Pd^+$).

Synthesis of L2Pd-(2,6-dihexyl*DMAP*)

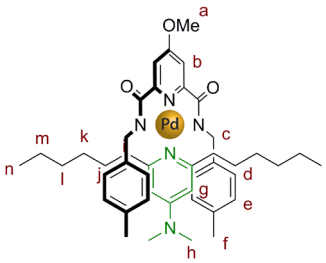

A solution of **S5** (60.0 mg, 0.11 mmol, 1.00 equiv) and **S2** (31.8 mg, 0.11 mmol, 1.00 equiv) in $CHCl_3$ (10 mL) was stirred at room temperature for 18 h. The solvent was removed under reduced pressure and the crude was purified by column chromatography (SiO_2, CH_2Cl_2/MeOH 95:5) to afford **L2**Pd-(2,6-dihexyl*DMAP*) (70.3 mg, 80%) as a yellow solid. m.p. 210 °C (dec.). ^1H NMR (500 MHz, $CDCl_3$): δ = 7.34 (s, 2H, H_b), 6.85 (d, *J* = 7.8 Hz, 4H, H_e), 6.65 (d, *J* = 7.9 Hz, 4H, H_d), 6.14 (s, 2H, H_g), 3.99 (s, 7H, H_{a+c}), 3.12 (s, 6H, H_h), 2.76 (m, 4H, H_i), 2.24 (s, 6H, H_f), 1.39–1.10 (m, 16H, $H_{j+k+l+m}$), 0.86 (t, *J* = 7.2 Hz, 6H, H_n). ^{13}C NMR (125 MHz, $CDCl_3$): δ = 171.3, 169.6, 162.4, 155.7, 154.6, 138.6, 135.5, 128.6, 127.7, 110.4, 103.5, 56.7, 49.7, 39.6, 38.8, 32.0, 29.4, 27.9, 22.8, 21.1, 14.2. HRMS (NSI$^+$): *m/z* = 798.3586 $[M+H]^+$ (calcd. 798.3585 for $C_{43}H_{58}N_5O_3Pd^+$).

Synthesis of L2Pt-(3,5-dihexyl*Py*)

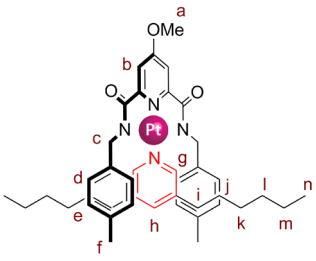

S6 (30.0 mg, 0.05 mmol, 1.00 equiv) and **S3** (11.0 mg, 0.05 mmol, 1.00 equiv) were dissolved in CH_2Cl_2 and the resulting mixture was stirred at room temperature for 12h. The solvent was removed under reduced pressure and the residue purified by column

chromatography (SiO_2, CH_2Cl_2/MeOH 98:2) to give **L2**Pt-(3,5-dihexyl*Py*) (36.0 mg, 95%) as a yellow solid. m.p. 230 °C (dec.). ^{1}H NMR (400 MHz, $CDCl_3$): δ = 7.70 (d, J = 1.7 Hz, 2H, H_g), 7.35 (s, 2H, H_b), 7.16 (s, 1H, H_h), 6.84 (d, J = 7.8 Hz, 4H, H_e), 6.68 (d, J = 7.8 Hz, 4H, H_d), 4.35 (s, 4H, H_c), 4.00 (s, 3H, H_a), 2.28–2.23 (m, 4H, H_i), 2.22 (s, 6H, H_f), 1.47–1.36 (m, 4H, H_j), 1.35–1.22 (m, 12H, H_{k+l+m}), 0.90 (t, J = 6.8 Hz, 6H, H_n). ^{13}C NMR (100 MHz, $CDCl_3$): δ = 171.8, 169.8, 153.6, 149.9, 140.1, 137.6, 137.2, 135.4, 128.7, 126.7, 110.7, 56.8, 49.6, 32.5, 31.6, 30.4, 29.1, 22.7, 21.1, 14.2. HRMS (NSI$^+$): m/z = 844.3766 $[M+H]^+$ (calcd. 844.3763 for $C_{41}H_{53}N_4O_3Pt^+$).

Synthesis of L2Pt-*DMAP*

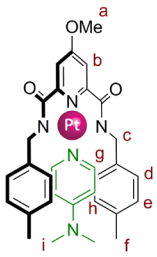

A dry 50 mL round bottom flask was charged with **S6** (29.0 mg, 0.05 mmol, 1.00 equiv) and 4-dimethylaminopyridine (6.0 mg, 0.05 mmol, 1.00 equiv) in CH_2Cl_2 (1.5 mL) and the solution stirred at room temperature for 16 h. The solvent was removed under reduced pressure and the crude product was purified by flash column chromatography (SiO_2, CH_2Cl_2/MeOH 98:2) to yield **L2**Pt-*DMAP* (26.0 mg, 83%) as an orange crystalline solid. m.p. 250 °C (dec.). ^{1}H NMR (400 MHz, $CDCl_3$): δ = 7.61 (d, J = 7.2 Hz, 2H, H_g), 7.31 (s, 2H, H_b), 6.88 (d, J = 8.0 Hz, 4H, H_e), 6.81 (d, J = 8.0 Hz, 4H, H_d), 6.10 (d, J = 7.2 Hz, 2H, H_h), 4.35 (s, 4H, H_c), 3.98 (s, 3H, H_a), 3.05 (s, 6H, H_i), 2.24 (s, 6H, H_f). ^{13}C NMR (125 MHz, $CDCl_3$): δ = 171.8, 169.5, 153.7, 150.9, 137.8, 135.3, 128.5, 127.1, 110.4, 107.4, 56.6, 49.7, 39.3, 21.1. HRMS (NSI$^+$): m/z = 719.2292 $[M+H]^+$ (calcd. 719.2309 for $C_{31}H_{34}N_5O_3Pt^+$).

General Procedures for Model Ligand Exchange Experiments

Ligand exchange experiments in CD_3CN

Stock solutions of complexes **L2**Pd-(2,6-dihexyl*Py*) and **L2**Pd-(3,5-dihexyl*Py*), and ligands **S1** and **S3** (0.4 mM in CD_3CN) were independently prepared. 0.6 mL aliquots of the relevant complex solution and 0.6 mL of the corresponding ligand solution were mixed to get 1:1 solutions (0.2 mM) of the Pd(II) complexes with respect to the exchange ligand. The reaction mixtures were then either left at room temperature or heated at 65 °C and monitored by ^{1}H NMR spectroscopy.

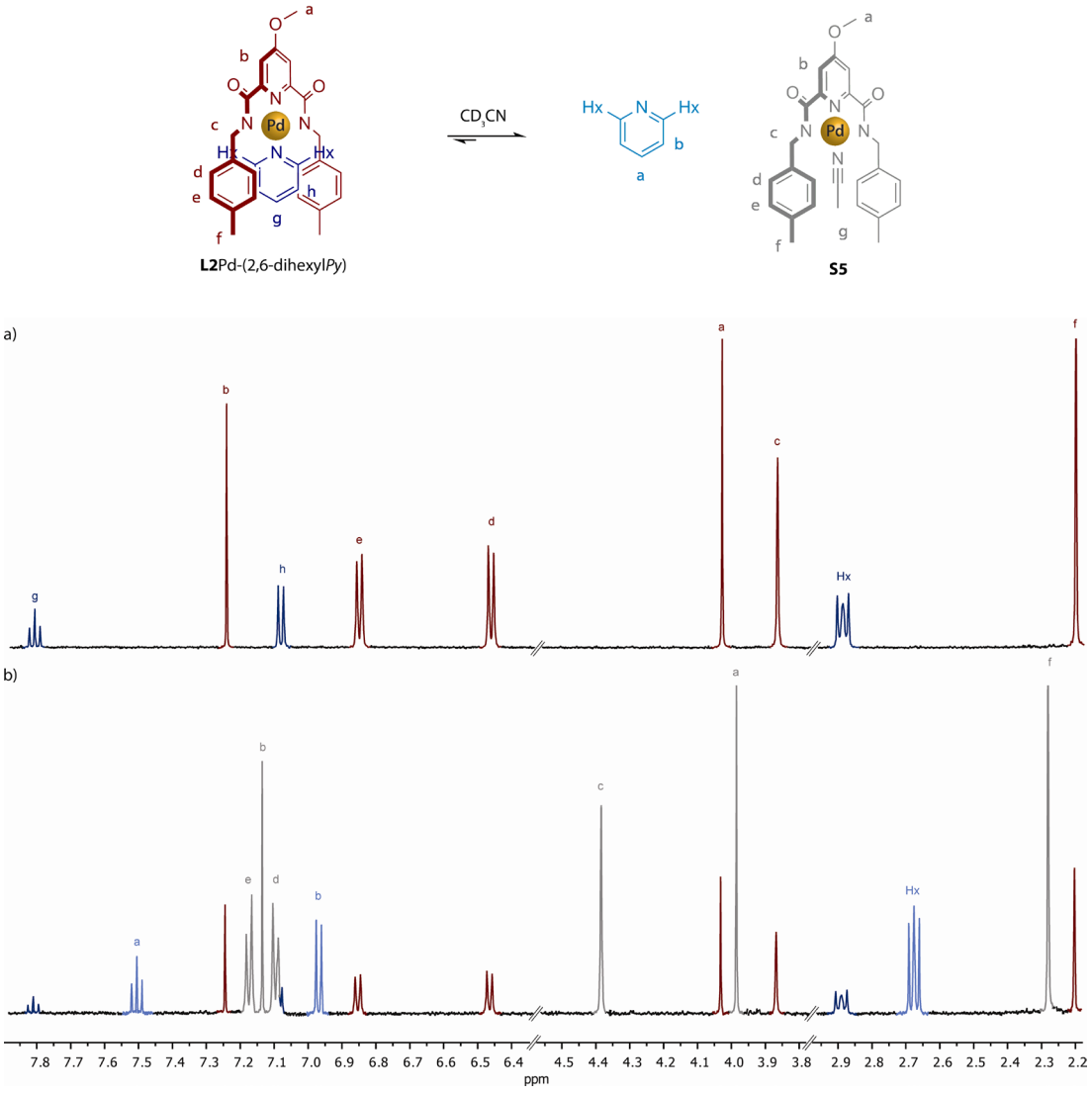

Figure 2.4 *- Elevated temperature (338 K) exchange of 2,6-dihexylPy for CD_3CN by Pd(II) complex **L2**Pd-(2,6-dihexylPy) in CD_3CN. Partial ^{1}H NMR (500 MHz, CD_3CN) of: (a) **L2**Pd-(2,6-dihexyl*Py*) (0.2 mM); (b) solution (a) after heating at 338 K for 5 h.*

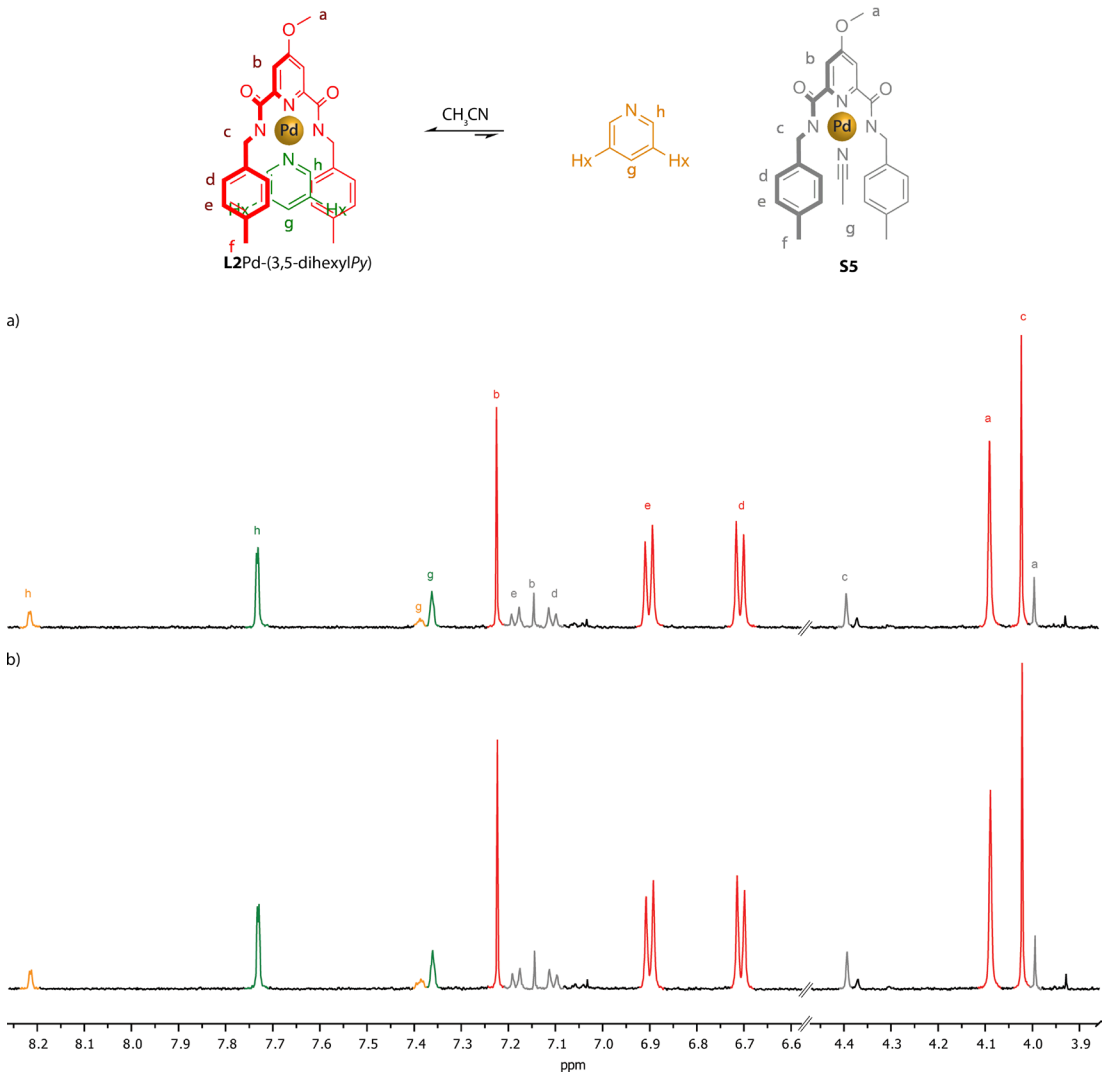

Figure 2.5 *- Elevated temperature (338 K) exchange of 3,5-dihexylPy for CD_3CN by Pd(II) complex* ***L2****Pd-(3,5-dihexylPy) in CD_3CN. Partial ^1H NMR (500 MHz, CD_3CN) of: (a)* ***L2****Pd-(3,5-dihexylPy) (0.2 mM); (b) solution (a) after heating at 338 K for 5 h.*

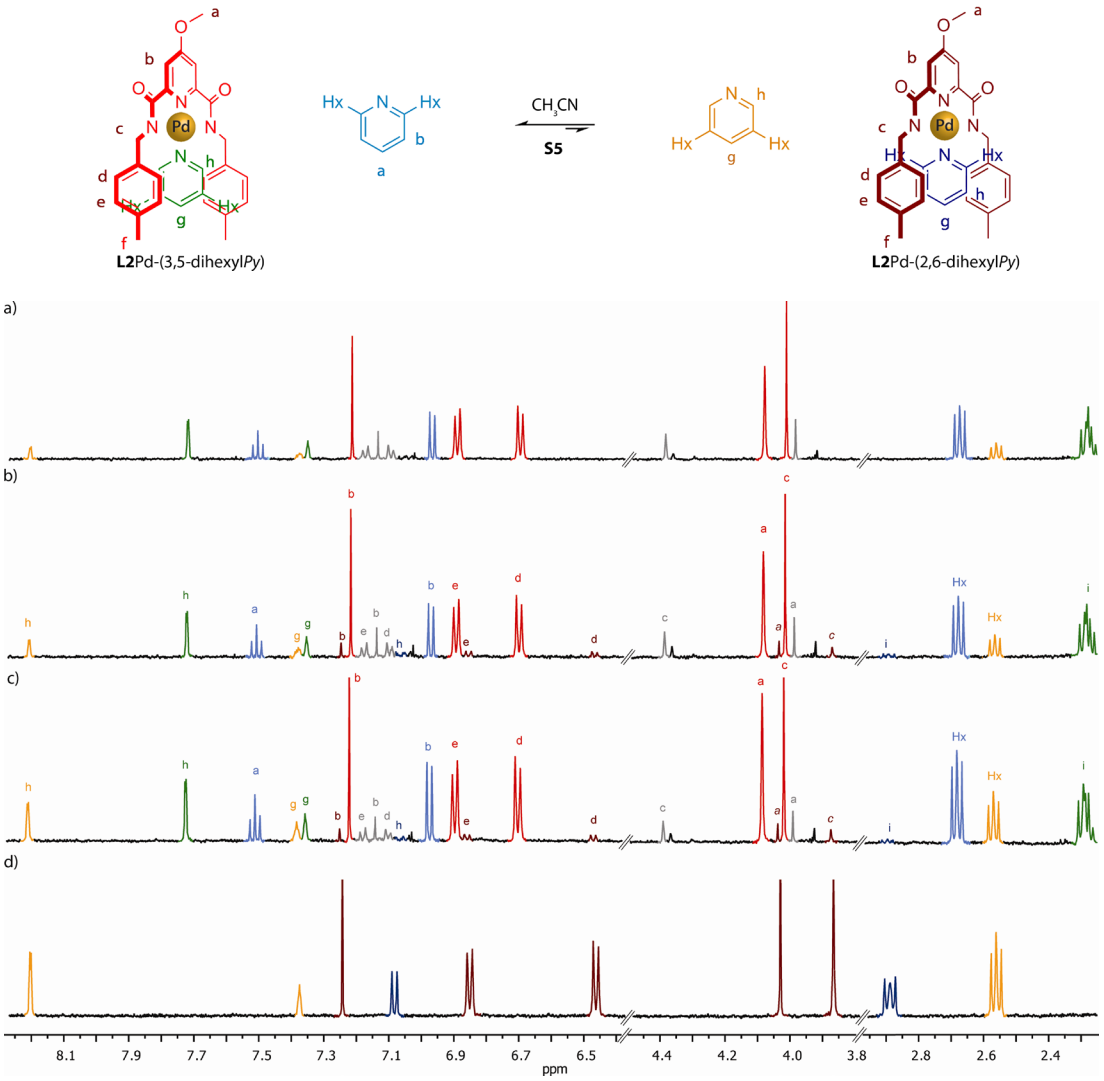

Figure 2.6 *- Elevated temperature (338 K) exchange of 3,5-dihexylPy for 2,6-dihexylPy or CD_3CN by Pd(II) complex* ***L2****Pd-(3,5-dihexylPy) and* ***L2****Pd-(2,6-dihexyl-Py) in CD_3CN. Partial ^1H NMR (500 MHz, CD_3CN) of: (a) 0.2 mM 1:1 mixture of* ***L2****Pd-(3,5-dihexylPy) (0.2 mM) and 2,6-dihexylPy; (b) solution (a) heated at 338 K for 12 h; (c) solution (d) heated at 338 K for 12 h; (d) 1:1 mixture of* ***L2****Pd-(2,6-dihexylPy) (0.2 mM) and 3,5-dihexylPy.*

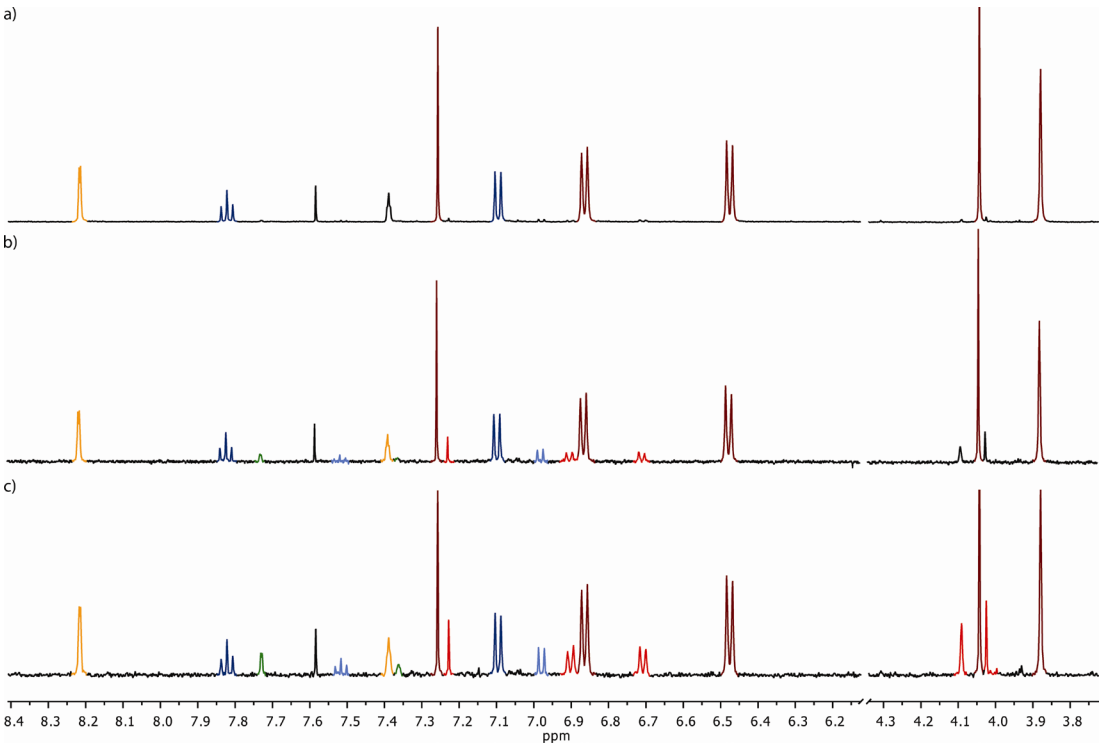

Figure 2.7 *- Room temperature exchange of 3,5-dihexyl*Py *for 2,6-dihexylPy or CD_3CN by Pd(II) complex* ***L2****Pd-(3,5-dihexylPy) in CD_3CN. Partial ^1H NMR (500 MHz, CD_3CN) of a 1:1 solution of* ***L2****Pd-(2,6-dihexylPy) (0.2 mM) and 3,5-dihexylPy maintained at room temperature for: (a) 0 h; (b) 5 h; (c) 15 h.*

Ligand exchange experiments in $CDCl_3$

Stock solutions of complexes **L2**Pd-(2,6-dihexyl*Py*), **L2**Pd-(2,6-dihexyl*DMAP*) and **L2**Pt-(3,5-dihexyl*Py*), ligands **S1**, **S2** and **S3** and CH_3SO_2H were prepared (45.0 mM in $CDCl_3$). Aliquots of the relevant metal complex (0.33 mL), the corresponding exchange ligand (0.33 mL) and methanesulfonic acid solution (0.33 mL, for acid-driven ligand exchange experiments) or $CDCl_3$ (0.33 mL, for ligand exchange experiments in neutral conditions) were combined in order to obtain equimolar solutions of the Pd(II) or Pt(II) complex and the exchange ligand (and acid where appropriate). Aliquots of $CDCl_3$ (0.42 mL) were added to these mixtures and the resulting solution (10 mM of each of the components) were divided into two samples (0.60 mL): one heated at 65 °C and the other one maintained at room temperature. The samples were monitored by ^1H NMR spectroscopy.

Ligand exchange experiments in $CDCl_3/CD_3CN$ (7:3)

Stock solutions of complexes **L2**Pd-(2,6-dihexyl*Py*), **L2**Pd-(2,6-dihexyl*DMAP*) and **L2**Pt-(3,5-dihexyl*Py*), exchange ligands **S1**, **S2** and **S3** and CH_3SO_2H were prepared (45.0 mM

in $CDCl_3$). Aliquots of the relevant metal complex (0.33 mL), the corresponding exchange ligand (0.33 mL) and the methanesulfonic acid solution (0.33 mL for acid-driven ligand exchange experiments) or $CDCl_3$ (0.33 mL for ligand exchange experiments in neutral conditions) were combined in order to obtain equimolar solutions of the Pd(II) or Pt(II) complex and the exchange ligand (and acid where appropriate). Aliquots of CD_3CN (0.42 mL) were added to these mixtures and the resulting solution (10 mM of each of the components) were each divided into two samples (0.60 mL): one heated at 65 °C and the other one maintained at room temperature. The samples were monitored by ^1H NMR spectroscopy.

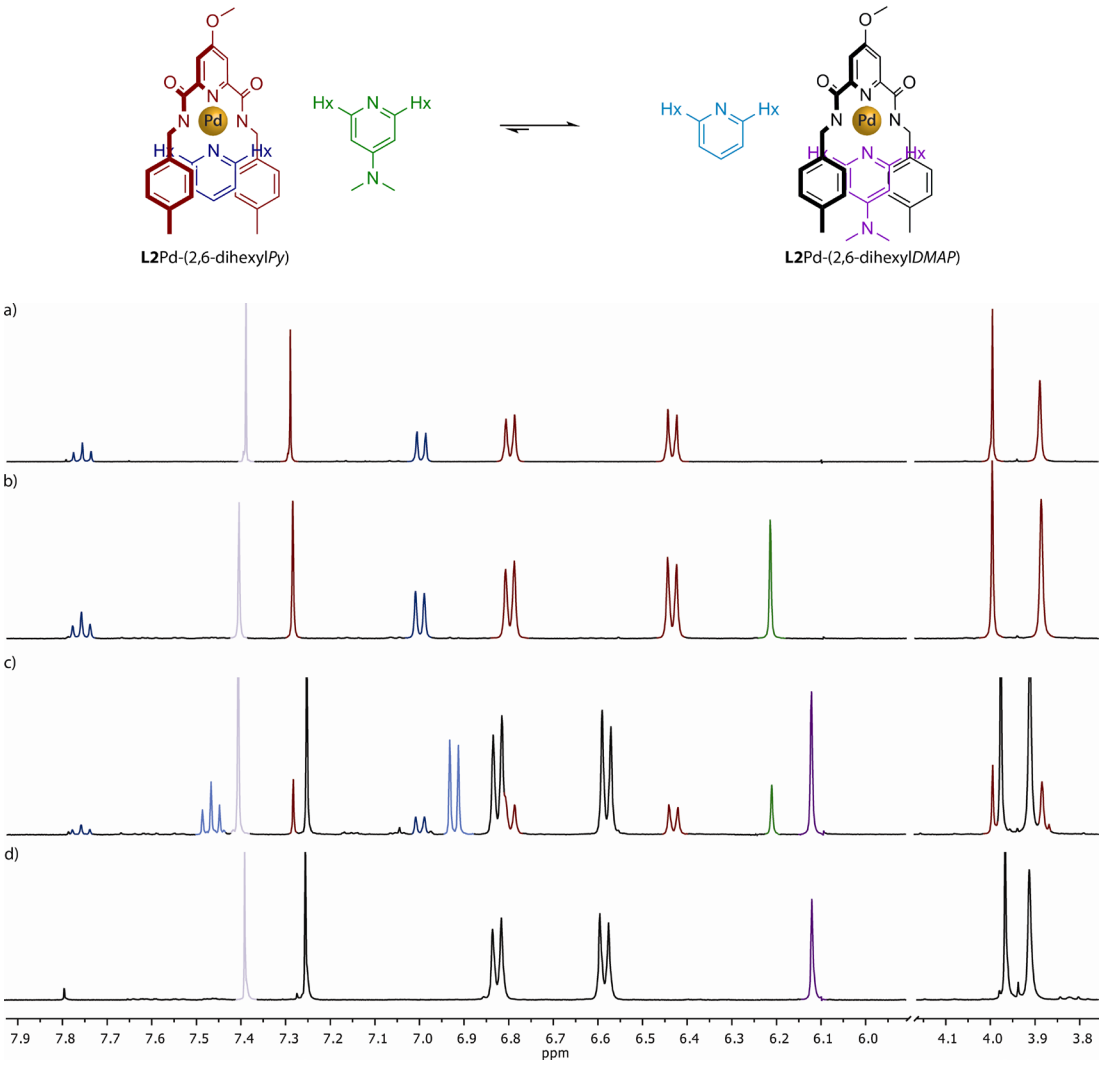

Figure 2.8 *- Elevated temperature (338 K) exchange of 2,6-dihexylPy for 2,6-dihexylDMAP by Pd(II) complex* ***L2****Pd-(2,6-dihexylPy) in $CDCl_3/CD_3CN$. Partial ^1H NMR (400 MHz, $CDCl_3/CD_3CN$ 7:3) of: (a) reference spectrum of* ***L2****Pd-(2,6-dihexylPy); (b) 1:1 mixture of* ***L2****Pd-(2,6-dihexylPy) (10 mM) and 2,6-dihexylDMAP; (c) mixture (a) heated at 338 K for 12 h showing 80% exchange; (d) reference spectrum of* ***L2****Pd-(2,6-dihexylDMAP).*

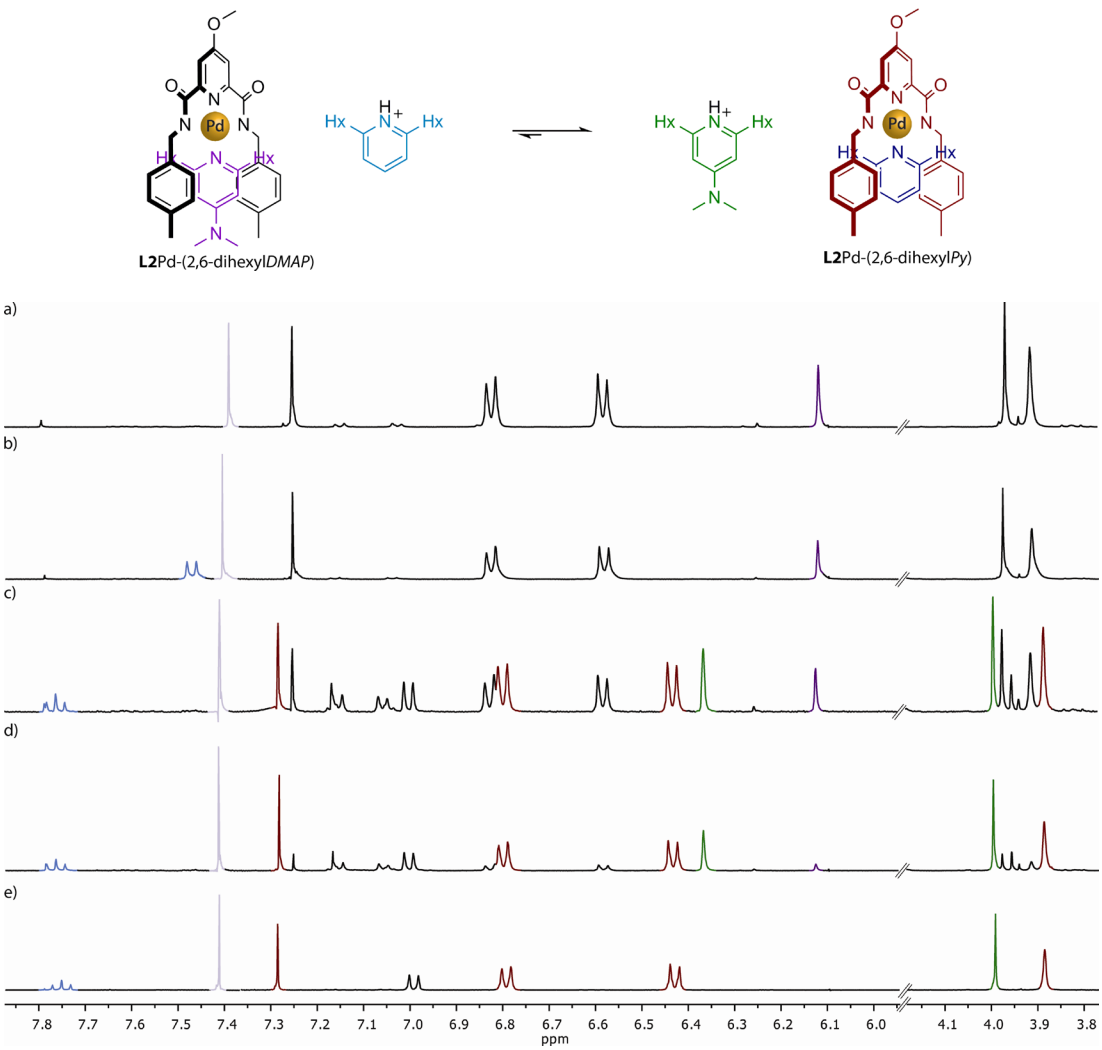

Figure 2.9 *- Elevated temperature (338 K) acid-driven exchange of 2,6-dihexylDMAP for 2,6-dihexylPy by Pd(II) complex* ***L2****Pd-(2,6-dihexylDMAP) in* $CDCl_3/CD_3CN$*. Partial* ^1H *NMR (400 MHz,* $CDCl_3/CD_3CN$ *7:3) of: (a) reference spectrum of* ***L2****Pd-(2,6-dihexylDMAP); (b) 1:1:1 mixture of* ***L2****Pd-(2,6-dihexylDMAP) (10 mM), 2,6-dihexylPy and* CH_3SO_2H*; (c) mixture (a) heated at 338 K for 20 h; (d) mixture (a) heated at 338 K for 40 h showing 85% exchange; (e) reference spectrum of* ***L2****Pd-(2,6-dihexylPy).*

Synthesis of Track 19

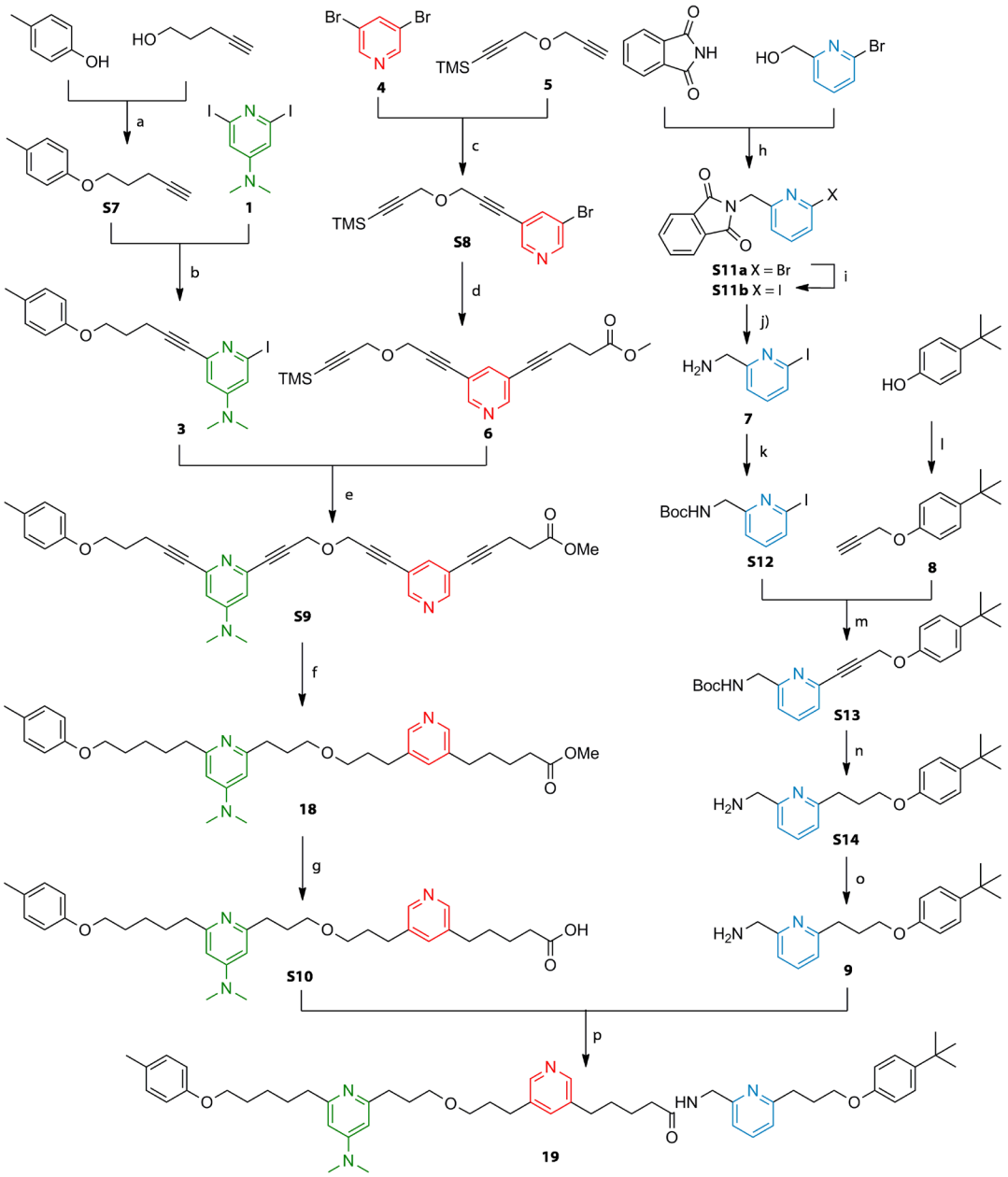

Scheme 2.7 *- Synthesis of molecular track. Reagents and conditions: (a) 4-pentyn-1-ol, PPh_3, DIAD, THF, 92%; (b) $PdCl_2(PPh_3)_2$, CuI, THF/Et_3N, 56%; (c) $PdCl_2(PPh_3)_2$, CuI, Et_3N/THF, 85%; (d) methyl-4-pentynoate, $PdCl_2(PPh_3)_2$, CuI, Et_3N/THF, 71%; (e) (i) TBAF, THF/H_2O (9:1), 95%, (ii) $PdCl_2(PPh_3)_2$, CuI, Et_3N/THF, 74%; (f) H_2, $Pd(OH)_2$/C, K_2CO_3, THF, 78%; (g) LiOH, MeOH/H_2O/THF 6:3:1, 97%; (h) phthalimide, PPh_3, DIAD, THF, 92%; (i) NaI, CuI, N,N'-dimethylethylenediamine, 90%; (j) hydrazine monohydrate, EtOH, 92%; (k) Boc_2O, CH_2Cl_2, 97%; (l) propargyl bromide, K_2CO_3, 2-butanone, 91%; (m) CuI, $Pd(PPh_3)_4$, THF/Et_3N, 88%; (n) H_2, $Pd(OH)_2$/C, K_2CO_3, THF, 98%; (o) CF_3COOH, $CHCl_3$, 96%; (p) PyBroP, DIPEA, DMF, 86%.*

Synthesis of 2

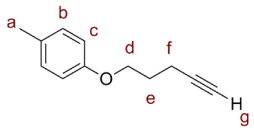

To a solution of triphenylphosphine (15.5 g, 59.5 mmol, 1.00 equiv) in THF (100 mL) was added DIAD (12.0 g, 59.5 mmol, 1.00 equiv) at 0 °C under an atmosphere of nitrogen and the mixture stirred for 30 min. 4-Pentyn-1-ol (5.00 g, 59.5 mmol, 1.00 equiv) was added dropwise and the mixture stirred for 20 min. 4-Cresol (6.10 g, 56.5 mmol, 0.95 equiv) was added slowly over 30 min and the solution was allowed to warm to room temperature. The solvent was removed under reduced pressure and the residue purified by column chromatography (SiO_2, petroleum ether/EtOAc 95:5) to yield **2** (9.00 g, 92%) as a colourless oil. ^{1}H NMR (500 MHz, $CDCl_3$): δ = 7.07 (d, J = 8.5 Hz, 2H, H_b), 6.80 (d, J = 8.5 Hz, 2H, H_c), 4.04 (t, J = 6.1 Hz, 2H, H_d), 2.40 (td, J = 7.0, 2.6 Hz, 2H, H_f), 2.28 (s, 3H, H_a), 1.99 (p, 2H, H_e), 1.96 (t, J = 2.6 Hz, 1H, H_g). ^{13}C NMR (125 MHz, $CDCl_3$): δ = 156.9, 130.1, 130.0, 114.5, 83.7, 68.9, 66.4, 53.6, 28.4, 20.6. HRMS (EI$^+$): m/z = 174.1038 $[M]^+$ (calcd. 174.1039 for $C_{12}H_{14}O^+$).

Synthesis of 3

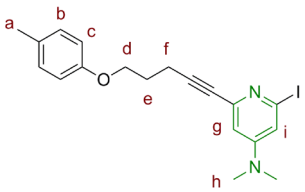

To a solution of **2** (2.79 g, 16.0 mmol, 1.00 equiv) and 2,6-diiodo-4-(*N,N*-dimethylamino)-pyridine (**1**) (6.00 g, 16.0 mmol, 1.00 equiv) in degassed THF/NEt_3 (5:3, 80 mL) was added $PdCl_2(PPh_3)_2$ (1.12 g, 1.60 mmol, 0.10 equiv) and CuI (610 mg, 3.20 mmol, 0.20 equiv) and the solution stirred at 55 °C for 15 h. The reaction mixture was cooled to room temperature, poured into ammonia solution (10%, 300 mL), and extracted with CH_2Cl_2 (3 × 75 mL). The organic layer was washed with brine (2 × 150 mL), dried over $MgSO_4$, filtered, and concentrated under reduced pressure. The residue was purified by column chromatography (SiO_2, petroleum ether/EtOAc 9:1) to yield **3** (4.10 g, 61%) as a colourless solid. m.p. 68-70 °C. ^{1}H NMR (400 MHz, $CDCl_3$): δ = 7.07 (d, J = 8.5 Hz, 2H, H_b), 6.81 (m, 3H, H_{c+i}), 6.55 (d, J = 2.3 Hz, 1H, H_g), 4.05 (t, J = 6.1 Hz, 2H, H_d), 2.95 (s, 6H, H_h), 2.60 (t, J = 7.1 Hz, 2H, H_f), 2.28 (s, 3H, H_a), 2.09–2.03 (m,

2H, H_e). ^{13}C NMR (100 MHz, $CDCl_3$): δ = 156.8, 154.6, 143.3, 130.0, 118.4, 115.9, 114.5, 109.8, 89.5, 80.6, 66.5, 39.4, 28.2, 20.6, 16.3. HRMS (ESI^+): *m/z* = 421.0777 $[M+H]^+$ (calcd. 421.0771 for $C_{19}H_{22}IN_2O^+$).

Synthesis of S8

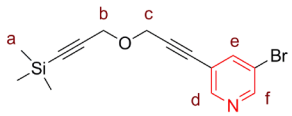

To a solution of 2,6-dibromopyridine (1.99 g, 7.03 mmol, 1.00 equiv) in THF (50 mL) and Et_3N (25 mL) was added CuI (260 mg, 1.40 mmol, 0.20 equiv) and $PdCl_2(PPh_3)_2$ (490 mg, 0.70 mmol, 0.10 equiv). Trimethyl-(3-prop-2-ynyloxyprop-1-ynyl)-silane (1.16 g, 7.03 mmol, 1.00 equiv) was added to the reaction mixture *via* syringe and the solution stirred at 65 °C for 16 h. The solvents were removed under reduced pressure, the resulting residue re-dissolved in EtOAc and washed with aqueous NH_4Cl (2 × 50 mL) and brine (50 mL). The organic extracts were collected and dried over Na_2SO_4. After concentration under reduced pressure, the crude residue was purified by flash column chromatography (SiO_2, hexane/Et_2O 9:1) to yield **S8** (1.93 g, 85%) as a white solid. m.p. 64-66 °C. ^1H NMR (500 MHz, $CDCl_3$): δ = 8.61 (br, 2H, H_{d+f}), 7.88 (s, 1H, H_e), 4.48 (s, 2H, H_c), 4.30 (s, 2H, H_b), 0.19 (s, 9H, H_a). ^{13}C NMR ($CDCl_3$, 100 MHz): δ = 150.5, 150.3, 141.1, 121.3, 120.3, 100.3, 92.7, 89.5, 82.0, 57.9, 57.2, 0.0. HRMS (ESI^+): *m/z* = 322.0258 $[M+H]^+$ (calcd. 322.0257 for $C_{14}H_{17}BrNOSi^+$).

Synthesis of 6

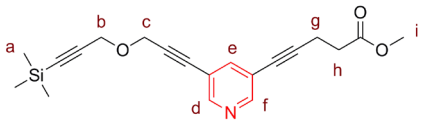

S8 (5.07 g, 16.0 mmol, 1.00 equiv) was dissolved in THF/Et_3N (1:1, 100 mL) and purged with nitrogen for 20 min. Methyl-4-pentynoate (5.90 g, 35.0 mmol, 1.10 equiv) was added and the solution purged for an additional 5 min. $PdCl_2(PPh_3)_2$ (2.20 g, 3.30 mmol, 0.10 equiv) and CuI (310 mg, 1.7 mmol, 0.05 equiv) were added and the reaction stirred at 50 °C for 15 h. The reaction mixture was cooled to room temperature, filtered and the filtrate concentrated under reduced pressure. The residue was dissolved in CH_2Cl_2 (150 mL) and washed with sat. NH_4Cl (2 × 100 mL). The organic layer was dried over $MgSO_4$, filtered, and concentrated under reduced pressure. The

residue was purified by column chromatography (SiO_2, petroleum ether/EtOAc 9:1) to yield **6** (3.96 g, 71%) as an orange oil. ^{1}H NMR (400 MHz, $CDCl_3$): δ = 8.56 (br, 2H, H_{d+f}), 7.71 (s, 1H, H_e), 4.47 (s, 2H, H_c), 4.30 (s, 2H, H_b), 3.73 (s, 3H, H_i), 2.75 (m, 2H, H_g), 2.64 (m, 2H, H_h), 0.19 (s, 9H, H_a). ^{13}C NMR (125 MHz, $CDCl_3$): δ = 172.1, 151.4, 150.7, 141.0, 135.9, 124.8, 120.2, 119.1, 100.3, 92.5, 88.3, 82.7, 57.7, 57.1, 52.0, 33.1, 15.4, 0.0. HRMS (ESI$^+$): *m/z* = 354.1522 $[M+H]^+$ (calcd. 354.1520 for $C_{20}H_{24}NO_3Si^+$).

Synthesis of S9

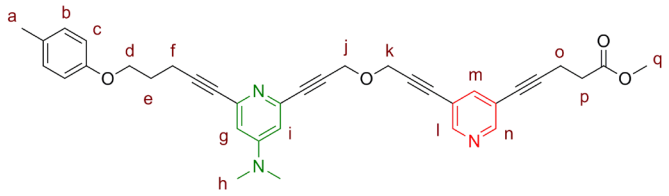

Compound **6** (5.86 g, 16.7 mmol, 1.00 eq.) was dissolved in THF/H_2O (9:1, 60 mL), and tetrabutylammonium fluoride solution in THF (20 mL, 1.20 equiv) was added dropwise to the reaction mixture. The reaction was monitored by TLC and after 2 h, the reaction mixture was directly adsorbed onto silica and purified by column chromatography (SiO_2, petroleum ether/EtOAc 8:2) to yield an oil (4.39 g, 94%) which was immediately added to a solution of **3** (5.66 g, 13.5 mmol, 1.00 equiv) in degassed THF/Et_3N (5:2, 70 mL). $Pd(PPh_3)_4$ (780 mg, 0.68 mmol, 0.05 equiv) and CuI (0.19 g, 1.01 mmol, 0.08 equiv) were added and the solution was stirred at 50 °C for 18 h. The reaction mixture was cooled to room temperature, poured into ammonia solution (10%, 500 mL), and extracted with CH_2Cl_2 (3 × 100 mL). The organic layer was washed with brine (2 × 200 mL), dried over $MgSO_4$, filtered, and concentrated under reduced pressure. The residue was purified by column chromatography (SiO_2, CH_2Cl_2/MeOH 97:3) to yield **S9** (6.61 g, 86%) as a colourless oil. ^{1}H NMR (500 MHz, $CDCl_3$): δ = 8.54 (d, *J* = 2.0 Hz, 1H, H_l), 8.52 (d, *J* = 2.0 Hz, 1H, H_n), 7.70 (t, *J* = 2.0 Hz, 1H, H_m), 7.06 (d, *J* = 8.3 Hz, 2H, H_b), 6.80 (d, *J* = 8.5 Hz, 2H, H_c), 6.61 (d, *J* = 2.5 Hz, 1H, H_i), 6.56 (d, *J* = 2.5 Hz, 1H, H_g), 4.54 (s, 2H, H_k), 4.51 (s, 2H, H_j), 4.06 (t, *J* = 6.1 Hz, 2H, H_d), 3.73 (s, 3H, H_s), 2.98 (s, 6H, H_h), 2.75 (t, *J* = 7.2 Hz, 2H, H_o), 2.64 (t, *J* = 7.2 Hz, 2H, H_p), 2.61 (t, *J* = 7.1 Hz, 2H, H_f), 2.26 (s, 3H, H_a), 2.09–2.04 (m, 2H, H_e). ^{13}C NMR (125 MHz, $CDCl_3$): δ = 172.3, 156.9, 154.5, 151.5, 150.9, 143.9, 142.5, 141.2, 130.0, 120.4, 119.3, 114.6, 109.4, 109.4, 92.6, 88.6, 88.5, 87.2, 82.9, 82.4, 81.3, 77.3, 66.6, 57.6, 57.5, 52.1, 39.3, 33.2, 28.3, 20.6, 16.3, 15.5. HRMS (ESI$^+$): *m/z* = 574.2693 $[M+H]^+$ (calcd. 574.2700 for $C_{36}H_{36}N_3O_4^+$).

Synthesis of 18

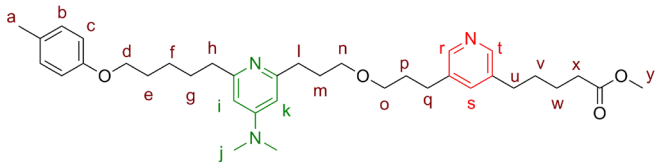

S9 (1.20 g, 2.10 mmol, 1.00 equiv) was dissolved in THF/ethanol (4:1, 50 mL) and degassed with N_2, followed by H_2. K_2CO_3 (14.0 mg, 0.10 mmol, 0.05 equiv) and $Pd(OH)_2/C$ (20 % Pd, 120 mg, 10 wt. %) were added and the reaction continued to be purged with H_2 for an additional 10 min before being allowed to stir for 16 h under an H_2 atmosphere. The crude residue was filtered through Celite® and purified by column chromatography (SiO_2, CH_2Cl_2/MeOH 9:1) to yield **18** (0.993 g, 78%) as a brown oil. ^{1}H NMR (500 MHz, $CDCl_3$): δ = 8.27 (d, J = 1.9 Hz, 1H, H_r), 8.25 (d, J = 1.9 Hz, 1H, H_t), 7.30 (s, 1H, H_s), 7.05 (d, J = 8.3 Hz, 2H, H_b), 6.77 (d, J = 8.5 Hz, 2H, H_c), 6.25 (d, J = 2.2 Hz, 1H, H_k), 6.22 (d, J = 2.2 Hz, 1H, H_i), 3.91 (t, J = 6.6 Hz, 2H, H_d), 3.66 (s, 3H, H_y), 3.47 (t, J = 6.5 Hz, 2H, H_n), 3.42 (t, J = 6.3 Hz, 2H, H_o), 2.98 (s, 6H, H_j), 2.75 (m, 2H, H_l), 2.71–2.65 (m, 4H, H_{h+q}), 2.59 (t, J = 7.2 Hz, 2H, H_u), 2.33 (t, J = 7.0 Hz, 2H, H_x), 2.26 (s, 3H, H_a), 1.99 (m, 2H, H_m), 1.87 (m, 2H, H_p), 1.83–1.73 (m, 4H, H_{e+g}), 1.67–1.63 (m, 4H, H_{v+w}), 1.53 (m, 2H, H_f). ^{13}C NMR (125 MHz, $CDCl_3$): δ = 174.0, 157.1, 155.6, 147.7, 147.6, 137.0, 136.9, 135.9, 129.9, 129.7, 114.5, 103.2, 103.1, 70.6, 69.8, 68.1, 51.7, 39.4, 38.7, 35.2, 33.9, 32.7, 31.3, 30.7, 30.4, 30.2, 29.6, 29.4, 26.1, 24.6, 20.6. HRMS (ESI$^+$): m/z = 590.3942 $[M+H]^+$ (calcd. 590.3952 for $C_{36}H_{52}N_3O_4^+$).

Synthesis of S10

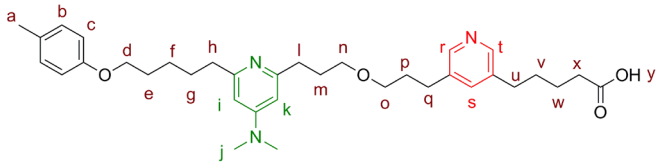

To a solution of **18** (700 mg, 1.20 mmol, 1.00 equiv) in MeOH/H_2O/THF (6:3:1, 22.5 mL) was added LiOH (145 mg, 6.00 mmol, 6.00 equiv) and the reaction mixture stirred at room temperature for 16 h. The mixture was poured into sat. NH_4Cl (150 mL) and extracted with $CHCl_3$/^{i}PrOH (3:1, 10 × 30 mL). The organic layer was washed with brine (2 × 50 mL), dried over $MgSO_4$, filtered, and concentrated under reduced pressure to yield **S10** (685 mg, 97%) as a yellow oil. ^{1}H NMR (500 MHz, $CDCl_3$): δ = 8.24 (s, 2H, H_{r+t}), 7.36 (s, J = 18.4 Hz, 1H, H_s), 7.04 (d, J = 8.4 Hz, 2H, H_b),

6.75 (d, J = 8.4 Hz, 2H, H_c), 6.31 (d, J = 2.5 Hz, 1H, H_i), 6.26 (d, J = 2.5 Hz, 1H, H_k), 3.90 (t, J = 6.4 Hz, 2H, H_d), 3.43 (t, J = 6.2 Hz, 2H, H_n), 3.30 (t, J = 6.1 Hz, 2H, H_o), 3.10 (s, 6H), 3.00 (m, 2H, H_l), 2.94 (m, 2H, H_h), 2.67 (t, J = 7.0 Hz, 2H, H_q), 2.61 (m, 2H, H_u), 2.32 (m, 2H, H_x), 2.25 (s, 3H, H_a), 2.02 (m, 2H, H_m), 1.89–1.75 (m, 6H, H_{e+g+p}), 1.68 (m, 4H, H_{v+w}), 1.54 (m, 2H, H_f). ^{13}C NMR (125 MHz, $CDCl_3$): δ = 177.9, 157.2, 157.0, 156.8, 156.5, 147.1, 147.0, 137.6, 137.0, 136.6, 129.9, 129.8, 114.5, 103.7, 103.6, 70.2, 68.7, 67.8, 39.9, 35.8, 33.8, 32.6, 30.9, 30.8, 30.6, 30.3, 29.8, 29.5, 29.4, 29.0, 29.0, 25.8, 25.4, 20.6.

Synthesis of S11a

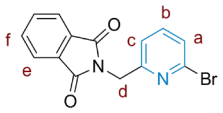

To a solution of PPh_3 (950 mg, 3.62 mmol, 1.20 equiv) in dry THF (30 mL) was added DIAD (0.65 mL, 3.30 mmol, 1.10 equiv) dropwise at 0 ˚C. The mixture was stirred for 15 min at this temperature during which time a suspension formed. 2-Bromo-6-(hydroxymethyl)-pyridine (567 mg, 3.02 mmol, 1.00 equiv) in THF (2 mL) was added dropwise at 0 ˚C and the mixture stirred for another 20 min at 0 ˚C. Phthalimide (485 mg, 3.30 mmol, 1.10 equiv) was added as a solid in one portion. The resulting orange solution was stirred for 16 h without further cooling. The solution was concentrated under vacuum and the residue purified by column chromatography (SiO_2, CH_2Cl_2) to give **S11a** (813 mg, 85%) as an off-white solid. m.p. 124-126 ˚C. ^{1}H NMR (400 MHz, $CDCl_3$): δ = 7.88–7.92 (m, 2H, H_e), 7.74–7.78 (m, 2H, H_f), 7.48 (t, J = 7.6, 1H, H_b), 7.37 (d, J = 7.6, 1H, H_a), 7.16 (d, J = 7.6, 1H, H_c), 4.99 (s, 2H, H_d),). ^{13}C NMR (100 MHz, $CDCl_3$): δ = 167.9, 156.9, 141.9, 139.0, 134.2, 132.1, 127.0, 123.6, 119.9, 42.5. HRMS (ESI$^+$): m/z = 316.9923 $[M+H]^+$ (calcd. 316.9920 for $C_{14}H_{10}BrN_2O_2^+$).

Synthesis of S11b

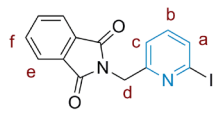

A solution of *N*,*N*'-dimethylethylenediamine (41.0 mg, 50.0 μL, 0.47 mmol, 0.10 equiv) in dry dioxane (35 mL) was degassed with nitrogen for 30 minutes. CuI (45.0 mg, 0.24 mmol, 0.05 equiv), NaI (8.90 g, 59.0 mmol, 12.5 equiv), and **S11a** (1.50 g, 4.73 mmol, 1.00 equiv) were added and the mixture stirred vigorously at 105 ˚C for 48 h. The reaction mixture was then allowed to cool to room temperature, before

aqueous ammonia (20 % w, 25 mL) was added and the mixture extracted into EtOAc (3 × 50 mL). The combined organic layers were washed with brine and water, and dried over $MgSO_4$. The crude product was purified by column chromatography (Al_2O_3 basic, activity II, CH_2Cl_2), to give **S11b** (1.55 g, 90%) as a colourless solid. m.p. 138-140 °C. ^{1}H NMR (400 MHz, $CDCl_3$): δ = 7.88–7.92 (m, 2H, H_e), 7.74–7.78 (m, 2H, H_f), 7.60 (t, J = 7.8, 1H, H_a), 7.25 (t, J = 7.8, 1H, H_b), 7.15 (d, J = 7.8, 1H, H_c), 4.98 (s, 2H, H_d). ^{13}C NMR (100 MHz, $CDCl_3$): δ = 167.9, 157.3, 138.0, 134.2, 133.8, 132.1, 123.6, 120.1, 117.8, 42.5. HRMS (ESI$^+$): m/z = 364.9784 $[M+H]^+$ (calcd. 364.9782 for $C_{14}H_{10}IN_2O_2^+$).

Synthesis of 7

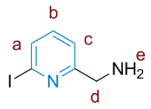

S11b (2.18 g, 6.00 mmol, 1.00 equiv) and hydrazine monohydrate (0.35 mL, 6.00 mmol, 1.00 equiv) were suspended in EtOH (50 mL) and the mixture heated to reflux for 2 h. Additional hydrazine monohydrate (50.0 μL, 0.86 mmol, 0.15 equiv) was added and the solution stirred at reflux for a further 2 h. The reaction mixture was allowed to cool to room temperature, diluted with Et_2O (300 mL) and the solids removed *via* filtration. The filtrate was concentrated under reduced pressure and the resulting crude residue purified by column chromatography (SiO_2, CH_2Cl_2/MeOH/Et_3N 79:20:1) to give **7** (1.29 g, 92%) as a yellow solid. m.p. 30-32 °C. ^{1}H NMR ($CDCl_3$, 400 MHz): δ = 7.58 (dd, J_1 = 6.5, J_2 = 2.1, 1H, H_c), 7.24–7.30 (m, 2H, $H_{a,b}$), 3.92 (s, 2H, H_d). ^{13}C NMR ($CDCl_3$, 100 MHz): δ = 164.2, 137.9, 132.8, 120.2, 117.8, 47.2. HRMS (ESI$^+$): m/z = 234.9726 $[M+H]^+$ (calcd. 234.9727 for $C_6H_8IN_2^+$).

Synthesis of S12

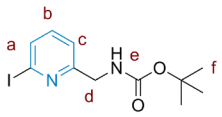

Boc_2O (3.60 g, 16.5 mmol, 1.10 equiv) was dissolved in CH_2Cl_2 (35 mL) and the solution cooled to 0 °C. To this solution was added **7** (3.51 g, 15.0 mmol, 1.00 equiv) as a solid in one portion and the reaction mixture stirred at room temperature for 14 h. Removal of the solvents under reduced pressure, followed by column chromatography (SiO_2, CH_2Cl_2/EtOAc 8:2) yielded **S12** (4.86 g, 97%) as a white solid. m.p 84-86 °C. ^{1}H NMR ($CDCl_3$, 400 MHz): δ = 7.59–7.63 (m, 1H, H_c), 7.23–7.32 (m, 2H, $H_{a,b}$), 5.34–5.48

(br, 1H, H_e), 4.38 (d, J = 5.8, 2H, H_d), 1.46 (s, 9H, H_f). ^{13}C NMR ($CDCl_3$, 100 MHz): δ = 159.9, 155.9, 138.1, 133.4, 120.8, 117.4, 79.7, 45.4, 28.4. HRMS (ESI^+): m/z = 335.0250 $[M+H]^+$ (calcd. 335.0251 for $C_{11}H_{16}IN_2O_2^+$).

Synthesis of 8

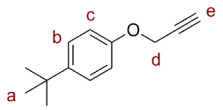

To a solution of 4-*tert*-butylphenol (300 mg, 1.99 mmol, 1.00 equiv) in 2-butanone (35 mL), was added K_2CO_3 (1.38 g, 9.95 mmol, 5.00 equiv) and propargyl bromide (80 wt.% in toluene, 0.70 mL, 5.99 mmol, 3.00 equiv) and the mixture was stirred at 70 °C for 15 h. H_2O (40 mL) was added and the phases separated. The aqueous layer was extracted with ether (2 × 30 mL). The combined organic extracts were dried over $MgSO_4$ and the solvent removed under reduced pressure. The crude was purified by column chromatography (SiO_2, petroleum ether/CH_2Cl_2 2:1) to yield **8** (341 mg, 91%) as a yellow oil. ^1H NMR (400 MHz, $CDCl_3$): δ = 7.39 (d, J = 8.9 Hz, 2H, H_b), 6.99 (d, J = 8.9 Hz, 2H, H_c), 4.72 (d, J = 2.4 Hz, 2H, H_d), 2.56 (t, J = 2.4 Hz, 1H, H_e), 1.38 (s, 9H, H_a). ^{13}C NMR (100 MHz, $CDCl_3$): δ = 155.4, 144.3, 126.4, 114.4, 79.0, 75.5, 55.8, 34.2, 31.6. HRMS ($APCI^+$): m/z = 189.1272 $[M+H]^+$ (calcd. 189.1274 for $C_{13}H_{17}O^+$).

Synthesis of S13

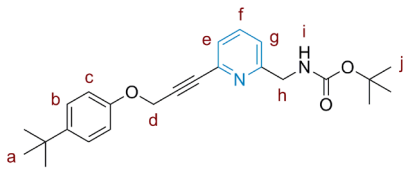

To a solution of **S12** (2.50 g, 7.50 mmol, 1.00 equiv) and **8** (1.66 g, 9.35 mmol, 1.25 equiv) in degassed THF/Et_3N (3:1 40 mL), was added $Pd(PPh_3)_4$ (433 mg, 0.38 mmol, 0.05 equiv) and CuI (107 mg, 0.56 mmol, 0.08 equiv) and the solution stirred at 45 °C for 22 h. The reaction mixture was cooled to room temperature, poured into ammonia solution (10%, 200 mL), and extracted with CH_2Cl_2 (3 × 50 mL). The organic layer was washed with brine (2 × 50 mL), dried over $MgSO_4$, filtered, and concentrated under reduced pressure. The residue was purified by column chromatography (SiO_2, CH_2Cl_2/MeOH 99.5:0.5) to yield **S13** (2.60 g, 88%) as a brown solid. ^1H NMR (500 MHz, $CDCl_3$): δ = 7.60 (t, J = 7.8 Hz, 1H, H_f), 7.35–7.28 (m, 3H, H_{b+e}), 7.23 (d, J = 7.8 Hz, 1H, Hg), 6.96 (d, J = 8.9 Hz, 2H, H_c), 5.52 (br, 1H, H_i), 4.90 (s, 2H, H_d),

4.41 (d, J = 5.4 Hz, 2H, H_h), 1.45 (s, 9H, H_j), 1.29 (s, 9H, H_a). ^{13}C NMR (125 MHz, $CDCl_3$): δ = 158.4, 156.1, 155.7, 144.5, 141.9, 137.1, 126.5, 126.1, 121.6, 114.5, 86.1, 84.7, 79.8, 56.7, 45.9, 34.3, 31.6, 28.5. HRMS (ESI$^+$): m/z = 395.2332 $[M+H]^+$ (calcd. 395.2329 for $C_{24}H_{31}O_3N_2^+$).

Synthesis of S14

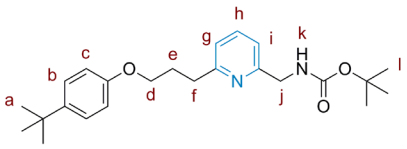

A mixture of **S13** (200 mg, 0.51 mmol, 1.00 equiv), K_2CO_3 (0.35 g, 2.53 mmol, 5.00 equiv) and $Pd(OH)_2/C$ (20.0 mg, 10%w) in THF (20 mL) was stirred under a H_2 atmosphere at room temperature for 5h. The resulting mixture was filtered through a pad of Celite® and the filtrate concentrated under reduced pressure to afford **S14** (200 mg, 98%) as a brown oil. ^1H NMR (400 MHz, $CDCl_3$): δ = 7.60 (t, J = 7.7 Hz, 1H, H_h), 7.32 (d, J = 8.8 Hz, 2H, H_b), 7.11 (m, 2H, H_{g+i}), 6.85 (d, J = 8.8 Hz, 2H, H_c), 5.63 (br, 1H, H_k), 4.45 (d, J = 4.7 Hz, 2H, H_j), 4.01 (t, J = 6.2 Hz, 2H, H_d), 3.00 (t, J = 7.5 Hz, 2H, H_f), 2.34–2.17 (m, 2H, H_e), 1.49 (s, 9H, H_l), 1.32 (s, 9H, H_a). ^{13}C NMR (125 MHz, $CDCl_3$): δ = 160.8, 156.8, 156.8, 156.1, 143.3, 137.0, 126.2, 121.4, 119.0, 114.0, 79.4, 67.1, 45.8, 34.5, 34.1, 31.6, 29.2, 28.5. HRMS (ESI$^+$): m/z = 399.2640 $[M+H]^+$ (calcd. 399.2642 for $C_{24}H_{35}O_3N_2^+$).

Synthesis of 9

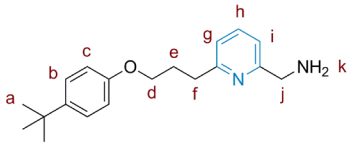

A solution of **S14** (200 mg, 0.50 mmol, 1.00 equiv) in $CHCl_3/CF_3COOH$ (1:1, 8 mL) was stirred at room temperature for 4 h. The resulting mixture was basified with K_2CO_3 until pH>10 and the extracted with CH_2Cl_2 (3 × 25 mL). The combined organic extracts were dried with $MgSO_4$ and the solvent was reduced under reduced pressure to yield **9** (140 mg, 96%) as a brown oil. ^1H NMR (500 MHz, $CDCl_3$): δ = 7.54 (t, J = 7.6 Hz, 1H, H_h), 7.28 (d, J = 8.8 Hz, 2H, H_b), 7.09 (d, J = 7.8 Hz, 1H, H_i), 7.05 (d, J = 7.7 Hz, 1H, H_g), 6.82 (d, J = 8.8 Hz, 2H, H_c), 3.99 (m, 4H, H_{d+j}), 3.58 (br, 2H, H_k), 2.95 (t, J = 7.6 Hz, 2H, H_f), 2.21 (m, 2H, H_e), 1.29 (s, 9H, H_a). ^{13}C NMR (125 MHz, $CDCl_3$): δ = 161.0, 159.4,

156.8, 143.3, 137.1, 126.3, 121.4, 118.8, 114.0, 67.1, 46.8, 34.7, 34.1, 31.6, 29.3. HRMS (ESI$^+$): *m/z* = 299.2122 [M+H]$^+$ (calcd. 299.2118 for $C_{19}H_{27}ON_2^+$).

Synthesis of 19

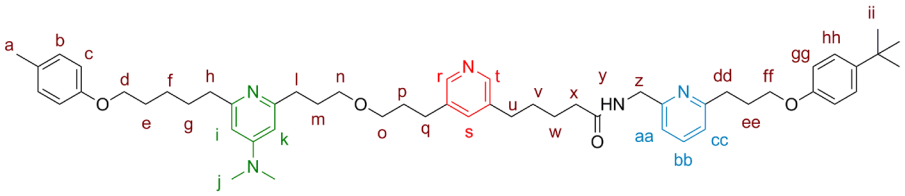

To a solution of **S10** (200 mg, 0.34 mmol, 1.00 equiv), **9** (120 mg, 0.40 mmol, 1.20 equiv) and PyBroP (190 mg, 0.40 mmol, 1.20 equiv) in DMF (15 mL) under N_2 at 0 °C, was added DIPEA (0.18 mL, 1.02 mmol, 3.00 equiv). The resulting mixture was allowed to reach room temperature while stirring for 4 h. The reaction was quenched by addition of aqueous $KHSO_4$ 1 M (10 mL). The mixture was diluted with brine (40 mL) and extracted with CH_2Cl_2 (3 × 75 mL). The combined organic extracts were washed with brine (75 mL) and aqueous LiCl 5% (2 × 75 mL) and dried over $MgSO_4$. The solvent was removed under reduced pressure and the crude mixture purified by column chromatography (SiO_2, CH_2Cl_2/MeOH/Et_3N 94.5:5:0.5) to afford **19** (250 mg, 86%) as a colourless oil. ^{1}H NMR (400 MHz, $CDCl_3$): δ = 8.23 (m, 2H, H_{r+t}), 7.52 (t, *J* = 7.7 Hz, 1H, H_{bb}), 7.30 (s, 1H, H_s), 7.26 (d, *J* = 8.7 Hz, 2H, H_{gg}), 7.05 (d, *J* = 8.4 Hz, 2H, H_b), 7.09–6.98 (m, 2H, H_{aa+cc}), 6.79 (d, *J* = 8.7 Hz, 2H, H_{hh}), 6.74 (d, *J* = 8.4 Hz, 2H, H_c), 6.32 (d, *J* = 2.4 Hz, 1H, H_i), 6.26 (d, *J* = 2.4 Hz, 1H, H_k), 4.49 (d, *J* = 4.9 Hz, 2H, H_z), 3.95 (t, *J* = 6.2 Hz, 2H, H_{ff}), 3.89 (t, *J* = 6.3 Hz, 2H, H_d), 3.47 (t, *J* = 6.0 Hz, 2H, H_n), 3.39 (t, *J* = 6.2 Hz, 2H, H_o), 3.11 (s, 6H, H_j), 3.05 (t, *J* = 7.5 Hz, 2H, H_l), 2.98 (t, *J* = 7.7 Hz, 2H, H_q), 2.92 (t, *J* = 7.6 Hz, 2H, H_{dd}), 2.65–6.54 (m, 4H, H_{h+u}), 2.30 (t, *J* = 7.1 Hz, 2H, H_x), 2.24 (s, 3H, H_a), 2.21–2.13 (m, 2H, H_{ee}), 2.12–2.00 (m, 2H, H_m), 1.88–1.74 (m, 6H, H_{e+g+p}), 1.72–1.59 (m, 4H, H_{v+w}), 1.60–1.48 (m, 2H, H_f), 1.26 (s, 9H, H_{ii}). ^{13}C NMR (100 MHz, $CDCl_3$): δ = 172.9, 160.8, 157.0, 156.8, 156.0, 147.6, 143.4, 137.2, 136.0, 129.9, 129.8, 126.3, 121.5, 119.4, 114.4, 114.0, 103.9, 103.6, 69.9, 69.7, 67.8, 67.1, 44.5, 40.0, 36.4, 34.6, 34.1, 32.8, 31.6, 31.1, 30.9, 30.0, 29.5, 29.5, 29.3, 29.0, 25.7, 25.4, 20.5. HRMS (ESI$^+$): *m/z* = 856.5727 [M+H]$^+$ (calcd. 856.5735 for $C_{54}H_{74}N_5O_4^+$).

Synthesis of L1Pd-(2,6-DMAP)

Synthesis of 11

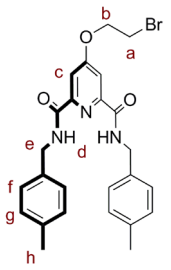

To a solution of **10** (1.50 g, 3.85 mmol, 1.00 equiv) and 1,2-dibromoethane (3.62 g, 19.2 mmol, 5.00 equiv) in acetone (30 mL), was added K_2CO_3 (2.65 g, 19.2 mmol, 5.00 equiv) and the suspension was refluxed for 18 h. The solvent was removed under reduced pressure and the residue washed with water, extracted with butanone, and dried over $MgSO_4$. The crude product was purified by column chromatography (SiO_2, CH_2Cl_2/MeOH 95:5) to give **11** (1.38 g, 72%) as a brown solid. m.p. 121-123 °C. ^{1}H NMR (400 MHz, $CDCl_3$): δ = 7.92 (t, 2H, H_d), 7.90 (s, 2H, H_c), 7.22 (d, J = 8.0 Hz, 4H, H_f), 7.14 (d, J = 8.0 Hz, 4H, H_g), 4.62 (d, J = 6.1 Hz, 4H, H_e), 4.47 (t, J = 6.1 Hz, 2H, H_b), 3.68 (t, J = 6.1 Hz, 2H, H_a), 2.34 (s, 6H, H_h). ^{13}C NMR (100 MHz, $CDCl_3$): δ = 166.9, 163.5, 151.0, 137.3, 135.1, 129.5, 127.8, 111.4, 68.3, 43.3, 28.0, 21.2. HRMS (ESI$^+$): m/z = 496.1225 $[M+H]^+$ (calcd. 496.1230 for $C_{25}H_{27}BrN_3O_3^+$).

Synthesis of 12

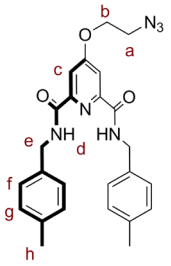

A solution of **11** (1.08 g, 2.17 mmol, 1.00 equiv), NaN_3 (1.43 g, 22.0 mmol, 10.0 equiv) and NaI (50.0 mg, 0.33 mmol, 0.15 equiv) in DMF (10 mL) was stirred at 90 °C for 18 h. The solvent was removed under reduced pressure. The residue was dissolved in CH_2Cl_2, washed with H_2O, and dried over $MgSO_4$. The crude product was purified by flash column chromatography (SiO_2, petroleum ether/EtOAc 3:1) to yield **12** (810 mg, 81%) as a pale, yellow oil. ^{1}H NMR (500 MHz, $CDCl_3$): δ = 7.97 (t, J = 6.1 Hz, 2H, H_d),

7.90 (s, 2H, H_c), 7.21 (d, J = 8.0 Hz, 4H, H_f), 7.12 (d, J = 8.0 Hz, 4H, H_g), 4.61 (d, J = 6.1 Hz, 4H, H_e), 4.30 (t, J = 6.1 Hz, 2H, H_a), 3.67 (t, J = 6.1 Hz, 2H, H_b), 2.33 (s, 6H, H_h). ^{13}C NMR (125 MHz, $CDCl_3$): δ = 167.2, 163.3, 151.2, 137.5, 135.1, 129.6, 127.9, 111.6, 67.8, 49.8, 43.5, 21.3. HRMS (ESI$^+$): m/z = 459.2137 $[M+H]^+$ (calcd. 459.2139 for $C_{25}H_{27}N_6O_3^+$).

Synthesis of 13

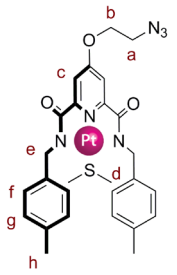

Azide **12** (1.51 g, 3.30 mmol, 1.00 equiv) was dissolved in THF (20 mL) and purged with nitrogen for 20 min. NaH (290 mg, 7.26 mmol, 2.20 equiv) was added and the mixture stirred at room temperature for 2 h. The reaction mixture was then cooled to 0 °C and protected from light. $PtCl_2(SMe_2)_2$ (2.32 g, 5.93 mmol, 1.80 equiv) was added and the reaction stirred for 18 h. The solvent was removed under reduced pressure and the residue purified by flash column chromatography (SiO_2, CH_2Cl_2/MeOH 99:1) to give **13** (1.50 g, 64%) as an orange solid. m.p. 260 °C (dec.). ^{1}H NMR (500 MHz, $CDCl_3$): δ = 7.40 (s, 2H, H_c), 7.16 (d, J = 7.9 Hz, 4H, H_f), 7.06 (d, J = 7.9 Hz, 4H, H_g), 4.77 (s, 6H, H_e), 4.33 (t, J = 4.8 Hz, 2H, H_b), 3.71 (t, J = 4.8 Hz, 2H, H_a), 2.27 (s, 6H, H_h), 1.81 (s, 6H, H_d). ^{13}C NMR (125 MHz, $CDCl_3$): δ = 172.2, 169.1, 152.3, 137.0, 136.1, 129.2, 126.6, 111.2, 68.6, 50.2, 49.7, 22.1, 21.2. HRMS (ESI$^+$): m/z = 714.1823 $[M+H]^+$ (calcd. 714.1821 for $C_{27}H_{31}N_6O_3PtS^+$).

Synthesis of 15

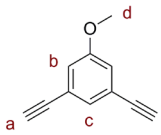

To a solution of 3,5-dibromoanisole (2.66 g, 10.0 mmol, 1.00 equiv) and trimethylsilylacetylene (4.30 mL, 30.0 mmol, 3.00 equiv) in degassed THF/Et_3N (2:1, 30 mL) was added $PdCl_2(PPh_3)_2$ (705 mg, 1.00 mmol, 0.10 equiv) and CuI (285 mg, 1.50 mmol, 0.15 equiv) and the solution was stirred at 65 °C for 16 h. The reaction mixture was cooled to room temperature, and a solution of KOH in methanol (1 M,

50 mL) was added. The reaction mixture was stirred for 1 h at room temperature, poured into brine (150 mL), and extracted with CH_2Cl_2 (3 × 50 mL). The organic layer was dried over $MgSO_4$, filtered, and concentrated under reduced pressure. The residue was purified by column chromatography (SiO_2, petroleum ether/EtOAc 98:2) to yield **15** (1.47 g, 94%) as colourless crystals. m.p. 63-65 °C. ^{1}H NMR (400 MHz, $CDCl_3$): δ = 7.22 (t, J = 1.3 Hz, 1H, H_c), 7.01 (d, J = 1.3 Hz, 2H, H_b), 3.80 (s, 3H, H_d), 3.07 (s, 2H, H_a). ^{13}C NMR (100 MHz, $CDCl_3$): δ = 159.2, 128.41, 123.5, 118.4, 82.7, 77.8, 55.6. HRMS (EI$^+$): m/z = 156.0572 $[M]^+$ (calcd. 156.0570 for $C_{11}H_8O^+$).

Synthesis of 16

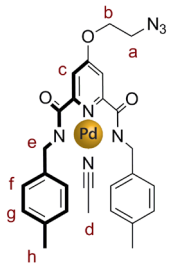

To a solution of **12** (780 mg, 1.72 mmol, 1.00 equiv) in MeCN (25 mL) was added $Pd(OAc)_2$ (460 mg, 2.06 mmol, 1.15 equiv) and the resulting mixture was stirred at room temperature for 16 h. A yellow precipitate was formed, filtered off and rinsed with ice-cold CH_3CN to give **16** as a yellow/green solid (870 mg, 84%). ^{1}H NMR (400 MHz, $CDCl_3$/CD_3CN): δ = 7.22 (s, 2H, H_c), 7.17 (d, J = 7.9 Hz, 4H, H_g), 7.06 (d, J = 7.9 Hz, 4H, H_f), 4.46 (s, 4H, H_e), 4.25 (t, J = 4.8 Hz, 2H, H_b), 3.64 (m, 2H, H_a), 2.28 (s, 6H, H_h), 1.98 (s, 3H, H_d). ^{13}C NMR (125 MHz, $CDCl_3$): δ = 170.5, 168.7, 154.9, 138.7, 135.8, 129.0, 127.4, 111.5, 111.0, 68.5, 50.1, 43.3, 21.2, 2.1. HRMS m/z = 602.1094 $[M–2H+H]^+$ (calcd. 602.1132 for $C_{27}H_{26}N_7O_3Pd^+$).

Synthesis of 17

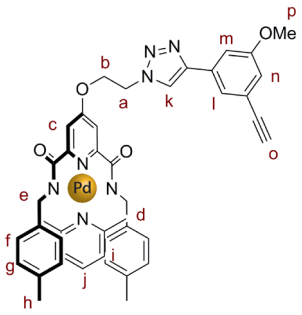

To a solution of compound **16** (300 mg, 0.50 mmol, 1.00 equiv) in CH_2Cl_2 (6.0 mL) was added 2,6-lutidine (60 µL, 0.50 mmol, 1.00 equiv) and the reaction stirred at room temperature for 3 h. The solution was purged with N_2 for 20 min. and DIPEA (130 µl, 1.50 equiv) and **15** (320 mg, 5.00 equiv) were added. The reaction was stirred at room temperature for 5 min. $Cu(CH_3CN)_4{\cdot}PF_6$ (37.0 mg, 20% mol) and a catalytic amount of TBTA were added to the reaction which was stirred at room temperature for 12 h. The solvent was removed under reduced pressure and the residue purified by column chromatography (SiO_2, CH_2Cl_2/MeOH 98:2) to yield **17** (330 mg, 80%) as a pale, yellow solid. ^{1}H NMR (500 MHz, $CDCl_3$): δ = 7.95 (s, 1H, H_k), 7.62 (t, J = 7.7 Hz, 1H, H_j), 7.52 (t, J = 1.3 Hz, 1H, H_m), 7.49 (dd, J = 2.4, 1.3 Hz, 1H, $H_{l/n}$), 7.36 (s, 2H_c), 7.01 (dd, J = 2.4, 1.3 Hz, 1H, $H_{l/n}$), 6.94 (d, J = 7.7 Hz, 2H, H_i), 6.80 (d, J = 7.8 Hz, 4H, H_g), 6.44 (d, J = 7.8 Hz, 4H, H_f), 4.91 (t, J = 4.8 Hz, 2H, H_a), 4.63 (t, J = 4.8 Hz, 2H, H_b), 4.00 (s, 4H, H_e), 3.88 (s, 3H, H_p), 3.09 (s, 1H, H_o), 2.41 (s, 6H, H_d), 2.24 (s, 6H, H_h). ^{13}C NMR (125 MHz, $CDCl_3$): δ = 170.8, 167.9, 160.5, 160.0, 154.9, 147.4, 138.7, 138.0, 136.1, 131.9, 128.8, 127.4, 123.8, 122.8, 122.2, 121.2, 117.7, 112.2, 110.8, 83.3, 77.6, 67.7, 55.7, 55.5, 53.8, 49.4, 25.6, 21.2. HRMS (ESI$^+$): m/z = 826.2346 $[M+H]^+$ (calcd. 826.2333 for $C_{43}H_{42}N_7O_4Pd^+$); 848.2159 $[M+Na]^+$ (calcd. 848.2147 for $C_{43}H_{41}N_7NaO_4Pd^+$).

Synthesis of 20

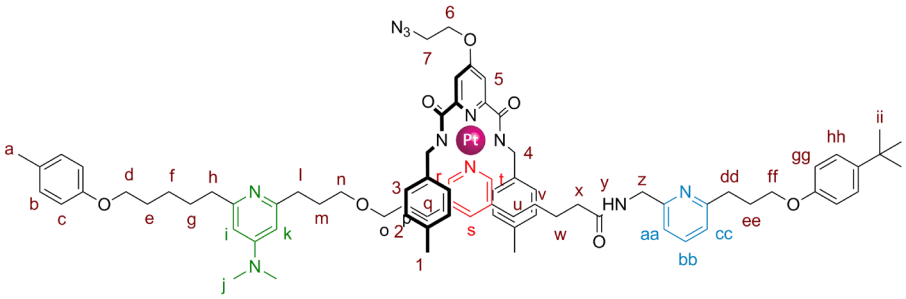

To a solution of **19** (150 mg, 0.18 mmol, 1.00 equiv) under N_2 in DMF (10 mL), was added a solution of **13** (150 mg, 0.21 mmol, 1.20 equiv) in CH_2Cl_2 (3 mL). The solution was stirred vigorously at room temperature for 16 h. The resulting mixture was concentrated under reduced pressure and the residue purified by column chromatography (SiO_2, CH_2Cl_2/MeOH/Et_3N 96.5:3:0.5) to yield **20** (173 mg, 62 %) as an orange solid. ^1H NMR (500 MHz, $CDCl_3$): δ = 7.78 (s, 1H, H_t), 7.62 (s, J = 1.2 Hz, 1H, H_r), 7.53 (t, J = 7.7 Hz, 1H, H_{bb}), 7.31 (s, 2H, H_5), 7.30 (br, 1H, H_s), 7.27 (d, J = 8.9 Hz, 2H, H_{gg}), 7.06 (d, J = 7.7 Hz, 2H, H_b), 7.03 (m, 2H, H_{aa+cc}), 6.96 (t, J = 5.0 Hz, 1H, H_y), 6.83 (d, J = 7.9 Hz, 4H, H_2), 6.81 (d, J = 8.8 Hz, 2H, H_{hh}), 6.73 (d, J = 8.6 Hz, 2H, H_c), 6.67 (d, J = 7.9 Hz, 4H, H_3), 6.41 (d, J = 2.5 Hz, 1H, $H_{k/i}$), 6.33 (d, J = 2.5 Hz, 1H, $H_{k/i}$), 4.50 (d, J = 5.0 Hz, 2H, H_z), 4.39 (d, J = 14.9 Hz, 2H, $H_{4/4'}$), 4.32 (m, 2H, H_6), 4.23 (d, J = 15.1 Hz, 2H, $H_{4/4'}$), 3.97 (t, J = 6.2 Hz, 2H, H_{ff}), 3.86 (t, J = 6.3 Hz, 2H, H_d), 3.67 (m, 2H, H_7), 3.43 (t, J = 6.0 Hz, 2H, H_n), 3.33 (t, J = 6.1 Hz, 2H, H_o), 3.13 (s, 6H, H_j), 2.93 (d, J = 7.9 Hz, 2H, H_{dd}), 2.83 (m, 2H, H_l), 2.72 (m, 2H, H_h), 2.36 (m, 2H, H_u), 2.30 (t, J = 7.4 Hz, 2H, H_x), 2.25 (m, 5H, H_{a+q}), 2.19 (m, 8H, H_{1+ee}), 1.98–1.88 (m, 2H, H_m), , 1.78–1.67 (m, 4H, H_{e+p}), 1.67–1.57 (m, 4H, H_{v+w}), 1.52–1.38 (m, 4H, H_{f+g}), 1.28 (s, 9H, H_{ii}). HRMS (ESI$^+$): m/z = 1507.7276 $[M+H]^+$ (calcd. 1507.7293 for $C_{79}H_{97}N_{11}O_7Pt^+$).

Synthesis of L1Pd-(2,6-*lutidine*)

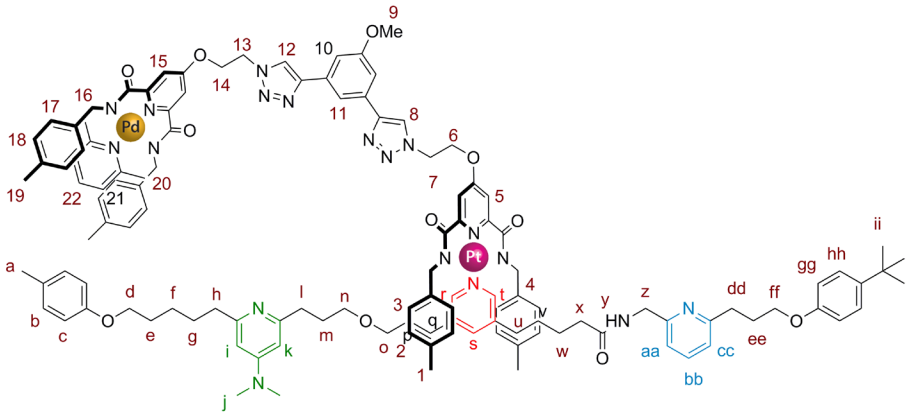

To a solution of **20** (150 mg, 0.10 mmol, 1.00 equiv) and **17** (90.0 g, 0.11 mmol, 1.10 equiv) in CH_2Cl_2 was added DIPEA (20.0 mg, 0.17 mmol, 1.50 equiv) *via* syringe. $Cu(CH_3CN)_4PF_6$ (15.0 mg, 0.04 mmol, 0.40 equiv) and a catalytic amount of TBTA were added forming an orange solution which was stirred under a nitrogen environment at room temperature for 12 h. The solvent was removed under reduced pressure and the crude residue purified by flash column chromatography (SiO_2, CH_2Cl_2/MeOH/Et_3N 95.5:4:0.5) to yield **L1**Pd-(2,6-*lutidine*) (220 mg, 85%) as a yellow solid. ^{1}H NMR (500 MHz, $CDCl_3$): δ = 8.35 (s, 1H, H_{12}), 8.29 (s, 1H, H_8), 7.69 (s, 1H, H_t), 7.66 (s, 1H, H_r), 7.61 (s, 1H, H_{11}), 7.60 (t, J = 6.4 Hz, 1H, H_{22}), 7.55 (s, 2H, H_{10}), 7.54 (t, 1H, H_{bb}), 7.42 (s, 2H, H_{15}), 7.40 (s, 2H, H_5), 7.28 (d, J = 8.9 Hz, 2H, H_{gg}), 7.19 (s, 1H, H_s), 7.02–7.09 (m, 2H, H_{aa+cc}), 7.05 (d, J = 8.3 Hz, 2H, H_b), 6.92 (d, J = 7.6 Hz, 2H, H_{21}), 6.83–6.75 (m, 12H, $H_{c+hh+2+18}$), 6.65 (d, J = 7.9 Hz, 4H, H_3), 6.43 (d, J = 7.9 Hz, 4H, H_{17}), 6.24 (d, J = 2.3 Hz, 1H, H_k), 6.22 (d, J = 2.3 Hz, 1H, H_i), 4.85–4.79 (m, 4H, H_{7+13}), 4.62 (br s, 4H, H_{6+14}), 4.52 (d, J = 4.7 Hz, 2H, H_z), 4.39–4.21 (m, 4H, H_4), 3.98 (s, 4H, H_{16}), 3.97 (t, J = 6.3 Hz, 2H, H_{ff}), 3.95 (s, 3H, H_9), 3.91 (t, J = 6.5 Hz, 2H, H_d), 3.46 (t, J = 6.5 Hz, 2H, H_n), 3.33 (t, J = 6.1 Hz, 2H, H_o), 2.97 (s, 6H, H_j), 2.96–2.92 (m, 2H, H_{dd}), 2.74 (t, J = 7.1 Hz, 2H, H_l), 2.68 (t, J = 7.2 Hz, 2H, H_h), 2.39 (s, 6H, H_{20}), 2.33–2.30 (m, 2H, H_q), 2.30–2.27 (m, 4H_{u+x}), 2.26 (s, 3H, H_a), 2.22 (s, 6H, H_{19}), 2.19 (s, 6H, H_1), 2.19–2.15 (m, 2H, H_{ee}), 2.02–1.95 (m, 2H, H_m), 1.82–1.77 (m, 2H, H_e), 1.77–1.73 (m, 2H, H_g), 1.69–1.63 (m, 2H, H_v), 1.62–1.54 (m, 2H, H_p), 1.48–1.52 (m, 2H, H_f), 1.48–1.43 (m, 2H, H_w), 1.28 (s, 9H, H_{ii}). ^{13}C NMR (125 MHz, $CDCl_3$): δ = 172.4, 171.6, 170.9, 168.3, 168.2, 160.9, 160.9, 160.5, 157.1, 156.8, 155.7, 154.8, 153.9, 150.0, 149.8, 147.9, 147.9, 143.5, 139.7, 138.7, 138.0, 137.5, 137.4, 137.3, 136.1, 135.4, 132.4, 130.1, 129.8, 128.8, 127.3, 126.5, 126.4, 122.8, 122.0, 121.9, 121.7, 119.5, 116.3, 114.5, 114.0, 111.4, 111.4, 111.1, 103.3, 103.1, 70.9, 69.5, 68.0, 67.8, 67.1,

55.8, 49.6, 49.4, 49.3, 46.4, 44.5, 39.4, 36.0, 34.7, 34.2, 32.3, 31.7, 30.4, 30.2, 30.1, 30.0, 29.8, 29.4, 29.3, 29.2, 26.1, 25.6, 25.3, 21.2, 20.6. HRMS (ESI$^+$): *m/z* = 2332.9570 $[M+H]^+$ (calcd. 2332.9548 for $C_{122}H_{139}N_{18}O_{11}PdPt^+$).

Synthesis of L1Pd-(2,6-*DMAP*)

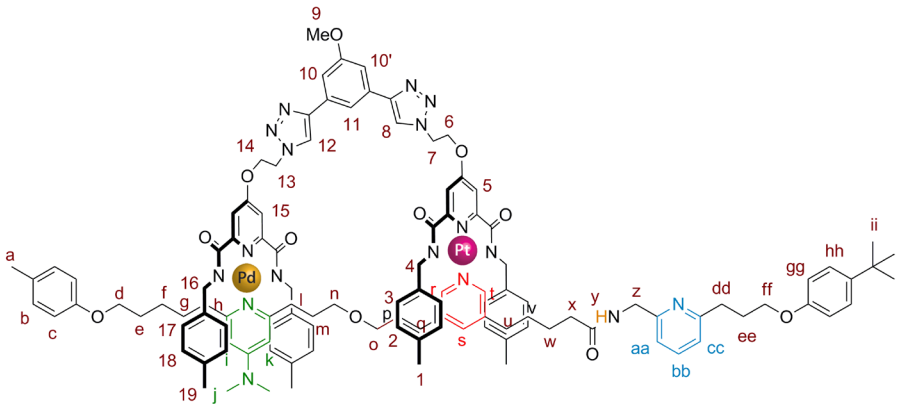

A solution of **L1**Pd-(2,6-*lutidine*) (96.0 mg, 0.04 mmol, 1.00 equiv) in CH_3Cl/CH_3CN (7:3, 250 mL, 0.16 mM) was stirred at 65 °C for 14 h. The solvent was removed under reduced pressure and the crude mixture purified by column chromatography (SiO_2, CH_2Cl_2/MeOH/Et_3N 95.5:4:0.5) to yield **L1**Pd-(2,6-*DMAP*) (69.0 mg, 76%) as a yellow solid. ^{1}H NMR (500 MHz, $CDCl_3$): δ = 8.55 (s, 1H, H_{12}), 8.17 (s, 1H, H_8), 7.78 (s, 1H, H_t), 7.70 (dd, *J* = 2.4, 1.4 Hz, 1H, $H_{10/10'}$), 7.60 (dd, *J* = 2.4, 1.4 Hz, 1H, $H_{10/10'}$), 7.53 (t, *J* = 7.7 Hz, 1H, H_{bb}), 7.42 (s, 2H, H_{15}), 7.42 (s, 1H, H_{11}), 7.38 (s, 1H, H_r), 7.28 (d, *J* = 8.9 Hz, 2H, H_{gg}), 7.19 (s, 1H, H_s), 7.19–7.17 (m, 1H, H_y), 7.06–7.03 (m, 4H, $H_{aa+cc+b}$), 6.98 (s, 2H, H_5), 6.81 (d, *J* = 8.7 Hz, 2H, H_{hh}), 6.81 (d, *J* = 7.7 Hz, 4H, H_{18}), 6.75 (d, *J* = 8.6 Hz, 2H, H_c), 6.70 (d, *J* = 7.6 Hz, 4H, H_2), 6.58 (d, *J* = 7.7 Hz, 4H, H_{17}), 6.56 (d, *J* = 7.6 Hz, 4H, H_3), 6.15 (d, *J* = 2.4 Hz, 1H, H_k), 6.10 (d, *J* = 2.4 Hz, 1H, H_i), 4.96 (t, *J* = 6.5 Hz, 2H, H_7), 4.92 (t, *J* = 4.6 Hz, 2H, H_{13}), 4.59 (t, *J* = 4.6 Hz, 2H, H_{14}), 4.52 (d, *J* = 4.9 Hz, 2H, H_z), 4.49 (d, *J* = 15.5 Hz, 2H, $H_{4/4'}$), 4.26 (t, *J* = 6.5 Hz, 2H, H_6), 4.10 (d, *J* = 15.5 Hz, 2H, $H_{4/4'}$), 4.03 (d, *J* = 14.0 Hz, 2H, $H_{16/16'}$), 3.97 (t, *J* = 6.1 Hz, 2H, H_{ff}), 3.96 (s, 3H, H_9), 3.89 (d, *J* = 14.0 Hz, 2H, $H_{16/16'}$), 3.85 (t, *J* = 6.4 Hz, 2H, H_d), 3.31–3.25 (m, 4H, H_{n+o}), 3.11 (s, 6H, H_j), 2.95–2.92 (m, 2H, H_{dd}), 2.94–2.90 (m, 2H, H_l), 2.73–2.67 (m, 2H, H_h), 2.33 (t, *J* = 7.8 Hz, 2H, H_x), 2.30 (t, *J* = 7.3 Hz, 2H, H_u), 2.27 (s, 3H, H_a), 2.21 (s, 6H, H_{19}), 2.19–2.17 (m, 2H, H_{ee}), 2.18–2.15 (m, 2H, H_q), 2.14 (s, 6H, H_1), 1.73–1.61 (m, 6H, H_{e+m+v}), 1.60–1.47 (m, 6H, H_{f+p+w}), 1.28 (s, 9H, H_{ii}), 1.28–1.24 (m, 2H, H_g). ^{13}C NMR (125 MHz, $CDCl_3$): δ = 172.6, 171.5, 171.0, 167.9, 167.7, 162.4, 161.5, 161.1, 160.9, 157.0, 156.8, 156.0, 155.7, 154.3, 154.2, 150.1, 149.8,

148.3, 147.2, 143.5, 139.9, 139.3, 138.5, 137.3, 137.3, 137.1, 135.6, 135.6, 132.6, 132.2, 131.3, 130.0, 129.9, 128.8, 128.6, 127.8, 126.4, 126.4, 122.5, 122.2, 121.6, 119.3, 116.5, 114.5, 114.4, 114.4, 113.9, 111.4, 111.3, 111.2, 110.6, 103.8, 103.5, 103.3, 70.4, 70.0, 68.2, 67.8, 67.2, 67.1, 55.8, 53.6, 49.7, 49.6, 49.0, 48.3, 46.2, 44.6, 40.1, 39.6, 38.7, 36.0, 35.5, 34.7, 34.2, 32.5, 31.7, 30.2, 29.8, 29.7, 29.4, 29.3, 29.0, 28.7, 27.9, 27.5, 26.2, 25.3, 21.2, 20.6, 14.3, 9.2. LRMS (ESI$^+$): *m/z* = 2225.6 [M+H]$^+$; 2247.9 [M+Na]$^+$. HRMS (ESI$^+$): *m/z* = 1113.4441 [M+2H]$^{2+}$ (calcd. 1113.4448 for $C_{115}H_{131}N_{17}O_{11}PdPt^{2+}$).

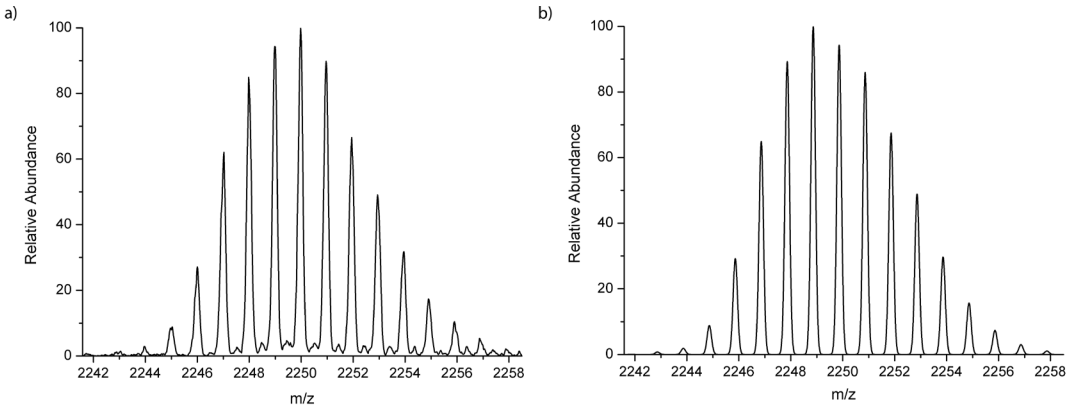

Figure 2.10 *- Isotopic mass distribution for* ***L1****Pd-(2,6-DMAP). LRESI$^+$: m/z = 2247.98 [M+Na]$^+$ (calcd. 2247.86 for $C_{115}H_{129}N_{17}O_{11}PdPtNa^+$): a) experimental; b) theoretical.*

Synthesis of L1Pd-(2,6-*Py*)

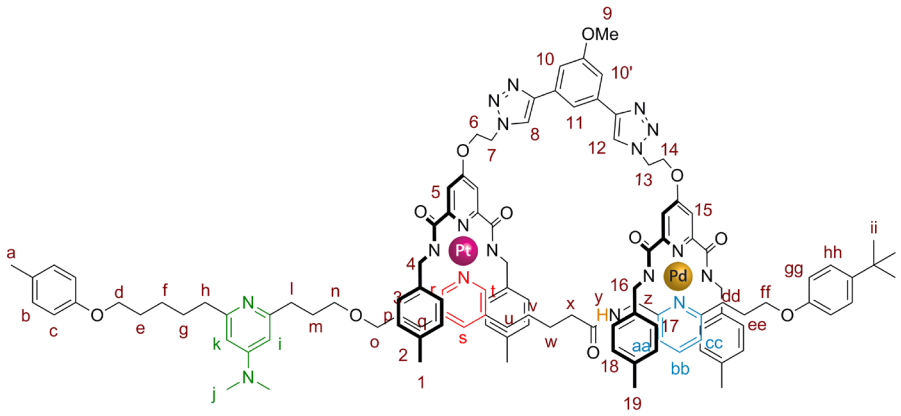

L1Pd-(2,6-*DMAP*) (17.0 mg, 7.60 μmol, 1.00 equiv) and CH_3SO_3H (1.00 equiv) were dissolved in a $CHCl_3/CH_3CN$ mixture (7:3, 76 mL, 0.1 mM) and heated at 65 ºC for 40 h. Toluene (50 mL) was added and the solvent slowly removed under reduced pressure. The residue was purified by preparative thin layer chromatography (SiO_2, CH_2Cl_2/MeOH 95:5) to yield **L1**Pd-(2,6-*Py*) (4.5 mg, 26%) as a yellow solid. ^{1}H NMR (500 MHz, CD_2Cl_2): δ = 8.69 (t, J = 6.3 Hz, 1H, H_y), 8.12 (s, 1H, H_{12}), 8.07 (s, 1H, H_8),

7.82 (s, 2H, H_5), 7.81 (s, 1H, H_r), 7.74 (t, *J* = 6.1 Hz, 1H, $H_{y'}$), 7.72 (s, 1H, H_t), 7.70 (t, *J* = 6.4 Hz, 1H, H_{bb}), 7.60 (t, *J* = 1.4 Hz, 1H, H_{11}), 7.54 (dd, *J* = 2.4, 1.4 Hz, 1H, $H_{10'}$), 7.46 (dd, *J* = 2.4, 1.4 Hz, 1H, H_{10}), 7.36 (dd, *J* = 7.6, 1.0 Hz, 1H, H_{aa}), 7.32 (s, 1H, H_s), 7.30–7.27 (m, 1H, H_{cc}), 7.29 (d, *J* = 8.8 Hz, 2H, H_{gg}), 7.19 (s, 2H, H_{15}), 7.09 (d, *J* = 8.0 Hz, 4H, H_{17}), 7.04 (d, *J* = 8.2 Hz, 2H, H_b), 6.97 (d, *J* = 8.0 Hz, 4H, H_{18}), 6.90 (d, *J* = 7.9 Hz, 4H, H_2), 6.86 (d, *J* = 8.8 Hz, 2H, H_{hh}), 6.76 (d, *J* = 8.2 Hz, 2H, H_c), 6.74 (d, *J* = 7.9 Hz, 4H, H_3), 6.34 (d, *J* = 2.8 Hz, 1H, H_i), 6.32 (d, *J* = 2.8 Hz, 1H, H_k), 5.90 (d, *J* = 6.0 Hz, 1H, $H_{z'}$), 4.89–4.85 (m, 4H, H_{7+13}), 4.67 (t, *J* = 4.8 Hz, 2H, H_{14}), 4.58 (t, *J* = 4.8 Hz, 2H, H_6), 4.49–4.44 (m, 8H, $H_{dd+z+16}$), 4.29 (d, *J* = 14.4 Hz, 4H, H_4), 4.16–4.12 (m, 2H, H_{ff}), 4.11–4.07 (m, 2H, H_h), 4.05–4.00 (m, 2H, H_l), 3.93 (s, 3H, H_9), 3.90 (t, *J* = 6.4 Hz, 3H, H_d), 3.56 (t, *J* = 6.7 Hz, 2h, H_n), 3.17 (t, *J* = 5.8 Hz, 2H, H_o), 3.02 (s, 6H, H_j), 2.60–2.55 (m, 2H, H_{ee}), 2.50–2.47 (m, 2H, H_q), 2.38–2.27 (m, 6H, H_{m+u+x}), 2.26 (s, 3H, H_a), 2.23 (s, 12H, H_{1+19}), 2.07–2.02 (m, 2H, H_g), 1.84–1.77 (m, 2H, H_e), 1.73–1.66 (m, 2H, H_f), 1.67–1.57 (m, 4H, H_{p+w}), 1.48 (s, 2H, H_v), 1.28 (s, 9H, H_{ii}). ^{13}C NMR (125 MHz, CD_2Cl_2): δ = 174.2, 172.4, 172.3, 171.9, 168.4, 167.4, 164.3, 163.8, 162.5, 161.4, 161.3, 161.3, 159.9, 157.6, 157.2, 156.0, 154.1, 152.0, 150.7, 150.6, 148.0, 147.9, 144.1, 140.1, 139.9, 139.6, 139.4, 137.9, 137.3, 136.2, 136.1, 133.1, 133.0, 130.3, 130.2, 129.6, 129.3, 128.0, 126.8, 126.8, 124.7, 124.4, 122.4, 121.8, 116.2, 114.8, 114.5, 111.6, 111.5, 111.2, 111.1, 105.8, 105.6, 70.8, 70.5, 68.9, 68.6, 68.3, 68.0, 67.6, 67.0, 65.7, 65.6, 63.9, 56.2, 50.1, 49.8, 49.7, 46.2, 43.5, 40.2, 39.7, 36.8, 36.5, 36.4, 34.6, 34.5, 33.6, 32.5, 32.3, 31.8, 30.3, 30.2, 30.2, 30.1, 30.1, 30.1, 30.0, 29.9, 29.9, 29.8, 29.7, 29.6, 29.4, 28.9, 28.9, 28.7, 26.5, 25.5, 25.4, 25.3, 23.3, 21.4, 21.3, 20.7, 14.4, 1.3. LRMS (ESI$^+$): *m/z* = 2226.0 $[M+H]^+$; 2248.0 $[M+Na]^+$.

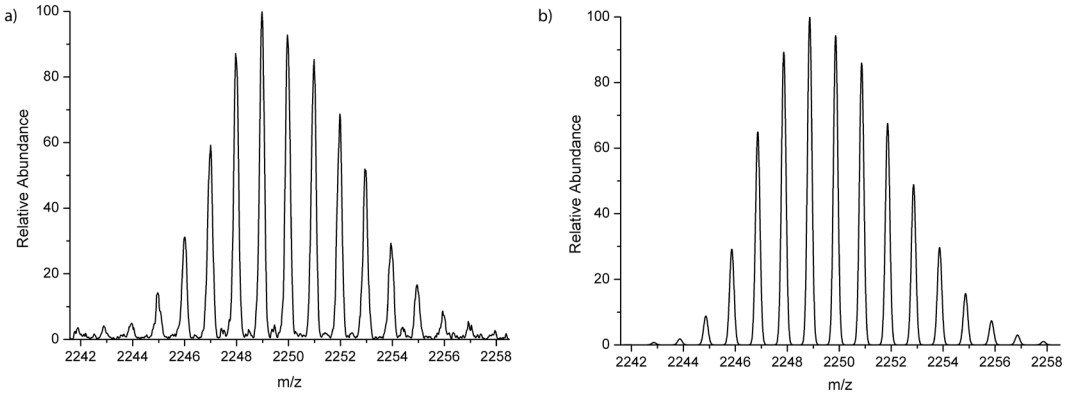

Figure 2.11 *- Isotopic mass distribution for* ***L1****Pd-(2,6-Py). LRESI$^+$: m/z = 2247.96 $[M+Na]^+$ (calcd. 2247.86 for $C_{115}H_{129}N_{17}O_{11}PdPtNa^+$): a) experimental; b) theoretical.*

Synthesis of Bimetallic Complex 21

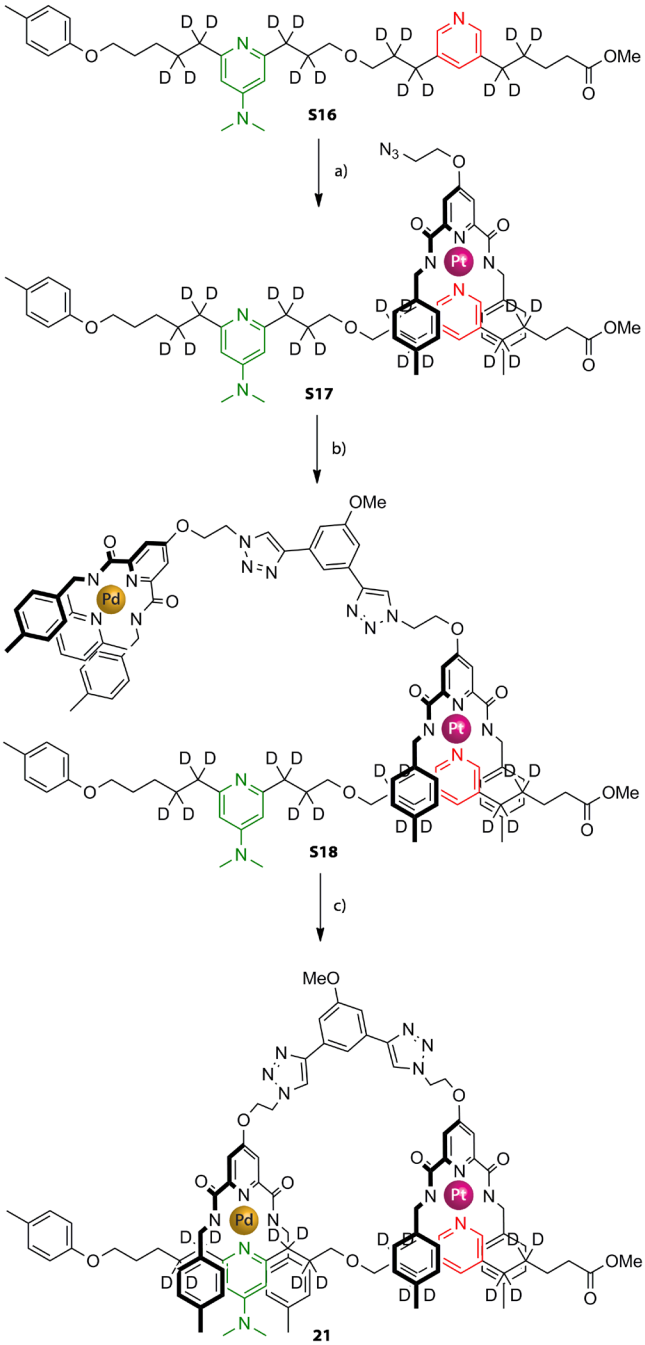

Scheme 2.8 *- Synthesis of bimetallic complex. Reagents and conditions: (a)* ***13****, DMF, 85%; (b)* ***17****, DIPEA, Cu(CH₃CN)₄·PF₆, TBTA, 88%; (c) DMF/CH₃CN (1:1), 0.2 mM, 67%.*

Synthesis of S16

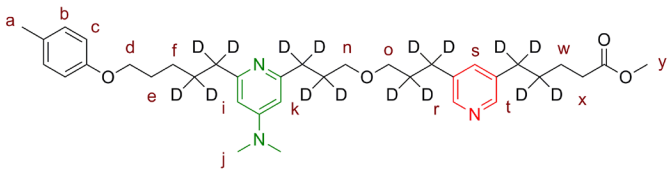

$Pd(OH)_2/C$ was stirred in D_2O for 16 h. D_2O was removed under reduced pressure and dried under high vacuum before use. **S9** (1.20 g, 2.10 mmol, 1.00 equiv) was dissolved in THF/methanol-d_4 (4:1, 50 mL) and degassed with N_2, followed by D_2. K_2CO_3 (14.0 mg, 0.10 mmol, 0.05 equiv) and $Pd(OH)_2/C$ (120 mg, 10 % weight) were added and the reaction continued to be purged with D_2 for an additional 10 min. before being allowed to stir for 16 h under a D_2 atmosphere. The crude residue was filtered through Celite®, and purified by column chromatography (SiO_2, CH_2Cl_2/MeOH 9:1) to yield **S16** (994 mg, 78%) as a colourless oil. ^1H NMR (500 MHz, $CDCl_3$): δ = 8.27 (d, J = 1.8 Hz, 1H, H_r), 8.26 (d, J = 1.8 Hz, 1H, H_y), 7.30 (t, J = 2.1 Hz, 1H, H_s), 7.05 (d, J = 8.4 Hz, 2H, H_b), 6.77 (d, J = 8.4 Hz, 2H, H_c), 6.25 (d, J = 2.3 Hz, 1H, H_k), 6.22 (d, J = 2.3 Hz, 1H, H_i), 3.91 (t, J = 6.6 Hz, 2H, H_d), 3.66 (s, 3H, H_y), 3.46 (s, 2H, H_n), 3.41 (s, 2H, H_o), 2.98 (s, 6H, H_j), 2.33 (t, J = 7.5 Hz, 2H, H_x), 2.27 (s, 3H, H_a), 1.83–1.76 (m, 2H, H_e), 1.65 (t, J = 7.5 Hz, 2H, H_w), 1.54–1.49 (m, 2H, H_f). ^{13}C NMR (125 MHz, $CDCl_3$): δ = 174.0, 161.5, 161.5, 157.1, 147.8, 147.6, 147.6, 136.9, 136.9, 135.9, 130.0, 130.0, 129.7, 114.5, 114.5, 103.2, 103.1, 70.5, 69.7, 68.1, 67.9, 51.7, 39.4, 33.9, 29.8, 29.3, 25.9, 25.9, 25.8, 24.5, 24.4, 20.6. HRMS (ESI$^+$): m/z = 606.4933 $[M+H]^+$ (calcd. 606.4940 for $C_{36}H_{36}D_{16}N_3O_4^+$).

Synthesis of S17

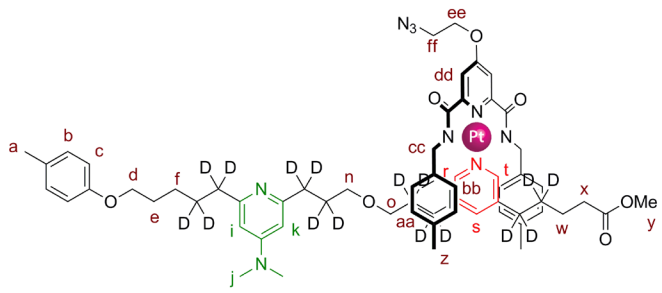

S16 (319 mg, 0.53 mmol, 1.00 equiv) was dissolved in DMF (5 mL) and a CH_2Cl_2 (5 mL) solution of **13** (375 mg, 0.53 mmol, 1.00 equiv) was added dropwise. The reaction was stirred vigorously for 16 h. The solvent was removed under reduced pressure and the crude product was purified by column chromatography (SiO_2, CH_2Cl_2/MeOH/Et_3N

98.5:2:0.5) to yield **S17** (568 mg, 85%) as a yellow solid. ^{1}H NMR (500 MHz, $CDCl_3$): δ = 7.72 (d, J = 1.9 Hz, 1H, H_t), 7.71 (d, J = 1.9 Hz, 1H, H_r), 7.37 (s, 2H, H_{dd}), 7.20 (t, J = 1.9 Hz, 1H, H_s), 7.06 (d, J = 8.4 Hz, 2H, H_c), 6.85 (d, J = 7.9 Hz, 4H, H_{aa}), 6.78 (d, J = 8.4 Hz, 2H, H_b), 6.69 (d, J = 7.9 Hz, 4H, H_{bb}), 6.24 (d, J = 2.3 Hz, 1H, H_k), 6.22 (d, J = 2.3 Hz, 1H, H_i), 4.36 (s, 4H, H_{cc}), 4.33 (t, J = 4.3 Hz, 2H, H_{ee}), 3.92 (t, J = 6.6 Hz, 2H, H_d), 3.73–3.69 (m, 2H, H_{ff}), 3.69 (s, 3H, H_y), 3.47 (s, 2H, H_n), 3.36 (s, 2H, H_o), 2.97 (s, 6H, H_j), 2.33 (t, J = 7.4 Hz, 2H, H_x), 2.27 (s, 3H, H_a), 2.22 (s, 6H, H_z), 1.84–1.76 (m, 2H, H_e), 1.60 (t, J = 7.4 Hz, 2H, H_w), 1.55–1.48 (m, 2H, H_f). ^{13}C NMR (125 MHz, $CDCl_3$): δ = 173.7, 171.7, 168.4, 162.0, 157.1, 155.5, 153.9, 150.1, 149.9, 137.6, 137.4, 135.4, 130.0, 129.8, 128.8, 126.6, 114.5, 111.0, 103.2, 103.0, 70.9, 69.4, 68.4, 68.1, 51.8, 49.5, 49.6, 39.4, 33.8, 33.6, 32.1, 30.3, 29.9, 29.5, 29.4, 26.9, 25.9, 24.4, 22.8, 21.1, 20.6, 14.3. HRMS (ESI$^+$): m/z = 1257.6444 $[M+H]^+$ (calcd. 1257.6449 for $C_{61}H_{60}D_{16}N_9O_7Pt^+$).

Synthesis of S18

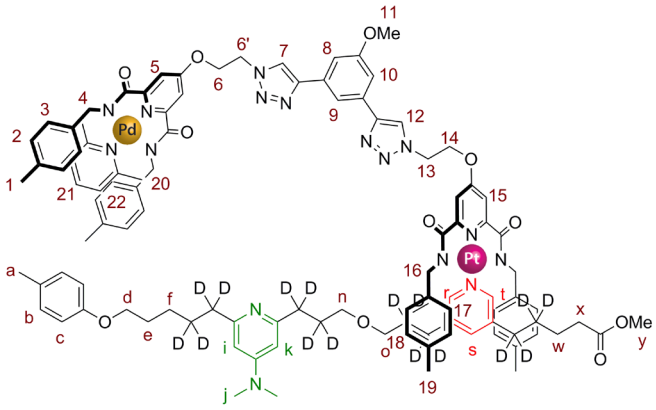

Compounds **S17** (480 mg, 0.38 mmol, 1.00 equiv) and **17** (318 g, 0.38 mmol, 1.00 equiv) were dissolved in CH_2Cl_2 (25 mL) and the reaction mixture purged with N_2 for 20 min. DIPEA (100 μL, 1.50 equiv) was added and the mixture stirred for 5 min. $Cu(CH_3CN)_4{\cdot}PF_6$ (37.0 mg, 0.20 equiv) and a catalytic amount of TBTA were added to the reaction which was stirred at room temperature for 14 h. The solvent was removed under reduced pressure and the residue purified by flash column chromatography (SiO_2, CH_2Cl_2/MeOH/Et_3N 94.5:5:0.5) to yield **S18** (706 mg, 88%) as an orange oil. ^{1}H NMR (400 MHz, $CDCl_3$): δ = 8.35 (s, 1H, $H_{7/12}$), 8.28 (s, 1H, $H_{7/12}$), 7.70 (d, J = 1.5 Hz, 1H, H_t), 7.66 (d, J = 1.5 Hz, 1H, H_r), 7.63–7.60 (m, 1H, H_9), 7.61–7.57 (m, 1H, H_{22}), 7.56–7.53 (m, 2H, H_{8+10}), 7.43 (s, 2H, H_5), 7.41 (s, 2H, H_{15}), 7.19 (s, 1H, H_s), 7.05 (d, J = 8.2 Hz, 2H, H_b), 6.92 (d, J = 7.8 Hz, 2H, H_{21}), 6.81 (d, J = 7.9 Hz, 4H, H_{18}), 6.79 – 6.75 (m, 6H, H_{2+c}),

6.66 (d, J = 7.9 Hz, 4H, H_{17}), 6.42 (d, J = 7.9 Hz, 4H, H_3), 6.24 (d, J = 1.5 Hz, 1H, H_k), 6.23 (d, J = 1.5 Hz, 1H, H_i), 4.86–4.79 (m, 4H, $H_{6'+13}$), 4.60–4.65 (m, 4H, H_{6+14}), 4.32 (d, J = 6.2 Hz, 4H, H_{16}), 3.98 (s, 4H, H_4), 3.95 (s, 3H, H_{11}), 3.91 (t, J = 6.5 Hz, 2H, H_d), 3.67 (s, 3H, H_y), 3.47 (s, 2H, H_n), 3.35 (s, 2H, H_o), 3.00 (s, 6H, H_j), 2.38 (s, 6H, H_{20}), 2.31 (t, J = 7.4 Hz, 2H, H_x), 2.26 (s, 3H, H_a), 2.22 (s, 6H, H_1), 2.20 (s, 6H, H_{19}), 1.84–1.76 (m, 2H, H_e), 1.57 (t, J = 7.4 Hz, 2H, H_f), 1.54–1.48 (m, 2H, H_2).

Synthesis of 21

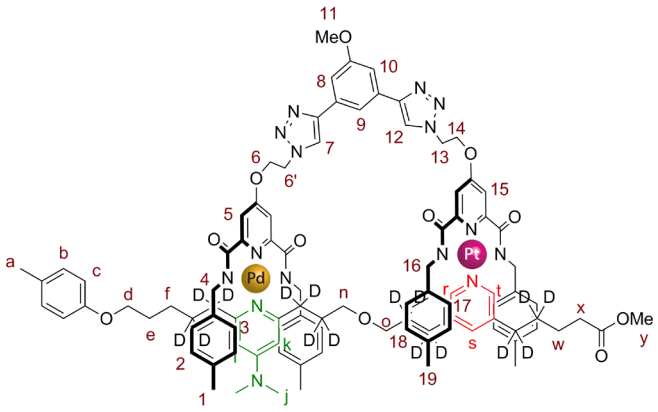

S18 (1.85 g, 0.89 mmol) was dissolved in DMF/MeCN 1:1 (4.0 L, 0.2 mM) and the reaction stirred at 65 °C for 5 h. The solvent was removed at 60 °C under reduced pressure. The orange residue was purified by column chromatography (SiO_2, CH_2Cl_2/MeOH 95:5) to yield **21** (1.18 g, 67%) as a yellow solid. ^{1}H NMR (500 MHz, $CDCl_3$): δ = 8.52 (s, 1H, H_{12}), 8.18 (s, 1H, H_7), 7.75 (d, J = 1.3 Hz, 1H, $H_{r/t}$), 7.69 (s, 1H, $H_{8/10}$), 7.62 (s, 1H, $H_{8/10}$), 7.48 (d, J = 1.3 Hz, 1H, $H_{r/t}$), 7.44 (s, 2H, H_5), 7.41 (s, 1H, H_9), 7.18 (t, J = 1.7 Hz, 1H, H_s), 7.08 (s, 2H, H_{15}), 7.05 (d, J = 8.4 Hz, 2H, H_b), 6.81 (d, J = 7.9 Hz, 4H, H_3), 6.75 (d, J = 8.4 Hz, 4H, H_c), 6.73 (d, J = 8.1 Hz, 4H, H_{17}), 6.62 (d, J = 8.1 Hz, 4H, H_{18}), 6.58 (d, J = 7.9 Hz, 4H, H_2), 6.16 (d, J = 2.6 Hz, 1H, H_i), 6.10 (d, J = 2.6 Hz, 1H, H_k), 4.96 (t, J = 6.3 Hz, 2H, H_{13}), 4.92 (t, J = 4.3 Hz, 2H, $H_{6'}$), 4.60 (t, J = 4.4 Hz, 2H, H_6), 4.42 (d, J = 15.0 Hz, 2H, H_{16}), 4.31 (t, J = 6.3 Hz, 2H, H_{14}), 4.20 (d, J = 15.0 Hz, 2H, $H_{16'}$), 4.08 (d, J = 13.9 Hz, 2H, H_4), 3.96 (s, 3H, H_a), 3.86 (d, J = 13.9 Hz, 2H, $H_{4'}$), 3.85 (t, J = 6.3 Hz, 2H, H_d), 3.68 (s, 3H, H_y), 3.28 (s, 4H, H_{n+o}), 3.11 (s, 6H, H_j), 2.34 (t, J = 7.3 Hz, 2H, H_x), 2.27 (s, 3H, H_a), 2.21 (s, 6H, H_1), 2.16 (s, 6H, H_{19}), 1.62–1.58 (m, 2H, H_w), 1.27–1.22 (m, 2H, H_f). ^{13}C NMR (125 MHz, $CDCl_3$): δ = 173.8, 172.5, 171.5, 171.1, 167.8, 167.7, 162.4, 162.4, 161.4, 161.0, 161.0, 156.9, 155.6, 154.3, 154.2, 154.1, 150.1, 149.8, 148.3, 147.2, 140.8, 139.5, 139.2, 139.2, 138.5, 137.3, 137.1, 135.6, 135.5, 132.5, 132.1, 132.1,

130.0, 129.8, 128.7, 128.6, 127.8, 127.7, 126.5, 126.4, 116.5, 114.3, 111.4, 111.3 111.2, 110.6, 103.4, 103.3, 70.3, 69.9, 68.1, 67.8, 67.2, 55.8, 51.8, 49.6, 48.9, 48.4, 46.0, 39.7, 33.6, 29.8, 29.4, 25.9, 24.4, 22.8, 21.2, 20.6. HRMS (ESI^+): *m/z* = 1996.7784 $[M–H+Na]^+$ (calcd. 1996.7764 for $C_{97}H_{90}D_{16}N_{15}O_{11}PdPtNa^+$).

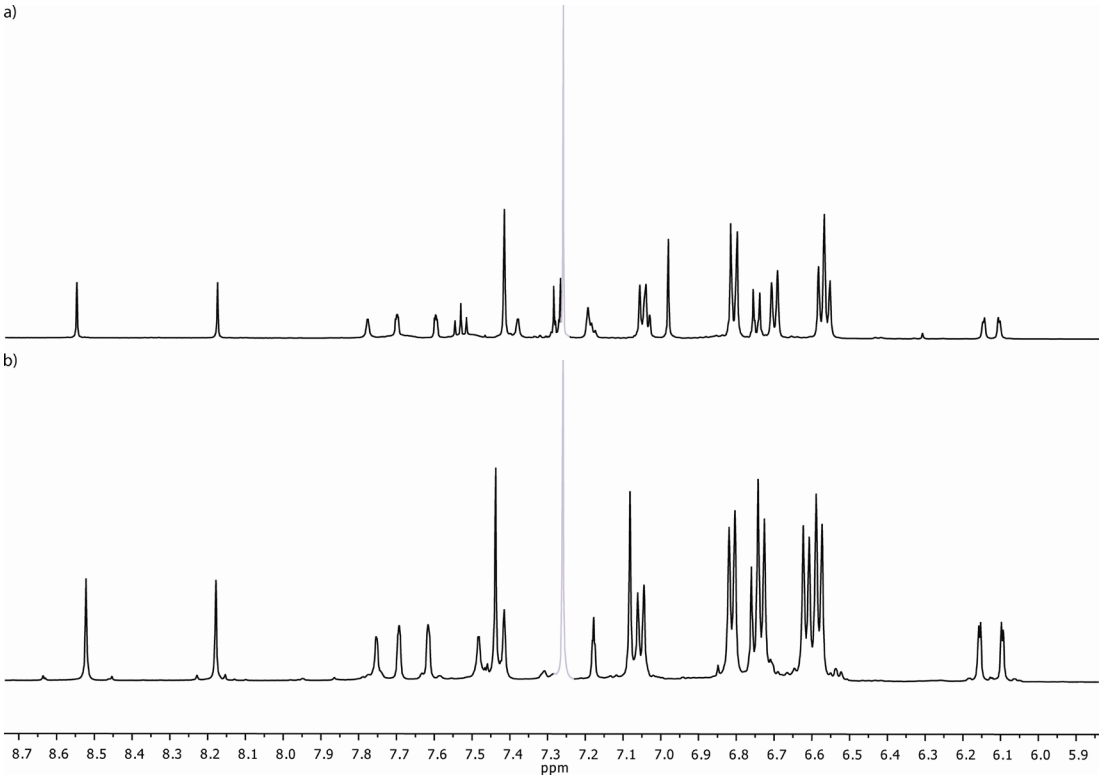

Figure 2.12 - *Partial ^1H NMR (500 MHz, $CDCl_3$) of : a)* ***21****; (b)* ***L1****Pd-(2,6-DMAP).*

General Procedure for the Protonation-Driven Switching of L1Pd

Stock solutions of **L1**Pd-(2,6-*DMAP*) (2.0 mM in $CDCl_3$) and CH_3SO_2H (2.0 mM in $CDCl_3$) were prepared. Aliquots (0.5 mL) of each solution were mixed and $CDCl_3$ (6.0 mL) and CD_3CN (3.0 mL) were added to obtain a 1:1 solution of **L1**Pd-(2,6-*DMAP*) (0.1 mM) and CH_3SO_2H (0.1 mM) in $CDCl_3/CD_3CN$ (7:3). Aliquots of this solution (0.5 mL) were heated at 65 °C or maintained at room temperature and monitored by ^1H NMR spectroscopy.

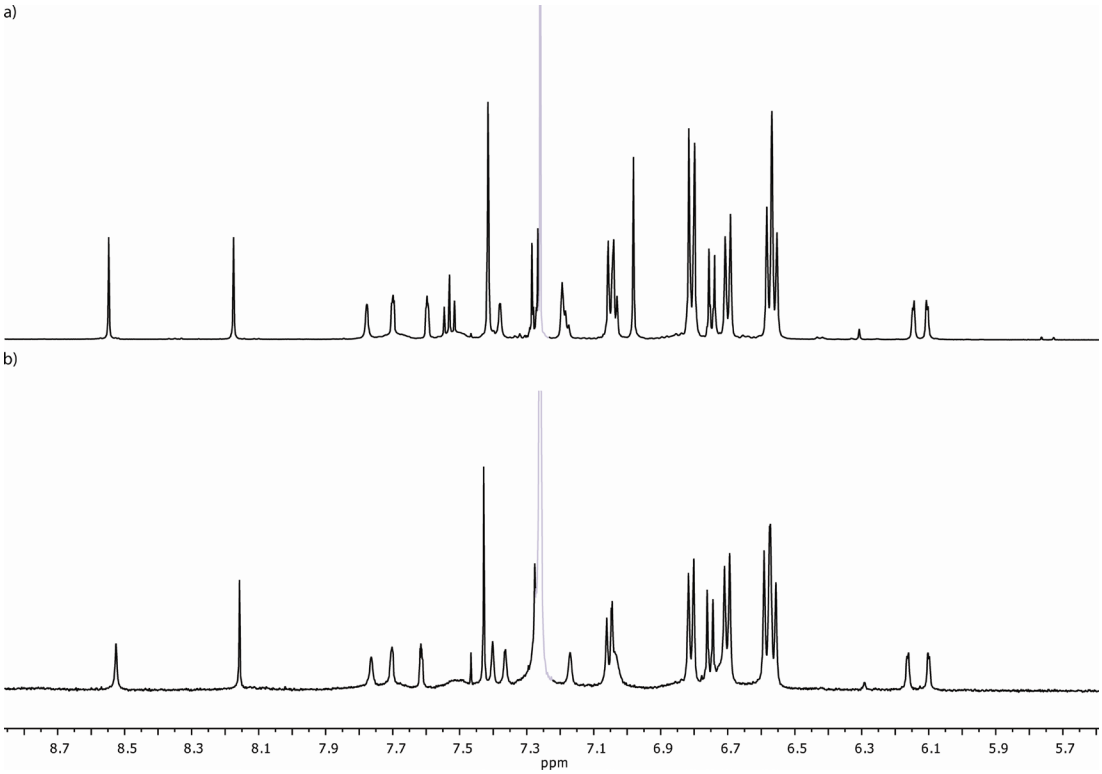

Figure 2.13 *- Partial [1]H NMR (500 MHz, $CDCl_3$) of* ***L1****Pd-(2,6-*DMAP*) before (a) and after (b) the addition of 1 equivalent of CH_3SO_2H.*

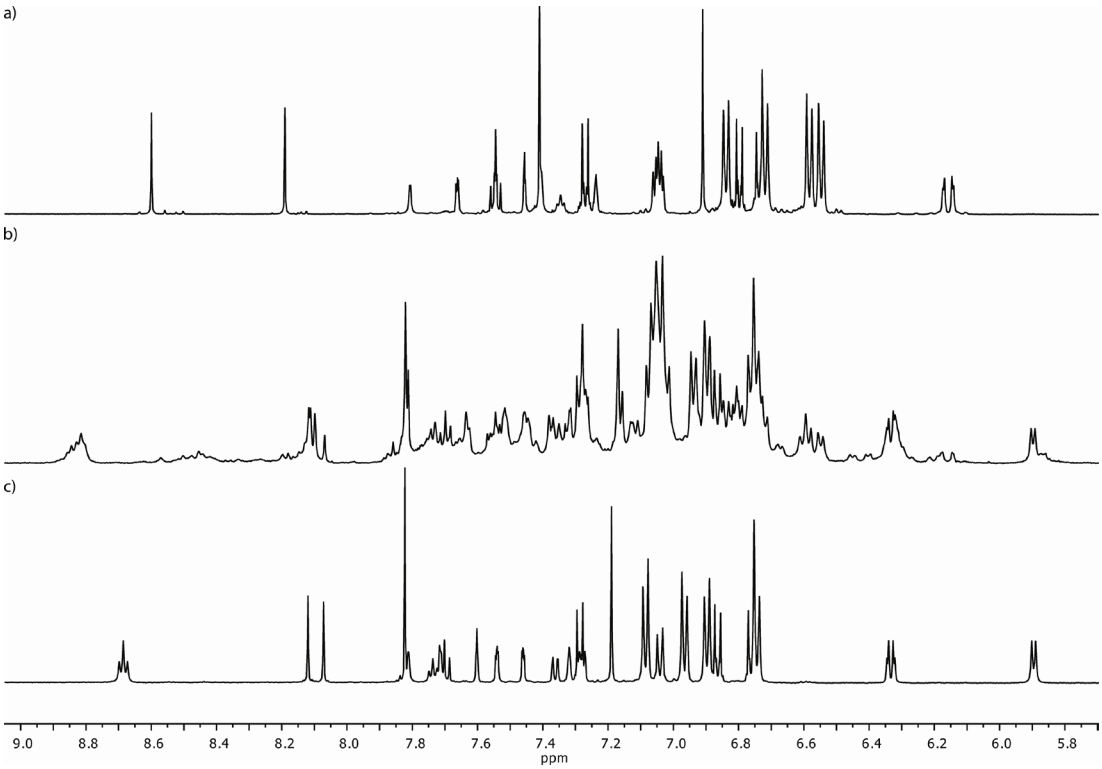

Figure 2.14 *- Partial [1]H NMR (500 MHz, CD2Cl2) of: (a)* ***L1****Pd-(2,6-DMAP); (b) crude operation mixture after work-up; (c)* ***L1****Pd-(2,6-Py).*

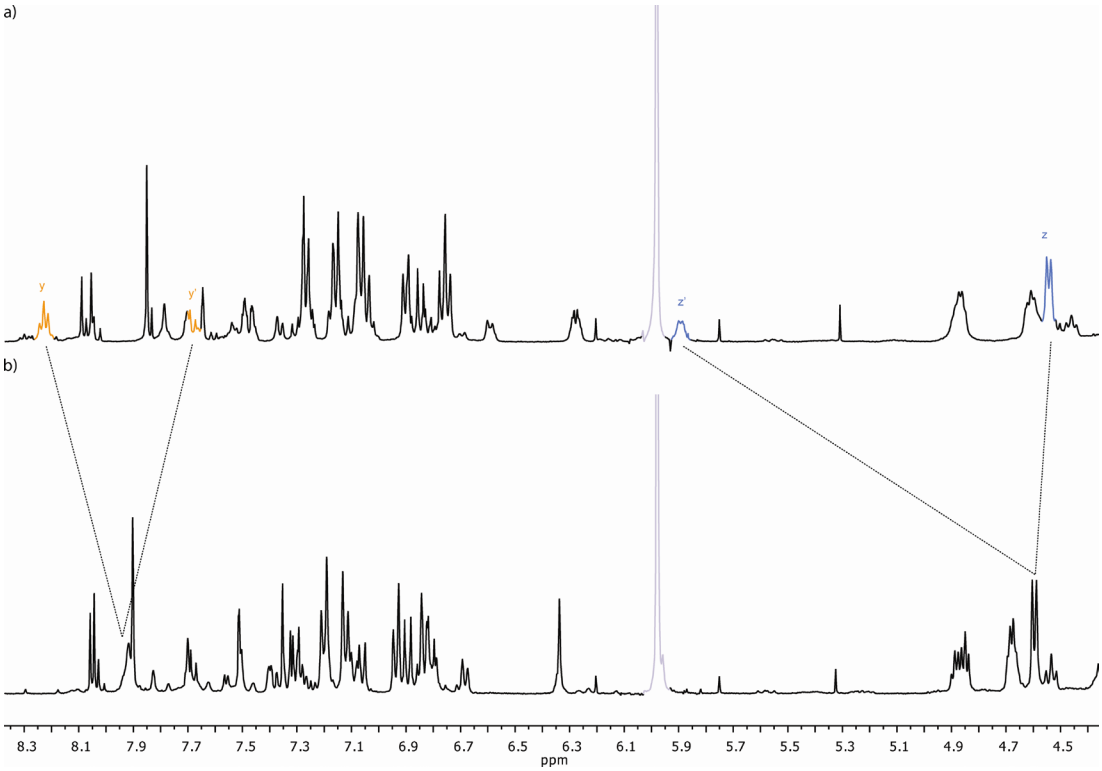

Figure 2.15 *- Partial ^{1}H NMR (400 MHz, $C_2D_2Cl_4$) of* ***L1****Pd-(2,6-Py) at: (a) 298 K; (b) 380 K.*

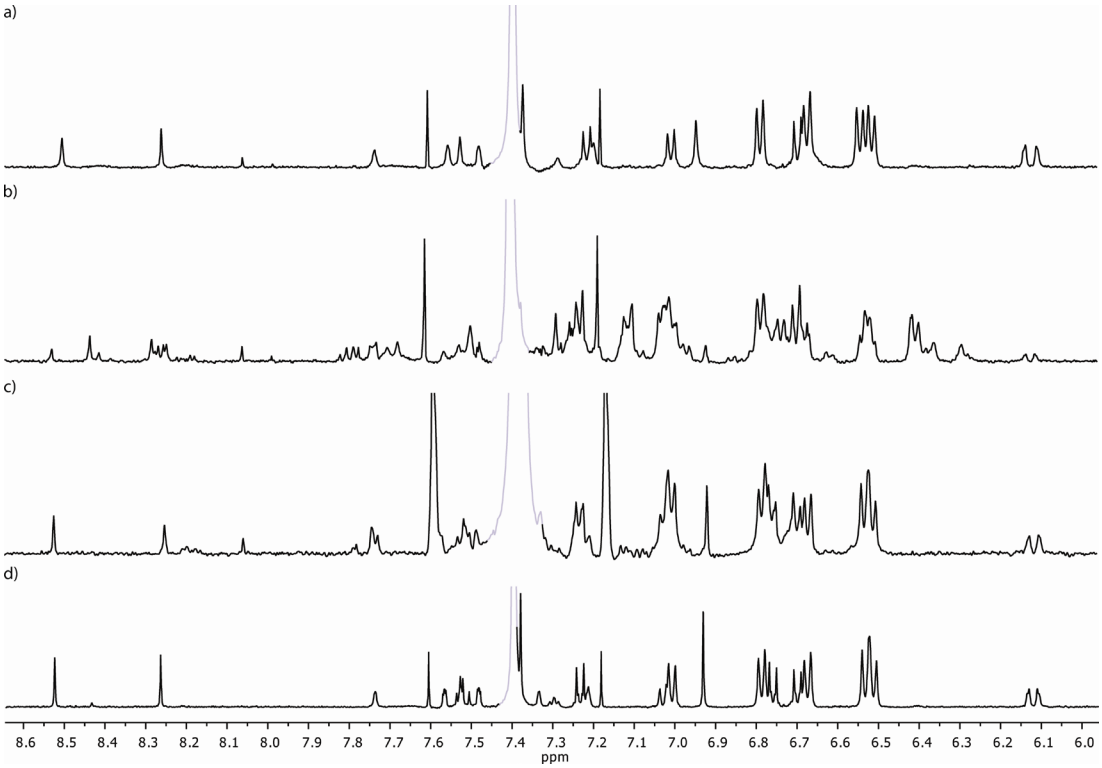

Figure 2.16 *- Partial 1H NMR (500 MHz, CDCl3/CD3CN 7:3) of: (a) 1:1 solution of* ***L1****Pd-(2,6-DMAP) (0.1 mM) and CH_3SO_2H; (b) mixture (a) heated at 338 K for 40 h; (c) mixture (b) heated at 338 K for 24 h in the presence of excess K_2CO_3; (d) reference spectrum of* ***L1****Pd-(2,6-DMAP).*

2.9 Crystallographic Data

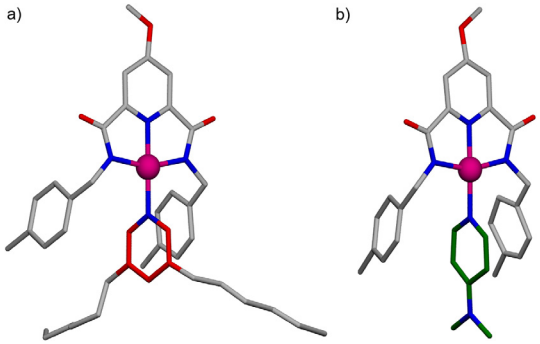

Figure 2.17 *- X-ray crystal structures of: (a)* ***L2****Pt-(3,5-dihexylPy); (b)* ***L2****Pt-DMAP. Hydrogen atoms and solvent molecules are omitted for clarity. Nitrogen atoms are shown in blue, oxygen atoms red, platinum atoms pink and carbon atoms in grey (DMAP and pyridine carbon atoms are shown in green and red respectively).*

	L1Pd-(2,6-*DMAP*)	**L2**Pt-(3,5-dihexyl*Py*)	**L2**Pt-*DMAP*
Chemical formula	$C_{101}H_{103}D_{16}N_{15}O_{13}PdPt$	$C_{82}H_{110}N_8O_9Pt_2$	$C_{62}H_{68}N_{10}O_7Pt_2$
Formula Mass	2068.70	1742.00	1455.46
Crystal system	Triclinic	Triclinic	Monoclinic
Space group	*P*-1	*P*-1	*C*2/*c*
Crystal size/mm	0.03 × 0.20 × 0.20	0.04 × 0.10 × 0.12	0.20 × 0.20 × 0.20
a/Å	14.238(4)	13.963(5)	24.018(12)
b/Å	18.939(5)	16.442(5)	20.103(8)
c/Å	19.681(5)	19.176(5)	16.238(8)
α/°	104.533(6)	90.185(5)	90
β/°	96.912(8)	106.795(7)	125.402(8)
γ/°	94.763(4)	108.246(5)	90
V/Å^3	5064(2)	3981(2)	6391(5)
Temperature/K	93(2)	93(2)	93(2)
Z	2	2	4
D_{calc}/Mgm^{-3}	1.357	1.448	1.513
μ/mm^{-1}	1.624	3.556	4.413
F(000)	2116	1772	2888
θ limits	2.16º to 25.33º	2.22º to 25.35º	0º to 25.46º
hkl limits	-17,15/-22,17/-23,23	-16,16/-12,19/-20,23	-24,29/-21,24/-19,19
No. of reflections measured	32421	25292	19911
No. of independent reflections	17832	14087	5872
R_{int}	0.0554	0.0345	0.114
Data/restraints/ parameters	17832 / 35 / 1168	14087/20/900	5872/43/366
$R(I> 2\sigma(I))$	R_1 = 0.1041	R_1 = 0.0521	R_1 = 0.092
R (all data)	wR_2 = 0.3374	wR_2 = 0.1517	wR_2 = 0.2694
Goodness of fit on F^2	1.231	1.083	1.052

Table 1 *- X-ray crystallographic experimental and refinement data for* ***L1****Pd-(2,6-DMAP),* ***L2****Pt-(3,5-dihexylPy) and* ***L2****Pt-DMAP.*[a] *In common: Refinement method: full-matrix least-squares on F². Wavelength: 0.71073 Å (Mo/Kα), Temperature: 93(2) K. Absorption correction method: multi-scan (only for L1Pd-(2,6-DMAP) and L2Pt-(3,5-dihexylPy)).*

2.10 References

1. Kay, E. R.; Leigh, D. A.; Zerbetto, F. *Angew. Chem., Int. Ed.* **2007**, *46*, 72–191.

2. *For discussion on eletrochemically powered molecular machines, see:*

a) Ballardini, R.; Balzani, V.; Credi, A.; Gandolfi, M. T.; Venturi, M. *Acc. Chem. Res.* **2001**, *34*, 445–455;

For a review of electrochemical control of supramolecular systems, see:

b) Nijhuis, C. A.; Ravoo, B. J.; Huskens, J.; Reinhoudt, D. N. *Coord. Chem. Rev.* **2007**, *251*, 1761–1780;

Changes in metal oxidation state can alter the coordination geometry preferences of some metal ions which has proven to be an effective means of generating intramolecular ligand re-arrangements, for selected examples, see:

c) Zahn, S.; Canary, J. W. *Angew. Chem., Int. Ed.* **1998**, *37*, 305–307;

d) He, Z.; Colbran, S. B.; Craig, D. C. *Chem.-Eur. J.* **2003**, *9*, 116–129;

e) Fabbrizzi, L.; Foti, F.; Patroni, S.; Pallavicini, P.; Taglietti, A. *Angew. Chem., Int. Ed.* **2004**, *43*, 5073–5077;

f) Amendola, V.; Dallacosta, C.; Fabbrizzi, L.; Monzani, E. *Tetrahedron* **2008**, *64*, 8318–8323;

g) Kuwamura, N.; Kitano, K. I.; Hirotsu, M.; Nishioka, T.; Teki, Y.; Santo, R.; Ichimura, A.; Hashimoto, H.; Wright, L. J.; Kinoshita, I. *Chem.-Eur. J.* **2011**, *17*, 10708–10715.

For examples of redox-driven translocation of metal ions, see:

h) Zelikovich, L.; Libman, J.; Shanzer, A. *Nature* **1995**, *374*, 790–792;

i) Amendola, V.; Fabbrizzi, L.; Mangano, C.; Pallavicini, P. *Acc. Chem. Res.* **2001**, *34*, 488–493;

j) Champin, B.; Mobian, P.; Sauvage, J.-P. *Chem. Soc. Rev.* **2007**, *36*, 358–366;

k) Colasson, B.; Poul, N. L.; Mest, Y. L.; Reinaud, O. *J. Am. Chem. Soc.* **2010**, *132*, 4393–4398;

l) Murahashi, T.; Shirato, K.; Fukushima, A.; Takase, K.; Suenobu, T.; Fukuzumi, S.; Ogoshi, S.; Kurosawa, H. *Nature Chem.* **2012**, *4*, 52–58;

For the mechanical movement of macrocycle-bound metal ions using redox processes, see:

m) Livoreil, A.; Dietrich-Buchecker, C. O.; Sauvage, J.-P. *J. Am. Chem. Soc.* **1994**, *116*, 9399–9400;

n) Cárdenas, D. J.; Livoreil, A.; Sauvage, J.-P. *J. Am. Chem. Soc.* **1996**, *118*, 11980–11981;

o) Gaviña, P.; Sauvage, J.-P. *Tetrahedron Lett.* **1997**, *38*, 3521–3524;

p) Livoreil, A.; Sauvage, J.-P.; Armaroli, N.; Balzani, V.; Flamigni, L.; Ventura, B. *J. Am. Chem. Soc.* **1997**, *119*, 12114–12124;

q) Armaroli, N.; Balzani, V.; Collin, J.-P.; Gaviña, P.; Sauvage, J.-P.; Ventura, B. *J. Am. Chem. Soc.* **1999**, *121*, 4397–4408;

r) Raehm, L.; Kern, J.-M.; Sauvage, J.-P. *Chem.-Eur. J.* **1999**, *5*, 3310–3317;

s) Weber, N.; Hamann, C.; Kern, J.-M.; Sauvage, J.-P. *Inorg. Chem.* **2003**, *42*, 6780–6792;

t) Poleschak, I.; Kern, J.-M.; Sauvage, J.-P. *Chem. Commun.* **2004**, 474–476;

u) Létinois-Halbes, U.; Hanss, D.; Beierle, J. M.; Collin, J.-P.; Sauvage, J.-P. *Org. Lett.* **2005**, *7*, 5753–5756;

v) Bonnet, S.; Collin, J.-P.; Koizumi, M.; Mobian, P.; Sauvage, J.-P. *Adv. Mater.* **2006**, *18*, 1239–1250;

w) Durola, F.; Sauvage, J.-P. *Angew. Chem., Int. Ed.* **2007**, *46*, 3537–3540;

x) Collin, J.-P.; Durola, F.; Lux, J.; Sauvage, J.-P. *Angew. Chem., Int. Ed.* **2009**, *47*, 8532–8535;

y) Collin, J.-P.; Levine, R. D.; Periyasamy, J.-P.; Remacle, F.; Sauvage, J.-P. *Chem.-Eur. J.* **2009**, *15*, 1310–1313;

z) Durola, F.; Lux, J.; Sauvage, J.-P. *Chem.-Eur. J.* **2009**, 4124–4134;

a') McNitt, K. A.; Parimal, K.; Share, A. I.; Fahrenbach, A. C.; Witlicki, E. H.; Pink, M.; Bediako, D. K.; Plaisier, C. L.; Le, N.; Heeringa, L. P.; Griend, D. A. V.; Flood, A. H. *J. Am. Chem. Soc.* **2009**, *131*, 1305–1313;

b') Durot, S.; Reviriego, F.; Sauvage, J.-P. *Dalton Trans.* **2010**, *39*, 10557–10570.

3. *For a discussion of chemically-driven molecular machines, see:*

a) Crowley, J. D.; Kay, E. R.; Leigh, D. A. *Intell. Mater.* **2008**, 1–47;

For examples of large amplitude molecular motion achieved by reversible metal ion binding, see:

b) Barboiu, M.; Vaughan, G.; Kyritsakas, N.; Lehn, J.-M. *Chem.-Eur J.* **2003**, *9*, 763–769;

c) Guenet, A.; Graf, E.; Kyritsakas, N.; Hosseini, M. W. *Inorg. Chem.* **2010**, *49*, 1872–1883;

d) Haberhauer, G. *Angew. Chem., Int. Ed.* **2010**, *49*, 9286–9289;

e) Haberhauer, G. *Angew. Chem., Int. Ed.* **2011**, *50*, 6415–6418;

For examples of "molecular muscle" rotaxanes stimulated by switchable Cu(I)/Zn(II) binding, see:

f) Jiménez, M. C.; Dietrich-Buchecker, C.; Sauvage, J.-P. *Angew. Chem., Int. Ed.* **2000**, *39*, 3284–3287;

g) Collin, J.-P.; Dietrich-Buchecker, C.; Gaviña, P.; Jimenez-Molero, M. C.; Sauvage, J.-P. *Acc. Chem. Res.* **2001**, *34*, 477–487;

For an example of large amplitude molecular motion achieved by solvent mediated hydrogen bond manipulation in transition metal-porphyrin systems, see:

h) Guenet, A.; Graf, E.; Kyritsakas, N.; Hosseini, M. W. *Chem.-Eur. J.* **2011**, *17*, 6443–6452.

4. *For examples of photo-driven molecular machines, see:*

a) Koumura, N.; Geertsema, E. M.; van Gelder, M. B.; Meetsma, A.; Feringa, B. L. *J. Am. Chem. Soc.* **2002**, *124*, 5037–5051;

b) Kay, E. R.; Leigh, D. A. *Nature* **2006**, *440*, 286–287;

c) Saha, S.; Stoddart, J. F. *Chem. Soc. Rev.* **2007**, *36*, 77–92;

For examples of a photo-driven motion of a transition metal based machines, see:

d) Mobian, P.; Kern, J.-M.; Sauvage, J.-P. *Angew. Chem., Int. Ed.* **2004**, *43*, 2392–2395;

e) Bonnet, S.; Collin, J.-P. *Chem. Soc. Rev.* **2008**, *37*, 1207–1217;

f) Balzani, V.; Bergamini, G.; Marchioni, F.; Ceroni, P. *Coord. Chem. Rev.* **2006**, *250*, 1254–1266.

5. Chatterjee, M. N.; Kay, E. R.; Leigh, D. A. *J. Am. Chem. Soc.* **2006**, *128*, 4058–4073.

6. *For Pd(II)-based molecular shuttles driven by acid-base changes, see:*

a) Crowley, J. D.; Leigh, D. A.; Lusby, P. J.; McBurney, R. T.; Perret-Aebi, L.-E.; Petzold, C.; Slawin, A. M. Z.; Symes, M. D. *J. Am. Chem. Soc.* **2007**, *129*, 15085–15090;

b) Leigh, D. A.; Lusby, P. J.; McBurney, R. T.; Symes, M. D. *Chem. Commun.* **2010**, *46*, 2382–2384.

7. To the best of the author's knowledge, none of the previously reported systems, with the exception of the Haberhauer's motor[3e] and the two Pd(II)

rotaxane shuttles,[6] possess ratcheting mechanisms, and are therefore switches.

8. *For examples of interlocked molecular motors, see:*

a) Leigh, D. A.; Wong, J. K. Y.; Dehez, F.; Zerbetto, F. *Nature* **2003**, 424, 174–179;

b) Hernández, J. V.; Kay, E. R.; Leigh, D. A. *Science* **2004**, *306*, 1532–1537.

9. Berná, J.; Leigh, D. A.; Lubomska, M.; Mendoza, S. M.; Pérez, E. M.; Rudolf, P.; Teobaldi, G.; Zerbetto, F. *Nature Mater.* **2005**, *4*, 704–710.

10. a) Fletcher, S. P.; Dumur, F.; Pollard, M. M.; Feringa, B. L. *Science* **2005**, *310*, 80–82;

b) Fujita, T.; Kuwahara, S.; Harada, N. *Eur. J. Org. Chem.* **2005**, 4533–4543;

c) Kuwahara, S.; Fujita, T.; Harada, N. *Eur. J. Org. Chem.* **2005**, 4544–4556;

d) Kudernac, T.; Ruangsupapichat, N.; Parschau, M.; Maciá, B.; Katsonis, N.; Harutyunyan, S. R.; Ernst, K.-H.; Feringa, B. L. *Nature* **2011**, *479*, 208–211;

e) Conyard, J.; Addison, K.; Heisler, I. A.; Cnossen, A.; Browne, W. R.; Feringa, B. L.; Meech, S. R. *Nature Chem.* **2012**, *4*, 547–551.

11. a) von Delius, M.; Geertsema, E. R.; Leigh, D. A. M. *Nature Chem.* **2010**, *2*, 96–101;

b) von Delius, M.; Geertsema, E. R.; Leigh, D. A.; Tang, T. D. M. *J. Am. Chem. Soc.* **2010**, *132*, 16134–16145;

c) Barrell, M. J.; Campaña, A. G.; Geertzema, E. M.; Leigh, D. A.; von Delius, M. *Angew. Chem., Int. Ed.* **2011**, *50*, 285–290;

d) Perl, A.; Gomez-Casado, A.; Thompson, D.; Dam, H. H.; Jonkheijm, P.; Reinhoudt, D. N.; Huskens, J. *Nature Chem.* **2011**, *3*, 217–322;

e) Campaña, A. G.; Carlone, A.; Chen, K.; Dryden, D. T. F.; Leigh, D. A.; Lewandowska, U.; Mullen, K. M. *Angew. Chem., Int. Ed.* **2012**, *51*, 5480–5483;

f) Kovaříček, P.; Lehn, J.-M. *J. Am. Chem. Soc.* **2012**, *134*, 9446–9455.

12. a) Fuller, A.-M. L.; Leigh, D. A.; Lusby, P. J.; Slawin, A. M. Z.; Walker, D. B. *J. Am. Chem. Soc.* **2005**, *127*, 12612–12619;

b) Leigh, D. A.; Lusby, P. J.; Slawin, A. M. Z.; Walker, D. B. *Chem. Commun.* **2005**, 4919–4921.

13. a) Fuller, A.-M. L.; Leigh, D. A.; Lusby, P. J.; Oswald, I. D. H.; Parsons, S.; Walker, D. B. *Angew. Chem., Int. Ed.* **2004**, *43*, 3914–3918;

b) Furusho, Y.; Matsuyama, T.; Takata, T.; Moriuchi, T.; Hirao, T. *Tetrahedron Lett.* **2004**, *45*, 9593–9597;

c) Fuller, A.-M. L.; Leigh, D. A.; Lusby, P. J. *Angew. Chem., Int. Ed.* **2007**, *46*, 5015–5019;

d) Hung, W.-C.; Wang, L.-Y.; Lai, C.-C.; Liu, Y.-H.; Peng, S.-M.; Chiu, S.-H. *Tetrahedron Lett.* **2009**, *50*, 267–270;

e) Fuller, A.-M. L.; Leigh, D. A.; Lusby, P. J. *J. Am. Chem. Soc.* **2010**, *132*, 4954–4959.

14. Slagt, M. Q.; van Zwieten, D. A. P.; Moerkerk, A. J. C. M.; Gebbink, R. J. M. K.; van Koten, G. *Coord. Chem. Rev.* **2004**, *248*, 2275–2282.

15. Pike, S. J.; Lusby, P. J. *Chem. Commun.* **2010**, *46*, 8338–8340.

16. The italicized suffixes *-DMAP*, *-Py*, and *-2,6-lutidine* denote the monodentate ligand is coordinated to the aforementioned metal.

17. *For a recent review on the design principes of small molecule molecular walkers, see:*

Leigh, D. A.; von Delius, M. *Chem. Soc. Rev.* **2011**, *40*, 3656–3676.

18. Hx = *n*-hexyl

19. *For exchange of various 4-substituted pyridine ligands at the fourth coordination site of Pd-pincer complexes, see:*

a) van Manen, H.-J.; Nakashima, K.; Shinkai, S.; Kooijman, H.; Spek, A. L.; van Veggel, F. C. J. M.; Reinhoudt, D. N. *Eur. J. Inorg. Chem.* **2000**, 2533–2540;

b) Yount, W. C.; Loveless, D. M.; Craig, S. L. *J. Am. Chem. Soc.* **2005**, *127*, 14488–14496.

20. *For proton-driven ligand exchange of lutidine coordinated Pd(II), see:*

a) Hamann, C.; Kern, J.-M.; Sauvage, J.-P. *Dalton Trans.* **2003**, 3770–3775;

For proton-driven exchange of various amines within copper-coordinated imine ligands, see:

b) Nitschke, J. R.; Schultz, D.; Bernardinelli, G.; Gérard, D. *J. Am. Chem. Soc.* **2004**, *126*, 16538–16543;

c) Schultz, D.; Nitschke, J. R. *Proc. Natl. Acad. Sci. U.S.A.* **2005**, *102*, 11191–11195;

d) Nitschke, J. R. *Acc. Chem. Res.* **2007**, *40*, 103–112.

21. Sonogashira, K.; Tohda, Y.; Hagihara, N. *Tetrahedron Lett.* **1975**, *16*, 4467–4470.

22. Kolb, H. C.; Finn, M. G.; Sharpless, K. B. *Angew. Chem., Int. Ed.* **2001**, *40*, 2004–2021.

23. Prior to its synthesis it was postulated that such a molecule might prove difficult to characterize by ^{1}H NMR spectroscopy and thus, deuteration of the alkyl chain linkers between the footholds was employed to simplify the spectra. This technique would also prove useful in differentiating between similar footholds in extended and iterative tracks of potential molecular walker systems.

24. Investigation of a compatible protecting group could still make this a viable route to extended systems with 2-(trimethylsilyl)ethyl ester (TMSE) as a possible alternative.

25. Crystal data for **21**·2EtOH: yellow prism, 0.03×0.20×0.20 mm, M_w = 2068.70, $C_{101}H_{103}D_{16}N_{15}O_{13}PdPt$, triclinic, space group *P*-1, a = 14.238(4) Å, b = 18.939(5) Å, c = 19.681(5) Å, α = 104.533(6)°, β = 96.912(8)°, γ = 94.763(4)°, V = 5064(2) Å^3, Z = 2, D_c = 1.357 g/cm^3, $Mo_{K\alpha}$ radiation (graphite monochromator, λ = 0.71075 Å), μ = 1.624 mm^{-1}, T = 93(2) K, F(000) = 2116. 32421 data (17832 unique, R_{int}=0.055, 2.16<θ<25.3). 1168 parameters, 35 restraints, R = 0.1041 [$I_o > 2\sigma(I_o)$], wR =0.3374 (all reflections), S = 1.23.

26. <5% exchange to the alternative positional isomer oserved after 30 h.

27. When the concentration of **L1**Pd was increased in neat coordinating solvent a significant degree of intermolecular ligand exchange was observed, leading to the formation of polymeric material. In order to avoid this, when removing the solvent, the temperature was maintained below 40 °C, and the concentration with respect to coordinating solvent was never increased above the exchange reaction concentration (0.1 mM).

28. Chang, H.-T.; Jeganmohan, M.; Cheng, C.-H. *Org. Lett.* **2007**, *9*, 505–508.

29. Hill, G. S.; Irwin, M. J.; Levy, C. J.; Rendina, L. M.; Puddephatt, R. J., Andersen, R. A.; Mclean, L. Platinum(II) complexes of Dimethyl Sulfide, *Inorganic Synthesis*, John Wiley and Sons; Hoboken, NJ, USA, **1998**.

30. (a) Lee, B.-Y.; Park, S. R.; Jeon, H. B.; Kim, K. S. *Tetrahedron Lett*. **2006**, *47*, 5105–5109.

Chapter III

Design, Synthesis and Investigation of Stimuli for a Switchable Platinum(II)-Complexed Molecular Shuttle

Acknowledgements

Dr Victor Blanco and Dr Romen Carrillo are gratefully acknowledged for their work on a previous generation of the molecular shuttle presented herein.

3.1 Synopsis

Switchable mechanically interlocked molecules have shown promise in the field of molecular electronics with potential applications in processors and information storage devices. Further progress in this area demands improvement in molecular switching efficiencies during operation and an increase in the lifetimes of resting states. Herein, the design, synthesis, and characterisation of a novel bistable [2]rotaxane is described incorporating a platinum(II)-complexed macrocycle interlocked with a two-station thread comprising 4-dimethyaminopyridine and pyridine binding sites. The use of both thermodynamic and kinetic stimuli are investigated with the aim of achieving efficient and selective translocation of the metal-complexed macrocycle between stations through reversible protonation, thus constituting a stimuli-responsive molecular shuttle. The substitution pattern of the ligands and the kinetic stability of the Pt-N bond afford exceptional metastability to the co-conformers of the molecule in the resting state; a prerequisite in the procurement of long-term information storage.

In terms of this thesis, the investigation of photoinitiated ligand exchange in platinum(II) complexes is also pursued as a potential orthogonal stimulus to the heat/protonation switch outlined in Chapter II for use in a bimetallic molecular walker system.

3.2 Introduction

The past half-century has witnessed an incredible advancement in the fields of technology and electronics; a progression inextricably linked with man's ability to miniaturise components in the quest for evermore powerful and efficient devices. In 1965, Gordon E. Moore famously laid out a vision for the future of integrated electronics and computing in his seminal paper "*Cramming more components onto integrated circuits*"[1] where he predicted the number of transistors that could be placed into a given area would double every two years. Although he only foresaw this trend holding for a decade or so, innovative engineering and improved manufacturing techniques have resulted in the remarkable endurance of so-called Moore's Law up to the present day, fuelling the continued progression of electronic device capabilities including computer processing-power and data-storage capacity. After nearly half a century and with transistors now registering at an individual length of little over 20 nm, the end of the law's limits may soon be realised. Keeping components cool and error-free becomes more and more difficult as their dimensions decrease, as do the complex and expensive optical lithography and etching techniques required to accurately arrange them on integrated circuits from a bulk material.[2] In order to match the modern-day information society's seemingly insatiable thirst for faster, more powerful and portable electronic devices, there is a growing demand for smaller, cheaper and more energy efficient alternatives to the silicon chip[3] as the predicted zenith of its capabilities approaches.

The field of molecular electronics[4] has garnered significant interest as one such avenue and involves superlative miniaturisation of parts by incorporating complete electronic components within single molecules. This "bottom-up" approach holds the potential to substitute costly factory assembly lines with large-scale laboratory synthesis of components, all intricately designed and tuned at the atomic level to meet the ultimate goal of molecular electronics, that is: to control macroscopic device properties as a function of chemical structure. This has already been achieved to a certain degree in molecular electronic devices where molecules act as solid-state molecular resistors,[5] rectifiers,[6] and transistors.[7]

Catenanes and rotaxanes that can act as molecular switches and shuttles through manipulation of non-covalent interactions[8] have shown real promise as active

molecular electronic devices[9] because their operation can instigate changes in experimentally measureable parameters such as calorimetric transformations,[10] shifts in electrochemical potentials,[11] and temperature-dependent kinetics,[10,11a,b,12] thus facilitating a tangible correlation between the properties of chemical solution-phase switching and the resultant responses of the electronic device. To date, most examples have been based around bistable [2]catenane or [2]rotaxane molecular switches and shuttles[4b,8c,13] that possess two experimentally differentiable, metastable co-conformers. These two states can be translated into a simple binary output where the switch is defined as either ON or OFF, very similar to the binary code that has acted as the core of computing over the past half-century. In principle, each single molecule can store the 'one' or the 'zero' of a bit of information according to its positional isomeric state offering an alternative method of making computer memory[14] on an unprecedented scale.

A major challenge facing this approach is the degree of metastability afforded to each state. An effective memory storage system would require fast and facile manipulation of the switches when writing information but, equally, each state would need to be completely kinetically locked once the data had been stored to ensure long-term retention. This equates to a chemical switch not dissimilar to those already discussed for use in the operable feet of molecular walkers and stimuli switchable molecular shuttles (Chapter II). Accordingly, the same beneficial control of binding event kinetics and thermodynamics that made metal coordination motifs amenable to these aforementioned fields stands them in good stead to play a role in the achievement of high integrity information storage through molecular memory.

Over the past fifteen years or so, J. P. Sauvage *et al*. have continued to carry out ground-breaking research in the field of redox-responsive Cu(I)/Cu(II) and Cu(II)/Zn(II) mechanically interlocked molecules.[15] This work has given rise to an impressive wealth of literature and provided the pretext for the palladium(II)-based acid-base switchable molecular shuttles[16] discussed in Chapter I. Although these latter Pd(II)-based examples do possess an intelligible ON/OFF level and can be fixed in thermodynamically unfavourable states by means of an energy ratchet mechanism,[17] the metastability of the co-conformers is not absolute under ambient conditions and the systems were reported to gradually return to their equilibrium distributions over time. This aspect needs to be vastly improved if such chemistry is to be used for long-

term memory storage where there is a requirement for complexes to be completely kinetically stable unless subjected to switching conditions.

One approach to improving the retention time of positional integrity in metal-coordinated molecular shuttles in the absence of their operating stimuli is simply to use metal-ligand complexes with greater levels of stability. The platinum(II)-pyridine derivative complexes (**L2**Pt-) investigated in Chapter II exhibited significantly improved stabilities compared to their palladium(II) counterparts (**L2**Pd-), making motifs of this kind attractive for potential use in stimuli switchable molecular shuttles aiming to achieve exceptional metastability of co-conformers. The upshot of this increased stability is of course the need for a more rigorous stimulus when operating the machine. Although this would be an issue in the palladium-based shuttles that were reported to decompose at very high temperatures used in attempts to accelerate shuttling, it was predicted that platinum analogues could withstand far harsher conditions whilst still facilitating translocation of the macrocycle on a reasonable timescale. An energetically more efficient alternative would be to employ a different stimulus to labilise the macrocycle and the potential for photonically driven platinum(II) molecular shuttling is explored in this chapter. It was postulated that such a stimulus may also prove to be effective as an independently operable switch for use with an opposing foot to the successful palladium(II) motif laid out in Chapter II and aid the design of extended bimetallic molecular walker systems.

3.3 Basis of Design: Protonation/Deprotonation Driven Ligand Exchange

The concept outlined in Figure 3.1 is very similar to that of the palladium-based molecular shuttles discussed previously[16] only with slight structural adjustments to the binding sites' (stations') substitution patterns on account of platinum(II) complexes' inability to bind 2,6-disubstituted pyridines. To accommodate these preferences the thread was altered to incorporate a 3,5-substituted pyridine, and a DMAP moiety functionalised through the nitrogen at the 4-position.

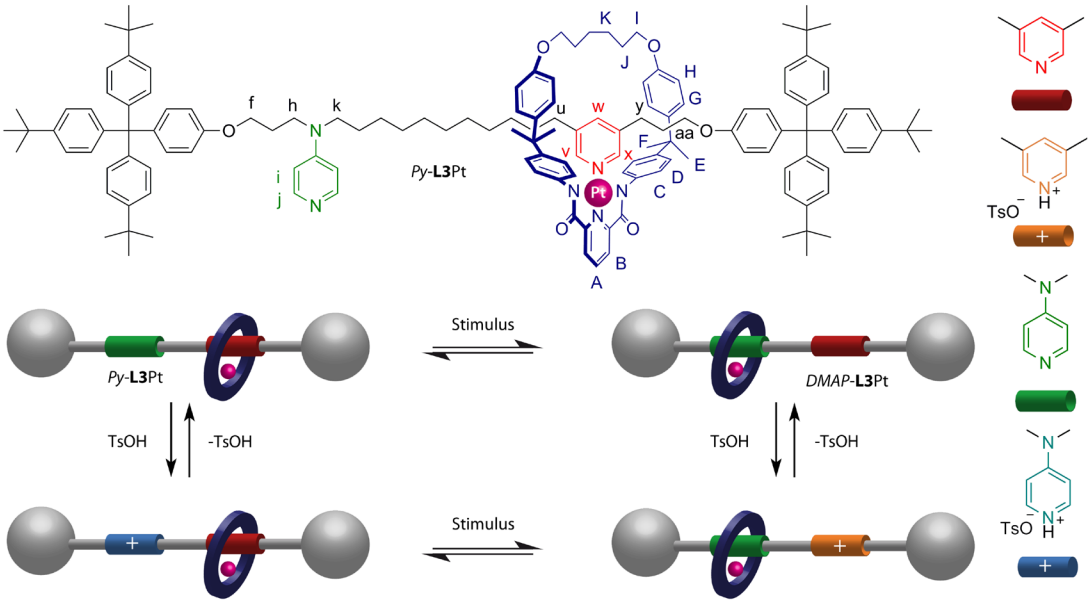

Figure 3.1 *- Structure and proposed operation method for a pH-switchable Pt(II)-complexed molecular shuttle, Py-**L3**Pt.*

The system's design was based around the hypothesis that, upon application of a suitable stimulus, the otherwise kinetically inert Pt-ligand bond will be significantly labilised. Assuming the platinum remains coordinated to the tridentate *N,N,N*-pincer motif of the macrocycle (**L3**) throughout the application, metal-ligand complex **L3**Pt will act as a brownian particle free to explore both potential ligand binding sites of the thread. Maintenance of the stimulus will drive the system towards a thermodynamic minimum at which the relative populations of the *Py*-**L3**Pt[18] and *DMAP*-**L3**Pt states will be defined by the energy difference between them. This ratio could then be fixed upon suspension of the stimulus when the macrocycle becomes kinetically locked to the thread. When *Py*-**L3**Pt is operated under neutral conditions, labilisation would invoke a significant shift in relative populations as the majority of macrocycles in the sample translocate to coordinate to the DMAP station on account of its superior ligand strength. The addition of one equivalent of acid and subsequent application of the stimulus will bring about a different equilibrium defined by the relative basicities of the two heterocycles. Acidic operation of the system would instigate protonation of the more basic DMAP moeity and a net migration of macrocycle units to the Py-station. The exceptional kinetic stability of the Pt-*N*-heterocycle bonds means that shuttling should be completely prohibited in the absence of a stimulus for extensive periods of time. Whilst in this state, the addition or removal of protons to the thread should not

automatically induce translocation of the macrocycle. These operating conditions would allow the thread do work on the macrocycle by ultimately ratcheting it energetically uphill (from DMAP to Py), an act notoriously difficult to achieve in molecular shuttles that operate *via* non-covalent interactions. Because resetting the thread (deprotonation) in the absence of a stimulus was not expected to undo the initial translocation task, the macrocycle could be locked in a thermodynamically unfavourable distribution. This method of operation would render the platinum-complexed [2]rotaxane an acid-base switchable molecular shuttle predicted to possess improved levels of metastability from previous examples.[16]

3.4 Ligand Exchange Experiments

The synthesis of a platinum(II)-complexed [2]rotaxane of the kind proposed in Figure 3.1 by a threading-and-stoppering strategy[19] is inherently more difficult than for their palladium counterparts because the metal of the macrocycle is more likely to coordinate to the stations on the thread by "perching' (that is, without forming the desired interlocked species) because the binding sites are far less sterically hindered due to differences in substitution patterns. This issue can be overcome through manipulation of the steric environment of the macrocycle by using a rigid bis-anilide ring,[16b,20] as opposed to a more flexible benzylic amide macrocycle.[16a] However, although this choice of shuttling component has been shown to improve positional bias in previous systems, it has also proven to facilitate superior dynamics in terms of rate of equilibration during operation. Considering the aim of this project is to increase the metastability of co-conformers rather than the dynamics between them, some model ligand exchange experiments were carried out to investigate the relative stabilities of the different kinds of platinum(II)-pyridine complexes and assess their respective potentials for use as a components in this new system.

The tridentate pyridine 2,6-dicarboxamide motif (**L2**) used to model the palladium(II) and platinum(II) complexes in Chapter II also provides a good mimic for a potential benzylic amide macrocycle. A simple exchange experiment (Scheme 3.1) showed **L2**Pt-(3,5-dihexyl*Py*) to be stable in coordinating solvent mixture DMF-d_7/MeCN-d_3 (1:1) in the presence of DMAP at room temperature indefinitely and, even at 348 K, it took 2 weeks to reach an equilibrium state of 25:75 **L2**Pt-(3,5-dihexyl*Py*):*DMAP* (Figure 3.2). Although this rate of exchange is too slow for practical use, the

metastability of **L2**Pt-(3,5-*Py*) in the presence of the superior DMAP ligand was shown to be considerably better than it's Pd(II) analogue. Additionally, the exchange process observed when heated was incredibly clean with no decomposition products observed at all providing precedent for the theory of dramatically increased overall stability.

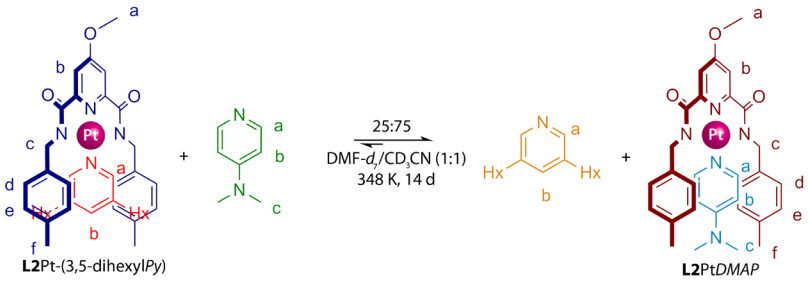

Scheme 3.1 *- Substitution of 3,5-dihexylPy for DMAP ligands in N,N,N-pincer-platinum(II) complex* ***L2****Pt-(3,5-dihexylPy) in DMF-d_7/MeCN-d_3 (1:1). Time required to reach equilibrium: 2 weeks at 348 K. No ligand exchange was observed at room temperature after 2 weeks.*

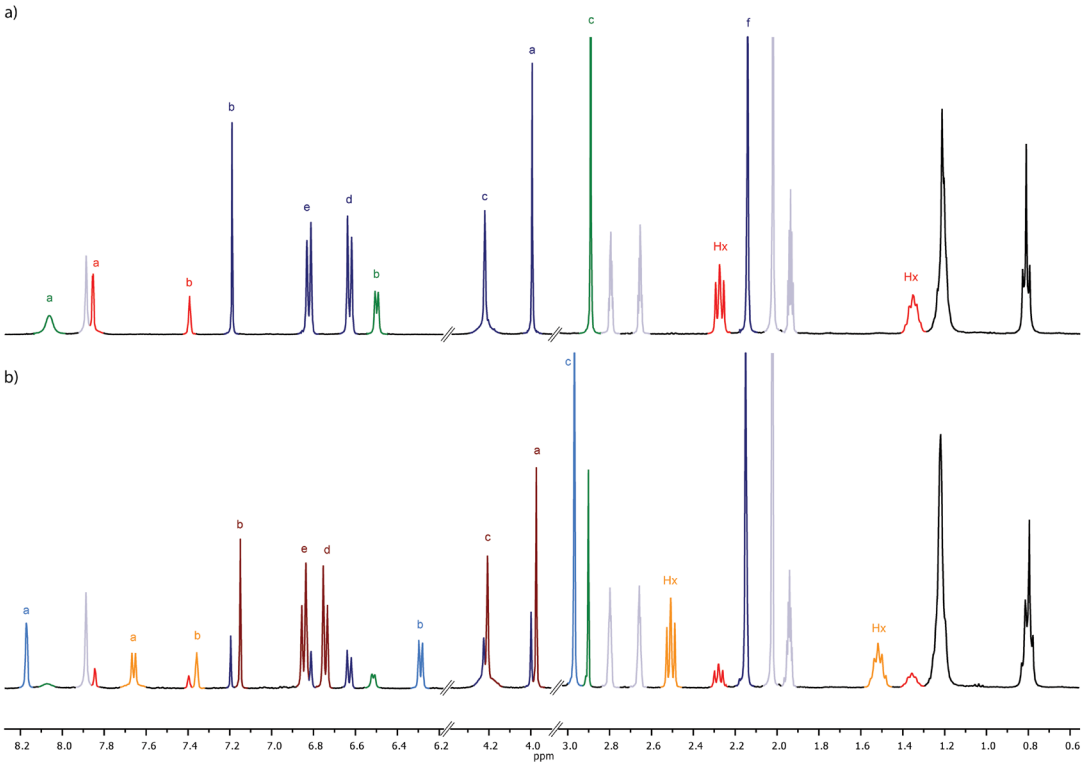

Figure 3.2 - *^{1}H NMR spectra (500 MHz, DMF-d_7/MeCN-d_3 (1:1), 298 K)* ***L2****Pt-(3,5-dihexylPy) and DMAP (1:1, 1 mM): (a) t = 0 h; (b) t = 2 weeks at 348 K. The lettering and colours in the figure refer to the assignments in Scheme 3.1.*

Similar exchange experiments were carried out with bis-anilide macrocycle **L3** (Scheme 3.2) to monitor how structural alterations to the *N,N,N*-pincer ligand affected the dynamics of the system. Encouragingly, there was no observable difference in

ambient stability with all complexes shown to be stable in the reaction mixture at room temperature for 2 weeks. At elevated temperature, however, there was a significant increase in the rate of ligand exchange compared to the bis-amide analogues. The lutidine group of **L3**Pt-(*3,5-lutidine*) was exchanged for DMAP (Scheme 3.2a) reaching an equilibrium distribution of 25:75 (**L3**Pt-(*3,5-lutidine*):*DMAP*) within just 18 h. This process could be reversed by adding an equivalent of *p*-toluenesulfonic acid (Scheme 3.2b). The results suggested that the platinum-complexed [2]rotaxane proposed in Figure 3.1, incorporating both DMAP and Py binding sites and a bis-anilide macrocycle, could operate as an acid-base switchable molecular shuttle with a thermal stimulus in a coordinating solvent.

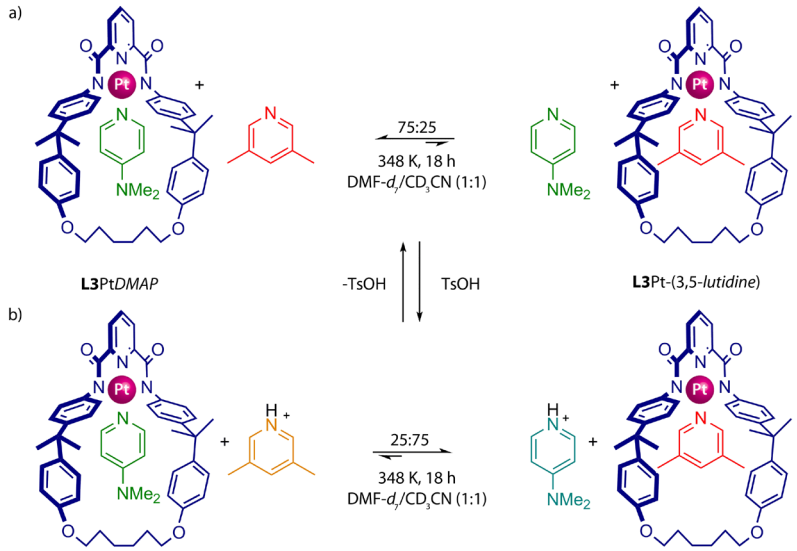

Scheme 3.2 *- Reversible substitution of 3,5-dihexlypyridine and DMAP ligands in macrocycle-platinum complex* ***L3****Pt-(3,5-lutidine)/DMAP in DMF-d_7/MeCN-d_3 (1:1): (a) neutral conditions; (b) in the presence of TsOH (1 equiv). Time required to reach equilibrium: 18 h at 348 K. No ligand exchange was observed in $CDCl_3$, either under neutral conditions, nor in the presence of TsOH, even after heating at reflux for 5 days.*

The method proposed here to increase the metastability of far-from-equilibrium states depends very simply upon raising the kinetic barrier to equilibration from either of the fixed co-conformers of the [2]rotaxane. Although this is beneficial because it results in longer-term information storage, it comes at the cost of a heavier energy penalty to intentional metal-ligand bond labilisation. One way of offsetting this is with the use of a kinetic stimulus[21] to lower the energy barrier during operation and it has indeed been demonstrated that platinum(II)-ligand exchange can be increased upon photoirradiation.[22]

3.5 Photophysics and Photochemistry of Platinum(II)-Py Bonds

To date, the majority of work relating to the photophysical and photochemical properties of platinum(II) complexes has focused upon electronic and spectroscopic characteristics with a view of gaining control over their photoluminescence.[23] Reported applications include use in light-emitting devices,[24] chemical sensors,[25] bioimaging and labelling,[26] solar energy conversion,[27] and photogeneration of hydrogen from water.[28] Although the elucidation of relevant excited states of these complexes is a *sine qua non* for obtaining a general understanding in any of the bespoken fields, the collective primary incentive for further research is provided by the allure of chemo-stable systems with high luminescent quantum yields and electronic properties that can be easily tuned by means of simple synthetic manipulation. The main challenges facing these systems are competitive non-radiative decay pathways and photodecomposition of the platinum species. An area that has received far less attention, however, is one in which these pathways, previously deemed deleterious, are actively encouraged within platinum(II) complexes specifically designed to undergo controlled photodissociation to yield pre-ordained, desirable photoisomerisation products.[22] Regardless of the respective goals of these systems, a comprehensive understanding of the relevant photophysical and electronic processes involved is essential to enable their effective incorporation as functioning components into advanced molecular machines.

As a coordination centre, platinum(II) has a strong thermodynamic preference for dsp^2 hybridisation and hence, has proved to be an interesting alternative to the more extensively studied metal ions within the world of inorganic photochemistry, such as ruthenium(II), chromium(III) and rhodium(III) that generally form 6-coordinate octahedral complexes. It is the 4-coordinate square-planar geometry that predominantly dictates the character of the excited states.[29] Platinum in the +2 oxidation state has a d^8 electron configuration defined by discrete energy levels according to the well-established ligand field theory.[30] This equates to four filled bonding or non-bonding metal-based d-orbitals (d_{z2}, d_{xy}, d_{xz}, and d_{yz}) and a strongly antibonding d_{x2-y2} orbital. For platinum(II) complexes solely comprised of simple inorganic ligands such as $[PtCl_2]^{2-}$ or $[Pt(NH_3)_4]^{2+}$, the d_{x2-y2} provides the only empty orbital accessible to the ground state upon irradiation. However, such a transition is Laporte forbidden and would therefore be very weak. Furthermore, due to unfavourable interactions with the ligands, the excited state molecule would undergo

significant D_{2d} distortion away from the D_{4h} square-planar configuration towards a tetrahedral conformation.[31] Such rearrangements promote coupling to the ground state and thus facilitate rapid radiationless deactivation of the excited species.[32] Hence, simple complexes generally have short-lived ligand field excited states and rarely show any significant luminescence.[29]

It is possible to influence the relative positions of the energy levels involved *via* careful ligand selection according to steric and electronic properties. However, the inauguration of more electronically complex ligands, such as conjugated aromatics, complicates the picture somewhat by introducing new accessible excited states and consequently, a new range of possible photo-induced transitions including ligand centred (π-π^*) and metal to ligand charge transfer (d-π^*, MLCT), among others. Consider the system described in the Figure 3.3a where an electron residing in a ground state d-orbital is promoted into a π^*-orbital centred on the ligand *via* a Laporte allowed photoinduced MLCT. The molecule then undergoes radiationless decay from the upper vibrational states, dissipating energy to the surroundings until it reaches the lowest vibrational level of the electronically excited molecular state (π_1^*, υ=0). From here, it can either return to the ground state by spontaneously emitting the remaining excess energy in the form of fluorescence, or it can thermally populate the adjacent d* excited state centred on the metal, from whence it can undergo subsequent non-radiative decay to the ground state. It is clear from this generic example that the luminescence properties and, to some extent, the excited state lifetimes of such systems are dictated by the disparity between the two excited state energy levels. In order to obtain highly emissive compounds this energy gap must be maximised either by raising the d*-state to inaccessible energies, or by lowering the potentially emissive π^*-state.

Figure 3.3a displays a simplified description of the potential energy landscape because it is only concerned with the ground and first two singlet excited states. However, platinum's high spin-orbit coupling constant (ε) brings states of higher multiplicity into play by promoting rapid inter-system crossing (ISC). Figure 3.3b accounts for this by describing a similar system but with the ^{1}d*-state raised to an inaccessible energy, and a readily accessible excited triplet state available to the first singlet excited state *via* ISC. The triplet state lies below its singlet analogue in energy in accordance with Hund's maximum multiplicity rule, which dictates that the state of the complex with spins parallel will lie lower in energy than the state in which they are paired.[33]

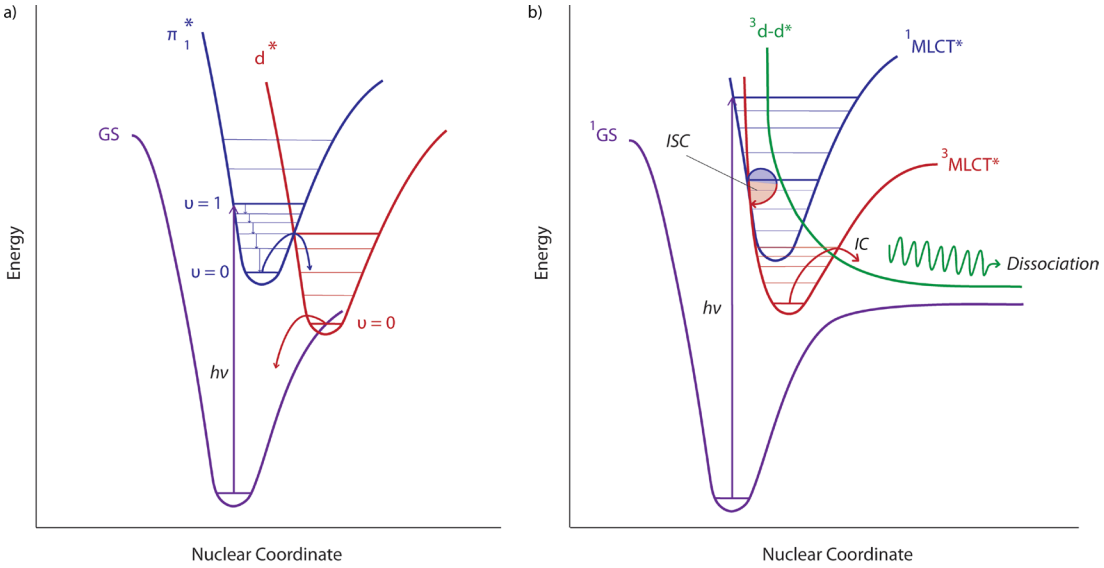

Figure 3.3 *- Potential energy profile showing the possible pathways of a platinum(II) complex promoted from the ground state (GS) via UV-irradiation (h ν) into: (a) the first excited singlet ligand-based state (π_1*). The molecule descends to the lowest vibrational level from whence it can thermally access a metal-based state (d*) and thence non-radiatively return to the ground state; (b) the first singlet excited state (^{1}MLCT*). Intersystem crossing (ISC) mediates transfer into a triplet state of ligand parentage (^{3}MLCT*), where it rapidly descends to the lowest vibrational level. The molecule can then radiatively dissipate energy via phosphorescence or undergo thermally activated internal conversion (IC) to a highly dissociative metal-based antibonding orbital state (^{3}d-d*) leads to Pt-ligand bond breaking.*

Similar to the previous example, irradiation induces a metal to ligand charge transfer to the first singlet excited state, followed by rapid relaxation, non-radiatively transferring energy to the surroundings as the molecule descends through the vibrational levels. At the intersect of the potential energy surfaces, the ligand-based triplet and singlet states share a common geometry where spin-orbit coupling can mediate the unpairing of electron spins and thus facilitate a non-radiative transition between the two states *via* ISC. From there the molecule continues to dissipate energy to the surroundings descending the triplet's vibrational ladder until it reaches the lowest vibrational level where it is trapped because the solvent cannot absorb the final large quantum of energy and radiative return to the ground state is spin forbidden. These conditions manifest themselves in the formation of a relatively long-lived, paramagnetic state and it is from this state that various possibilities to manipulate the system arise depending on the desired application of the molecule. For the majority of systems mentioned previously in which high luminosity is the ultimate goal, the final step would involve radiative decay back to the ground state in the form of phosphorescence. Although this process is formally spin-forbidden, the same spin-orbit coupling that mediates ISC

breaks the selection rule and can render the triplet state a slowly radiating reservoir.[33] Alternatively, for systems with ambitions more akin to those of this project in which organised bond dissociation is the coveted concluding process, an additional element of control over decay from the ligand-based triplet excited state must be introduced.

Because the photolability of transition metal compounds is generally associated with the enforced population of metal-centred (MC) antibonding orbitals,[34] this can be realised by means of a low-lying metal-centred triplet state (such as ^{3}d-d* in Figure 3.3b) that is thermally accessible from the triplet MLCT state (^{3}MLCT*). Thermal energy can excite the molecule to a higher vibrational level causing its electrons to undergo a reorganisation that results in internal conversion (IC); a radiationless transition to another state of identical multiplicity that occurs most readily when the two states share a common nuclear geometry (i.e. at the intersect of their respective potential energy profiles). If the metal-centred antibonding state into which the molecule converts is dissociative, there will be no ground state analogue and such a conversion will result in the breaking of a chemical bond where the photolability of the compound will be related to the energy difference between the emitting ^{3}MLCT and the dissociative ^{3}MC states.

These mechanisms have been studied extensively for ruthenium(II) complexes[35] and in 2004, Sauvage *et al*. reported two such complexes in which the motility of one component of a catenane molecule could be photochemically controlled by means of photoinduced ligand exchange as a result of orchestrated population of a dissociative excited state.[36] Although ruthenium(II) systems stand as a useful paradigm for predicting the possible photophysical mechanisms, apart from a few reports of photoisomerisations,[27a,f] there has not been substantial literature precedent for successful photonically stimulated ligand dissociation in platinum(II) complexes until quite recently. In 2007, Fujita *et al*. reported the potential to labilise an otherwise inert platinum(II)-Py bond by irradiating with ultraviolet (UV) light.[22b]

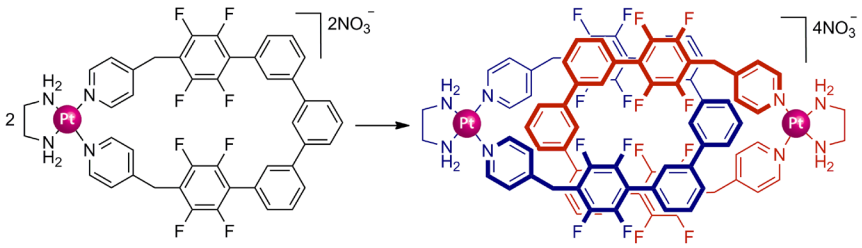

Scheme 3.3 *- One-way catenane formation of a Pt(II)-linked coordination ring via the photolabilisation of a Pt(II)-pyridine bond. Reagents and Conditions: DMSO/H_2O (1:2), hv, 15 min, quant. yield.*[22b]

This property was exploited to accommodate efficient photoinduced catenane formation in the synthesis of a so-called "molecular lock" where a pyridyl ligand was reversibly coordinated to platinum dependent upon aqueous/non-aqueous solvent environment (Scheme 3.3). Kinetic studies supported the theory of a photoinduced, dissociative mechanism, however, there is some debate as to the specific orbitals and excited states involved. DFT calculations showed a "reasonable" agreement with the authors' theory that photo-excitation induces a direct transition from the ground state highest occupied molecular orbital (HOMO) into an antibonding orbital dominated by metal d_{x2-y2} character and consequently inducing dissociation of the pyridine ligand. Although the HOMO was not officially assigned, calculated projections showed a large coefficient on the metal centre implying that this excitation equates to a Laporte forbidden d-d* transition corresponding to an indiscernible band in the UV-visible absorption spectrum. Considering the unprecedented efficiency of the catenation, it seems more likely that the reaction proceeds *via* a mechanism more akin to that proposed earlier for ruthenium(II) complexes. Regardless of this contention, the overall result of the study is indisputable: platinum(II)-pyridine bonds can be significantly labilised upon UV irradiation providing a clear mandate for further research in this area. Indeed, Lusby and Pike later reported the use of light as a kinetic stimulus in *N*-heterocyclic ligand exchange between cyclometalated platinum(II) complexes.[22e]

In order to transform these systems from simple ligand exchange processes into a fully functioning component of a synthetic molecular machine, the fundamental mechanism must be considered and each aspect tuned appropriately to meet the goals of the new design. Taking each facet in turn; the basis of a selectively labilisable metal-ligand bond in these species equates to a platinum(II) complex in a perfect square-planar

conformation. Distortion of D_{2d} symmetry in the complex can lead to reduction of the ligand field and lowering of the deleterious d-d* singlet excited states to a thermally accessible level, the end result being rapid non-radiative deactivation of the excited state. One way in which the conformation can be locked is by using rigid chelate ligands. Cyclometalating ligands can also serve as strong σ-donors that increase the splitting of the platinum d-orbitals and therefore help to raise the d_{x2-y2} to inaccessible energies.[37] Additionally, multidentate ligands can help avoid unwanted decomposition products, as the idealised labilising stimulus should specifically target only the bond that coordinates the platinum to the exchanging ligand. Selecting a tridentate *N,N,N*-pincer ligand to occupy the other three coordination sites on the platinum reduces the chance of complete metal dissociation from the pincer motif and favours the permanent breaking of the metal-monodentate ligand coordinate bond, which will be the most photolabile in the complex as a result of the chelate effect. MLCT transitions can be maximised by introducing low lying π*-orbitals facilitated through the introduction of good π-donor ligands. Swift ISC crossing is accommodated by platinum's high spin-orbit coupling constant. It has also been reported that the use of strongly ligating solvents can increase the quantum yield of ligand exchange.[34] With these preconditions in mind, macrocycle **L3** provides a reasonable starting point in the search for a rigid, π-donor, tridentate ligand with the prediction that irradiation with an appropriate wavelength of light in the presence of a coordinating solvent will lower the activation energy to platinum(II)-pyridyl bond labilisation, thus acting as a kinetic stimulus for use in the pH-switchable molecular shuttle outlined in Figure 3.1.

This chemistry could also find useful application in the designs of advanced bimetallic molecular walker systems similar to the one described in Chapter II. Although both metals reside in the same group of the periodic table, irradiation of platinum(II) complexes is far more likely to promote population of dissociative triplet states than in their palladium(II) counterparts on account of the former's greater size and therefore spin orbit coupling constant. If two opposing complexes could be effectively tuned to accommodate a labilising process in the platinum(II) moiety at sufficiently low temperatures to render a Pd-N bond inert, such a stimulus would be orthogonal to the heat/protonation switch proposed previously and could therefore function in tandem as the basis for a bimetallic molecular walker.

3.6 Synthesis and Characterisation of [2]Rotaxane L3Pt

The synthetic strategy of [2]rotaxane *Py*-**L3**Pt is outlined in Schemes 3.4-3.6 and full details are given in the Experimental Section 3.10.

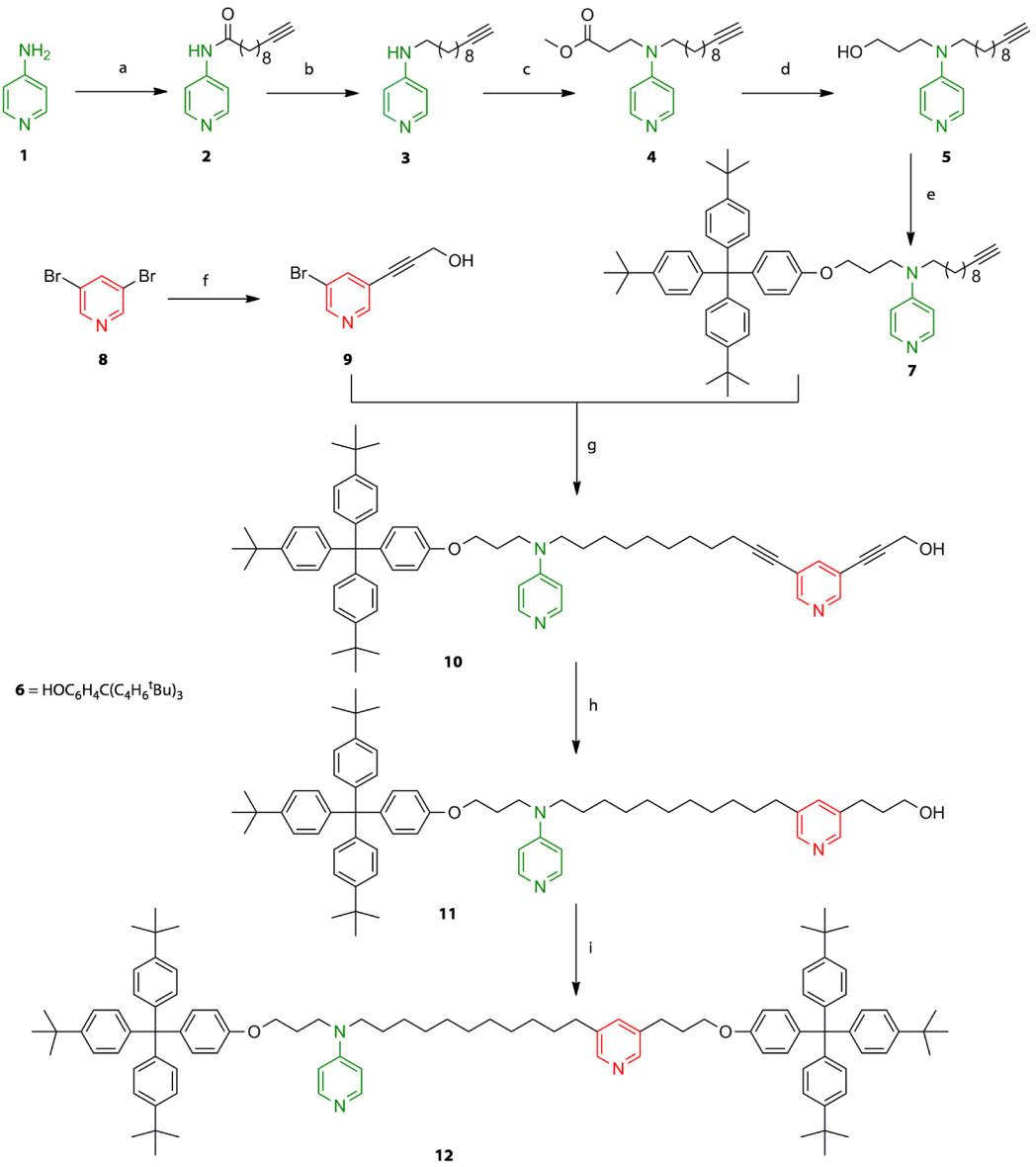

Scheme 3.4 *- Synthesis of molecular thread. Reaction conditions: (a) 10-undecynoic acid, DCC, $CHCl_3$, RT, 18 h, 99%; (b) $LiAlH_4$, THF, 40 °C, 10 h, 98%; (c) methyl acrylate, 98 °C, 3 days, 90%; (d) $LiAlH_4$, THF, RT, 18 h, 73%; (e)* **6**, *PPh_3, DIAD, THF, RT, 4 h, 61%; (f) propargyl alcohol, $Pd(PPh_3)_4$, CuI, Et_3N, THF, RT, 15 h, 55%; (g) $Pd(PPh_3)_4$, CuI, Et_3N, THF, 50 °C, 6 h, 64%; (h) $Pd(OH)_2/C$, H_2, K_2CO_3, $CHCl_3$/THF (1:1), RT, 18 h, 95%; (i)* **6**, *PPh_3, DIAD, THF, RT, 12 h, 56%.*

DCC coupling of commercially available 4-amniopyridine (**1**) and 10-undecynoic acid afforded amide **2** and subsequent reduction ($LiAlH_4$) gave rise to amine derivative **3** (Scheme 3.4a & 3.4b). The unsymmetrical DMAP-station, **5**, was achieved by reflux of **3**

in methyl acrylate (excess) to give **4**, followed by reduction ($LiALH_4$). Subjection of **5** to Mitsunobu reaction conditions[38] with bulky phenol **6**[39] gave rise to compound **7**. The synthesis of the Py-station fragment was achieved by desymmertrisation of commercially available 3,5-dibromopyridine (**8**) through Sonagashira cross-coupling with 1 equivalent of propargyl alcohol to give **9**, which was subsequently submitted to Pd-catalysed Sonagashira cross-coupling with **7** to yield **10**, the hydrogenation of which ($Pd(OH)_2/C$) afforded the saturated monostoppered thread **11**. The isolated full thread was synthesised for reference purposes to aid in the characterisation of the shuttle using a Mitsunobu reaction to couple **11** with phenol **6** to give **12** in 56% yield.

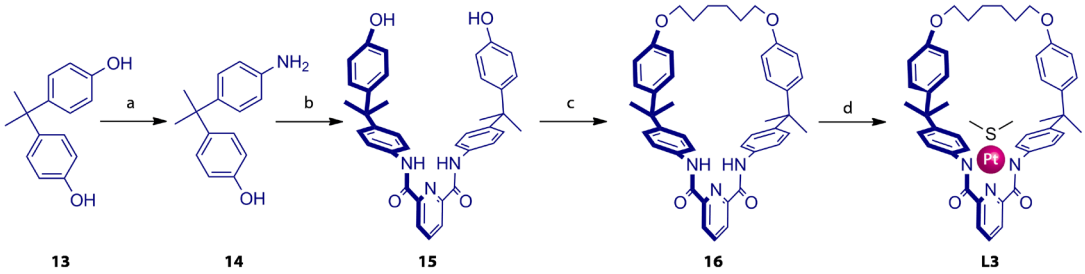

Scheme 3.5 *- Synthesis of Pt(II)-complexed macrocycle. Reaction conditions: (a) aniline hydrochloride, 180 °C, 45 min, 31%; (b) pyridine-2,6-dicarboyl dichloride, Et_3N, THF, RT, 18 h, 87%; (c) 1,6-dibromohexane, K_2CO_3, DMF, RT, 3 days, 45%; (d) NaH, $PtCl_2(SMe_2)_2$, THF, RT, 15 h, 78%.*

The platinum(II)-coordinated macrocycle was synthesised by first heating commercially available aniline hydrochloride with 2,2-bis(*p*-hydroxyphenyl)propane) (**13**) to afford 2-aniline-(2-phenolpropane) (**14**) which was subsequently reacted with pyridine-2,6-dicarboyl dichloride (0.5 equiv) at 0 °C to yield diol **15** (Scheme 3.5a & 3.5b). The free macrocycle **16** was synthesised *via* Williamson reaction of 1,6-dibromohexane with **15**, which was then metallated by reaction with $PtCl_2(SMe_2)_2$ and sodium hydride to give **L3**. Combining monostoppered thread, **11**, with 1 equivalent of trifluoroacetic acid led to selective protonation of the more basic DMAP station and subsequent addition of **L3** resulted in complexation of the macrocycle-platinum moiety exclusively to the Py binding site to yield pseudo-rotaxane **17** (Scheme 3.6a). Attempts to mimic the synthesis of isolated thread **12** using the stopper and pseudo-rotaxane **17** under Mitsunobu conditions proved unsuccessful, possibly as a consequence of using a triphenylphosphine mediated reaction with a platinum-complexed species. To circumnavigate this problem, the alcohol group of **13** was converted to the corresponding mesylate and Williamson coupled to **6** to give the target [2]rotaxane **L3**Pt in a yield of 56%.

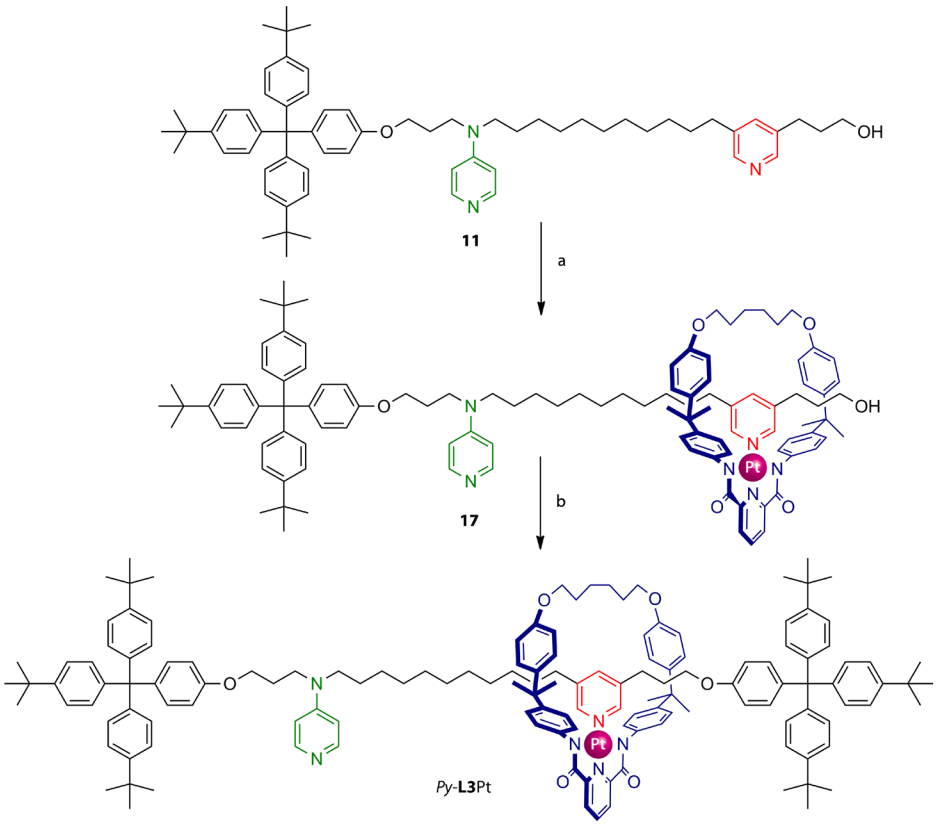

Scheme 3.6 - *Synthesis of Pt(II)-complexed molecular shuttle. Reaction conditions: (a)* ***L3****, TsOH (1 equiv),* $CHCl_3$*, 50 ℃, 18 h, 63%. b) (i) MsCl,* Et_3N*,* $CHCl_3$*, RT, 1 h, (ii)* ***6****, NaH, THF, RT, 4 h, (iii) 15-crown-5, DMSO, 48 ℃, 48 h, 56%.*

Electrospray mass spectrometry confirmed the product's constitution as **L3**Pt with a mass peak at 2276.29 *m/z* corresponding to $[M+H]^+$ and an isotopic distribution concordant with theoretical predictions. ^1H NMR spectroscopy (Figure 3.4) showed exclusive formation of the *Py*-**L3**Pt co-conformation; i.e. the platinum-macrocycle fragment, **L3**Pt, was solely coordinated to the Py-station. A comparison of the spectra of free thread **12** (Figure 3.4a) and *Py*-**L3**Pt in $CDCl_3$ (Figure 3.4b) shows significant upfield shifts of between 0.55-0.59 ppm for resonances associated with the Py-station ($H_{v\text{-}x}$) upon threading. Similarly the signals of the protons adjacent to the Py-station (H_{u+y}) are shifted upfield by 0.55 and 0.67 ppm respectively as they are shielded by the presence of the macrocycle. Meanwhile, the DMAP-station signals (H_{i+j}) of the rotaxane occur at very similar values (6.6-6.8 and 8.1-8.2 ppm respectively) to those of the free thread.

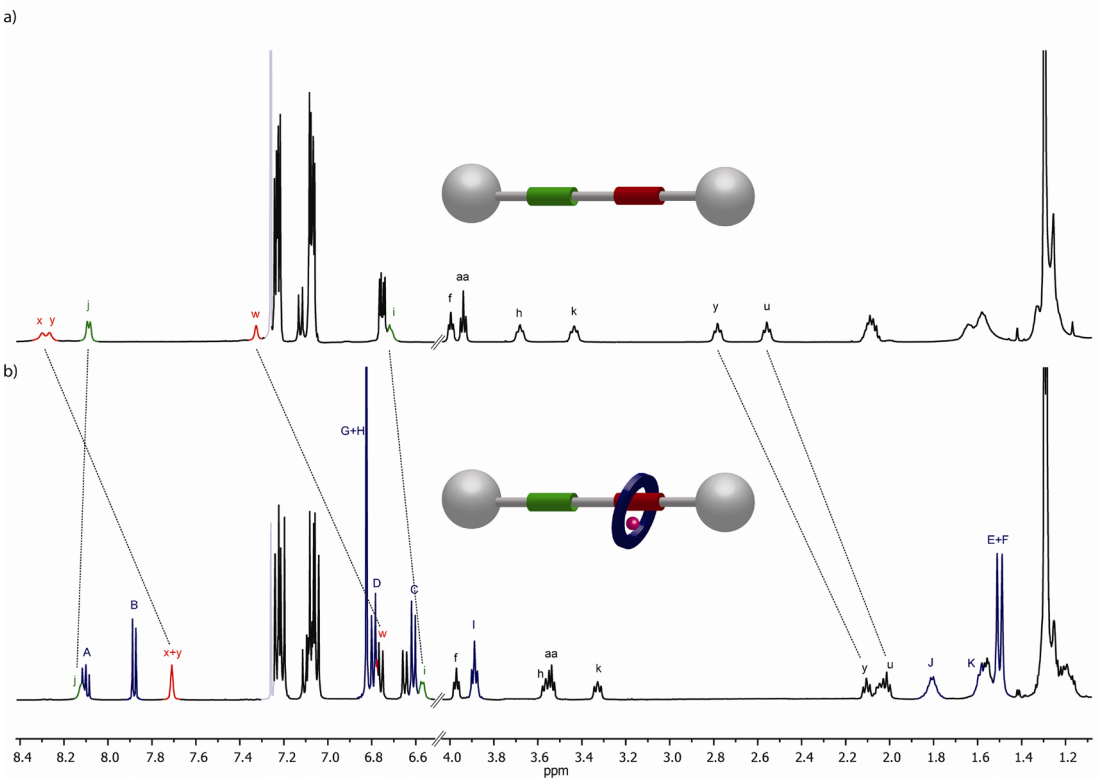

Figure 3.4 - *^{1}H NMR spectra (500 MHz, $CDCl_3$, 298 K) of [2]rotaxane **L3**Pt and free thread for comparison: (a) thread **12**; (b) Py-**L3**Pt. The lettering in the figure refers to assignments in Figure 3.1.*

3.7 Macrocycle to DMAP-Station Shuttling Experiments

In an attempt to translocate the platinum(II)-coordinated macrocycle from the Py-station to its thermodynamically favoured DMAP counterpart, *Py*-**L3**Pt was subjected to the neutral ligand exchange reaction conditions developed for the non-interlocked model experiments (DMF-d_7/MeCN-d_3 (1:1), 348 K, Scheme 3.2a), and the reaction followed by ^{1}H NMR spectroscopy. However, no changes were observed in the [2]rotaxane resonances during 6 weeks of heating after which solvent decomposition started to occur. It was postulated that the lack of macrocycle translocation might be the result of remnant trace acid from the synthesis in the solution meaning the DMAP-station would in fact be protonated. In this event, the platinum-Py bond may be labilised under the reaction conditions but the protonated DMAP-station would be inaccessible meaning no shuttling would be observed as the system would thermodynamically favour the starting co-conformer under the conditions. This hypothesis was tested by submitting a fresh sample of *Py*-**L3**Pt to the same conditions in the presence of excess K_2CO_3, however, the results remained unaltered. There were

also no changes seen in the chemical shifts of the resonances relating to the DMAP-station (H_{j+i}) upon the addition of base, implying that the reaction mixture was already neutralised in the previous experiment.

Another explanation for the lack of shuttling could be that the interlocked nature of the [2]rotaxane affords the system a considerable increase in stability in comparison to the free macrocycle analogues. Such a phenomenon could be explained from a steric perspective: if the alkyl chain between the two stations provides a sufficient steric barrier to translocation, the labilised macrocycle would remain in the vicinity of the Py-station under the reaction conditions and, therefore, simply reform the starting co-conformer upon suspension of the stimulus. The simplest method of overcoming such a thermodynamic barrier is to increase the energy input into the system. Fresh independent samples of *Py*-**L3**Pt were made up in the solvent mixture as well as in neat DMF and each refluxed for 7 days but to no avail. Identical samples were heated to their respective boiling points whilst exposing them to microwave radiation for 48 h but showed no sign of isomerisation or decomposition.

An alternative method of probing this theory is to increase the relative stability of the intermediate platinum(II)-solvent complex, facilitating incremental escapement of the macrocycle from the local thermodynamic minimum of the Py-station. This was done by incorporating solvents with increased coordinating ability (neat MeCN, DMSO). Unsuccessful attempts were also made in neat pyridine and in the presence of excess un-tethered DMAP. Heating the system at 348 K in $C_2H_4Cl_2/CH_3CN$ (2:8) for 5 days resulted in alkylation of the nitrogen at the 1-position of the DMAP-station through decomposition of the dichloroethane. This product was confirmed by mass spectrometry (*m/z* = 2341.48, $[M+H]^+$).

The labilisation of kinetically inert platinum(II)-pyridine coordination bonds by salt-mediated nucleophilic activation has previously been reported[40] and attempts were made to synthesise an intermediate platinum(II)-chloride complex by heating *Py*-**L3**Pt in DMF at 383 K in the presence of tetrabutyl ammonium chloride (5 equiv) for 4 weeks. Although this resulted in some unidentified variations in the ^{1}H NMR spectrum over time, the product could not be isolated from the starting material in the crude mixture. Attempts to remove the chloride ion to allow the macrocycle to equilibrate and coordinate to one of the two stations in the thread were made by the addition of silver triflate (0.5 equiv) in DMF. However, after 12 h at room temperature multiple

decomposition products were observed and the expected favoured product of *DMAP*-**L3**Pt could not be isolated by column chromatography.

Considerable labilisation of platinum(II)-pyridine bonds has also been reported in the presence of strong hydrogen-bond donor solvents[41] such as 2,2,2-trifluoroethanol (TFE) which exhibits a hydrogen bond donating ability equivalent to that of phenol[42] and weakly acidic character resulting in the formation of a 1:1 acid-base complex with pyridine. Platinum(II)-pyridine bonds are said to be labilised in TFE due to the stabilisation afforded to the dissociated pyridine ligands through strong hydrogen bonding to the solvent. Although such an approach would certainly make the DMAP-station inaccessible as well, it was attempted to see if the platinum-complexed macrocycle could at least be moved away from the Py-station to form an intermediate metal-solvent complex. A clean sample of *Py*-**L3**Pt was dissolved in DMSO/TFE (3:7) and heated at 358 K whilst being subjected to microwave radiation for 48 h. No change was observed in the ^{1}H NMR. Following a similar theory of blocking the Py-station once the metal-ligand bond had been labilised, the [2]rotaxane was dissolved in DMSO in the presence of TsOH (2 equiv) and heated at 358 K with microwave irradiation for 48 h but, again, no changes were observed from the starting material.

3.8 Kinetic Stimulus: Photoirradiation

Although the conditions developed for the non-interlocked model experiments sufficed in overcoming the kinetic barrier to equilibration in intermolecular ligand exchange (Scheme 3.2a), it is possible that the slight differences between these systems and the [2]rotaxane have a profound effect on the kinetic stability of the Pt(II)-N bond, thus rendering the conditions inadequate for bond labilisation in the interlocked structure. The application of a kinetic stimulus to reduce the magnitude of the energy barrier could vastly increase the degree of bond dissociation under the conditions and accelerate the rate of shuttling. Photoirradiation was proposed as one such stimulus in Section 3.5 and so the photochemistry of *Py*-**L3**Pt was investigated to assess the applicability of using light as an additional stimulus to instigate shuttling of the macrocycle component. The UV-visible spectrum for the [2]rotaxane is shown in Figure 3.5.

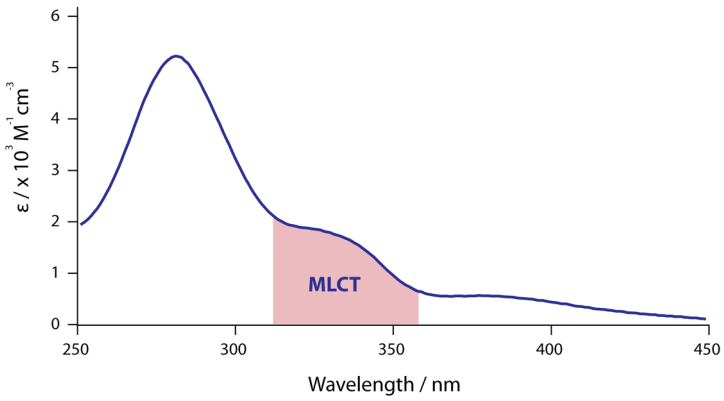

Figure 3.5 *- UV-visible absorption spectrum for Py-**L3**Pt: molar extinction coefficient (ε) vs irradiation wavelength.*

The broad, bell-shape of the peak centred at 340 nm is indicative of a charge transfer transition and represents the population of the first MLCT singlet excited state. It was predicted that from this state the system could undergo intersystem crossing to a dissociative triplet state and thus promote increased metal-ligand bond lability. A solution of *Py*-**L3**Pt in DMF-d_7/MeCN-d_3 (1:1, 1 mM) was irradiated at 340 nm at 348 K and the reaction followed by ^{1}H NMR (Figure 3.6)

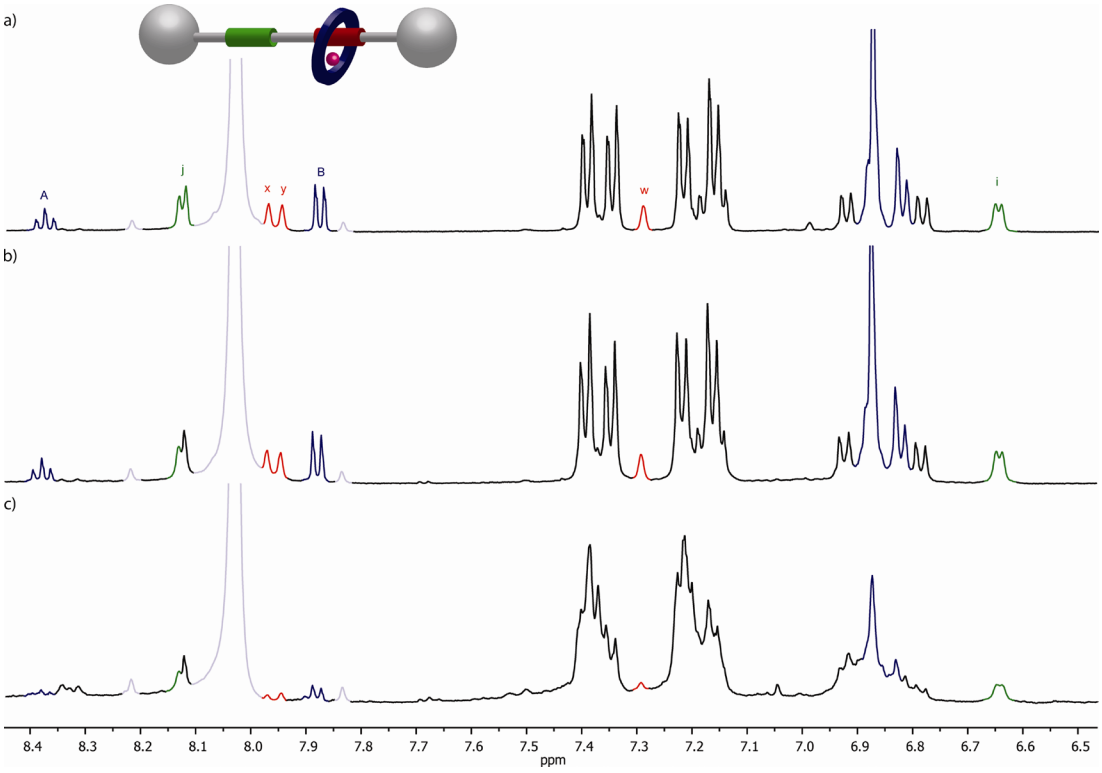

Figure 3.6 *- ^{1}H NMR spectra (500 MHz, DMF-d_7/MeCN-d_3 (1:1), 298 K) of Py-**L3**Pt upon irradiation with UV-light (340 nm ± 40 nm) at 348 K: (a) t = 0 h; (b) t = 4 h; (c) t = 20 h.*

No signs of shuttling were observed and, after 20 h of irradiation, considerable decomposition had taken place. In an attempt to reduce this deterioration, the irradiation wavelength was varied within the proposed MLCT absorption bracket using a range of bandwidth filters, the solvents were degassed with argon using a freeze-thaw technique to remove any air which could lead to the formation of reactive singlet oxygen species, and the temperature of the reaction varied. Figure 3.6 demonstrates the best results obtained using this method. It was clear from these experiments that the complex structure and electronics needed to be tuned in order to achieve the desired metal-ligand bond dissociation without significant decomposition of the complex. More worrying, however, was that Figure 3.6c appears to show decomposition not only of the metal complex, but also of the thread which had been predicted to be stable under the conditions. Before tinkering with the subtle photophysics of the Pt(II) complex to improve the efficiency of the system, experiments were carried out to test the photostability of the free ligand sites in the track.

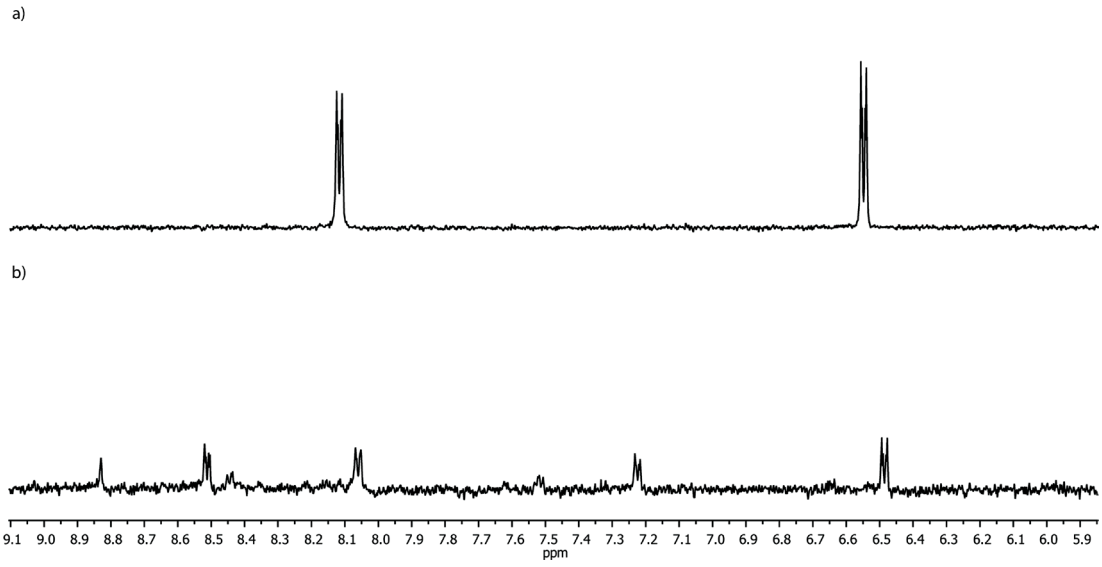

Figure 3.7 - *^{1}H NMR spectra (500 MHz, MeCN-d_3, 298 K) of DMAP upon irradiation with UV-light (340 nm ± 40 nm) at 298 K: (a) t = 0 h; (b) t = 4 h.*

A solution of DMAP in MeCN-d_3 was irradiated with UV-light at 298 K and the reaction followed by ^{1}H NMR (Figure 3.7). Significant decomposition was observed after just 4 h and, although this process could be retarded by running the experiments at high concentrations and by removing oxygen from the system, it could never be completely prevented in any solvent tested. This discovery marked the end of investigations into using UV-light as a kinetic stimulus as they clearly show that it is not compatible with the pyridine derivatives used in the threads and tracks of these systems. In order to

overcome this problem whilst retaining a pyridyl thread, a platinum(II) complex would have to be devised with an MLCT absorption band at higher wavelengths where DMAP can be irradiated without initiating photodecomposition.

3.9 Conclusion

The development of switchable components with high degrees of metastability is important for the advancement of molecular machinery such as synthetic molecular walkers and stimuli-responsive shuttles for use in molecular electronics. Manipulation of metal coordination motif energetics can help in this progression by providing operational control over submolecular components.

The system described in this chapter looked to enhance the kinetic stability of previous pH-switchable molecular shuttles through the incorporation of platinum(II) ions. Considering the relative ease with which this goal was achieved in non-interlocked model experiments, the exceptional stability of the [2]rotaxane under a large range of conditions was certainly surprising and ultimately prevented operation of the final interlocked system. This is thought to be due to steric restrictions causing a dearth of sufficient pathways for the coordinating solvent, scavenger ligand or anion to reach the platinum(II) centre meaning that, once the platinum-*Py* bond has been labilised under the applied stimulus, it simply reforms the original complex due to a lack of alternative ligand partners. This steric restriction around the metal-centre may also explain the difficulties encountered when trying to form the rotaxane *via* a Mitsunobu reaction in the final step of the synthesis. Further work on this system could involve extending the alkyl chain between the stations and their adjacent bulky stoppers to alleviate the steric restrictions and more closely mimic the model systems where the coordinating solvent species enjoy free passage to the metal ion. Attempts to employ photoirradiation as a kinetic stimulus proved unsuccessful due in part to photodecomposition of the thread at the required wavelengths for metal-ligand labilisation meaning further in-depth investigation and tuning of the relevant energy levels of the excited states involved is required.

One point is certain, however; the migration from palladium(II) to platinum(II) metal-ligand complexes in these types of rotaxane allows for an exceptional increase in molecular stability and metastability of co-conformers and may well prove useful in the continued research into molecular electronic devices.

3.10 Experimental Section

General Information

4-[tris-(4-*tert*-butylphenyl)methyl]phenol (**6**)[39] was prepared according to a modified literature procedure. 10-Undecynoic acid, propargyl alcohol, 1,6-dibromohexane, bis(*p*-hydroxyphenyl)propane), pyridine-2,6-dicarboyl dichloride, 3,5-lutidine, 4-dimethylaminopyridine and compounds **1** and **8** were purchased from Sigma Aldrich. The syntheses of **L2**Pt-(3,5-dihexyl*Py*), **L2**Pt*DMAP* and 3,5-dihexyl*Py* are described in Chapter II, Section 2.8.

Synthesis of [2]Rotaxane L3Pt

Synthesis of 2

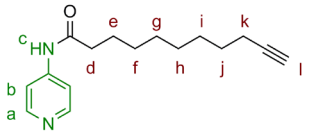

To a solution of 4-aminopyridine (5.16 g, 55.0 mmol, 2.00 equiv) and 10-undecynoic acid (5.00 g, 27.0 mmol, 1.00 equiv) in $CHCl_3$ (250 mL) was added dicyclohexylcarbodiimide (7.36 g, 36.0 mmol, 1.30 equiv) and the solution allowed to stir at room temperature for 15 h. A white precipitate was observed, filtered off and the solvent was removed under reduced pressure. The resulting crude residue was purified by column chromatography (SiO_2, MeOH/EtOAc 5:95) to give **2** (7.01 g, 99%) as a colourless oil. ^{1}H NMR (400 MHz, $CDCl_3$): δ = 8.47 (d, J = 6.3 Hz, 2H, H_a), 7.79 (s, 1H, H_c), 7.59 (d, J = 6.3 Hz, 2H, H_b), 2.42 (t, J = 7.5 Hz, 2H, H_d), 2.18 (td, J = 7.0, 2.6 Hz, 2H, H_k), 1.94 (t, J = 2.6 Hz, 1H, H_l), 1.81 – 1.66 (m, J = 14.5, 7.2 Hz, 2H, H_e), 1.56 – 1.46 (m, 2H, H_j), 1.44 – 1.23 (m, 8H, $H_{f+g+h+i}$). ^{13}C NMR (101 MHz, $CDCl_3$): δ = 172.60, 149.15, 113.78, 84.85, 68.29, 37.94, 34.09, 29.33, 29.24, 29.03, 28.78, 28.54, 25.28, 18.51. HRMS (NSI$^+$): m/z = 259.1806 $[M+H]^+$ (calcd. 259.1810 for $C_{16}H_{23}N_2O^+$).

Synthesis of 3

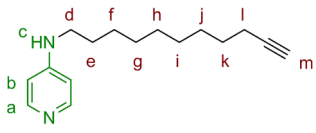

A 500 mL, oven-dried round-bottom flask was charged with **2** (7.01 g, 27.0 mmol, 1.0 equiv). THF (300 mL) was added and the resulting solution cooled to 0 °C. $LiAlH_4$

tablets (10.0 g, 263 mmol, 9.8 equiv) were added and the solution stirred for 1 h. Effervescence and a grey precipitate were observed. The ice bath was removed and the solution left to stir at 40 °C for 12 h. The reaction was quenched with H_2O, added dropwise. The grey precipitate was filtered off and the solution dried over $MgSO_4$. The solvent was removed under reduced pressure to give **3** (6.47 g, 98%) as a pale yellow oil. ^{1}H NMR (500 MHz, $CDCl_3$): δ = 8.17 (dd, J = 4.9, 1.5 Hz, 2H, H_a), 6.42 (dd, J = 4.9, 1.5 Hz, 2H, H_b), 4.20 (s, 1H, H_c), 3.13 (td, J = 7.1, 5.6 Hz, 2H, H_d), 2.18 (td, J = 7.1, 2.6 Hz, 2H, H_l), 1.94 (t, J = 2.6 Hz, 1H, H_m), 1.61 (m, 2H, H_e), 1.52 (m, 2H, H_k), 1.44 – 1.35 (m, 4H, H_{f+k}), 1.35 – 1.25 (m, 8H, $H_{g+h+i+j}$). ^{13}C NMR (126 MHz, $CDCl_3$): δ = 153.63, 149.91, 107.58, 84.87, 68.25, 42.80, 29.51, 29.41, 29.26, 29.14, 28.82, 28.57, 27.11, 18.52. HRMS (NSI$^+$): m/z = 245.2003 $[M+H]^+$ (calcd. 245.2018 for $C_{16}H_{25}N_2^+$).

Synthesis of 4

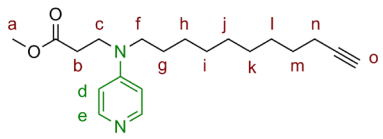

3 (6.47 g, 26.4 mmol, 1 equiv) was dissolved in methyl acrylate (48 g, 555 mmol, 35 equiv) and refluxed at 98 °C for 3 days. Excess methyl acrylate was removed under reduced pressure yielding a brown, oily residue. The crude product was purified by column chromatography (SiO_2, acetone/MeOH 9:1) to give **4** (7.17 g, 90%) as a pale, yellow oil. ^{1}H NMR (400 MHz, $CDCl_3$): δ = 8.20 (dd, J = 5.2, 1.4 Hz, 2H, H_e), 6.48 (dd, J = 5.2, 1.4 Hz, 2H, H_d), 3.70 (s, 3H, H_a), 3.66 (t, J = 7.1 Hz, 2H, H_c), 3.31 (t, J = 7.8 Hz, 2H, H_f), 2.61 (t, J = 7.1 Hz, 2H, H_b), 2.18 (td, J = 7.1, 2.6 Hz, 2H, H_n), 1.94 (t, J = 2.6 Hz, 1H, H_o), 1.63 – 1.54 (m, 2H, H_g), 1.54 – 1.47 (m, 2H, H_m), 1.45 – 1.36 (m, 2H, H_l), 1.37 – 1.16 (m, 8H, $H_{h+i+j+k}$). ^{13}C NMR (126 MHz, $CDCl_3$): δ = 172.06, 152.75, 148.84, 106.68, 84.85, 77.16, 68.27, 52.12, 50.50, 45.96, 31.95, 29.55, 29.49, 29.13, 28.81, 28.56, 27.06, 18.52. HRMS (NSI$^+$): m/z = 331.2376 $[M+H]^+$ (calcd. 331.2386 for $C_{20}H_{31}N_2O_2^+$).

Synthesis of 5

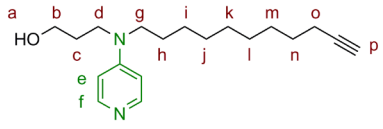

A solution of **4** (7.17 g, 21.8 mmol, 1.0 equiv) in THF (240 mL) was cooled to 0 °C and purged with nitrogen for 20 min. $LiAlH_4$ tablets (9.55 g, 252 mmol, 12.0 equiv) were

added and the reaction mixture stirred for 1 h. The ice bath was removed and the solution stirred at room temperature for 15 h. The reaction was quenched with H_2O, added dropwise. Violent effervescence and a grey precipitate were observed. The precipitate was filtered off and rinsed with THF. The rinsings and remaining solvent were combined and dried over $MgSO_4$. The solvent was removed under reduced pressure to give **5** (4.77 g, 73%) as a yellow oil. ^{1}H NMR (400 MHz, $CDCl_3$): δ = 8.15 (d, J = 6.6 Hz, 2H, H_f), 6.51 (d, J = 6.6 Hz, 2H, H_e), 3.72 (t, J =5.7 Hz, 2H, H_b), 3.47 (t, J = 7.1 Hz, 2H, H_d), 3.30 (t, J = 7.6 Hz, 2H, H_g), 2.18 (td, J = 7.0, 2.6 Hz, 2H, H_o), 1.94 (t, J = 2.6 Hz, 1H, H_p), 1.89 – 1.80 (m, J = 6.6, 3.3 Hz, 2H, H_c), 1.64 – 1.55 (m, 2H, H_h), 1.55 – 1.47 (m, 2H, H_n), 1.42 – 1.35 (m, 2H, H_m), 1.35 – 1.23 (m, 8H, $H_{i+j+k+l}$). ^{13}C NMR (101 MHz, $CDCl_3$): δ = 153.15, 148.40, 106.63, 84.87, 68.26, 59.90, 50.41, 47.00, 29.91, 29.56, 29.50, 29.13, 28.81, 28.55, 27.09, 26.95, 18.51. HRMS (NSI$^+$): m/z = 303.2435 $[M+H]^+$ (calcd. 303.2436 for $C_{19}H_{31}N_2O^+$).

Synthesis of 7

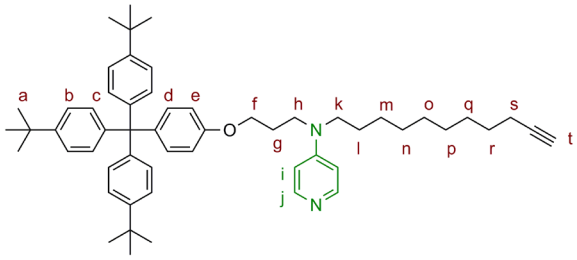

PPh_3 (4.99 g, 19.0 mmol, 1.2 equiv) was dissolved in the minimum volume of THF (20 mL) and the solution cooled to 0 °C. DIAD (4.48 g, 22.2 mmol, 1.4 equiv) was added dropwise *via* syringe over 30 min. The reaction mixture turned cloudy. A solution of **5** (4.77 g, 15.8 mmol, 1.0 equiv) in THF (15 mL) was added *via* syringe and the mixture stirred for 30 min. A solution of **6** (8.79 g, 17.4 mmol, 1.1 equiv) in THF (30 mL) cooled to 0 °C was added dropwise, and the solution stirred for 30 min. The reaction mixture was allowed to warm to room temperature and stirred for 12 h. The solvent was removed under reduced pressure and the crude product chromatographed (SiO_2, CH_2Cl_2/MeOH 99:1) to give **7** (7.59 g, 61%) as a brown solid. m.p. 107-110 °C. ^{1}H NMR (400 MHz, $CDCl_3$): δ = 8.19 (d, J = 6.4 Hz, 2H, H_j), 7.26 (d, J = 8.6 Hz, 6H, H_c), 7.16 – 7.12 (m, 2H, H_e), 7.11 (d, J = 8.6 Hz, 6H, H_b), 6.80 (d, J = 8.9 Hz, 2H, H_d), 6.54 (d, J = 6.4 Hz, 2H, H_i), 4.00 (t, J = 5.6 Hz, 2H, H_f), 3.57 (t, J = 7.2 Hz, 2H, H_h), 3.33 (t, J = 7.3, 2H, H_k), 2.20 (td, J = 7.0, 2.6 Hz, 2H, H_s), 2.14 – 2.01 (m, 2H, H_g), 1.95 (t, J = 2.6 Hz, 1H, H_t), 1.67 –

1.58 (m, 2H, H_l), 1.57 – 1.48 (m, 2H, H_r), 1.46 – 1.37 (m, 2H_q), 1.33 (m, 35H, $H_{m+n+o+p+a}$). ^{13}C NMR (101 MHz, $CDCl_3$) δ = 156.5, 152.9, 148.9, 148.5, 144.2, 140.1, 132.5, 130.8, 124.2, 113.0, 106.6, 84.8, 68.3, 64.8, 63.2, 50.5, 47.1, 34.4, 31.5, 29.5, 29.4, 29.1, 28.8, 28.5, 27.1, 27.0, 26.9, 18.5. HRMS (NSI$^+$): *m/z* = 789.5684 $[M+H]^+$ (calcd. 789.5717 for $C_{56}H_{73}N_2O^+$).

Synthesis of 9

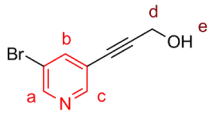

To a mixture of THF/Et_3N (1:1, 200 mL) was added 3,5-dibromopyridine (9.01 g, 38.0 mmol, 1.00 equiv) and the solution purged with nitrogen for 50 min. Propargyl alcohol (2.13 g, 38.0 mmol, 1.00 equiv) was added and the mixture purged for a further 30 min. $Pd(PPh_3)_4$ (2.63 g, 2.28 mmol, 0.06 equiv) and CuI (0.87 g, 4.56 mmol, 0.12 equiv) were added and the reaction stirred under nitrogen at room temperature for 16 h. The solvent was removed under reduced pressure and the crude product dissolved in CH_2Cl_2, and washed with sat. NH_4Cl and H_2O. A deep blue aqueous layer was observed. The organic layers were combined and dried over $MgSO_4$. The solvent was removed under reduced pressure and the crude product purified by column chromatography (SiO_2, CH_2Cl_2/MeOH 98:2) to give **9** (4.25 g, 53%) as a yellow/brown solid. m.p. 99-102 °C. ^{1}H NMR (400 MHz, $CDCl_3$): δ = 8.63 – 8.58 (m, 2H, H_{a+c}), 7.87 (t, *J* = 2.0 Hz, 1H, H_b), 4.51 (d, *J* = 6.2 Hz, 2H, H_d), 2.61 (t, *J* = 6.3 Hz, 1H, H_e). ^{13}C NMR (126 MHz, $CDCl_3$): δ = 150.23, 149.97, 141.12, 132.19, 128.73, 92.59, 80.96, 51.45.

Synthesis of 10

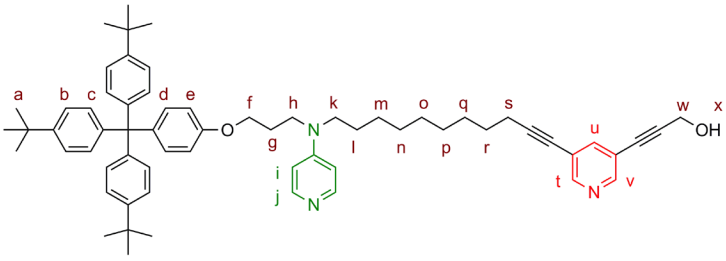

To a mixture of THF/Et_3N (3:1, 80 mL) was added **7** (7.59 g, 9.63 mmol, 1.00 equiv) and the solution purged with nitrogen for 40 min. To the mixture was added **9** (2.04 g, 9.63 mmol, 1.00 equiv) and the solution purged for 30 min. $Pd(PPh_3)_4$ (0.51 g, 0.41 mmol, 0.05 equiv) and copper iodide (0.205 g, 1.10 mmol, 0.10 equiv) were added and

the reaction stirred at 50 °C for 5 h. The solvent was removed under reduced pressure and the crude product dissolved in CH_2Cl_2 and washed with ammonia solution (1 M, 2 x 20 mL). The organic layer was dried over $MgSO_4$ and the solvent removed under reduced pressure. The resulting residue was purified by flash column chromatography (SiO_2, CH_2Cl_2/MeOH 85:15) to give **10** (5.69 g, 64%) as a brown solid, m.p. 124-127 °C. ^{1}H NMR (400 MHz, $CDCl_3$): δ = 8.51 (d, J = 2.0 Hz, 1H, H_v), 8.50 (d, J = 2.0 Hz, 1H, H_t), 8.15 (d, J = 6.5 Hz, 2H, H_j), 7.67 (t, J = 2.0 Hz, 1H, H_u), 7.23 (d, J = 8.6 Hz, 6H, H_b), 7.10 (d, J = 8.9 Hz, 2H, H_e), 7.08 (d, J = 8.6 Hz, 6H, H_c), 6.77 (d, J = 8.9 Hz, 2H, H_d), 6.50 (d, J = 6.5 Hz, 2H, H_i), 4.48 (s, 2H, H_w), 3.97 (t, J = 5.6 Hz, 2H, H_f), 3.53 (t, J = 7.1 Hz, 2H, H_h), 3.30 (t, J = 7.9 Hz, 2H, H_k), 2.42 (t, J = 6.7 Hz, 2H, H_s), 2.10 – 1.98 (m, 2H, H_g), 1.65 – 1.52 (m, 4H, H_{r+l}), 1.51 – 1.40 (m, 2H, H_q), 1.36 – 1.31 (m, 8H, $H_{m+n+o+p}$), 1.30 (s, J = 4.3 Hz, 27H, H_a). ^{13}C NMR (101 MHz, $CDCl_3$): δ = 156.5, 153.1, 151.1, 150.4, 148.5, 148.4, 144.2, 140.9, 140.1, 132.5, 130.8, 124.2, 120.9, 119.8, 113.0, 106.6, 94.9, 92.6, 80.9, 76.9, 64.8, 63.2, 50.9, 50.5, 47.1, 34.4, 31.5, 29.4, 29.1, 29.0, 28.7, 28.3, 27.0, 26.9, 26.7, 19.5. HRMS (NSI$^+$): m/z = 920.6095 $[M+H]^+$ (calcd. 920.6094 for $C_{64}H_{78}N_3O_2^+$).

Synthesis of 11

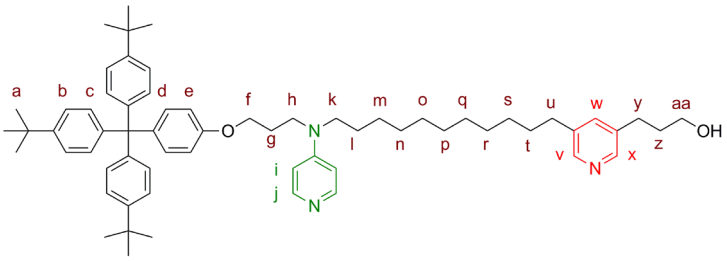

To a mixture of THF/$CHCl_3$ (1:1, 100 mL) was added **10** (4.32 g, 4.70 mmol, 1.00 equiv) and the solution purged with nitrogen for 20 min. $Pd(OH)_2$/C (large excess) and K_2CO_3 (0.035 g, 0.24 mmol, 0.05 equiv) were added and the solution purged with hydrogen for 30 min. The reaction was left to stir under hydrogen at room temperature for 12 h. The reaction mixture was filtered through Celite® and the solvent removed under reduced pressure. The crude black residue was purified by column chromatography (SiO_2, CH_2Cl_2/MeOH 95:5) to give **11** (4.16 g, 95%) as an off-white solid. m.p. 157-160 °C. ^{1}H NMR (400 MHz, $CDCl_3$): δ = 8.28 (d, J = 2.0 Hz, 1H, H_w), 8.26 (d, J = 2.0 Hz, 1H, H_x), 8.12 (d, J = 6.5 Hz, 2H, H_j), 7.32 (t, J = 2.0 Hz, 1H, H_v), 7.23 (d, J = 8.6 Hz, 6H, H_c), 7.11 (d, J = 8.9 Hz, 2H, H_e), 7.07 (d, J = 8.6 Hz, 6H, H_b), 6.77 (d, J = 8.9 Hz, 2H, H_d), 6.62 (d, J = 6.25 Hz, 2H, H_i), 3.99 (t, J = 5.4 Hz, 2H, H_f), 3.68 (t, J = 6.4 Hz, 2H, H_{aa}), 3.62 (t, J =

7.0 Hz, 2H, H_h), 3.38 (t, *J* = 7.4 Hz, 2H, H_k), 2.69 (t, *J* = 7.6 Hz, 2H, H_y), 2.56 (t, *J* = 7.5 Hz, 2H, H_u), 2.13 – 2.03 (m, 2H, H_g), 1.88 (m, 2H, H_z), 1.66 – 1.52 (m, 4H, H_{l+t}), 1.30 (s, 27H, H_a), 1.36 – 1.22 (m, 14H, $H_{m+n+o+p+q+r+s}$). ^{13}C NMR (101 MHz, $CDCl_3$): δ = 156.2, 155.3, 148.6, 147.7, 147.5, 144.1, 140.5, 137.7, 136.8, 136.0, 132.6, 130.8, 124,2, 113.0, 106.6, 77.4, 64.4, 61.9, 51.2, 47.9, 36.2, 34.5, 34.1, 33.0, 31.5, 31.3, 29.6, 29.5, 29.4, 29.3, 29.2, 27.0, 26.9, 26.8, 26.7, 26.3. HRMS (ESI$^+$): *m/z* = 928.6689 $[M+H]^+$ (calcd. 928.6720 for $C_{64}H_{86}N_3O_2^+$).

Synthesis of 12

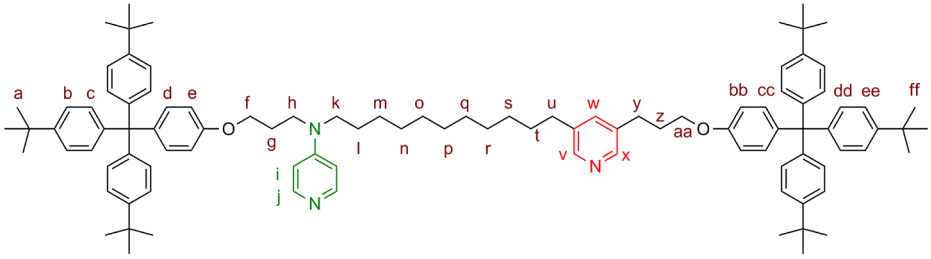

An oven-dried 5 mL round bottom flask was charged with PPh_3 (0.035 g, 0.132 mmol, 1.2 equiv) in THF (1 mL) and the solution cooled to 0 °C. DIAD (0.031 g, 0.154 mmol, 1.4 equiv) was added dropwise and the solution stirred under nitrogen for 40 min. **11** (0.102 g, 0.110 mmol, 1.0 equiv) was added in THF (1 mL) and the solution stirred for 40 min. **6** (0.083 g, 0.165 mmol, 1.5 equiv) dissolved in minimum THF (1 mL) was added and the reaction allowed to warm to room temperature over 12 h. The solvent was removed under reduced pressure and the crude product purified by column chromatography (SiO_2, CH_2Cl_2/MeOH 98:2) to give **12** (53 mg, 56%) as an off-white solid. m.p. 240 °C (dec.). ^{1}H NMR (500 MHz, $CDCl_3$): δ = 8.30 (s, 1H, H_x), 8.27 (s, 1H, H_v), 8.09 (d, *J* = 6.9 Hz, 2H, H_j), 7.33 (s, 1H, H_w), 7.23 (d, *J* = 8.6 Hz, 6H, H_c), 7.22 (d, *J* = 8.6 Hz, 6H, H_{dd}), 7.12 (d, *J* = 8.9 Hz, 2H, H_e), 7.08 (d, *J* = 8.9 Hz, 10H, H_{bb}), 7.08 (d, *J* = 8.6 Hz, 6H, H_b), 7.07 (d, *J* = 8.6 Hz, 6H, H_{cc}), 6.76 (d, *J* = 8.9 Hz, 2H, H_d), 6.75 (d, *J* = 8.9 Hz, 2H, H_{cc}), 4.00 (t, *J* = 5.3 Hz, 2H, H_f), 3.94 (t, *J* = 6.1 Hz, 2H, H_{aa}), 3.68 (t, *J* = 6.9 Hz, 2H, H_h), 3.44 (t, *J* = 7.4 Hz, 2H, H_k), 2.78 (t, *J* = 7.5 Hz, 2H, H_y), 2.56 (t, *J* = 7.5 Hz, 2H, H_u), 2.15 – 2.03 (m, 4H, H_{g+z}), 1.68 – 1.61 (m, 2H, H_l), 1.61 – 1.53 (m, 2H, H_t), 1.36 – 1.31 (m, 2H, H_m), 1.30 (s, 27H, $H_{a,ff}$), 1.29 – 1.20 (m, 12H, $H_{n+o+p+q+r+s}$). ^{13}C NMR (126 MHz, $CDCl_3$): δ = 156.8, 156.3, 156.1, 148.6, 148.5, 147.8, 147.1, 144.3, 144.1, 140.7, 140.2, 139.5, 138.2, 136.7, 136.2, 132.6, 132.4, 130.9, 130.8, 124.3, 124.2, 113.1, 113.0, 106.7, 66.6, 64.2, 63.3, 63.2, 51.5, 48.3, 34.5, 34.4, 34.1, 33.0, 31.5, 31.2, 29.9, 29.8, 29.7, 29.6,

29.5, 29.4, 27.0, 26.9, 26.8, 26.7. HRMS (NSI+): *m/z* = 1415.9940 $[M+H]^+$ (calcd. 1416.0040 for $C_{101}H_{128}N_3O_2^+$).

Synthesis of 14

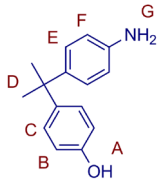

2,2-Bis(*p*-hydroxyphenyl)propane) (22.8 g, 100 mmol, 1.0 equiv) and aniline hydrochloride (38.9g, 300 mmol, 3.0 equiv) were added to a 150 mL round bottom flask and heated to 180 °C to give a clear liquid. The resulting liquid was stirred at 180 °C for 45 min and cooled to room temperature to give a sticky solid. Water (600 mL) was added to give a suspension. The pH adjusted to >13 by addition of 50% NaOH. The resulting mixture was extracted with toluene (3 x 100 mL) to remove aniline. The pH was adjusted to 5.5 by addition of 0.5 M HCl to give a white precipitate of the crude product which was collected and washed with water (20 mL). The powder was recrystallised from EtOH to give the pure **14** (7.1 g, 31 mmol, 31%) as a white microcrystalline solid. ^{1}H NMR (400 MHz, DMSO-d_6): δ = 9.15 (s, 1H, H_A), 6.96 (d, J = 8.7, 2H, H_E), 6.83 (d, J = 8.6, 2H, H_C), 6.61 (d, J = 8.7, 2H, H_F), 6.43 (d, J = 8.6, 2H, H_B), 4.83 (s, 2H, H_G), 1.49 (s, 6H, H_D). ^{13}C NMR (101 MHz, DMSO-d_6): δ = 154.8, 146.0, 141.5, 138.1, 127.3, 126.8, 114.5, 113.6, 40.8, 31.0. HRMS (NSI+): *m/z* = 228.1382 $[M+H]^+$ (calcd. 228.1388 for $C_{15}H_{18}NO^+$).

Synthesis of 15

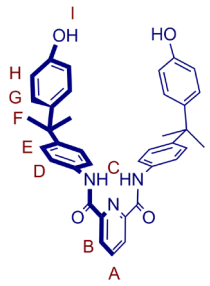

To a solution of **14** (0.560 g, 2.50 mmol, 2.3 equiv) and Et_3N (0.30 g, 3.00 mmol, 2.7 equiv) in dry THF (50 mL) was added pyridine-2,6-dicarboyl dichloride (0.227g, 1.10 mmol, 1 equiv) in THF (10 mL) slowly at 0 °C. A white precipitate formed immediately and became pale yellow after several hours. The solution was stirred at room

temperature for 20 h and the solution filtered to remove the white precipitate, which was washed with THF (100 mL). The solvent was removed under reduced pressure to give a fluffy solid which was recrystallised from EtOH/H_2O to give **15** (0.570 g, 87%) as a white powder. m.p. 270 °C (dec.). ^{1}H NMR (400 MHz, DMSO-d_6): δ = 10.97 (s, 2H, H_C), 9.23 (s, 2H, H_I), 8.39 (dd, J = 7.7, 0.8, 2H, H_B), 8.30 (dd, J = 8.6, 6.8, 1H, H_A), 7.76 (d, J = 8.7, 4H, H_H), 7.28 (d, J = 8.8, 4H, H_G), 7.04 (d, J = 8.7, 4H, H), 6.68 (d, J = 8.7, 4H, H_D), 1.63 (s, 12H, H_F). ^{13}C NMR (101 MHz, DMSO-d_6): δ = 161.6, 155.1, 148.9, 147.1, 140.6, 135.4, 127.4, 126.8, 125.3, 121.1, 114.7, 41.5, 30.70. HRMS (NSI$^+$): m/z = 586.2696 $[M+H]^+$, 608.2512 $[M+Na]^+$ (calcd. 586.2706 for $C_{37}H_{36}N_3O_4^+$, 608.2525 for $C_{37}H_{35}N_3NaO_4^+$).

Synthesis of 16

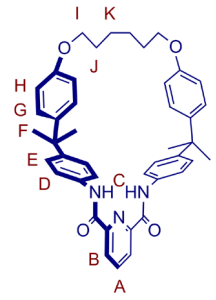

To a solution of **15** (1.77 g, 3.02 mmol, 1.0 equiv) in DMF (600 mL) was added K_2CO_3 (10 g, 76 mmol, 25 equiv). To the stirring suspension was added 1,6-dibromohexane (0.737 g, 3.02 mmol, 1.0 equiv) slowly *via* syringe over a period of 30 min and the mixture stirred at room temperature for 3 days. The solvent was removed under reduced pressure and the crude product dissolved in CH_2Cl_2, washed with H_2O and dried over $MgSO_4$. The crude residue was purified by column chromatography (SiO_2 CH_2Cl_2/cyclohexane/Et_2O 5:4:1) to give **16** (0.887 g, 45%) as a white crystalline solid. m.p. 330 °C (dec.). ^{1}H NMR (400 MHz, $CDCl_3$): δ = 9.47 (s, 2H, H_C), 8.47 (d, J = 7.8 Hz, 2H, H_B), 8.16 (t, J = 7.8 Hz, 1H, H_A), 7.56 (d, J = 8.6 Hz, 4H, H_D), 7.16 (d, J = 8.8 Hz, 4H, H_G), 7.14 (d, J = 8.6 Hz, 4H, H_E), 6.80 (d, J = 8.8 Hz, 4H, H_H), 3.96 (t, J = 6.2 Hz, 4H, H_I), 1.82 (t, J = 6.1 Hz, 4H, H_J), 1.68 (s, 12H, H_F), 1.53 (s, 4H, H_K). ^{13}C NMR (101 MHz, $CDCl_3$): δ = 160.7, 157.3, 148.9, 148.8, 142.5, 140.1, 134.5, 128.1, 127.8, 125.4, 119.4, 114.1, 67.7, 42.3, 30.1, 29.3, 25.6. HRMS (NSI$^+$): m/z = 690.3305 $[M+Na]^+$ (calcd. 690.3308 for $C_{43}H_{45}N_3NaO_4^+$).

Synthesis of L3

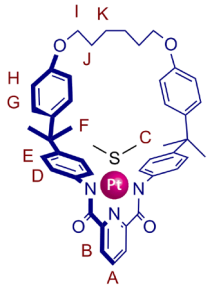

A 15 mL oven-dried round bottom flask was charged with **16** (0.167 g, 0.250 mmol, 1.0 equiv). THF (9 mL) was added and the solution purged with nitrogen for 20 min. NaH (0.017 g, 0.450 mmol, 1.7 equiv) was added and the reaction mixture stirred for 5 h. After a cloudy solution was observed the vessel was wrapped in tin foil and cooled to 0 °C. $PtCl_2(SMe_2)_2$ (0.176 g, 0.450 mmol, 1.8 equiv) was added and the reaction stirred under nitrogen for 12 h. A yellow solution was observed with some white precipitate. The solution was filtered through cotton wool and the solvent removed under vacuum. The crude residue was purified by column chromatography (SiO_2, CH_2Cl_2/MeOH 95.5:0.5) to give **L3** (0.070g, 78%) as an orange crystalline solid. m.p. 345 °C (dec.). ^{1}H NMR (400 MHz, $CDCl_3$): δ = 8.17 (t, J = 7.8, 1H, H_A), 7.96 (d, J = 7.8 Hz, 2H, H_B), 7.22 (d, J = 8.4 Hz, 4H, H_D), 7.13 (d, J = 8.4 Hz, 4H, H_E), 6.98 (d, J = 8.8 Hz, 4H, H_G), 6.67 (d, J = 8.8 Hz, 4H, H_H), 3.88 (t, J = 6.4 Hz, 4H, H_I), 1.85 – 1.76 (m, 4H, H_J), 1.67 (s, 12H_F), 1.55 – 1.49 (m, 4H_K), 1.38 (s, 6H_C). ^{13}C NMR (101 MHz, $CDCl_3$): δ = 170.4, 157.0, 150.5, 148.6, 145.1, 143.7, 141.0, 127.7, 127.5, 126.3, 126.1, 113.5, 67.7, 42.0, 30.23, 29.8, 29.1, 25.8, 21.1. HRMS (NSI$^+$) : m/z = 923.3159 $[M+H]^+$ (calcd. 923.3170 for $C_{45}H_{50}N_3O_4PtS^+$).

Synthesis of 17

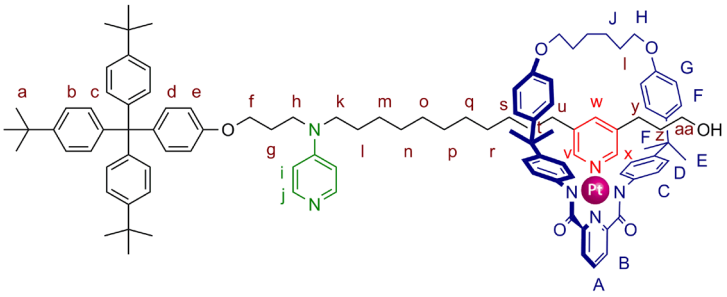

To a stirring solution of **11** (145 mg, 0.155 mmol, 1.0 equiv) in $CHCl_3$ (1.5 mL) under nitrogen was added trifluoroacetic acid (21 mg, 0.186mmol, 1.2 equiv) dropwise. The solution was stirred for 1 h. **L3** (143 mg, 0.155 mmol, 1.0 equiv) dissolved in $CHCl_3$ was

added *via* syringe. The solution was heated to 55 °C and stirred under nitrogen for 3 days. The solution was washed with $NaHCO_3$ solution and dried over $NaSO_4$. The solvent was removed under reduced pressure and the crude residue purified by column chromatography (SiO_2, CH_2Cl_2/MeOH 96:4) to give **17** (176 mg, 63%) as an orange crystalline solid. m.p. 230 °C (dec.). ^{1}H NMR (500 MHz, $CDCl_3$): δ = 8.10 (t, J = 7.9 Hz, 2H, H_A), 8.09 – 8.04 (m, 2H, H_j), 7.83 (d, J = 7.9 Hz, 2H, H_B), 7.78 (d, J = 1.1 Hz, 1H, H_v), 7.68 (d, J = 1.1 Hz, 1H, H_x), 7.23 (d, J = 8.6 Hz, 6H, H_c), 7.12 (d, J = 8.9 Hz, 2H, H_e), 7.07 (d, J = 8.6 Hz, 6H, H_b), 6.87 (d, J = 8.5 Hz, 4H, H_G), 6.80 (d, J = 8.5 Hz, 4H, H_H), 6.79 (d, J = 8.8 Hz, 4H, H_C), 6.75 (d, J = 8.9 Hz, 2H, H_d), 6.74 (s, 1H, H_w), 6.68 (d, J = 4.6 Hz, 2H, H_i), 6.63 (d, J = 8.8 Hz, 4H, H_D), 3.98 (t, J = 5.3 Hz, 2H, H_f), 3.94 (t, J = 6.5 Hz, 4H, H_I), 3.63 (t, J = 7.2 Hz, 2H, H_h), 3.39 (t, J = 7.6 Hz, 2H, H_k), 3.13 (t, J = 6.0 Hz, 2H, H_{aa}), 2.12 – 1.99 (m, 6H, H_{g+u+y}), 1.90 – 1.80 (s, 4H, H_J), 1.65 – 1.56 (m, 6H, H_{K+l}), 1.53 (s, 6H, $H_{E,F}$), 1.34 – 1.31 (m, J = 12.0 Hz, 4H, H_{m+z}), 1.30 (s, 27H, H_a), 1.27 – 1.09 (m, 12H, $H_{n+o+p+q+r+t}$), 1.04 – 0.96 (m, H, H_s). ^{13}C NMR (126 MHz, $CDCl_3$): δ = 169.86, 156.72, 156.17, 152.13, 149.58, 149.05, 148.56, 146.95, 144.11, 143.49, 143.16, 141.15, 140.55, 140.34, 139.52, 139.28, 137.74, 132.58, 130.81, 127.33, 126.42, 125.80, 125.29, 124.22, 113.53, 113.00, 106.71, 67.86, 64.37, 63.18, 59.97, 51.25, 48.06, 41.54, 34.44, 32.75, 32.39, 32.06, 31.51, 30.36, 30.17, 30.14, 29.75, 29.71, 29.65, 29.50, 29.18, 28.72, 28.10, 27.04, 26.88, 25.91, 22.82, 14.26. HRMS (ESI$^+$): m/z = 1789.9585 $[M+H]^+$ (calcd. 1789.9655 for $C_{107}H_{129}N_6O_6Pt^+$).

Synthesis of *Py*-L3Pt

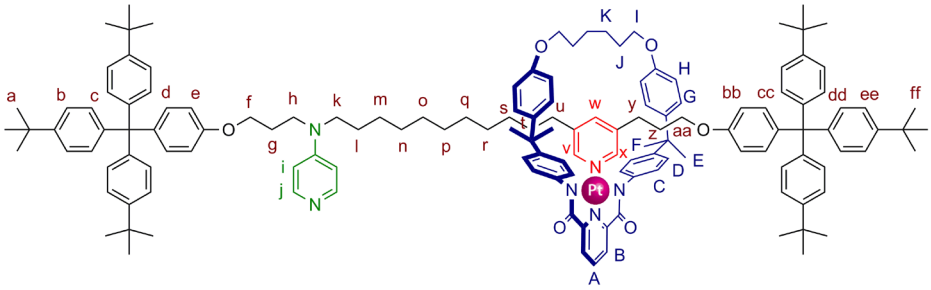

To a solution of **17** (0.060 g, 0.033 mmol, 1.0 equiv) in $CHCl_3$ (10 mL) as added MsCl (0.008 g, 0.067 mmol, 2.0 equiv) and Et_3N (0.014 g, 0.134 mmol, 4.0 equiv) and the reaction stirred at room temperature for 1 h. The reaction was quenched with H_2O and the crude product extracted with CH_2Cl_2, washed with brine and dried over $MgSO_4$. The solvent was removed under reduced pressure to give a yellow oil which was added

to a solution of NaH (0.024 g, 0.602 mmol, 4.9 equiv) and **6** (0.310 g, 0.614 mmol, 5.0 equiv) in THF (30 mL) that had been stirring at room temperature for 4 h.

15-crown-5 (0.135 g, 0.614 mmol, 5.0 equiv) and DMSO (1.5 mL) were added and the reaction stirred at 48 °C for 48 h. The solvents were removed under reduced pressure, the crude product dissolved in CH_2Cl_2 and washed with H_2O and brine. The organic fractions were dried over $MgSO_4$ and the solvent removed under reduced pressure. The crude residue was purified by column chromatography (SiO_2, CH_2Cl_2/MeOH 9:1) to give *Py*-**L3**Pt (0.158 g, 56%) as an orange solid m.p. 181-184 °C. ^{1}H NMR (500 MHz, $CDCl_3$): δ = 8.12 (s, 1H, H_j), 8.12 – 8.08 (m, 1H, H_A), 7.88 (d, J = 7.9 Hz, 2H, H_B), 7.73 – 7.69 (m, 2H, H_{v+x}), 7.25 – 7.22 (m, 4H, H_c), 7.22 – 7.15 (m, 12H, H_{c+dd}), 7.09 –7.04 (m, 16H, $H_{b,e,bb,ee}$), 6.83 (s, 8H, H_{G+H}), 6.79 (d, J = 8.8 Hz, 4H, H_D), 6.78 (s, 1H, H_w), 6.77 – 6.74 (m, 2H, H_d), 6.66 (d, J = 9.0 Hz, 2H, H_{cc}), 6.61 (d, J = 8.8 Hz, 4H, H_C), 6.57 (d, J = 5.6 Hz, 2H_i), 3.97 (t, J = 5.5 Hz, 2H, H_f), 3.92 – 3.85 (m, 4H, H_I), 3.57 (d, J = 7.1 Hz, 2H, H_h), 3.56 – 3.51 (m, 2H, H_{aa}), 3.36 – 3.28 (m, 2H, H_k), 2.11 (t, J = 7.6 Hz, 2H, H_y), 2.08 – 2.04 (m, 2H, H_g), 2.01 (t, J = 7.6 Hz, 2H, H_t), 1.81 (d, J = 6.1 Hz, 4H, H_J), 1.63 – 1.53 (m, 8H, $H_{K,l,z}$), 1.48 (s, 6$H_{E/F}$), 1.49 (s, 6$H_{E/F}$), 1.30 (s, 27H, $H_{a/ff}$), 1.28 (s, 27H, $H_{a/ff}$), 1.27 – 1.21 (m, 12H, $H_{m,n,o,p,q,r}$), 1.23 – 1.15 (m, 2H, H_t), 1.06 - 1.00 (m, 2H, H_s). ^{13}C NMR (126 MHz, $CDCl_3$): δ =169.89, 156.73, 156.45, 156.39, 154.07, 152.31, 149.40, 149.12, 148.52, 148.47, 146.88, 145.72, 144.16, 144.15, 143.44, 143.26, 140.29, 140.18, 140.15, 139.66, 138.69, 137.39, 132.52, 132.45, 130.83, 130.82, 127.30, 126.46, 125.76, 125.28, 124.20, 113.42, 113.04, 112.91, 106.64, 67.66, 65.65, 64.68, 63.18, 63.16, 50.75, 47.49, 41.48, 34.43, 34.42, 32.39, 30.39, 30.22, 30.01, 29.83, 29.81, 29.76, 29.70, 29.61, 29.52, 29.35, 29.14, 28.78, 28.55, 27.13, 26.98, 25.91, 22.83, 14.27. HRMS (NSI$^+$): m/z = 2276.2843 $[M+H]^+$ (calcd. 2276.2941 $C_{144}H_{171}N_6O_6Pt^+$).

Synthesis Model Compounds

Synthesis of L3Pt*DMAP*

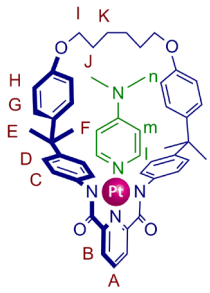

To a solution of **L3** (50 mg, 0.054 mmol, 1.0 equiv) in $CHCl_3$ (2 mL) was added DMAP (6.6 mg, 0.054 mmol, 1.0 equiv) and the mixture stirred at 50 °C under nitrogen for 15 h. The solvent was removed under reduced pressure and the crude residue purified by column chromatography (SiO_2, CH_2Cl_2/MeOH 98:2) to give **L3**Pt*DMAP* (45 mg, 83%) as an orange crystalline solid. m.p. 300 °C (dec.). ^{1}H NMR (400 MHz, $CDCl_3$): δ = 8.11 (t, J = 7.9 Hz, 1H, H_A), 7.90 (d, J = 7.8 Hz, 2H, H_B), 7.13 (d, J = 7.2 Hz, 2H, H_l), 6.97 – 6.84 (m, 12H, H_{C+D+G}), 6.60 (d, J = 8.7 Hz, 4H, H_h), 5.64 (d, J = 7.2 Hz, 2H, H_m), 3.88 (t, J = 5.8 Hz, 4H, H_I), 2.70 (s, 6H, H_n), 1.85 – 1.78 (m, 4H, H_J), 1.58 (s, 12H, H_{E+F}), 1.56 - 1.52 (m, 4H, H_K). ^{13}C NMR (126 MHz, $CDCl_3$): δ = 170.30, 156.88, 153.41, 152.49, 150.60, 146.39, 144.01, 143.35, 139.55, 127.68, 126.85, 125.87, 125.69, 113.29, 107.29, 67.46, 41.84, 39.48, 30.50, 29.59, 26.36. HRMS (NSI$^+$): m/z = 1005.3637 $[M+Na]^+$ (calcd. 1005.3643 for $C_{50}H_{53}N_5NaO_4Pt^+$).

Synthesis of L3Pt-(3,5-*lutidine*)

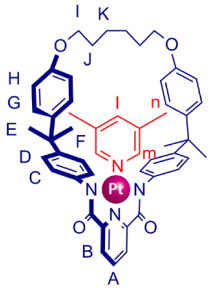

To a solution of **L3** (50 mg, 0.054 mmol, 1.0 equiv) in $CHCl_3$ (2 mL) was added 3,5-lutidine (5.8 mg, 0.054 mmol, 1.0 equiv) and the mixture stirred at 50 °C under nitrogen for 15 h. The solvent was removed under reduced pressure and the crude residue purified by column chromatography (SiO_2, CH_2Cl_2/MeOH 97:3) to give **L3**Pt-(3,5-*lutidine*) (44 mg, 85%) as an orange crystalline solid. m.p. 290 °C (dec.). ^{1}H NMR (400 MHz, $CDCl_3$): δ = 8.12 (t, J = 7.8 Hz, 1H, H_A), 7.90 (d, J = 7.8 Hz, 2H, H_B), 7.58 (s, 2H, H_m), 6.94 – 6.82 (m, 12H, H_{C+D+G}), 6.77 (s, 1H, H_l), 6.65 (d, J = 8.8 Hz, 4H, H_H), 3.94 (t, J = 6.3 Hz, 4H, H_I), 1.88 – 1.80 (m, 4H, H_J), 1.67 (s, 6H, H_n), 1.60 – 1.56 (m, 4H, H_K), 1.55 (s, 12H, H_{E+F}). ^{13}C NMR (126 MHz, $CDCl_3$): δ =170.06, 156.79, 149.47, 146.92, 143.41, 143.03, 140.05, 138.60, 134.77, 127.30, 126.39, 125.51, 113.57,67.80, 41.51, 30.05, 29.21, 25.92, 17.85. HRMS (NSI$^+$): m/z = 1022.3332 $[M+Na]^+$ (calcd. 1022.6335 for $C_{50}H_{52}N_4NaO_4Pt^+$).

General Procedures for Model Exchange Experiments

Exchange of 3,5-dihexylPy for DMAP in L2Pt-(3,5-dihexyl*Py*) (Scheme 3.1)

To two vacuum dried NMR tubes was added **L2**Pt-(3,5-dihexyl*Py*) (0.25 mL, 2.0 mM, 1 equiv) and DMAP (0.25 mL, 2.0 mM, 1 equiv) each from stock solutions in DMF-d_7/CD_3CN (1:1). The tubes were sealed. One was left at room temperature and the other heated at 348 K for two weeks during which time each was monitored by ^1H NMR spectroscopy. The room temperature sample shoed no changes throughout the duration of the experiment. The heated sample reached an equilibrium distribution of 25:75 **L2**Pt-(3,5-dihexyl*Py*):*DMAP* within 2 weeks.

Exchange of 3,5-lutidine for DMAP in L3Pt-(3,5-*lutidine*) (Figure 3.2a)

To two vacuum dried NMR tubes was added **L3**Pt-(3,5-*lutidine*) (0.25 mL, 2.0 mM, 1 equiv) and DMAP (0.25 mL, 2.0 mM, 1 equiv) each from stock solutions in DMF-d_7/CD_3CN (1:1). The tubes were sealed. One was left at room temperature and the other heated at 348 K and each monitored by ^1H NMR spectroscopy. The room temperature sample shoed no changes throughout the duration of the experiment (2 weeks). The heated sample reached an equilibrium distribution of 25:75 **L3**Pt-(*3,5-lutidine*):*DMAP* within 18 h.

Exchange of DMAP for 3,5-lutidine in L3Pt*DMAP* (Figure 3.2b)

To two vacuum dried NMR tubes was added **L3**Pt-(3,5-*lutidine*) (0.16 mL, 3.0 mM, 1 equiv), DMAP (0.16 mL, 3,0 mM, 1 equiv), and TsOH (0.16 mL, 3,0 mM, 1 equiv) each from stock solutions in DMF-d_7/CD_3CN (1:1). The tubes were sealed. One was left at room temperature and the other heated at 348 K and each monitored by ^1H NMR spectroscopy. The room temperature sample showed no changes throughout the duration of the experiment (2 weeks). The heated sample reached an equilibrium distribution of 25:75 **L3**Pt-(*3,5-lutidine*):*DMAP* within 18 h.

3.11 References

1. Moore, G. E. *Electronics* **1965**, *38*.

2. Radelaar, S. *Physics and Technology of Semiconductor Qunatum Devices*, Springer: Berlin, **1993**.

3. Galloway, J. M.; Bramble, J. P.; Rawlings, A. E.; Evans, S. D.; Staniland, S. S. *Small* **2012**, *8*, 204-208.

4. *For reviews on the progression of the field of molecuar electronics, see:*

a) Shipway, A. N.; Willner, I. *Acc. Chem. Res.* **2001**, *34*, 421-432;

b) Coskun, A.; Spruell, J. M.; Barin, G.; Dichtel, W. R.; Flood, A. H.; Botros, Y. Y.; Stoddart, J. F. *Chem. Soc. Rev.* **2012**, *41*, 4827-4859.

5. a) Polymeropoulos, E. E.; Sagiv, J. *J. Chem. Phys.* **1978**, *69*, 1836-1847;

b) Lee, T.; Wang, W.; Klemic, J. F.; Zhang, J. J.; Su, J.; Reed, M. A. *J. Phys. Chem. B* **2004**, *108*, 8742-8750.

6. a) Ashwell, G. J.; Ewington, J.; Moczko, K. *J. Mater. Chem.* **2005**, *15*, 1154-1159;

b) Ho, G.; Heath, J. R.; Kondratenko, M.; Perepichka, D. F.; Arseneault, K.; Pézolet, M.; Bryce, M. R. *Chem.- Eur. J.* **2005**, *11*, 2914-2922.

7. a) Whalley, A. C.; Steigerwald, M. L.; Guo, X.; Nuckolls, C. *J. Am. Chem. Soc.* **2007**, *129*, 12590-12591;

b) Feldman, A. K.; Steigerwald, M. L.; Guo, X.; Nuckolls, C. *Acc. Chem. Res.* **2008**, *41*, 1731-1741;

c) Guo, X.; Xiao, S.; Myers, M.; Miao, Q.; Steigerwald, M. L.; Nuckolls, C. *Proc. Natl Acad. Sci. U. S. A.* **2009**, *106*, 691-696.

8. *For recent articles on molecular shuttles that exploit weak non-covalent interactions, see:*

a) Aucagne, V.; Berná, J.; Crowley, J. D.; Goldup, S. M.; Hänni, K. D.; Leigh, D. A.; Lusby, P. J.; Ronaldson, V. E.; Slawin, A. M. Z.; Viterisi, A.; Walker, D. B. *J. Am. Chem. Soc.* **2007**, *129*, 11950-11963;

b) Barrell, M. J.; Leigh, D. A.; Lusby, P. J.; Slawin, A. M. Z. *Angew. Chem., Int. Ed.* **2008**, *47*, 8036-8039;

c) Umehara, T.; Kawai, H.; Fujiwara, K.; Suzuki, T. *J. Am. Chem. Soc.* **2008**, *130*, 13981-13988;

d) Angelos, S.; Khashab, N. M.; Yang, Y.-W.; Trabolsi, A.; Khatib, H. A.; Stoddart, J. F.; Zink, J. I. *J. Am. Chem. Soc.* **2009**, *131*, 12912-12914;

e) Coutrot, F.; Busseron, E. *Chem.- Eur. J.* **2009**, *15*, 5186-5190;

f) Fang, L.; Hmadeh, M.; Wu, J.; Olson, M. A.; Spruell, J. M.; Trabolsi, A.; Yang, Y.-W.; Elhabiri, M.; Albrecht-Gary, A.-M.; Stoddart, J. F. *J. Am. Chem. Soc.* **2009**, *131*, 7126-7134;

g) Lee, C.-F.; Leigh, D. A.; Pritchard, R. G.; Schultz, D.; Teat, S. J.; Timco, G. A.; Winpenny, R. E. P. *Nature* **2009**, *458*, 314-318;

h) Moretto, A.; Menegazzo, I.; Crisma, M.; Shotton, E. J.; Nowell, H.; Mammi, S.; Toniolo, C. *Angew. Chem., Int. Ed.* **2009**, *47*, 8986-8989;

i) Tokunaga, Y.; Kawabata, M.; Matsubara, N. *Org. Biomol. Chem.* **2011**, *9*, 4948-4953;

j) Panman, M. R.; Bodis, P.; J., S. D.; Bakker, D. H.; Newton, A. C.; Kay, E. R.; Leigh, D. A.; Buma, W. J. *Phys. Chem. Chem. Phys.* **2012**, *14*, 1865-1875;

k) Zhu, K.; Vukotic, N.; Loeb, S. J. *Angew. Chem., Int. Ed.* **2012**, *51*, 2168-2172.

For recent reviews highlighting the various aspects of molecular shuttles, see:

l) Bodis, P.; Panman, M. R.; Bakkert, B. H.; Mateo-Alonso, A.; Prato, M.; Buma, W. J.; Brouwer, A. M.; Kay, E. R.; Leigh, D. A.; Wourtersen, S. *Acc. Chem. Res.* **2009**, *42*, 1462, 1469;

m) Crowley, J. D.; Goldup, S. M.; Lee, A.-L.; Leigh, D. A.; McBurney, R. T. *Chem. Soc. Rev.* **2009**, *38*, 1530-1541;

n) Stoddart, J. F. *Chem. Soc. Rev.* **2009**, *28*, 1802-1820.

9. a) Flood, A. H.; Stoddart, J. F.; Steuerman, D. W.; Heath, J. R. *Science* **2004**, *306*, 2055-2056;

b) Balzani, V.; Credi, A.; Silvi, S.; Venturi, M. *Chem. Soc. Rev.* **2006**, *35*, 1135-1149.

10. Steuerman, D. W.; Tseng, H.-R.; Peters, A. J.; Flood, A. H.; Jeppesen, J. O.; Nielsen, K. A.; Stoddart, J. F.; Heath, J. R. *Angew. Chem., Int. Ed.* **2004**, *43*, 6486-6491.

11. a) Flood, A. H.; Peters, A. J.; Vignon, S. A.; Steuerman, D. W.; Tseng, H.-R.; Kang, S.; Heath, J. R.; Stoddart, J. F. *Chem. -Eur. J.* **2004**, *10*, 6558-6564;

b) Tseng, H.-R.; Wu, D.; Fang, N. X.; Zhang, X.; Stoddart, J. F. *Chem. Phys. Chem.* **2004**, *5*, 111-116;

c) Zhang, W.; Delonno, E.; Dichtel, W. R.; Fang, L.; Trabolsi, A.; Olsen, J.-C.; Benitez, D.; Heath, J. R.; Stoddart, J. F. *J. Mater. Chem.* **2011**, *21*, 1487-1495.

12. Choi, J. W.; Flood, A. H.; Steuerman, D. W.; Nygaard, S.; Braunschweig, A. B.; Moonen, N. N. P.; Luo, Y.; Delonno, E.; Peters, A. J.; Jeppesen, J. O.; Xe, K.; Stoddart, J. F.; Heath, J. R. *Chem. -Eur. J.* **2006**, *12*, 261-279.

13. Stoddart, J. F.; Colquhoun, H. M. *Tetrahedron* **2008**, *64*, 8231-8263.

14. Green, J. E.; Choi, J. W.; Boukai, A.; Bunimovich, Y.; Johnston-Halperin, E.; DeIonno, E.; Sheriff, B. A.; Xu, K.; Shin, Y. S.; Tseng, H.-R.; Stoddart, J. F.; Heath, J. R. *Nature* **2007**, *445*, 414-417.

15. a) Livoreil, A.; Dietrichbuchecker, C. O.; Sauvage, J.-P. *J. Am. Chem. Soc.* **1994**, *116*, 9399-9400;

b) Cardenas, D. J.; Livoreil, A.; Sauvage, J. P. *J. Am. Chem. Soc.* **1996**, *118*, 11980-11981;

c) Livoreil, A.; Sauvage, J.-P.; Armaroli, N.; Balzani, V.; Flamigni, L.; Ventura, B. *J. Am. Chem. Soc.* **1997**, *119*, 12114-12124;

d) Armaroli, N.; Balzani, V.; Collin, J. P.; Gavina, P.; Sauvage, J.-P.; Ventura, B. *J. Am. Chem. Soc.* **1999**, *121*, 4397-4408;

e) Durola, F.; Sauvage, J.-P. *Angew. Chem., Int. Ed.* **2007**, *46*, 3537-3540;

f) Collin, J. P.; Durola, F.; Lux, J.; Sauvage, J.-P. *Angew. Chem., Int. Ed.* **2009**, *48*, 8532-8535;

g) Periyasamy, G.; Collin, J. P.; Sauvage, J. P.; Levine, R. D.; Remacle, F. *Chem.-Eur. J.* **2009**, *15*, 1310-1313;

h) Durola, F.; Sauvage, J.-P.; Wenger, O. S. *Coord. Chem. Rev.* **2010**, *254*, 1748-1759;

i) Sauvage, J.-P.; Trolez, Y.; Canevet, D.; Sallé, M. *Eur. J. Org. Chem.* **2011**, 2413-2416;

j) Joosten, A.; Trolez, Y.; Collin, J.-P.; Heitz, V.; Sauvage, J.-P. *J. Am. Chem. Soc.* **2012**, *134*, 1802-1809.

16. a) Crowley, J. D.; Leigh, D. A.; Lusby, P. J.; McBurney, R. T.; Perret-Aebi, L. E.; Petzold, C.; Slawin, A. M. Z.; Symes, M. D. *J. Am. Chem. Soc.* **2007**, *129*, 15085-15090;

b) Leigh, D. A.; Lusby, P. J.; McBurney, R. T.; Symes, M. D. *Chem. Commun.* **2010**, *46*, 2382-2384.

17. Chatterjee, M. N.; Kay, E. R.; Leigh, D. A. *J. Am. Chem. Soc.* **2006**, *128*, 4058-4073.

18. The italicised prefixes -*DMAP* and -*Py* denote the position of the macrocycle on the thread in the rotaxane.

19. Amabilino, D. B.; Stoddart, J. F. *Chem. Rev.* **1995**, *95*, 2725-2828.

20. Goldup, S. M.; Leigh, D. A.; Lusby, P. J.; McBurney, R. T.; Slawin, A. M. Z. *Angew. Chem., Int. Ed.* **2008**, *47*, 3381-3384.

21. Heat cannot be termed a "kinetic stimulus" becasue it does not alter the magnitude of the energy barrier to re-equilibration.

22. a) Haake, P.; Hylton, T. A. *J. Am. Chem. Soc.* **1962**, *84*, 3774-3775;

b) Yamashita, K. I.; Kawano, M.; Fujita, M. *J. Am. Chem. Soc.* **2007**, *129*, 1850;

c) Wang, M.-S.; Xu, G.; Zhang, Z.-J.; Guo, G.-C. *Chem. Commun.* **2009**, *46*, 361-376;

d) Yamashita, K.; Sato, K.; Kawano, M.; Fujita, M. *New J. Chem.* **2009**, *33*, 264-270;

e) Pike, S. J.; Lusby, P. J. *Chem. Commun.* **2010**, *46*, 8338-8340;

f) Wang, M. S.; Xu, G.; Zhang, Z. J.; Guo, G. C. *Chem. Commun.* **2010**, *46*, 361-376.

23. McGuire Jr, R.; McGuire, M. C.; McMillin, D. R. *Coord. Chem. Rev.* **2010**, *254*, 2574-2583.

24. Cocchi, M.; Kalinowski, J.; Murphy, L.; Williams, J. A. G.; Fattori, V. *Org. Electron.* **2010**, *11*, 388-396.

25. a) Kunugi, Y.; Mann, K. R.; Miller, L. L.; Exstrom, C. L. *J. Am. Chem. Soc.* **1998**, *120*, 589-590;

b) Lanoe, P. H.; Fillaut, J. L.; Toupet, L.; Williams, J. A. G.; Le Bozec, H.; Guerchais, V. *Chem. Commun.* **2008**, 4333-4335;

c) Borisov, S. M.; Papkovsky, D. B.; Ponomarev, G. V.; DeToma, A. S.; Saf, R.; Klimant, I. *J. Photochem. Photobiol., A* **2009**, *206*, 87-92.

26. a) Ratilla, E. M. A.; Brothers, H. M.; Kostic, N. M. *J. Am. Chem. Soc.* **1987**, *109*, 4592-4599;

b) Siu, P. K. M.; Ma, D. L.; Che, C. M. *Chem. Commun.* **2005**, 1025-1027.

27. Wong, W. Y.; Wang, X. Z.; He, Z.; Chan, K. K.; Djurisic, A. B.; Cheung, K. Y.; Yip, C. T.; Ng, A. M. C.; Xi, Y. Y.; Mak, C. S. K.; Chan, W. K. *J. Am. Chem. Soc.* **2007**, *129*, 14372-14380.

28. Schneider, J.; Du, P. W.; Jarosz, P.; Lazarides, T.; Wang, X. Y.; Brennessel, W. W.; Eisenberg, R. *Inorg. Chem.* **2009**, *48*, 4306-4316.

29. Williams, J. A. G. *Photochemistry and photophysics of coordination compounds: Platinum*, vol. 281, Springer-Verlag: Berlin, **2007**.

30. Fenske, R. F.; Ruedenberg, K.; Martin, D. S. *Inorg. Chem.* **1962**, *1*, 441-452.

31. a) Ballhausen, C. J.; Bjerrum, N.; Dingle, R.; Eriks, K.; Hare, C. R. *Inorg. Chem.* **1965**, *4*, 514-518;

b) Balzani, V. C., V *J. Phys. Chem.* **1968**, *72*, 383-388.

32. Andrews, L. J. *J. Phys. Chem.* **1979**, *83*, 3203-3209.

33. Atkins, P.; de Paula, J. *Atkins' Physical Chemistry*; 7 ed.; Oxford University Press: Oxford, **2002**.

34. Vos, J. G.; Pryce, M. T. *Coord. Chem. Rev.* **2010**, *254*, 2519-2532.

35. a) van Houten, J.; Watts, R. J. *Inorg. Chem.* **1978**, *17*, 3381-3385;

b) Durham, B.; Caspar, J. V.; Nagle, J. K.; Meyer, T. J. *J. Am. Chem. Soc.* **1982**, *104*, 4803-4810;

c) Sullivan, B. P.; Meyer, T. J. *Inorg. Chem.* **1982**, *21*, 1037-1040;

d) Barigelletti, F.; Juris, A.; Balzani, V.; Belser, P.; Vonzelewsky, A. *Inorg. Chem.* **1983**, *22*, 3335-3339;

e) Wang, R.; Vos, J. G.; Schmehl, R. H.; Hage, R. *J. Am. Chem. Soc.* **1992**, *114*, 1964-1970.

36. Mobian, P.; Kern, J. M.; Sauvage, J.-P. *Angew. Chem., Int. Ed.* **2004**, *43*, 2392-2395.

37. Vezzu, D. A. K.; Deaton, J. C.; Jones, J. S.; Bartolotti, L.; Harris, C. F.; Marchetti, A. P.; Kondakova, M.; Pike, R. D.; Huo, S. *Inorg. Chem.* **2010**, *49*, 5107-5119.

38. Masaaki, Y. M., O *Bull. Chem. Soc. Jpn.* **1967**, *40*, 2380-2382.

39. Gibson, H. W.; Lee, S. H.; Engen, P. T.; Lecavalier, P.; Sze, J.; Shen, Y. X.; Bheda, M. *J. Org. Chem.* **1993**, *58*, 3748-3756.

40. Fujita, M.; Ibukuro, F.; Yamaguchi, K.; Ogura, K. *J. Am. Chem. Soc.* **1995**, *117*, 4175-4176.

41. Fujita, D.; Takahashi, A.; Sato, S.; Fujita, M. *J. Am. Chem. Soc.* **2011**, *133*, 13317-13319.

42. Middleton, W. J.; Lindsey, R. V. *J. Am. Chem. Soc.* **1964**, *86*, 4948-4952.

Chapter IV

The Orthogonal Addressability of Hydrazone and Palladium(II) Motifs Applied in the Design of a Molecular Walker

Acknowledgements

Dr Mustafa Ozser is gratefully recognised for his contribution to early synthetic work that is not described herein and Dr Victor Blanco is acknowledged for invaluable discussion and support throughout the project.

4.1 Synopsis

*The synthesis and characterisation of an unprecedented macrocycle (**M1**$_1$) containing a palladium(II)-pyridine motif and a hydrazone linkage is described. In the context of this thesis, **M1**$_1$ represents a model for a molecular walker unit featuring one palladium(II) and one hydrazone foot attached to a two-foothold section of a molecular track. The dynamic chemistry of **M1**$_1$ is investigated through various ring-opening experiments carried out under thermodynamic control. The results of these experiments indicated that the hydrazone bond exchanges only under acidic conditions, whereas the palladium(II)-ligand bond is only labile at elevated temperatures in the presence of a coordinating solvent.*

*These findings led to the design and synthesis of a first generation small-molecule walker-track system incorporating the core components of macrocycle **M1**$_1$ with an extended four-foothold track. This chapter addresses the teething problems associated with the initial design and lays out a proposal for improvements in a second generation model including discussion on how a thermodynamic bias might be introduced to facilitate directional walking.*

4.2 Introduction

Having discounted platinum(II) complexes as potential opposing feet to the palladium(II) chemistry developed in Chapter II, an alternative orthogonally operable switch was sought in the continued quest to integrate the palladium-foot into a fully functioning molecular walker system. Previous pursuits of this target have independently incorporated Cu(I)/Cu(II), and Co(II)/Co(III) redox ligand-exchange chemistry, however, the operation of both systems ultimately proved incompatible with that of the palladium(II) ligand exchange.[1] In broadening the search beyond the confines of bimetallic systems, other kinetically switchable linkages were considered along with their chemical compatibility with transition metal complexes of the kind used in this study.

Dynamic Covalent Chemistry

Synthetic organic chemistry to date has revolved around the design, synthesis and isolation of specific compounds that possess attractive properties and applications. The synthetic strategies employed to reach these target molecules are predominantly based on either individual, or ensembles of isolable kinetically controlled chemical reactions that irreversibly form stable covalently bonded products. Nature, on the other hand, more often makes use of dynamic chemical systems under thermodynamic control in which multiple components are interconnected through a range of reversible exchange reactions and where the final product distribution is defined by the relative free energies of all the possible products. This method provides the potential for real-time checks and control mechanisms and enables biological systems to respond rapidly to changes in their environments. The allure of attaining such reversible control over covalent bond formation inspired the dawn of dynamic covalent chemistry (DCC), an area that has given rise to a wealth of literature over the last decade[2] by bridging the fields of dynamic supramolecular chemistry[3] and traditional covalent synthesis. Although it has been heralded as a potential game-changer in the field of drug discovery where binding affinity towards target receptors can beneficially distinguish between members of dynamic combinatorial libraries,[4] dynamic covalent chemistry has also found applications in a wide range of other areas including dynamic polymers (dynamers),[5] sensors,[6] the synthesis and manipulation of mechanically interlocked architectures,[7] and systems chemistry.[8]

The complex behaviour of dynamic covalent systems can often be far more powerful than that attainable through the sum of their individually operated components and it is possible to use the chemistry to mimic the environment-responsive nature of biological systems. By integrating molecular networks of synthetic chemical species that interact with one another in a predesigned manner, the final thermodynamically favoured product can be selected and controlled using suitable external stimuli. However, predicting the resultant phenomena of an applied stimulus to these systems is not trivial, especially when the exchange reactions involved are said to be communicating,[9] i.e. when the reaction products of one component have an affect upon the procedure of another. Additional control can be attained by incorporating orthogonal[10] and non-concurrent exchange processes where reactions do not take place simultaneously and give products that have no influence over the operation of other components. Such control mechanisms have been incorporated into some of the molecular motor systems mentioned previously[11] to ratchet positional isomer distributions of molecular bipeds away form their thermodynamic minima,[12] thus facilitating the walking of small molecules down a track. These examples represent double-level[13] systems with two orthogonal, non-concurrent exchange reactions, each responsible for the stepping of an individual foot of the walker unit. There is a requirement that under the first set of conditions, only one of the two bond types is dynamic whilst the other remains kinetically locked. Similarly, under the second, mutually exclusive set of conditions, the relative rates of bond forming and bond breaking are reversed.

The implications and potential benefits of utilising multiple reactions instigated by orthogonal external stimuli have been impressively demonstrated[11] but by no means comprehensively explored or exploited. Reversible reactions form the toolbox of dynamic covalent chemistry[2d] and knowledge of the dynamism of different reaction types under mutually exclusive conditions empowers the designers of complex molecular machinery with the ability to integrate independent, yet ultimately cooperative reaction mechanisms into systems with a much greater consideration for the requirements of the surrounding environment (e.g. solubility, pH, temperature).

The palladium(II) motif described in Chapter II exhibited promise as a potential foot in a molecular walker system in which the inert Pt(II) anchor moiety could be replaced with an additional functioning foot. With a plethora of dynamic covalent processes to

choose from, the concept of a double-level, constitutionally dynamic[14] system combining DCC with transition metal coordination chemistry in the design of a molecular walker system was considered as an exciting advancement in the field.

Hydrazone Exchange

The reversible hydrolysis of hydrazone containing moieties has been studied and the general mechanism is shown in Scheme 4.1 where acid-catalysed hydrolysis of the initial hydrazone is the rate-limiting step followed by the condensation of the hemiaminal to the new mixture of products.

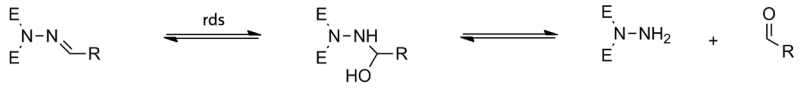

Scheme 4.1 - *Mechanism of reversible hydrolysis of a hydrazone: E = electron-withdrawing group (typically acyl); rds = rate determining step.*

The equilibrium distribution lies heavily in favour of the hydrazone product whilst allowing exchange to take place through a low but sufficient concentration of hydrolysed monomers. This provides an important and exploitable difference from the better-documented dynamic covalent chemistry of imines.[8d,15] Hydrazones are more stable than imines because the nitrogen substituent can participate in delocalisation of the imine double bond decreasing the partial charge on the carbon atom and raising the energy of the LUMO, thus making it less susceptible to nucleophilic attack. This increased stability means that, unlike imine exchange, hydrazones require acid[16] or nucleophilic base[17] to be hydrolysed and can therefore be kinetically locked under neutral conditions. Hydrazone exchange has proven to be a tremendously versatile tool effective in both organic[10b,11,18] and aqueous media.[19]

This chapter reports the synthesis and dynamic chemistry of macrocycle $\mathbf{M1_1}$, which incorporates both the palladium(II) moiety described in Chapter II, and a separate hydrazone unit within the bonds that make up the ring. Selective ring-opening of $\mathbf{M1_1}$ at either the hydrazone or palladium linkages was achieved by reversible covalent or metal-ligand bond formation respectively using one of two sets of mutually exclusive reaction conditions; namely, acid, or heat in the presence of a coordinating solvent. The dynamic chemistry was investigated in terms of competition between fully reversible intra- and intermolecular exchange processes carried out under thermodynamic

control. The results from this study, along with the developed synthetic strategy, were then incorporated into the synthesis of a small molecule designed to walk repetitively up and down a four-foothold molecular track in response to an oscillating chemical environment.

4.3 System Design and Independent Addressability

The successful operation of each of the proposed foot motifs in the design have been independently demonstrated with great success in previous systems, however, the potential to operate them in tandem within a single molecule requires that each foot is kinetically stable under the operating conditions of its partner. The hydrazone linkage is by no means an innocent functional group when working with transition metals[18c] and carrying out palladium(II)-ligand exchange processes in close proximity is without precedent. Experiments were therefore developed to test whether the palladium(II) complexes were stable under the conditions previously established for hydrazone exchange[11a] (Scheme 4.2).

After 22 h at room temperature under acidic conditions in $CDCl_3$, **L2**Pd-(2,6-dihexyl*Py*) remained unchanged while 30% of hydrazone **1** had been converted to **4** as shown in Figure 4.1. In a similar experiment in the absence of 2-picoline and **L2**Pd-(2,6-dihexyl*Py*), but with a greater excess of trifluoroacetic acid (TFA), the hydrazone exchange was shown to be much faster reaching an equilibrium state with 65% exchange from **1** to **4** within 20 h implying that the reaction rate can be controlled as a function of acid concentration.

To test a potential hydrazone foot's stability to the palladium(II)-stepping conditions, an equimolar solution of compound **1** and benzaldehyde (**2**) in $CDCl_3/CD_3CN$ (7:3, 0.1 mM) was heated to 228 K for 16 h, during which time no change was observed in the ^1H NMR spectrum.

These results provided precedent for a potential small molecule walker-track system with two different foot-foothold linkages based around the independently operable switches explored in this section.

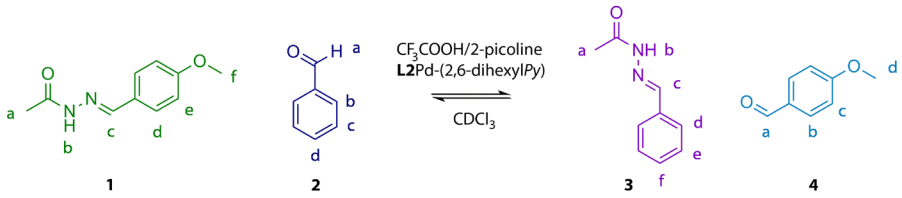

Scheme 4.2 *- Acid mediated hydrazone exchange in the presence of spectator compounds 2-picoline and* ***L2****Pd-(2,6-dihexylPy) with 1 drop of 20% CF_3COOH in $CDCl_3$.*

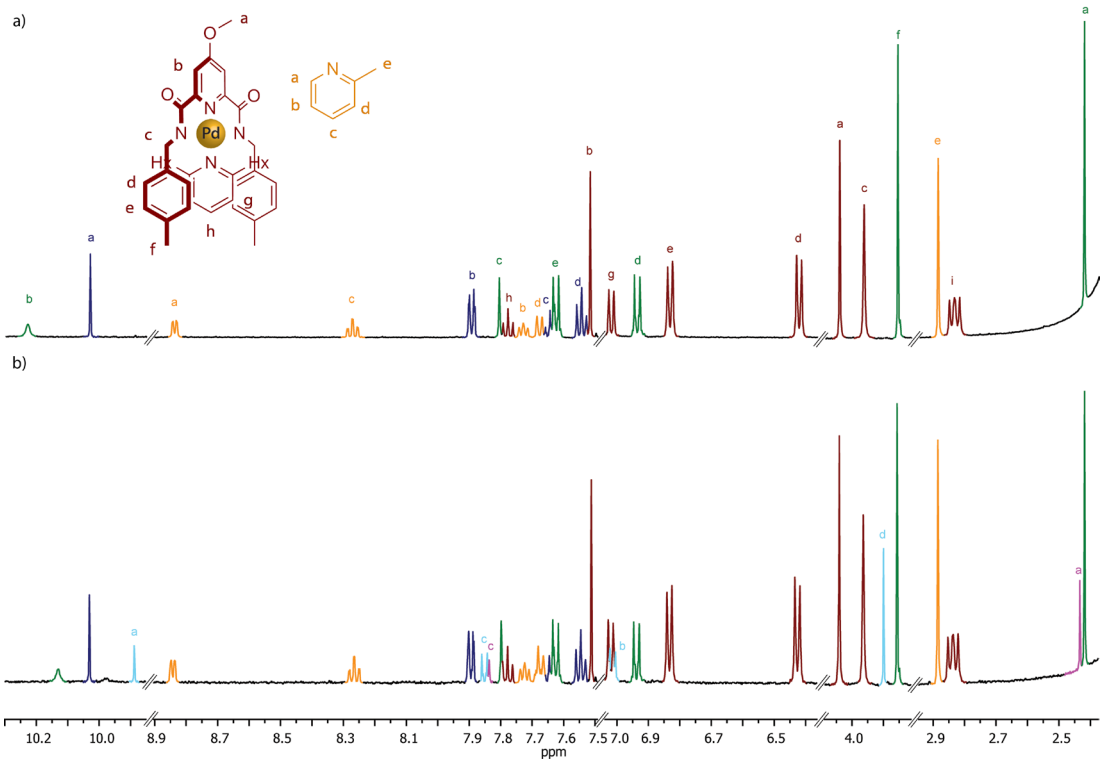

Figure 4.1 *- Partial ^1H NMR spectra (400 MHz, $CDCl_3$, 298 K) of a 0.1 mM mixture of* ***L2****Pd-(2,6-dihexyl*Py*),* ***1****,* ***2****, and 2-picoline in $CDCl_3$ with one drop of acid solution (20% TFA in $CDCl_3$) at: (a) t = 0 h; (b) solution (a) after 22 h at room temperature. The lettering and colours in the figure refer to assignments in Scheme 4.2.*

4.4 Synthesis of Macrocycle $M1_1$

So far, experiments have dealt with intermolecular exchanges. To ensure that the results could be extended into intramolecular systems, macrocycle $\mathbf{M1_1}$ was devised to further probe the dynamic chemistries involved. The target macrocycle can be viewed as a biped with an Pd(II)-*N,N,N*-pincer motif and a hydrazone moiety which act as opposing feet respectively attached to 2,6-substituted pyridine and benzaldehyde derivative footholds of a two-foothold track. The synthetic strategy for macrocycle

M1$_1$ is outlined in Scheme 4.3-4.5 and full details are given in the Experimental Section 4.11.

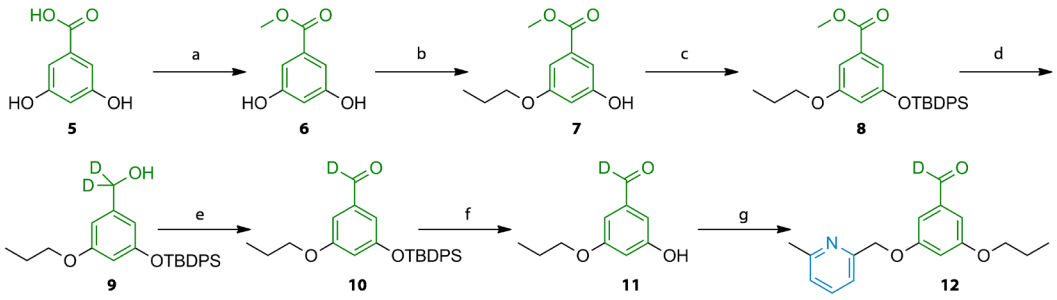

Scheme 4.3 *- Synthesis of 2-foothold track. Reagents and conditions: (a) $SOCl_2$, MeOH, RT, 15 h, quant.; (b) 1-bromopropane, K_2CO_3, DMF, RT, 3 days, 32%; (c) TBDPSCl, DIPEA, DMF, 328 K, 3 h, 94%; (d) $LiAlD_4$, THF, RT, 13 h, 94%; (e) Dess-Martin periodinane, CH_2Cl_2, RT, 16 h, 51%; (f) TBAF, THF, 273 K, 2 h, 90%; (g) 6-methyl-2-pyridine methanol, PPh_3, DIAD, THF, 8 h, 42%.*

Esterification of 3,5-dihydroxybenzoic acid (**5**) was achieved by stirring with thionyl chloride in MeOH for 12 h to give ester **6** in quantitative yield. Williamson coupling with 1-bromopropane (1 equiv) in DMF afforded monosubstituted substrate **7** within 3 days. The phenol group was protected by reaction with *tert*-butyldiphenylsilyl chloride (TBDPSCl) using *N,N*-diisopropylethylamine (DIPEA) in DMF to give **8**. The ester was reduced to deuterated alcohol **9** using $LiAlD_4$ (4 equiv) in THF before subsequent Dess-Martin oxidation to deuterated aldehyde **10**. The silyl ether was deprotected with tetrabutylammonium fluoride (TBAF) to give **11**, which was subsequently coupled to 6-methyl-2-pyridine methanol using Mitsunobu conditions to give two-foothold track **12**.

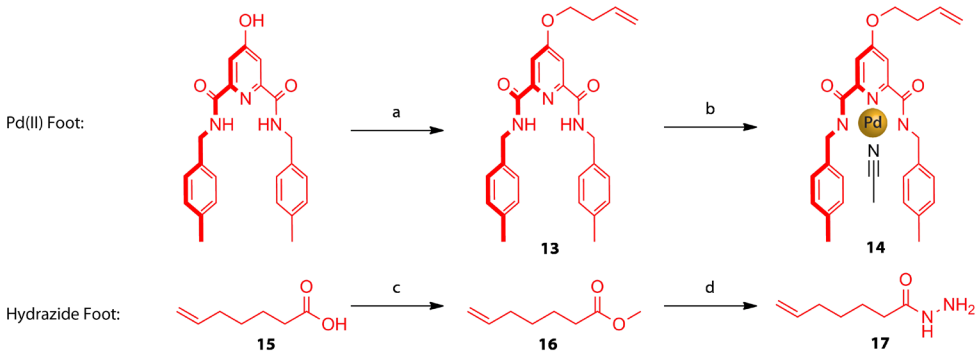

Scheme 4.4 *- Synthesis of Pd(II)- and hydrazone foot motifs. Reagents and conditions: (a) 4-bromobut-1-ene, K_2CO_3, butanone, 368 K, quant.; (b) $Pd(OAc)_2$, CH_3CN, RT, 16 h, 78% ; (c) $SOCl_2$, MeOH, RT, 14 h; (d) $H_2NNH_2{\cdot}H_2O$, MeOH, 335 K, 12 h, 63% from **15**.*

Palladium(II) complex **14** was prepared from the same pyridine-2,6-dicarboxamide unit described in Chapter II in two steps through Williamson alkylation with 4-bromobut-1-ene in butanone to give **13**, followed by reaction with palladium(II) acetate in CH_3CN to give the product as a yellow/green precipitate. The hydrazide moiety **17** was sourced from 6-heptanoic acid (**15**), which was esterified by reaction with thionyl chloride in methanol to give **16**, and subsequently converted to the product through reaction with hydrazine monohydrate in MeOH with a yield of 63% over the two steps.

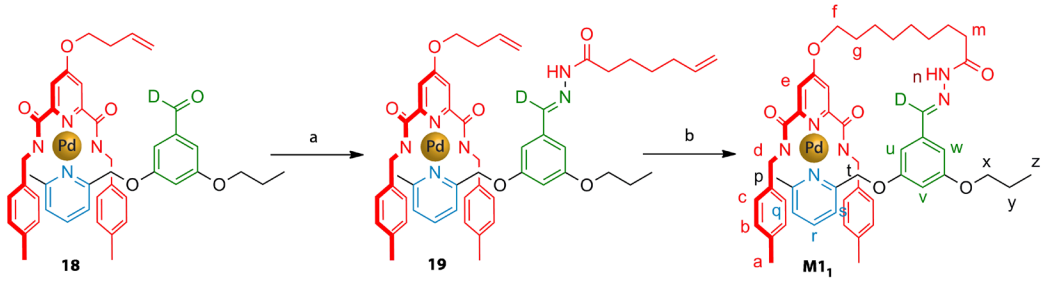

Scheme 4.5*- Synthesis of macrocycle* ***M1₁****. Reagents and conditions: (a)* ***17****, acetic acid, MeOH, RT, 12 h, 90%; (b) (i) Grubbs II, CH_2Cl_2, RT, 18 h, 58%, (ii) H_2, $Pd(OH)_2/C$, K_2CO_3, THF, RT, 4 h, 90%.*

Palladium(II) precursor **14** was coordinated to the pyridine binding site of track **12** by stirring the two in an equimolar solution with $CHCl_3$ for 5 h to give complex **18**. The opposing hydrazone foot (**17**) was attached by stirring with **18** and glacial acetic acid at room temperature to give **19**. Ring closing metathesis using Grubbs II catalyst in CH_2Cl_2 followed by hydrogenation of the resultant double bond ($Pd(OH)_2/C$, K_2CO_3, THF) afforded macrocycle **M1₁** in 52% yield over two steps.

Upon forming **M1₁**, the ^1H NMR spectrum became convoluted at room temperature on account of encapsulating the hydrazone linkage within the 25-membered ring resulting in the formation of different isomers of the amide bond that were not interchangeable at room temperature. The spectrum could be simplified using variable temperature ^1H NMR ($C_2D_2Cl_4$, 378 K) allowing full characterisation of the structure in solution (Figure 4.2).

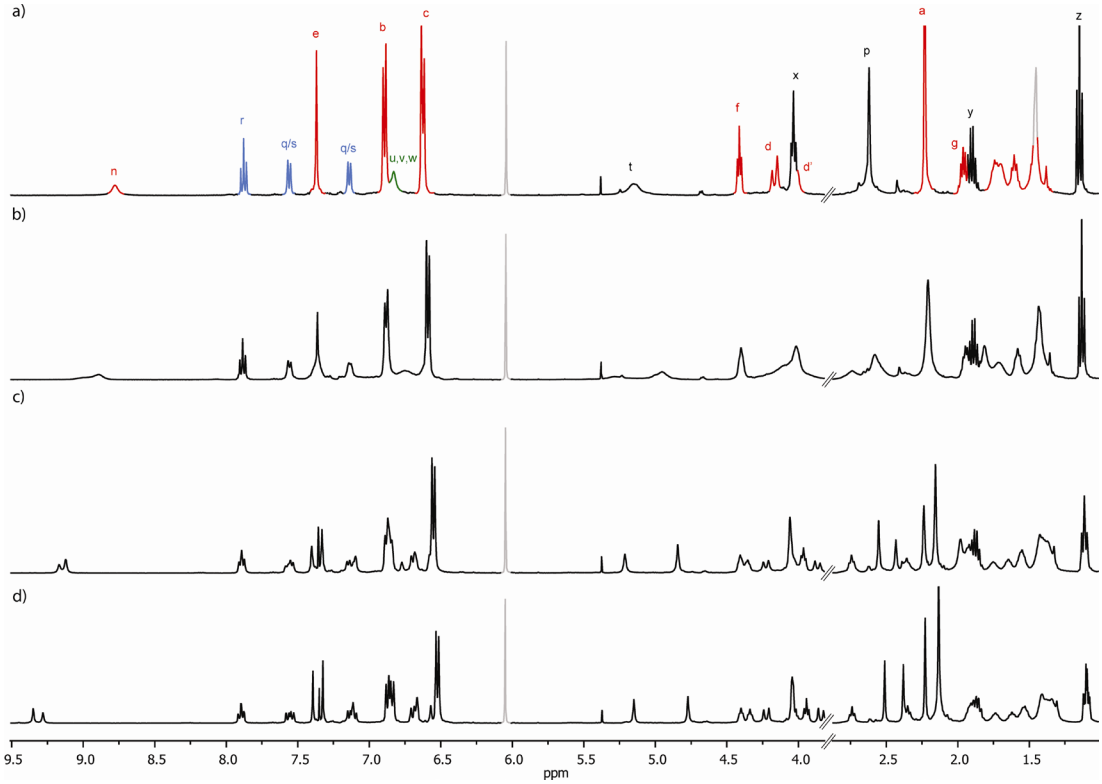

Figure 4.2 *- ^{1}H NMR spectra (400 MHz, $C_2D_2Cl_4$) of* ***M1$_1$****: (a) 378 K; (b) 348 K ;(c) 318 K; (d) 298 K. The lettering and colours in (a) refer to the assignments in Scheme 4.5.*

4.5 Cyclooligomerisation of Macrocycle M1$_1$

Macrocycle **M1$_1$** was independently subjected to the two different sets of chemical conditions optimised in the intermolecular model studies to establish their effectiveness in instigating cyclooligmerisation *via* hydrazone and palladium(II)-ligand exchange under thermodynamic control (Scheme 4.6).

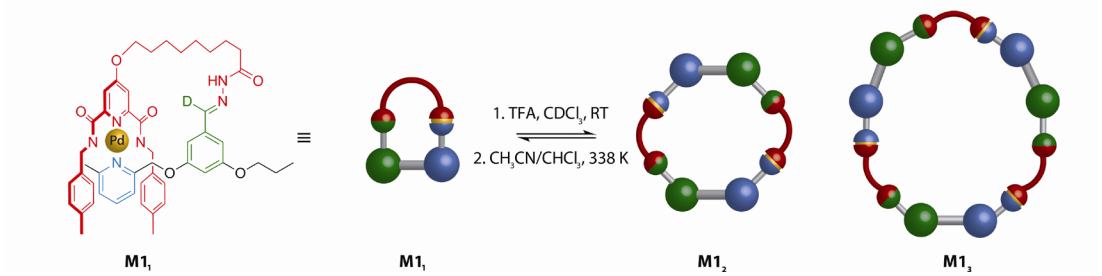

Scheme 4.6 *- Two sets of reaction conditions for the efficient conversion of macrocycle* ***M1$_1$*** *into a distribution of cyclic oligomers* ***M1$_n$*** *by dynamic bond formation: Conditions 1:* ***M1$_1$*** *(6 µmol, 1 equiv), 0.5 mL $CDCl_3$, TFA (30 µmol, 5 equiv), RT, 24 h; Conditions 2:* ***M1$_1$*** *(6 µmol, 1 equiv), 0.5 mL $CDCl_3$/CD_3CN (7:3), 338 K, 24 h.*

Under both sets of conditions (heating in $CDCl_3/CD_3CN$ (7:3) and TFA in $CDCl_3$) detectable amounts of dimeric ($\mathbf{M1_2}$) and trimeric ($\mathbf{M1_3}$) macrocyclic analogues of $\mathbf{M1_1}$ were observed in the equilibrium mixtures after typical equilibration times of 12-24 h (after which time the composition of reaction mixtures no longer changed). Although the progression of the reactions was hard to follow by ^1H NMR on account of the different isomers of the hydrazone linkages, the results were confirmed by electrospray ionisation-mass spectrometry (ESI-MS) (Figure 4.3).

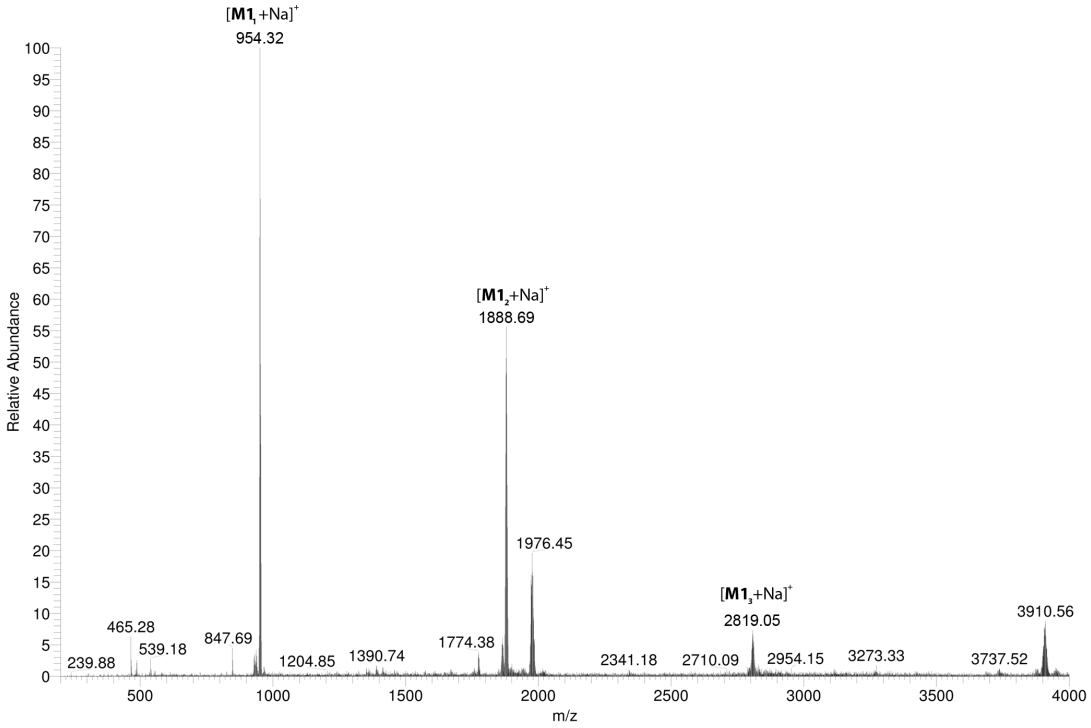

Figure 4.3 *-Mass spectrum (ESI⁺) of an equilibrium mixture containing* $\boldsymbol{M1_1}$ *and higher oligomers* $\boldsymbol{M1_n}$ *after treatment of* $\boldsymbol{M1_1}$ *under acidic conditions outlined in Scheme 4.6.*

4.6 Ring-Opening of Macrocycle $M1_1$ in the Presence of Scavengers

To confirm which linkage was dynamic under the different oligomerisation conditions, macrocycle $\mathbf{M1_1}$ was opened at each end in the presence of a suitable, acyclic "scavenger" molecule. $\mathbf{M1_1}$ was first subjected to conditions to labilise the Pd(II)-foot ($CDCl_3/CD_3CN$ (7:3), 1 mM, 338 K,) in the presence of 5 equivalents of 2,6-lutidine (Scheme 4.7a) which gave ring-opened compound **20** in a 75% isolated yield. A separate sample of $\mathbf{M1_1}$ was subjected to conditions to labilise the hydrazone foot ($CDCl_3$, 1 mM, TFA (5 equiv), RT) in the presence of 5 equivalents of *p*-anisaldehyde (Scheme 4.7b) which gave ring-opened compound **21** in a 40% isolated yield.

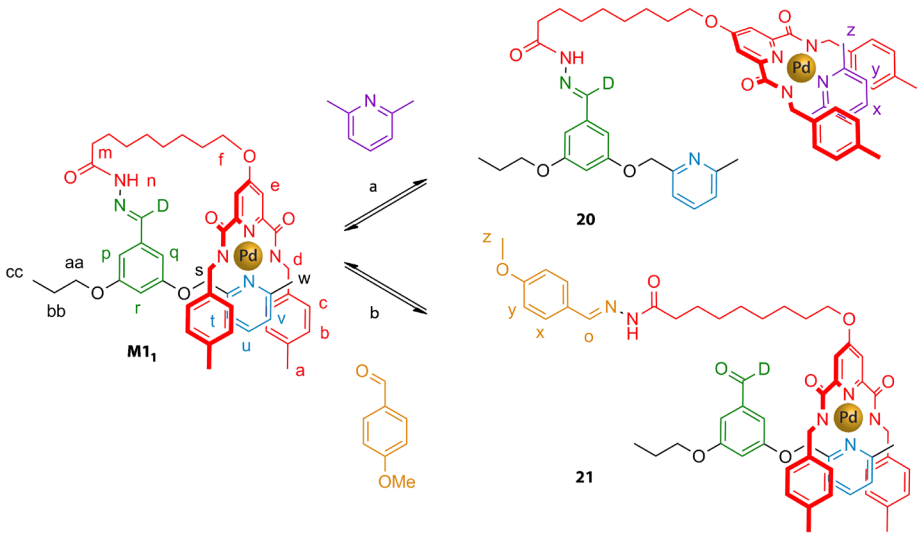

Scheme 4.7 *- Dynamic covalent ring-opening of macrocycle* ***M1₁*** *in the presence of an acyclic aldehyde or pyridyl scavenger: (a) Pd(II)-ligand exchange of* ***M1₁*** *(1 equiv) with metal scavenger 2,6-lutidine (5 equiv) in $CDCl_3/CD_3CN$ (7:3) (initial concentration of* ***M1₁*** *12 mM), 338 K, 15 h ; (b) acid-mediated (TFA, 5 equiv) hydrazone exchange of macrocycle* ***M1₁*** *(1 equiv) with aldehyde scavenger p-anisladehyde (5 equiv) in $CDCl_3$ (initial concentration of* ***M1₁*** *12 mM), RT, 15 h.*

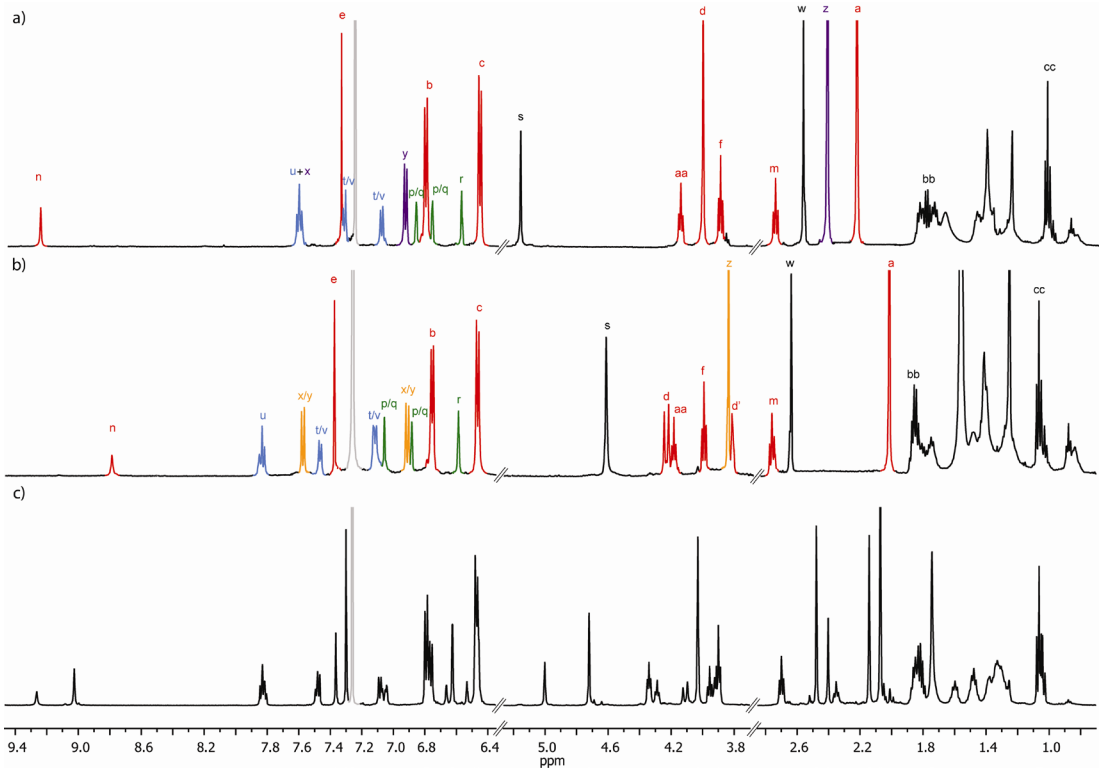

Figure 4.4 *- ^1H NMR spectra (400 MHz, $CDCl_3$, 298 K) of the isolated ring-opened products and the starting material for comparison: (a)* ***20****; (b)* ***21****; (c)* ***M1₁****. The lettering and colour refer to the assignments in Scheme 4.7.*

The ^{1}H NMR spectra of both isolated open products are shown in Figure 4.4 along with that of $\mathbf{M1_1}$. It can be clearly seen that the resonances of the two products are easily resolvable at room temperature compared to those of the starting material indicating that the hydrazone linkage is no longer constrained within the macrocycle and thus confirming the opening of the rings. Both products were isolated from a range of by-products by preparative thin layer chromatography on silica. These by-products were assumed to be oligomeric species formed as a result of running the experiments at higher concentrations than in previous intermolecular exchanges in order to favour the ring-opened products. This prediction was supported by mass spectrometry.

4.7 Design of a Dynamic Synthetic Small Molecule Walker-Track System

The dynamic behaviour of macrocycle $\mathbf{M1_1}$ meets the criteria required for the key operational components of a non-directional molecular walker laid out in Chapter I; in essence, it comprises two independently operable chemical switches. The goal of converting the simple macrocycle into a functioning walker system can be realised by extending the track to enable walking in the form of intramolecular dynamic exchange between footholds as opposed to the intermolecular stepping demonstrated in the presence of a high concentration of scavenger moieties. In this way, the biped unit of $\mathbf{M1_1}$ could be made to randomly walk up and down a 4-foothold track with a high degree of processivity by means of alternating the orthogonal stimuli developed in the macrocycle ring-opening (Figure 4.5).

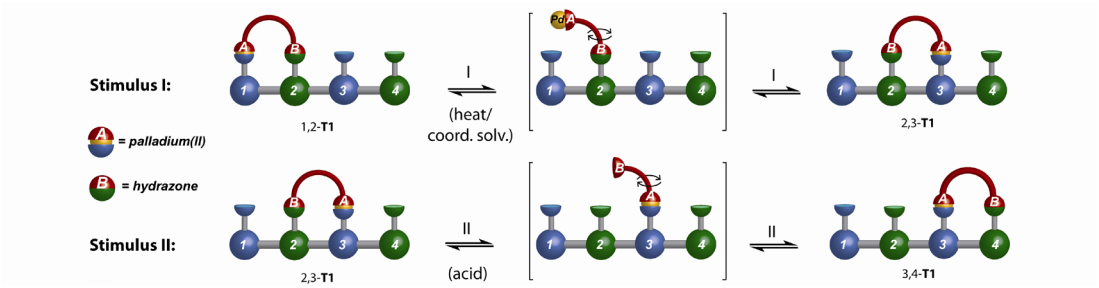

Figure 4.5 *- Proposed operation of walker track conjugate 1,2-**T1** (chemical structure shown in Scheme 4.9) when exposed to different sets of stimuli: Stimulus 1: heat in the presence of a coordinating solvent labilises Pd(II)-foot (A) from pyridyl footholds (1 & 3); Stimulus II: acid, labilises hydrazone foot (B) from benzaldehyde footholds (2 & 4).*

4.8 Synthesis, Characterisation and Operation of 1,2-T1

The synthetic strategy for the target walker-track conjugate 1,2-**T1** used macrocycle **M2$_1$** (a direct analogue of **M1$_1$**) as a core scaffold providing the potential for future compartmental extension of the track allowing for variations to be incorporated, such as branches or polymeric extensions. The synthetic route for the track is illustrated in Scheme 4.8, whilst the design of macrocycle **M2$_1$** is very similar to that described previously for **M1$_1$** and is outlined in Scheme 4.9. Full details are given in Experimental Section 4.11.

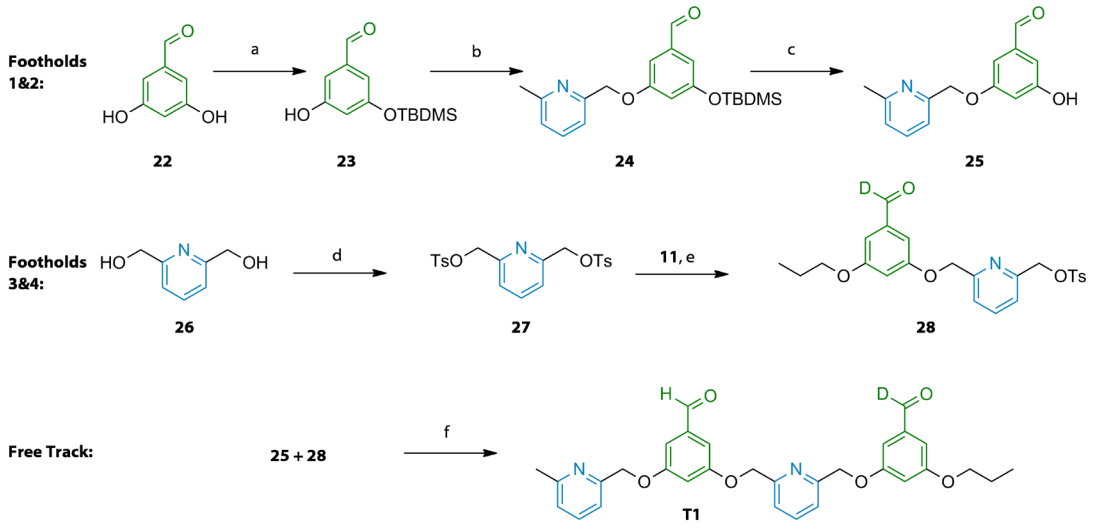

Scheme 4.8 *- Synthesis of free track. Reagents and conditions: (a) TBDMSCl, DIPEA, DMF, 328 K, 3 h, 51%; (b) 6-methyl-2-pyridine methanol, PPh_3, DIAD, THF, RT, 15 h, 74%; (c) TBAF, DIPEA, THF, 273 K, 2 h, 77%; (d) TsCl, THF/H_2O/ (3:1), RT, 16 h, 95%; (e)* ***11****, Cs_2CO_3, THF, RT, 89%; (f) Cs_2CO_3, THF, RT, 68%.*

3,5-dihydroxybenzaldehdyde (**22**) was mono-protected through reaction with one equivalent of *tert*-butyldimethylsilyl chloride and DIPEA in DMF to yield **23** (Scheme 4.8a), which was coupled to 6-methyl-2-pyridine methanol under Mitsunobu reaction conditions to afford track fragment **24**. Ditosylate **27** was synthesised according to a modified literature procedure[20] by reacting 2,6-pyridinemethanol (**26**) with tosyl chloride, in THF/H_2O (3:1). The second half of the four-foothold track was achieved by Williamson coupling of **11** and **27** to give the product in 89% yield (Scheme 4.8e). Free track **T1** was synthesised in a similar manner attaching **25** to **28** under Williamson reaction conditions (Scheme 4.8f).

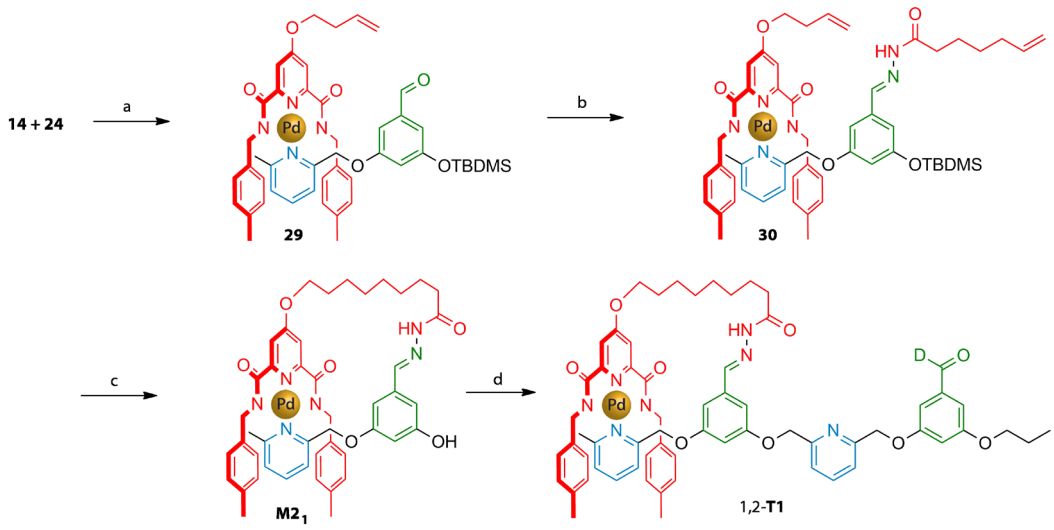

Scheme 4.9 *- Synthesis of walker-track conjugate. Reagents and conditions: (a) $CHCl_3$, RT, 16 h, 91%; (b)* ***17****, acetic acid, MeOH, RT, 12 h, 93%; (c) (i) Grubbs II, CH_2Cl_2, RT, 18 h, 58%, (ii) TBAF, DIPEA, THF, 273 K, 2 h, 78%, (iii) $Pd(OH)_2$, H_2, K_2CO_3, THF, RT, 4 h, 96%; (d) Conditions 1:* ***28****, Cs_2CO_3, THF, RT, 16%; Conditions 2:* ***28****, K_2CO_3, 18-crown-6, acetone, RT, 16 h, max 60%, min 42%; Conditions 3:* ***28****, K_2CO_3, 18-crown-6, acetone, RT, 6 days, 50%.*

The palladium(II) foot was attached by reacting an equimolar solution of **24** and **14** to give complex **29** (Scheme 4.9a), which was subjected to hydrazone forming conditions (acetic acid, MeOH) in the presence of **17** to give precursor **30**. Ring closing metathesis followed by silyl deprotection using TBAF in THF and subsequent hydrogenation gave the product **M2$_1$** (Scheme 4.9c). The ^{1}H NMR spectrum of this new macrocycle unsurprisingly showed the same hydrazone isomers as **M1$_1$** at room temperature but could be resolved at elevated temperature. Williamson reaction conditions were used in an attempt to couple **M2$_1$** and **28** in the synthesis of the target walker-track conjugate 1,2-**T1**, however, the product was only ever observed in poor yield. Conditions were screened varying the reaction times, the solvent and the base. The best results came from using K_2CO_3 in combination with 18-crown-6 in acetone for 16 h giving the product in a remarkable 60% yield. However, this result was not precisely reproducible. An alternative attempt was made with the same reagents in CH_2Cl_2 for 6 days, which afforded 1,2-**T1** in a more modest but reproducible 50% yield.

4.9 Heat-Driven Stepping of Palladium(II)-Foot

Walker-track conjugate 1,2-**T1** was submitted to the reaction conditions optimised in the intermolecular model studies and the ring-opening of macrocycle **M1$_1$** ($CDCl_3$/CD_3CN (7:3), 0.1 mM, 338 K, 25 h) and the progress was monitored by ^{1}H NMR

spectroscopy but, unfortunately, very little change was observed in the spectra. Due to the chemical similarity of the two pyridyl footholds within the track, only small variations were expected anyway, and they were predicted to be difficult to interpret in low concentration NMR experiments run at high temperature, however, when carried out on a larger scale full high temperature NMR analysis (^{13}C, HSQC, HMBC, COSY, ROESY, DOSY) showed the product to be identical to the starting material. Although the previous models implied that the palladium(II)-foot should indeed function under these conditions, the results from the attempted stepping either mean that the walker's first step actually worked and the product is simply indistinguishable from the starting material by NMR and HPLC analysis, or else the starting material is considerably more favoured and the equilibrium distribution lies completely in its favour. This first of these scenarios seems unlikely whilst the second could be explained by additional steric hindrance around foothold three. To test this theory and prove that the Pd-pyridyl bond was indeed being labilised under the chosen conditions, the stepping reaction was repeated with the addition of 5 equivalents of scavenger 2,6-lutidine (Scheme 4.10). The reaction showed formation (2,6-lutidine),2-**T1** in 70% yield.

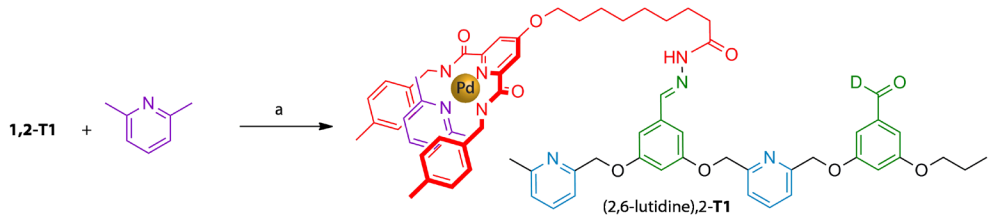

Scheme 4.10 *- Ring-opening of 1,2-**T1** in the presence of 2,6-lutidine. Reagents and conditions: (a) 2,6-lutidine (5 equiv), $CDCl_3/CD_3CN$ (7:3), 338 K, 23 h, 70%.*

These results give further evidence that the reaction conditions for palladium(II)-foot stepping are effective and suggest that foothold-1 is, in effect, unanimously favoured over its counterpart pyridyl foothold-3. This realisation means that the biped unit cannot be made to walk along the track of this system. Considering the degree of electronic similarity between the two stations in question, it can be inferred that this bias emanates from their disparate steric environments. Although CPK modelling had previously indicated that a single methylene spacer would be enough to comfortably accommodate the palladium(II) complex when coordinated to the central foothold, experimental evidence has shown otherwise.

4.10 Conclusions and Future Work

Whilst the first generation walker-track conjugate 1,2-**T1** has been found wanting in terms of the ultimate goal of this project, the information acquired through the synthesis, operation and model studies described in this chapter will be invaluable in the design of subsequent superior systems (Figure 4.6). The effective ring-opening of macrocycle $\mathbf{M1_1}$ gives precedent for the use of palladium(II) ligand chemistry and hydrazone exchange as effective components for use in conjunction with orthogonal chemical stimuli as independently addressable feet in a molecular biped.

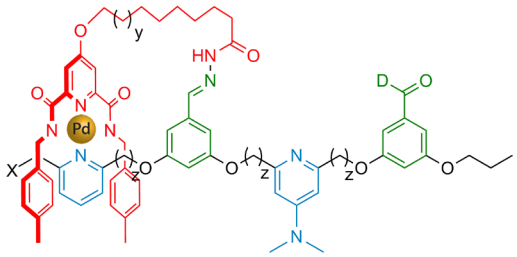

Figure 4.6 *- Potential adjustments to improve the functionality of 1,2-**T1**: (i) an increase in steric bulk at position **X** would help give a more even distribution between footholds 1 and 3 when operating the Pd(II)foot; (ii) increasing **y** would aid characterisation of the system by NMR spectroscopy by eliminating the hydrazone isomer issues that convolute the spectra at RT; (iii) increasing **z** would also help give a more even distribution between footholds 1 and 3 when operating the Pd(II) foot if **X** were left as a hydrogen atom; (iv) by incorporating a DMAP derivative in the foothold-3 position the Pd(II) step could be made directional conforming to an energy ratchet mechanism.*

It has been shown that encapsulating the hydrazone linkage within strained macrocycles can convolute the NMR spectra of these species. A second-generation design should try and avoid this by increasing the degree of flexibility afforded to the macrocycle formed by the two fixed feet and the track. Track **T1** was designed as an ABAB system with the potential for incremental extension. Although this is useful when trying to mimic the polymeric nature of biological molecular tracks, it makes ^{1}H NMR analysis of operation difficult. The introduction of deuterium labelling of the benzaldehyde footholds in **T1** proved effective in differentiating between them, however, the pyridine footholds (1 & 3) were almost indistinguishable by NMR. One method of labelling them would be to replace pyridine foothold-3 with a 2,6-substituted DMAP derivative. This would not only enable the operator to differentiate between ligand sites, but also allow for directionality to be introduced into the system by upgrading the palladium(II) component from a simple dynamic switch to an energy ratchet similar to the one described in Chapter II. The requirement for a large excess of

acid in order to operate the hydrazone foot means that processivity could still be maintained with the addition of a single equivalent of acid used to apply a bias between footholds during the palladium(II) stepping. Finally, the steric issue of the two pyridyl footholds would need to be addressed either by increasing the steric bulk of foothold-1 to match that of 3, or else, by increasing the alkyl chain lengths between footholds to ensure an even steric hindrance of both pyridyl moieties.

4.11 Experimental Section

General Information

Compounds **1**,[20] **23**[21] and **27**[22] were prepared according to modified literature procedures. Benzaldehyde (**2**), 3,5-dihydroxybenzoic acid (**5**), 6-heptenoic acid (**15**), 3,5-dihydroxybenzaldehyde (**22**), 1-bromopropane, 2,6-pyridinemethanol (**26**), 4-bromobutene and 6-methyl-2-pyridine methanol were purchased from Sigma Aldrich.

Synthesis of Macrocycle M1$_1$

Synthesis of 6

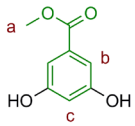

To a solution of 3,5-dihydroxybenzoic acid (**5**) (5.00 g, 32.0 mmol, 1.0 equiv) in dry MeOH (100 mL) was added $SOCl_2$ (5 mL) and the mixture stirred at room temperature under nitrogen for 12 h. The solvent was removed under reduced pressure to give **6** (5.35 g, quant.) as a pale yellow powder. m.p. 158-163 °C. ^{1}H NMR (400 MHz, MeOD): δ = 6.93 (d, J = 2.3 Hz, 2H, H_b), 6.48 (t, J = 2.3 Hz, 1H, H_c), 3.86 (s, 3H, H_a). ^{13}C NMR (101 MHz, MeOD): δ = 168.68, 159.74, 133.01, 108.79, 108.24, 52.52. HRMS (NSI$^+$): m/z = 191.0317 $[M+Na]^+$ (calcd. 191.0320 for $C_8H_8NaO_4^+$).

Synthesis of 7

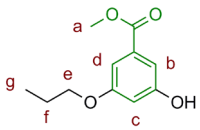

Under nitrogen, **6** (2.50 g, 15.0 mmol, 1.0 equiv) and K_2CO_3 (6.20 g, 45.0 mmol, 3.0 equiv) were added to dry DMF (100 mL) and stirred for 10 min. 1-bromopropane (1.80

g, 15.0 mmol, 1.0 equiv) was added *via* syringe over a period of 1 h. The reaction mixture was stirred at room temperature for 16 h. The solvent was removed under reduced pressure, the crude product dissolved in EtOAc and washed with H_2O, aqueous LiCl, and brine. The organic fractions were dried over $MgSO_4$ and the solvent removed under reduced pressure. The crude product was purified by column chromatography (SiO_2, EtOAc/petrol ether 1:4) to give **7** (1.00 g, 32%) as a white solid. m.p. 76-78 °C. ^{1}H NMR (400 MHz, MeOD): δ = 7.05 – 7.00 (m, 2H, H_{b+d}), 6.58 (t, J = 2.3 Hz, 1H, H_c), 3.94 (t, J = 6.5 Hz, 2H, H_e), 3.88 (s, 3H, H_a), 1.87 – 1.74 (m, 2H, H_f), 1.06 (t, J = 7.4 Hz, 3H, H_g). ^{13}C NMR (101 MHz, MeOD): δ = 168.6, 161.8, 159.9, 133.1, 109.9, 107.7, 107.5, 70.8, 52.6, 23.6, 10.8.

Synthesis of 8

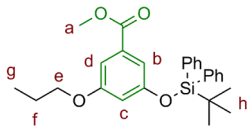

To a solution of **7** (0.620 g, 2.96 mmol, 1.0 equiv) in dry DMF (40 mL) at 0 °C was added DIPEA (1.22 g, 9.47 mmol, 3.2 equiv) and the solution stirred for 20 min. TBDPSCl (1.63 g, 5.91 mmol, 2.0 equiv) was added in dry DMF (10 mL) and the solution stirred at 55 °C for 3 h. Brine was added, the crude product extracted with CH_2Cl_2 and washed with HCl (1 M), H_2O, and brine. The organic phase was dried over $MgSO_4$. The solvent was removed under reduced pressure and the crude residues combined and purified by column chromatography (SiO_2, petrol ether/CH_2Cl_2 3:1) to give **8** (1.25 g, 94%) as a white solid. m.p. 121-123 °C. ^{1}H NMR (400 MHz, $CDCl_3$): δ = 7.82 – 7.74 (m, 4H, H_{Ar}), 7.52 – 7.37 (m, 6H, H_{Ar}), 7.21 – 7.15 (m, 2H, H_{b+d}), 6.48 (t, J = 2.3 Hz, 1H, H_c), 3.85 (s, 3H, H_a), 3.71 (t, J = 6.6 Hz, 2H, H_e), 1.73 – 1.63 (m, 2H, H_f), 1.18 (s, 9H, H_h), 0.95 (t, J = 7.4 Hz, 3H, H_g). ^{13}C NMR (101 MHz, $CDCl_3$): δ = 166.9, 159.8, 156.6, 135.6, 132.6, 131.8, 130.1, 127.9, 113.6, 111.2, 108.6, 69.7, 52.1, 26.6, 22.4, 19.6, 10.4. HRMS (ESI$^+$): m/z = 449.2142 $[M+H]^+$ (calcd. 449.2148 for $C_{27}H_{33}O_4Si^+$).

Synthesis of 9

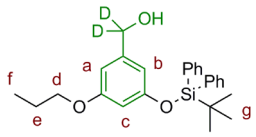

To a solution of **8** (0.380 g, 0.846 mmol, 1.0 equiv) in dry THF (35 mL) at 0 °C was added $LiAlD_4$ (0.140 g, 3.40 mmol, 4.0 equiv) and the reaction stirred at room temperature for 13 h. The reaction was quenched with H_2O followed by NaOH (0.1 M) and dried over $MgSO_4$. The solvent was removed under reduced pressure and the crude product purified by column chromatography (SiO_2, CH_2Cl_2/MeOH 98:2) to give **9** (0.340 g, 94%). m.p. 136-139 °C. ^{1}H NMR (400 MHz, $CDCl_3$): δ = 7.73 (d, J = 7.3 Hz, 4H, H_{Ar}), 7.46 – 7.34 (m, 6H, H_{Ar}), 6.46 (s, 1H, $H_{a/b}$), 6.37 (s, 1H, $H_{a/b}$), 6.22 (s, 1H, H_c), 3.65 (t, J = 6.6 Hz, 2H, H_d), 1.72 – 1.60 (m, 2H, H_e), 1.12 (s, 9H, H_g), 0.93 (t, J = 7.4 Hz, 3H, H_f). ^{13}C NMR (101 MHz, $CDCl_3$): δ = 160.2, 156.7, 142.9, 135.7, 133.0, 130.0, 127.9, 110.6, 106.3, 105.4, 69.5, 26.75, 22.5, 19.6, 10.5. HRMS (ESI$^+$): m/z = 423.2323 $[M+H]^+$ (calcd. 423.2324 for $C_{26}H_{31}D_2O_3Si^+$).

Synthesis of 10

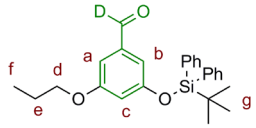

An equimolar solution of **9** (0.111 g, 0.260 mmol, 1.0 equiv) and Dess-Martin periodinane (0.110 g, 0.259 mmol, 1.0 equiv) was made up in CH_2Cl_2 and stirred at room temperature for 3 h. The reaction mixture was washed with H_2O and the organic fraction dried over $MgSO_4$. The solvent was removed under reduced pressure and the crude residue purified by column chromatography (SiO_2, petrol ether/CH_2Cl_2 3:2) to give **10** (76 mg, 51%) as a colourless oil. ^{1}H NMR (400 MHz, $CDCl_3$): δ = 7.74 – 7.68 (m, 4H, H_{Ar}), 7.48 – 7.34 (m, 6H, H_{Ar}), 6.94 (dd, J = 2.3, 1.3 Hz, 1H, $H_{a/b}$), 6.84 (dd, J = 2.3, 1.3 Hz, 1H, $H_{a/b}$), 6.53 (t, J = 2.3 Hz, 1H, H_c), 3.72 (t, J = 6.6 Hz, 2H, H_d), 1.73 – 1.62 (m, 2H, H_e), 1.12 (s, 9H, H_g), 0.94 (t, J = 7.4 Hz, 3H, H_f). ^{13}C NMR (126 MHz, $CDCl_3$): δ =191.8, 160.6, 157.3, 138.1, 135.6, 132.5, 130.3, 128.1, 114.5, 113.0, 107.5, 69.9, 26.6, 22.4, 19.6, 10.5. HRMS (NSI$^+$): m/z = 420.2097 $[M+H]^+$ (calcd. 420.2105 for $C_{26}H_{30}DO_3Si^+$)

Synthesis of 11

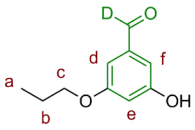

To a solution of **10** (76 mg, 0.17 mmol, 1.0 equiv) in dry THF (10 mL) was added TBAF (1 M in THF, 0.17 mL, 0.17 mmol, 1.0 equiv) at 0 °C forming a yellow solution which was stirred for 2 h. The reaction was quenched with H_2O (4 mL) at 0 °C and the crude product extracted with CH_2Cl_2, washed with H_2O and brine, and dried over $MgSO_4$. The crude product was purified by column chromatography (SiO_2, MeOH/CH_2Cl_2 1:99) to give **11** (28 mg, 90%) as a brown oil. ^{1}H NMR (400 MHz, $CDCl_3$): δ = 7.00 (dd, J = 2.3, 1.2 Hz, 1H, $H_{d/f}$), 6.94 (dd, J = 2.3, 1.2 Hz, 1H, $H_{d/f}$), 6.67 (t, J = 2.3 Hz, 1H, H_e), 3.95 (t, J = 6.6 Hz, 2H, H_c), 1.90 – 1.76 (m, 2H, H_b), 1.04 (t, J = 7.4 Hz, 3H, H_a). ^{13}C NMR (101 MHz, $CDCl_3$): δ = 192.92, 161.04, 157.82, 138.14, 109.14, 109.10, 108.05, 70.07, 22.51, 10.55. HRMS (NSI$^+$): m/z = 182.0923 $[M+H]^+$ (calcd. 082.0927 for $C_{10}H_{12}DO_3^+$).

Synthesis of 12

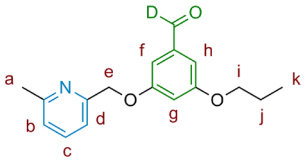

To a solution of PPh_3 (0.26 g, 0.99 mmol, 1.2 equiv) in dry THF (2 mL) was added DIAD (0.24 g, 1.2 mmol, 1.4 equiv) at 0 °C under nitrogen, forming a yellow cloudy solution which was stirred for 20 min. 6-methyl-2-pyridinemethanol (0.11 g, 0.91 mmol, 1.1 equiv) was added in THF (1 mL) and the solution stirred for 20 min. **11** (0.15 g, 0.83 mmol, 1.0 equiv) was added in THF (1.5 mL) and the solution turned clear yellow. The reaction mixture was allowed to warm to room temperature and stirred for 12 h. The solvent was removed under reduced pressure and the residue purified by column chromatography (SiO_2, MeOH/CH_2Cl_2 0.5:99.5) to give **12** (0.22 g, 93%) as a colourless oil. ^{1}H NMR (500 MHz, $CDCl_3$): δ = 7.60 (t, J = 7.7 Hz, 1H, H_c), 7.29 (d, J = 7.7 Hz, 1H, $H_{b/d}$), 7.09 (d, J = 7.7 Hz, 1H, $H_{b/d}$), 7.08 – 7.07 (m, 1H, $H_{f/h}$), 7.04 – 7.00 (m, 1H, $H_{f/h}$), 6.81 (t, J = 2.3 Hz, 1H, H_g), 5.19 (s, 2H, H_e), 3.94 (t, J = 6.6 Hz, 2H, H_i), 2.57 (s, 3H, H_a), 1.86 – 1.75 (m, 2H, H_j), 1.03 (t, J = 7.4 Hz, 3H, H_k). ^{13}C NMR (126 MHz, $CDCl_3$): δ = 192.0 – 191.4 (m), 161.0, 160.2, 158.3, 155.9, 138.4, 137.3, 122.6, 118.4, 108.5, 108.4, 107.9,

71.2, 70.1, 22.6, 22.1, 10.6. HRMS (NSI$^+$): *m/z* = 287.1501 [M+H]$^+$ (calcd. 287.1506 for $C_{17}H_{19}DNO_3^+$).

Synthesis of 13

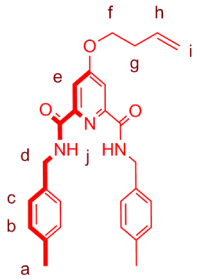

To a solution of compound **10** (Chapter II) (0.70 g, 1.8 mmol, 1.0 equiv) and K_2CO_3 (1.2 g, 9.0 mmol, 5.0 equiv) in butanone (60 mL) was added 4-bromobutene (1.2 g, 9.0 mmol, 5.0 equiv) and the solution stirred at 70 °C under nitrogen for 2 days. H_2O (50 mL) was added and the crude product extracted with butanone, dried over $MgSO_4$ and purified by column chromatography (SiO_2, MeOH/CH_2Cl_2 0.05:95.5) to give **13** (0.78 g, 99%) as a colourless oil. ^{1}H NMR (400 MHz, $CDCl_3$): δ = 8.51 (t, *J* = 6.1 Hz, 2H, H_j), 7.78 (s, 2H, H_e), 7.09 (d, *J* = 8.0 Hz, 4H, H_b), 6.99 (d, *J* = 8.0 Hz, 4H, H_c), 5.83 (ddt, *J* = 17.0, 10.2, 6.7 Hz, 1H, H_h), 5.22 – 5.09 (m, 2H, H_i), 4.48 (d, *J* = 6.2 Hz, 4H, H_d), 4.05 (t, *J* = 6.6 Hz, 2H, H_f), 2.54 (q, *J* = 6.6 Hz, 2H, H_g), 2.26 (s, 6H, H_a). ^{13}C NMR (101 MHz, $CDCl_3$): δ = 167.78, 163.58, 150.84, 137.39, 135.14, 133.50, 129.50, 127.87, 117.97, 111.61, 68.16, 43.37, 33.20, 21.24. HRMS (NSI$^+$): *m/z* = 444.2277 [M+H]$^+$ (calcd. 444.2287 for $C_{27}H_{30}N_3O_3^+$).

Synthesis of 14

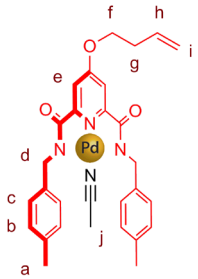

To a solution of **13** (0.80 g, 1.8 mmol, 1.0 equiv) in MeCN (55 mL) was added $Pd(OAc)_2$ (0.42 g, 1.8 mmol, 1.0 equiv) and the solution stirred at room temperature for 12 h. A bright yellow precipitate was filtered off and washed with cold MeCN. The product was dried under reduced pressure to give the product (0.79 g, 74%) as a grey/yellow

amorphous solid. ^{1}H NMR (400 MHz, $CDCl_3$): δ = 7.17 (s, 2H, H_e), 7.15 (d, J = 7.8 Hz, 4H, H_b), 7.04 (d, J = 7.8 Hz, 4H, H_c), 5.88 – 5.72 (m, 1H, H_h), 5.18 – 5.04 (m, 2H, H_i), 4.44 (s, 4H, H_d), 4.15 (t, J = 6.5 Hz, 2H, H_f), 2.59 – 2.48 (m, 2H, H_g), 2.26 (s, J = 13.1 Hz, 6H, H_a), 1.96 (s, J = 2.8 Hz, 3H, H_j). ^{13}C NMR (126 MHz, $CDCl_3$): δ = 170.7, 154.6, 138.7, 135.9, 133.1, 129.0, 128.6, 127.3, 118.3, 116.5, 111.2, 69.1, 50.1, 33.0, 21.2, 2.7, 2.0. HRMS (NSI$^+$): m/z = 589.1422 $[M+H]^+$ (calcd. 589.1431 for $C_{29}H_{31}N_4O_3Pd^+$).

Synthesis of 16

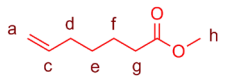

6-heptenoic acid (1.0 g, 7.8 mmol, 1.0 equiv) was added to MeOH (25 mL) at 0 °C. Thionyl chloride (2.0 g, 17 mmol, 2.2 equiv) was added *via* syringe and the solution stirred at room temperature for 16 h. The solvent was removed under reduced pressure to give **16** (1.1 g, quant.) as a colourless oil. ^{1}H NMR (400 MHz, $CDCl_3$): δ = 5.79 (ddt, J = 16.9, 10.2, 6.7 Hz, 1H, H_c), 5.05 – 4.91 (m, 2H, H_a) 3.66 (s, 3H, H_h), 2.31 (t, J = 7.5 Hz, 2H, H_g), 2.06 (q, J = 7.1 Hz, 2H, H_d), 1.65 - 1.61 (m, 2H, H_f), 1.47 – 1.36 (m, 2H, H_e). ^{13}C NMR (101 MHz, $CDCl_3$): δ = 174.3, 138.5, 114.8, 51.6, 48.5, 34.1, 33.5, 28.5, 24.5.

Synthesis of 17

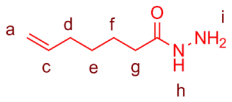

To a stirring solution of **16** (1.10 g, 7.80 mmol, 1.0 equiv) in MeOH (25 mL) was added hydrazine monohydrate (1.95 g, 39 .0mmol, 5.0 equiv) and the reaction mixture refluxed for 12 h. The solvent was removed under reduced pressure and the crude product purified by column chromatography (SiO_2, CH_2Cl_2/MeOH 95:5) to give **17** (0.70 g, 63%) as a white solid, m.p. 63 – 65 °C. ^{1}H NMR (400 MHz, $CDCl_3$): δ = 6.71 (s, 1H, H_h), 5.78 (ddt, J = 16.9, 10.2, 6.7 Hz, 1H, H_c), 5.03 – 4.93 (m, 2H, H_a), 3.89 (s, 2H, H_i), 2.20 – 2.11 (m, 2H, H_g), 2.11 – 2.01 (m, 2H, H_d), 1.73 – 1.57 (m, 2H, H_f), 1.48 – 1.35 (m, 2H, H_e). ^{13}C NMR (101 MHz, $CDCl_3$): δ = 174.0, 138.4, 114.9, 34.5, 33.5, 28.56, 25.1.

Synthesis of 18

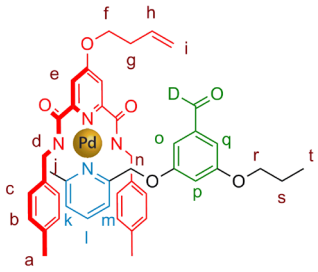

To a solution of **14** (0.25 g, 0.42 mmol, 1.0 equiv) in $CHCl_3$ (50 mL) was added **12** (0.12 g, 0.42 mmol, 1.0 equiv) and the solution stirred at room temperature for 5 h. The solvent was removed under reduced pressure and the crude residue purified by column chromatography (SiO_2, CH_2Cl_2/MeOH, 97:3) to yield **18** (0.32 g, 93%) as a yellow oil. ^{1}H NMR (500 MHz, $CDCl_3$): δ = 7.82 (t, J = 7.8 Hz, 1H, H_l), 7.45 (d, J = 7.8 Hz, 1H, $H_{k/m}$), 7.36 (s, 2H, H_e), 7.11 (d, J = 7.6 Hz, 1H, $H_{k/m}$), 7.05 (dd, J = 2.1, 1.1 Hz, 1H, $H_{q/o}$), 6.87 (dd, J = 2.2, 1.1 Hz, 1H, $H_{q/o}$), 6.74 (d, J = 7.8 Hz, 4H, H_b), 6.57 (t, J = 2.3 Hz, 1H, H_p), 6.45 (d, J = 7.9 Hz, 4H, H_c), 5.87 (ddt, J = 17.0, 10.3, 6.7 Hz, 1H, H_h), 5.22 – 5.12 (m, 2H, H_i), 4.59 (s, 2H, H_n), 4.28 – 4.18 (m, 4H, H_{d+f}), 3.98 (t, J = 6.6 Hz, 2H, H_r), 3.81 (d, J = 14.2 Hz, 2H, $H_{d'}$), 2.66 – 2.56 (m, 5H, H_{j+g}), 2.00 (s, 6H, H_a), 1.89 – 1.76 (m, 2H, H_s), 1.05 (t, J = 7.4 Hz, 3H, H_t). ^{13}C NMR (126 MHz, $CDCl_3$): δ = 191.44, 171.23, 169.37, 160.84, 160.47, 158.93, 154.33, 139.12, 138.09, 136.25, 133.18, 128.85, 127.30, 124.57, 120.67, 118.13, 111.25, 108.66, 108.40, 107.61, 77.41, 77.16, 76.91, 70.19, 68.94, 68.83, 53.54, 49.22, 33.02, 26.03, 22.54, 22.04, 20.86, 10.60. HRMS (NSI$^+$): m/z = 834.2608 $[M+H]^+$ (calcd. 834.2593 for $C_{44}H_{46}DN_4O_6Pd^+$).

Synthesis of 19

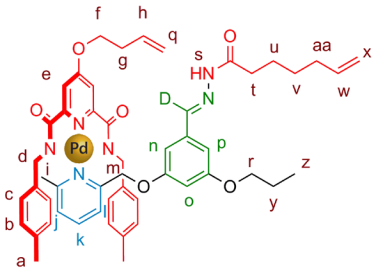

To a solution of **18** (0.25 g, 0.31 mmol, 1.0 equiv) and **17** (0.044 g, 0.31 mmol, 1.0 equiv) in dry MeOH (40 mL) was added glacial acetic acid (5 drops) and the solution stirred at room temperature for 16 h. The solvent was removed under reduced pressure and the crude residue purified by column chromatography (SiO_2,

CH_2Cl_2/MeOH 95:5) to yield **19** (0.27 g, 90%) as a yellow oily solid. ^{1}H NMR (500 MHz, $CDCl_3$): δ = 9.35 (s, 1H, H_s), 7.82 (t, J = 7.8 Hz, 1H, H_k), 7.48 (d, J = 7.9 Hz, 1H, $H_{j/l}$), 7.37 (s, 2H, H_e), 7.07 (d, J = 7.9 Hz, 1H, $H_{j/l}$), 6.88 (s, 1H, $H_{n/p}$), 6.76 (d, J = 7.8 Hz, 4H, H_b), 6.65 (s, 1H, $H_{n/p}$), 6.45 (d, J = 7.8 Hz, 4H, H_c), 6.36 (t, J = 2.2 Hz, 1H, H_o), 5.94 – 5.76 (m, 2H, H_{h+w}), 5.21 – 5.15 (m, 2H, H_q), 5.06 – 4.91 (m, 2H, H_x), 4.69 (s, 2H, H_m), 4.25 (t, J = 6.6 Hz, 2H, H_r), 4.14 (d, J = 14.2 Hz, 2H, H_d), 3.95 (t, J = 6.6 Hz, 2H, H_f), 3.92 (d, J = 14.3 Hz, 2H, $H_{d'}$), 2.75 (t, J = 7.5 Hz, 2H, H_t), 2.64 – 2.59 (m, 2H, H_g), 2.56 (s, 2H, H_i), 2.15 – 2.09 (m, 2H, H_{aa}), 1.88 – 1.79 (m, 2H, H_y), 1.77 – 1.70 (m, 2H, H_u), 1.52 – 1.44 (m, 2H, H_v), 1.06 (t, J = 7.4 Hz, 3H, H_z) . ^{13}C NMR (126 MHz, $CDCl_3$): δ = 207.13, 175.92, 171.24, 169.41, 160.63, 160.58, 159.19, 158.78, 154.38, 139.10, 138.76, 138.08, 136.33, 135.82, 133.20, 128.90, 127.33, 124.51, 120.72, 118.20, 114.73, 111.25, 107.23, 104.94, 103.76, 77.41, 77.16, 76.91, 70.18, 69.96, 69.02, 68.84, 53.56, 49.29, 33.67, 33.07, 32.63, 31.07, 28.74, 26.02, 24.34, 22.65, 22.09, 20.97, 10.70. HRMS (NSI$^+$): m/z = 958.3611 $[M+H]^+$ (calcd. 958.3594 for $C_{51}H_{58}DN_6O_6Pd^+$).

Synthesis of M1$_1$

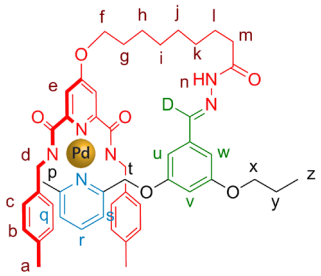

To an oven-dried round-bottom flask was added **19** (96.0 mg, 0.100 mmol, 1.0 equiv) and the flask purged with nitrogen. CH_2Cl_2 (110 mL, pre-purged with N_2) was added *via* syringe. Grubbs II (8.5 mg, 0.01 mmol, 0.1 equiv) was added and a light vacuum applied to the flask for 5 min. The flask was purged with nitrogen for 15 min and stirred at room temperature for 24 h. Additional Grubbs II (8.5 mg, 0.01 mmol, 0.1 equiv) was added and a light vacuum applied to the flask for 5 min. The flask was purged with nitrogen for 15 min and stirred at room temperature for 24 h. Ethyl vinyl ether (2 mL) was added and the solution stirred for 2 h. The solvent was removed under reduced pressure and the crude residue was purified by column chromatography (SiO_2, EtOAc) to give a yellow solid (54 mg, 58%), which was dissolved in dry THF (10 mL). K_2CO_3 (37.0 mg, 0.270 mmol, 5.0 equiv) was added with $Pd(OH)_2/C$ (5 mg) and the solution stirred at room temperature in the presence of

hydrogen gas for 4 h. The reaction mixture was filtered through Celite® and the solvent removed under reduced pressure. The crude residue was purified by column chromatography (SiO_2, CH_2Cl_2/MeOH 96:4) to yield **M1₁** (45 mg, 52% from **19**) as a yellow solid. ^{1}H NMR (400 MHz, $C_2Cl_4D_2$): δ = 8.78 (s, 1H, H_n), 7.88 (t, J = 7.8 Hz, 1H, H_r), 7.56 (d, J = 7.7 Hz, 1H, $H_{q/s}$), 7.37 (s, 2H, H_e), 7.14 (d, J = 7.7 Hz, 1H, $H_{q/s}$), 6.88 (t, J = 7.7 Hz, 4H, H_b), 6.83 (s, 3H, $H_{u\text{-}w}$), 6.63 (d, J = 7.7 Hz, 4H, H_c), 5.16 (s, 2H, H_t), 4.41 (t, J = 5.7 Hz, 2H, H_f), 4.17 (d, J = 14.4 Hz, 2H, H_d), 4.03 (t, J = 6.4 Hz, 2H, H_x), 4.01 (d, J = 14.4 Hz, 2H, $H_{d'}$), 2.62 (s, 3H, H_p), 2.23 (s, 6H, H_a), 2.00 – 1.93 (m, 2H, H_g), 1.94 – 1.85 (m, 2H, H_y), 1.81 – 1.65 (m, 4H, H_{h+m}), 1.65 – 1.55 (m, 4H, H_{k+j}), 1.53 – 1.46 (m, 2H, H_i), 1.15 (t, J = 7.4 Hz, 3H, H_z). HRMS (NSI$^+$): m/z = 932.3466 $[M+H]^+$ (calcd. 932.3437 for $C_{49}H_{56}DN_6O_6Pd^+$).

Ring-Opening Experiments

Synthesis of 20

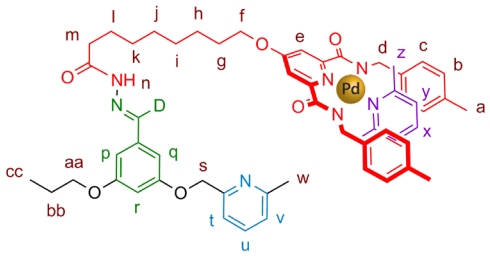

To a solution of **M1₁** (5.6 mg, 6.0 µmol, 1.0 equiv.) in CD_3CN (0.1 mL) and $CDCl_3$ (0.4 mL) was added 2,6-lutidine (3.2 mg, 30 µmol, 5.0 equiv.) and the solution heated at 65 °C for 15 hrs. Toluene (1 mL) was added and the solvent removed gradually under reduced pressure. The crude residue was purified by preparative thin layer chromatography (SiO_2, MeOH/CH_2Cl_2 5:95) to give **20** as a yellow solid (4.7 mg, 75%). m.p. 180 °C (dec.). ^{1}H NMR (500 MHz, $CDCl_3$): δ = 9.26 (s, 1H, H_n), 7.61 (t, J = 7.7 Hz, 1H, H_u), 7.61 (t, J = 7.7 Hz, 1H, H_x), 7.35 (s, 2H, H_e), 7.33 (d, J = 7.4 Hz, 1H, $H_{t/v}$), 7.09 (d, J = 7.6 Hz, 1H, $H_{t/v}$), 6.94 (d, J = 7.7 Hz, 2H, H_y), 6.87 (s, 1H, $H_{p/q}$), 6.81 (d, J = 7.8 Hz, 4H, H_b), 6.77 (s, 1H, $H_{p/q}$), 6.58 (t, J = 2.2 Hz, 1H, H_r), 6.47 (d, J = 7.8 Hz, 4H, H_c), 5.17 (s, 2H, H_s), 4.16 (t, J = 6.4 Hz, 2H, H_{aa}), 4.02 (s, 4H, H_d), 3.90 (t, J = 6.6 Hz, 2H, H_2), 2.76 (t, J = 7.3 Hz, 2H, H_2), 2.57 (s, 2H, H_w), 2.42 (s, 6H, H_z), 2.24 (s, 6H, H_a), 1.81 – 1.71 (m, 6H, $H_{g,l,bb}$), 1.50 – 1.37 (m, 6H, $H_{k,j,h}$), 1.03 (t, J = 7.4, Hz, 3H, H_{cc}). ^{13}C NMR (126 MHz, $CDCl_3$): δ = 175.78, 171.30, 169.52, 160.64, 160.57, 159.97, 158.13, 156.35, 154.37, 138.61, 138.22, 137.26, 135.96, 128.74, 127.46, 122.72, 122.45, 118.39, 111.16, 106.73,

105.47, 103.48, 70.98, 69.94, 69.85, 49.34, 32.64, 29.84, 29.13, 29.09, 28.87, 28.54, 25.61, 25.56, 24.57, 24.54, 22.64, 21.16, 10.66. HRMS (NSI+): *m/z* = 1039.4241 $[M+H]^+$ (calcd. 1039.4172 for $C_{56}H_{65}DN_7O_6Pd^+$).

Synthesis of 21

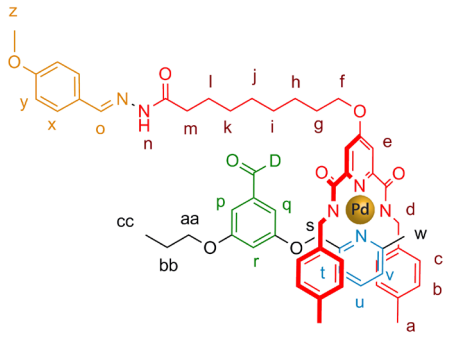

To a solution of **M1$_1$** (5.6 mg, 6.0 µmol, 1.0 equiv) in $CDCl_3$ (0.5 mL) was added *p*-anisaldehyde (4.1 mg, 0.03 mmol, 5.0 equiv) and TFA (2.2 µL, 0.03 mmol, 5.0 equiv) and the reaction left at room temperature for 15 h. The crude mixture was purified by preparative TLC (SiO_2, CH_2Cl_2/MeOH 95:5) to give **21** as a yellow solid. m.p. 175 °C (dec.) ^{1}H NMR (500 MHz, $CDCl_3$): δ = 8.79 (s, 1H, H_n), 7.86 (t, *J* = 7.7 Hz, 1H, H_u), 7.69 (s, 1H, H_o), 7.58 (d, *J* = 8.7 Hz, 1H, $H_{x/y}$), 7.47 (d, *J* = 7.7 Hz, 1H, $H_{t/v}$), 7.38 (s, 2H, H_e), 7.12 (d, *J* = 7.7, 1H, $H_{t/v}$), 7.06 (s, 1H, $H_{p/q}$), 6.91 (d, *J* = 8.7 Hz, 1H, $H_{x/y}$), 6.89 (s, 1H, $H_{p/q}$), 6.76 (d, *J* = 7.8 Hz, 4H, H_b), 6.59 (t, *J* = 2.0 Hz, 1H, H_r), 6.47 (d, *J* = 7.8 Hz, 4H, H_c), 4.61 (s, 2H, H_s), 4.23 (d, *J* = 14.1 Hz, 2H, H_d), 4.19 (t, *J* = 6.4 Hz, 2H$_f$), 3.99 (t, *J* = 6.6 Hz, 2H, H_{aa}), 3.84 (s, 3H, H_z), 3.83 (d, *J* = 14.1 Hz, 2H, $H_{d'}$), 2.76 (t, *J* = 7.4 Hz, 2H, H_m), 2.64 (s, 3H, H_w), 2.02 (s, 6H, H_a), 1.87 - 1.73 (m, 6H, $H_{bb,g,l}$), 1.50 – 1.39 (m, 8H, $H_{h,i,j,l}$) 1.07 (t, *J* = 7.4 Hz, 3H, H_{cc}). HRMS (NSI+): *m/z* = 1068.4001 $[M+H]^+$ (calcd. 1068.3961 for $C_{57}H_{64}DN_6O_8Pd^+$).

Synthesis of Molecular Walker-Track Conjugate 1,2-T1

Synthesis of 24

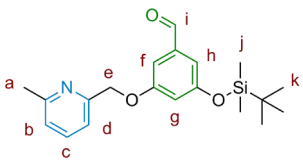

PPh_3 (0.24 g, 0.82 mmol, 1.2 equiv) was dissolved in dry THF (2 mL) and cooled to 0 °C under nitrogen. DIAD (0.21 g, 1.1 mmol, 1.4 equiv.) was added dropwise and the

solution stirred for 20 min. 6-methyl-2-pyridine methanol (0.10 g, 0.82 mmol, 1.2 equiv) was added in THF (1 mL) and the solution stirred for 20 min. **23** (0.19 g, 0.75 mmol, 1 equiv) was added in THF (1.5 mL) and stirred for 4.5 h. The solvent was removed under reduced pressure and the crude product purified by column chromatography (SiO_2, CH_2Cl_2) to give **24** (0.20 g, 74%) as a colourless oil. ^{1}H NMR (400 MHz, $CDCl_3$): δ = 9.87 (s, 1H, H_i), 7.61 (t, J = 7.7 Hz, 2H, H_c), 7.30 (d, J = 7.5 Hz, 1H, H_d), 7.12 (dd, J = 2.4, 1.3 Hz, 1H, H_f), 7.10 (d, J = 7.8 Hz, 1H, H_b), 6.95 (dd, J = 2.2, 1.3 Hz, 1H, H_h), 6.73 (t, J = 2.3 Hz, 1H, H_g), 5.18 (s, 2H, H_e), 2.58 (s, 3H, H_a), 0.97 (s, 9H, H_k), 0.22 (s, 6H, H_j). ^{13}C NMR (126 MHz, $CDCl_3$): δ = 191.90, 160.14, 158.30, 157.57, 155.94, 138.57, 137.31, 122.60, 118.49, 114.31, 113.54, 108.94, 71.21, 25.74, 24.50, 18.33, -4.33. HRMS (NSI$^+$): m/z = 358.1834 $[M+H]^+$ (calcd. 358.1838 for $C_{20}H_{28}NO_3Si^+$).

Synthesis of 25

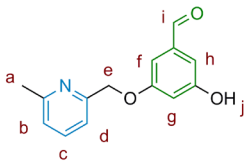

To a solution of **24** (76 mg, 0.21 mmol, 1.0 equiv) in dry THF (10 mL) was added TBAF (1 M in THF, 0.21 mL, 0.21 mmol, 1.0 equiv) at 0 °C forming a yellow solution which was stirred for 2 h. The reaction was quenched with H_2O (4 mL) at 0 °C and the crude product extracted with CH_2Cl_2, washed with H_2O and brine, and dried over $MgSO_4$. The crude product was purified by column chromatography (SiO_2, MeOH/CH_2Cl_2 1:99) to give **29** (46 mg, 90%) as a brown oil. ^{1}H NMR (400 MHz, MeOD): δ = 9.83 (s, 1H, H_i), 7.74 (t, J = 7.7 Hz, 1H, H_c), 7.39 (d, J = 7.6 Hz, 1H, H_d), 7.24 (d, J = 7.8 Hz, 1H, H_b), 7.03 (dd, J = 2.0, 1.1 Hz, 1H, H_f), 6.94 (dd, J = 2.0, 1.1 Hz, 1H, H_h), 6.74 (t, J = 2.0 Hz, 1H, H_g), 5.15 (s, 2H, H_e), 2.56 (s, 3H, H_a). ^{13}C NMR (126 MHz, MeOD): δ = 193.77, 161.57, 160.68, 159.31, 157.13, 140.15, 139.19, 124.07, 120.28, 110.53, 109.51, 107.66, 71.40, 23.79. HRES (ESI$^+$): m/z = 244.1001 $[M+H]^+$ (calcd. 244.0974 for $C_{14}H_{14}NO_3^+$).

Synthesis of T1

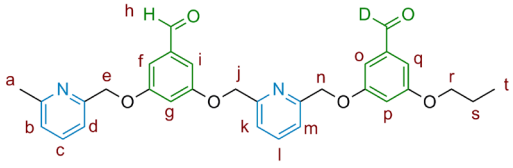

To a solution of **25** (29.5 mg, 0.122 mmol, 1.0 equiv) and **28** (61.0 mg, 0.134 mmol, 1.1 equiv) in dry THF (4 mL) was added $CsCO_3$ (119 mg, 0.365 mmol, 3.0 equiv) and the mixture stirred at room temperature for 15 h. The solvent was removed under reduced pressure and the crude residue purified by column chromatography (SiO_2, petroleum ether/EtOAc 6:4) to give **T1** (44 mg, 68%) as a colourless oil. ^{1}H NMR (500 MHz, $CDCl_3$): δ = 9.89 (s, 1H, H_{hz}), 7.77 (t, J = 7.8 Hz, 1H, H_{Ar}), 7.61 (t, J = 7.7 Hz, 1H, H_{Ar}), 7.45 (t, J = 7.6 Hz, 2H, H_{Ar}), 7.28 (d, J = 7.7 Hz, 1H, H_{Ar}), 7.13 (d, J = 2.3 Hz, 2H, H_{Ar}), 7.11 – 7.09 (m, 2H, H_{Ar}), 7.04 (dd, J = 2.2, 1.1 Hz, 1H, H_{Ar}), 6.93 (t, J = 2.3 Hz, 1H, H_{Ar}), 6.82 (t, J = 2.3 Hz, 1H, H_{Ar}), 5.24 (s, 4H, H_{j+n}), 5.20 (s, 2H, H_e), 3.96 (t, J = 6.6 Hz, 2H, H_r), 2.58 (s, 3H, H_a), 1.86 – 1.78 (m, 2H, H_s), 1.04 (t, J = 7.4 Hz, 3H, H_t). ^{13}C NMR (126 MHz, $CDCl_3$) δ 191.73, 161.02, 160.36, 160.19, 160.12, 158.38, 156.44, 156.30, 155.75, 138.68, 138.51, 137.93, 137.27, 122.64, 120.63, 118.47, 108.97, 108.66, 108.42, 108.26, 108.17, 71.32, 71.05, 70.98, 70.15, 24.55, 22.58, 10.61. HRMS (NSI$^+$): m/z = 528.228 $[M+H]^+$ (calcd. 528.2245 for $C_{31}H_{30}DN_2O_6^+$).

Synthesis of 28

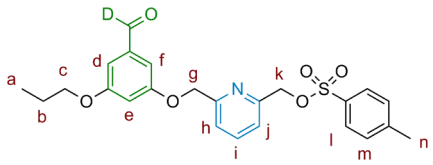

To a solution of **11** (0.310 g, 1.67 mmol, 1.0 equiv) and **27** (3.80 g, 8.50 mmol, 5.0 equiv) in dry THF (40 mL) was added $CsCO_3$ (2.77 g, 8.50 mmol, 5.0 equiv) and the solution stirred at room temperature under nitrogen for 16 h. CH_2Cl_2 (50 mL) and H_2O (50 mL) were added and the two phases separated. The organic layer was dried over $MgSO_4$, the solvent removed under reduced pressure and the crude product purified by column chromatography (SiO_2, petrol ether/EtOAc 2:1) to give **28** (0.58 g, 74%) as a colourless oil. ^{1}H NMR (500 MHz, $CDCl_3$): δ = 7.84 (d, J = 8.1 Hz, 2H, $H_{l/m}$), 7.73 (t, J = 7.8 Hz, 1H, H_i), 7.43 (d, J = 7.8 Hz, 1H, $H_{h/j}$), 7.37 (d, J = 7.8 Hz, 1H, $H_{h/j}$), 7.34 (d, J = 8.1 Hz, 1H, $H_{l/m}$), 7.06 – 7.04 (m, 1H, $H_{d/f}$), 7.04 – 7.02 (m, 1H, $H_{d/f}$), 6.78 (t, J = 2.2 Hz, 1H, H_e), 5.16 (s, 2H, $H_{g/k}$), 5.14 (s, 2H, $H_{g/k}$), 3.95 (t, J = 6.6 Hz, 2H, H_c), 2.44 (s, 3H, H_n), 1.87 – 1.74 (m, 2H, H_b), 1.03 (t, J = 7.4 Hz, 3H, H_a). ^{13}C NMR (126 MHz, $CDCl_3$): δ = 191.59, 161.03, 160.02, 156.43, 153.65, 145.24, 138.52, 138.02, 132.97, 130.07, 128.25, 121.09, 121.08, 108.38, 108.32, 108.07, 71.67, 70.74, 70.17, 22.57, 21.80, 10.60. HRES (ESI$^+$): m/z = 457.1532 $[M+H]^+$ (calcd. 457.1544 for $C_{24}H_{25}DNO_6S^+$).

Synthesis of 29

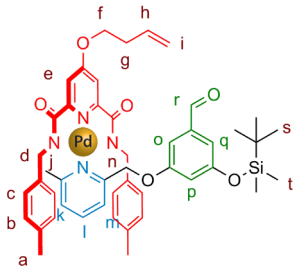

To a solution of **24** (0.22 g, 0.60 mmol, 1.0 equiv) in $CHCl_3$ (150 mL) was added **14** (0.36 g, 0.60 mmol, 1.0 equiv.) and the reaction mixture stirred at room temperature for 16 h. The solvent was removed under reduced pressure and the crude product purified by column chromatography (SiO_2, CH_2Cl_2/MeOH 97:3) to give **29** (0.42 g, 77%) as a yellow oily solid. ^{1}H NMR (400 MHz, $CDCl_3$): δ = 9.91 (s, 1H, H_r), 7.84 (t, J = 7.8 Hz, 1H, H_l), 7.46 (d, J = 7.7 Hz, 1H, $H_{k/m}$), 7.37 (s, 2H, H_e), 7.12 (d, J = 7.7 Hz, 1H, $H_{k/m}$), 6.99 (dd, J = 2.3, 1.2 Hz, 1H, $H_{q/o}$), 6.87 (dd, J = 2.3, 1.2 Hz, 1H, $H_{q/o}$), 6.74 (d, J = 7.7 Hz, 4H, H_b), 6.57 (t, J = 2.3 Hz, 1H, H_p), 6.45 (d, J = 7.9 Hz, 4H, H_c), 5.88 (ddt, J = 17.0, 10.2, 6.7 Hz, 1H, H_h), 5.26 – 5.13 (m, 2H, H_i), 4.60 (s, 2H, H_n), 4.28 = 4.20 (m, 4H, H_{d+f}), 3.82 (d, J = 14.2 Hz, 2H, $H_{d'}$), 2.65 – 2.60 (m, 5H, H_{g+j}), 2.02 (s, 6H, H_a), 0.99 (s, 9H, H_s), 0.22 (s, 6H, H_t). ^{13}C NMR (126 MHz, $CDCl_3$): δ = 191.66, 171.24, 169.42, 160.50, 158.98, 157.54, 154.41, 139.14, 138.52, 138.19, 136.30, 133.21, 128.90, 127.35, 124.54, 120.60, 118.20, 115.07, 113.27, 111.26, 107.96, 69.02, 68.89, 49.28, 33.08, 29.84, 26.07, 25.75, 20.93, 18.35, -4.24. HRMS (NSI$^+$): m/z = 905.2932 $[M+H]^+$ (calcd. 905.2926 for $C_{47}H_{55}N_4O_6PdSi^+$).

Synthesis of 30

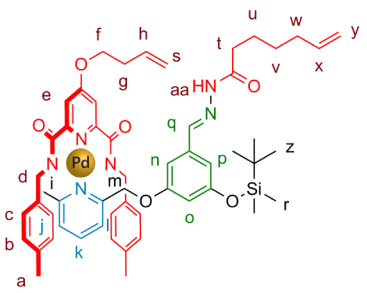

To a solution of **29** (0.077 g, 0.085 mmol, 1.0 equiv) in dry MeOH (20 mL) was added **17** (0.013 g, 0.085 mmol, 1.0 equiv). Glacial acetic acid (3 drops) was added and the solution stirred at room temperature under nitrogen for 12 h. The solvent was removed under reduced pressure and the crude product purified by column chromatography (SiO_2, CH_2Cl_2/MeOH 98:2) to yield **30** (0.083 g, 94%) as a yellow, oily solid. ^{1}H NMR (400 MHz, $CDCl_3$): δ = 8.98 (s, 1H, H_q), 7.83 (t, J = 7.8 Hz, 1H, H_k), 7.63 (s, 1H, H_{aa}), 7.47 (d, J = 7.7 Hz, 1H, $H_{j/l}$), 7.36 (s, 2H, H_e), 7.09 (d, J = 7.7 Hz, 1H, $H_{j/l}$), 6.84 (s, 1H, $H_{n/p}$), 6.74 (d, J = 7.8 Hz, 4H, H_b), 6.65 (s, 1H, $H_{n/p}$), 6.44 (d, J = 7.8 Hz, 4H, H_c), 6.34 (t, J = 2.2 Hz, 1H, H_o), 5.96 - 5.73 (m, 2H, H_{x+h}), 5.25 – 5.13 (m, 2H, H_s), 5.06 – 4.91 (m, 2H, H_y), 4.71 (s, 2H, H_m), 4.25 (t, J = 6.6 Hz, 2H, H_f), 4.15 (d, J = 14.2 Hz, 2H, $H_{d/d'}$), 3.90 (d, J = 14.2 Hz, 2H, $H_{d/d'}$), 2.74 (t, J = 7.5 Hz, 2H, H_t), 2.63 (q, J = 6.6 Hz, 2H, H_g), 2.55 (s, 3H, H_i), 2.16 – 2.08 (m, 2H, H_w), 2.07 (s, 6H, H_a), 1.79 – 1.68 (m, 2H, H_u), 1.56 – 1.42 (m, 2H, H_v), 0.96 (s, 9H_z), 0.20 (s, 6H, H_r). ^{13}C NMR (126 MHz, $CDCl_3$) δ 175.88, 174.09, 171.20, 169.41, 163.59, 160.55, 159.14, 158.77, 157.24, 154.42, 150.97, 142.56, 142.46, 139.12, 138.74, 138.11, 136.34, 135.82, 133.18, 129.52, 128.91, 127.90, 127.33, 124.46, 120.61, 118.24, 114.75, 111.64, 111.51, 111.43, 111.20, 108.52, 107.41, 107.35, 69.06, 68.88, 49.33, 33.67, 33.07, 32.74, 28.75, 25.83, 24.36, 21.01, 18.41, -4.18. HRMS (NSI$^+$): m/z = 1029.3939 $[M+H]^+$ (calcd. 1029.3926 for $C_{54}H_{67}N_6O_6PdSi^+$).

Synthesis of M2$_1$

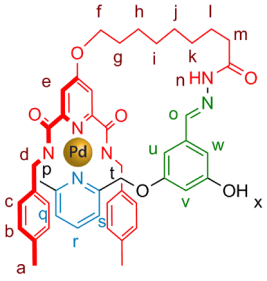

To an oven-dried round-bottom flask was added **30** (103 mg, 0.10 mmol, 1.0 equiv) and the flask purged with nitrogen. CH_2Cl_2 (110 mL, purged with N_2) was added *via* syringe. Grubbs II (8.5 mg, 0.01 mmol, 0.1 equiv) was added and a light vacuum applied to the flask for 5 min. The flask was purged with nitrogen for 15 min and stirred at room temperature for 24 h. Additional Grubbs II (8.5 mg, 0.01 mmol, 0.1 equiv) was added and a light vacuum applied to the flask for 5 min. The flask was purged with nitrogen for 15 min and stirred at room temperature for 24 h. Ethyl vinyl ether (2 mL) was added and the solution stirred for 2 h. The solvent was removed

under reduced pressure and the crude residue was purified by column chromatography (SiO_2, EtOAc) to give a yellow solid HRMS (NSI^+): *m/z* = 1001.3618 $[M+H]^+$ (calcd. 1001.3613 for $C_{52}H_{63}N_6O_6PdSi^+$)(58 mg, 58%), which was dissolved in dry THF (10 mL). TBAF (1 M in THF, 0.17 mL, 0.17 mmol, 1 equiv) at 0 °C forming a yellow solution which was stirred for 2 h. The reaction was quenched with H_2O (4 mL) at 0 °C and the crude product extracted with CH_2Cl_2, washed with H_2O and brine, and dried over $MgSO_4$. The crude product was purified by column chromatography (SiO_2, MeOH/CH_2Cl_2 1:99) to give a brown oil, which was dissolved in dry THF (10 mL). K_2CO_3 (37 mg, 0.27 mmol, 5 equiv) was added with $Pd(OH)_2/C$ (5 mg) and the solution stirred at room temperature in the presence of hydrogen gas for 4 h. The reaction mixture was filtered through celite and the solvent removed under reduced pressure. The crude residue was purified by column chromatography (SiO_2, CH_2Cl_2/MeOH 96:4) to yield **M2₁** (27 mg, 52% from **30**) as a yellow solid. ^1H NMR (400 MHz, $C_2D_2Cl_4$, 378 K): δ = 8.51 (s, 1H, H_o), 7.84 (t, *J* = 7.8 Hz, 1H, H_r), 7.49, (d, *J* = 7.8 Hz, 1H, $H_{q/s}$), 7.31 (s, 2H, H_e), 7.10 (d, *J* = 7.8 Hz, 1H, $H_{q/s}$), 6.88 (d, *J* = 7.6 Hz, 4H, H_b), 6.76 (s, 1H, $H_{u/w}$), 6.73 (s, 1H, H_v), 6.62 (d, *J* = 7.7 Hz, 4H, H_c), 6.53 (s, 1H, $H_{u/w}$), 5.18 (s, 2H, H_t), 4.36 (t, *J* = 5.7 Hz, 2H, H_f), 4.26 (d, *J* = 14.4 Hz, 2H, H_d), 3.91 (d, *J* = 14.4 Hz, 2H, $H_{d'}$), 2.62 – 2.59 (m, 2H, H_m), 2.55 (s, 3H, H_p), 2.23 (s, 6H, H_a), 2.00 – 1.89 (m, 2H, H_g), 1.78 – 1.69 (m, 2H, H_n), 1.63 – 1.54 (m, 2H, H_l), 1.50 – 1.45 (m, 8H, $H_{h,i,j,k}$). HRMS (NSI^+): *m/z* = 889.2914 $[M+H]^+$ (calcd. 889.2905 for $C_{46}H_{51}N_6O_6Pd^+$).

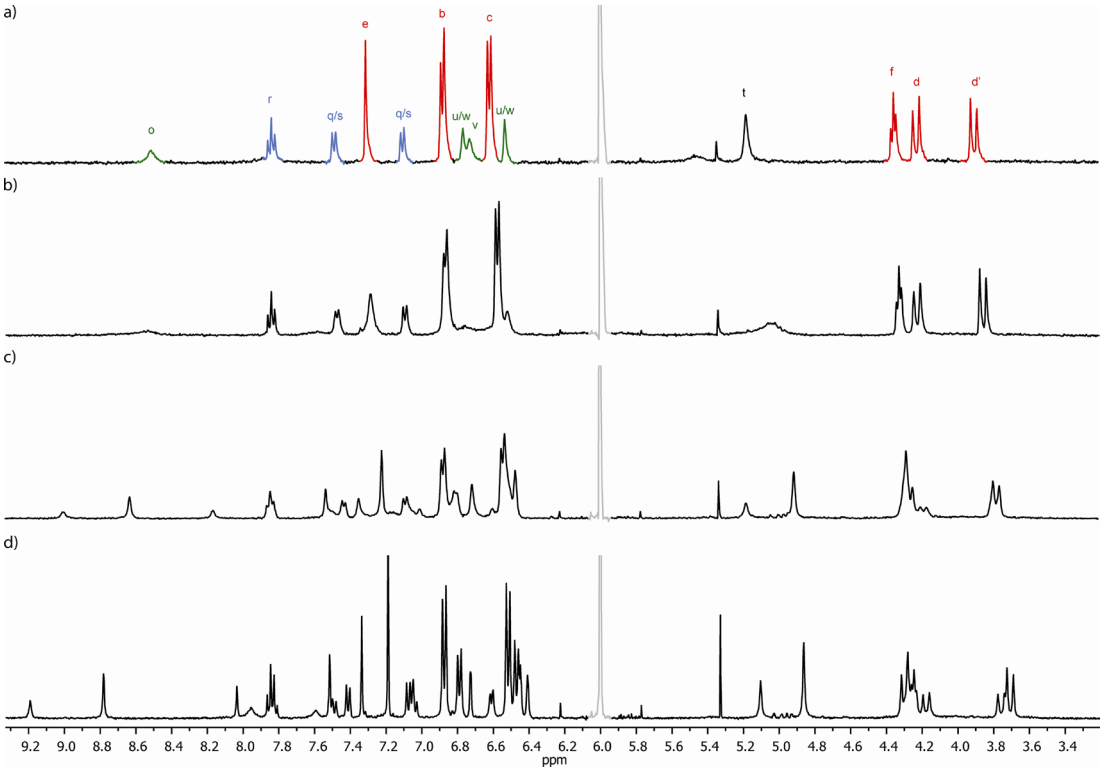

Figure 4.7 *- ^{1}H NMR spectra (400 MHz, $C_2D_2Cl_4$) of* ***M2$_1$****: (a) 378 K; (b) 348 K ;(c) 318 K; (d) 298 K.*

Synthesis of 1,2-T1

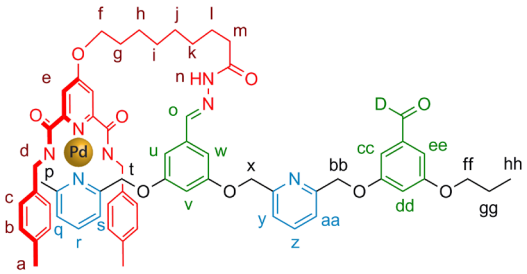

To a mixture of **M2$_1$** (30 mg, 0.034 mmol, 1.0 equiv) and $CsCO_3$ (55.4 mg, 0.17 mmol, 5.0 equiv) in dry THF (10 mL) was added **28** (31 mg, 0.067 mmol, 2.0 equiv) and the mixture stirred at room temperature for 15 h. The solvent was removed under reduced pressure and the crude residue purified by column chromatography (SiO_2, CH_2Cl_2/MeOH 95:5) to give 1,2-**T1** (24 mg, 61%) as a brown solid. ^{1}H NMR (400 MHz, $C_2D_2Cl_4$, 378 K): δ = 8.60 – 8.51 (m, 1H, H_o), 7.87 – 7.77 (m, 2H, H_{r+z}), 7.53 – 7.45 (m, 2H, $H_{q/s+y/aa}$), 7.31 (s, 2H, H_e), 7.17 – 7.13 (m, 1H, H_{cc}), 7.11 – 7.06 (m, 3H, $H_{q/s+y/aa+bb}$), 6.90 (t, J = 2.3 Hz, 1H, H_{dd}), 6.83 (d, J = 7.7 Hz, 4H, H_b), 6.82 – 6.78 (m, 1H, $H_{u/w}$), 6.71 (t, J = 2.1 Hz, 1H, H_v), 6.58 (d, J = 7.7 Hz, 4H, H_c), 6.56 – 6.55 (m, 1H, $H_{u/w}$), 5.33 (s, 2H, H_x),

5.29 (s, 2H, H_{bb}), 5.26 (s, 2H, H_t), 4.35 (t, J = 5.9 Hz, 2H, H_f), 4.12 (d, J = 14.5 Hz, 2H, H_d), 4.03 (t, J = 6.5 Hz, 2H, H_{ff}), 3.96 (d, J = 14.5 Hz, 2H, $H_{d'}$), 2.63 – 2.58 (m, 2H, H_m), 2.58 (s, 3H, H_p), 2.17 (s, 6H, H_a), 1.94 – 1.78 (m, 4H, H_{l+gg}), 1.73 – 1.35 (m, 10H, $H_{g,h,i,j,k}$), 1.08 (t, J = 7.4 Hz, 3H, H_{hh}).

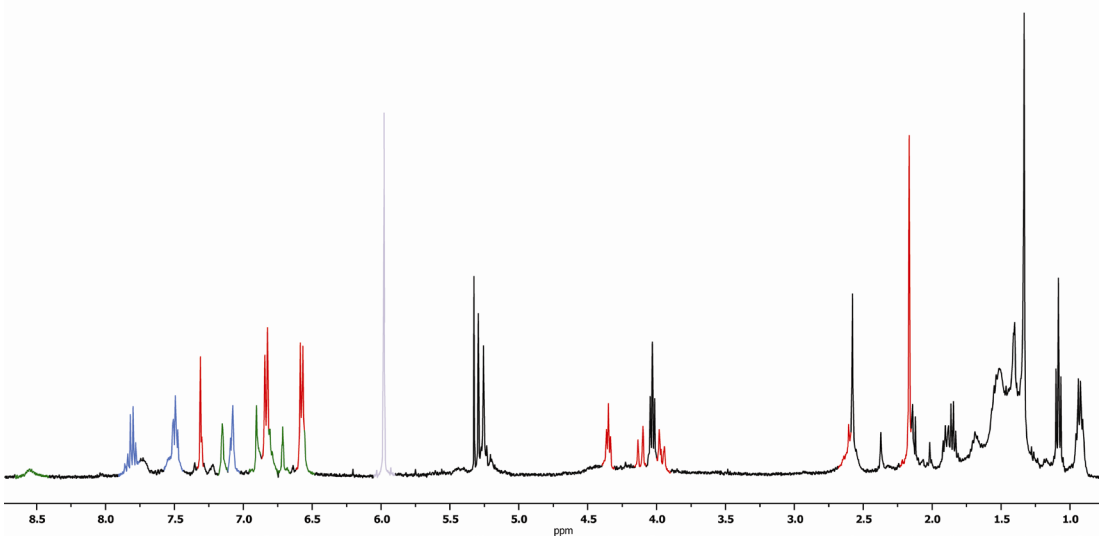

Figure 4.8 *- ^{1}H NMR spectra (400 MHz, $C_2D_2Cl_4$, 378 K) of 1,2-**T1**.*

Synthesis of (2,6-lutidine),2-T1

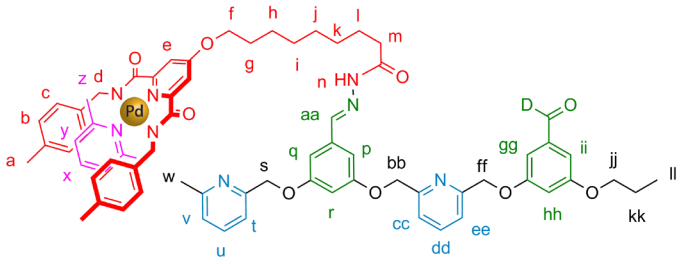

A solution of **1,2-T1** (5.0 mg, 4.26 µmol, 1.0 equiv) and 2,6-lutidine (2.3 mg, 21.0 µmol, 5.0 equiv) in $CDCl_3/CD_3CN$ (7:3, 0.50 mL) was heated at 65 °C for 23 h. The crude mixture was purified by preparative thin layer chromatography (SiO_2, CH_2Cl_2/MeOH 95:5) to give (2,6-lutidine),2-**T1** (3.50 mg, 70%) as a viscous yellow oil. ^{1}H NMR (500 MHz, $CDCl_3$): δ = 9.21 (s, 1H, H_n), 7.76 (t, J = 7.8 Hz, 1H, H_{dd}), 7.69 (s, 1H, H_{aa}), 7.61 (t, J = 7.7 Hz, 1H, H_x), 7.61 (t, J = 7.7 Hz, 1H, H_u), 7.47 – 7.43 (m, 2H, H_{cc+ee}), 7.34 (s, 2H, H_e), 7.33 (d, J = 6.3 Hz, 1H, $H_{t/v}$), 7.12 (d, J = 6.3 Hz, 1H, $H_{t/v}$), 7.08 (dd, J = 2.3, 1.2 Hz, 1H, H_{gg}), 7.04 (dd, J = 2.3, 1.2 Hz, 1H, H_{ii}), 6.95 (s, 1H, $H_{p/q}$), 6.94 (d, J = 7.7 Hz, 2H, H_y), 6.87 (s, 1H, $H_{p/q}$), 6.83 – 6.82 (m, 1H, H_{hh}), 6.81 (d, J = 7.9 Hz, 4H, H_b), 6.70 (t, J = 2.2 Hz, 1H,

H_r), 6.47 (d, J = 7.9 Hz, 4H, H_c), 5.24 (s, 4H, H_{bb+ff}), 5.21 (s, 2H, H_s), 4.15 (t, J = 6.5 Hz, 2H, H_{jj}), 4.02 (s, 4H, H_d), 3.96 (t, J = 6.6 Hz, 2H, H_f), 2.75 (t, J = 7.2 Hz, 2H, H_m), 2.43 (s, 6H, H_z), 2.24 (s, 6H, H_a), 1.84 – 1.79 (m, 2H_{kk}), 1.77 – 1.70 (m, 4H_{g+l}), 1.51 – 1.45 (m, 4H), 1.04 (t, J = 7.4 Hz, 3H, H_{ll}). ^{13}C NMR (126 MHz, $CDCl_3$): δ = 175.69, 171.31, 169.52, 161.03, 160.58, 160.15, 160.07, 159.88, 158.20, 156.77, 156.33, 156.20, 154.38, 142.54, 138.61, 138.51, 138.25, 137.91, 137.26, 136.29, 135.96, 129.50, 128.74, 127.88, 127.47, 122.73, 122.51, 120.58, 120.49, 118.41, 111.65, 111.17, 108.49, 108.43, 108.02, 106.80, 106.27, 103.96, 71.08, 71.02, 70.86, 70.17, 69.95, 49.35, 43.38, 32.60, 32.07, 29.85, 29.75, 29.61, 29.51, 29.40, 29.28, 29.22, 29.08, 28.83, 28.53, 25.63, 25.54, 24.55, 24.50, 22.84, 22.59, 21.23, 21.16, 14.26, 10.62. HRMS (NSI^+): m/z = 1280.4898 $[M+H]^+$ (calcd. 1280.4911 for $C_{70}H_{76}DN_8O_9Pd^+$).

4.12 References

1. Symes, M. D., *Walking Molecules*, University of Edinburgh, **2009**.

2. a) Lehn, J.-M. *Chem. -Eur. J.* **1999**, *5*, 2455-2463;

b) Lehn, J.-M.; Eliseev, A. V. *Science* **2002**, *291*, 2331-2332;

c) Rowan, S. J.; Cantrill, S. J.; Cousins, G. R. L.; Sanders, J. K. M.; Stoddart, J. F. *Angew. Chem., Int. Ed.* **2002**, *41*, 898-952;

d) Corbett, P. T.; Leclaire, J.; Vial, L.; West, K. R.; Wietor, J.-L.; Sanders, J. K. M.; Otto, S. *Chem. Rev.* **2006**, *106*, 3652-3711;

e) Lehn, J.-M. *Chem. Soc. Rev.* **2007**, *36*, 151-160;

f) Ladame, S. *Org. Biomol. Chem.* **2008**, *6*, 219-226;

g) Herrmann, A. *Org. Biomol. Chem.* **2009**, *7*, 3195-3204;

h) Mastalerz, M. *Angew. Chem., Int. Ed.* **2010**, *49*, 5042-5053.

3. a) Lehn, J.-M. *Science* **1985**, *227*, 849-856;

b) Lehn, J.-M. *Angew. Chem., Int. Ed.* **1988**, *27*, 89-112;

c) Lehn, J.-M. *Science* **1993**, *260*, 1762-1763;

d) Lehn, J.-M. *Supramolecular Chemistry*, Wiley-VCH: Weinheim, **1995**.

e) Fyfe, M. C. T.; Stoddart, J. F. *Acc. Chem. Rev.* **1997**, *30*, 393-401.

4. a) Otto, S.; Furlan, R. L. E.; Sanders, J. K. M. *Drug Discovery Today* **2002**, *7*, 117-125;

b) Otto, S.; Furlan, R. L. E.; Sanders, J. K. M. *Curr. Opin. Chem. Biol.* **2002**, *6*, 321-327;

c) Schmidt, M. F.; Rademann, J. *Trend Biotech.* **2009**, *27*, 512-521;

d) Bhat, V. T.; Caniard, A. M.; Luksch, T.; Brenk, R.; Campopiano, D. J.; Greaney, M. F. *Nature Chem.* **2010**, *2*, 490-497;

e) Miller, B. L. *Nature Chem.* **2010**, *2*, 433-434.

5. *Selected examples of dynamic polymers (dynamers):*

a) Odian, G. *Principles of Polymerization*, vol. 68,Wiley-Interscience: New York, **1991**;

b) H. D. Maynard, H. D.; R. H. Grubbs, R. H. *Macromol.* **1999**, *32*, 6917-6924;

c) Otsuka, H.; Aotani, K.; Higaki, Y.; Takahara, A. *Chem. Commun.* **2002**, 2838-2839;

d) Otsuka, H.; Aotani, K.; Higaki, Y.; Takahara, A. *J. Am. Chem. Soc.* **2003**, *125*, 4064-4065;

e) Skene, W. G.; Lehn, J.-M. *Proc. Natl. Acad. Sci. U. S. A.* **2004**, *101*, 8270-8275;

f) Kolomiets, E.; Lehn, J.-M. *Chem. Commun.* **2005**, 1519-1521;

g) Ono, T.; Nobori, T.; Lehn, J.-M. *Chem. Commun.* **2005**, 1522-1524;

h) Ruff, Y.; Lehn, J.-M. *Angew. Chem., Int. Ed.* **2008**, *47*, 3556-3559;

i) Ulrich, S.; Lehn, J.-M. *Angew. Chem., Int. Ed.* **2008**, *47*, 2240-2243;

j) Fuji, S.; Lehn, J.-M. *Angew. Chem., Int. Ed.* **2009**, *48*, 7635-7638;

k) Maeda, T.; Otsuka, H.; Takahara, A. *Prog. Polym. Sci.* **2009**, *34*, 581-604;

l) Reutenauer, P.; Buhler, E.; Boul, P. J.; Candau, S. J.; Lehn, J.-M. *Chem. -Eur. J.* **2009**, *15*, 1893-1900;

m) Lehn, J.-M. *Aust. J. Chem.* **2010**, *63*, 611-623;

n) Ruff, Y.; Buhler, E.; Candau, S. J.; Kesselman, E.; Talmon, Y.; Lehn, J.-M. *J. Am. Chem. Soc.* **2010**, *132*, 2573-2584.

o) Fan, J.; Saha, M. L.; Song, B.; Schonherr, H.; Schmittel, M. *J. Am. Chem. Soc.* **2012**, *134*, 150-153.

6. *Selected examples of DCC-based chemical sensors:*

a) Kubik, S.; Kirchner, R.; Nolting, D.; Seidel, J. *J. Am. Chem. Soc.* **2002**, *124*, 12752-12760;

b) Otto, S.; Severin, K. *Creative Chemical Sensor Systems*, vol. 267, Springer: Berlin, **2007.**

c) Hagihara, S.; Tanaka, H.; Matile, S. *J. Am. Chem. Soc.* **2008**, *130*, 5656-5657.

d) Herrmann, A. *Chem. -Eur. J.* **2012**, *18*, 8568-8577.

7. *Selected references in the use of DCC in the synthesis and dynamic manipulation of interlocked architectures:*

a) Rowan, S. J.; Stoddart, J. F. *Org. Lett.* **1913**, *1*, 1913-1916;

b) Cantrill, S. J.; Rowan, S. J.; Stoddart, J. F. *Org. Lett.* **1999**, *1*, 1363-1366;

c) Glink, P. T.; Oliva, A. I.; Stoddart, J. F.; White, A. J. P.; Williams, D. J. *Angew. Chem., Int. Ed.* **2001**, *40*, 1870-1875;

d) Leigh, D. A.; Lusby, P. J.; Teat, S. J.; Wilson, A. J.; Wong, J. K. Y. *Angew. Chem., Int. Ed.* **2001**, *40*, 1538-1543;

e) Badjic, J. D.; Cantrill, S. J.; Grubbs, R. H.; Guidry, E. N.; Orenes, R.; Stoddart, J. F. *Angew. Chem., Int. Ed.* **2004**, *43*, 3273-3278;

f) Chichak, K. S.; Cantrill, S. J.; Pease, A. R.; Chiu, S.-H.; Cave, G. W. V.; Atwood, J. L.; Stoddart, J. F. *Science* **2004**, *304*, 1308-1312;

g) Leigh, D. A.; Perez, E. M. *Chem. Commun.* **2004**, 2262-2263;

h) Lam, R. T. S.; Belenguer, A.; Roberts, S. L.; Naumann, C.; Jarrosson, T.; Otto, S.; Sanders, J. K. M. *Science* **2005**, *308*, 667-669;

i) Northrop, B. H.; Arico, F.; Tangchiavang, N.; Badjic, J. D.; Stoddart, J. F. *Org. Lett.* **2006**, *8*, 3899-3902;

j) Hsueh, S.-Y.; Cheng, K.-W.; Lai, C.-C.; Chiu, S.-H. *Angew. Chem., Int. Ed.* **2008**, *47*, 4436-4439;

k) Jiang, Y.; Wu, J.; He, L.; Tu, C.; Zhu, X.; Chen, Q.; Yao, Y.; Yan, D. *Chem. Commun.* **2008**, 6351-6353;

l) Patel, K.; Miljanic, O. S.; Stoddart, J. F. *Chem. Commun.* **2008**, 1853-1855;

m) Umehara, T.; Kawai, H.; Fujiwara, K.; Suzuki, T. *J. Am. Chem. Soc.* **2008**, *130*, 13981-13988;

n) Au-Yeung, H. Y.; Pantos, G. D.; Sanders, J. K. M. *J. Am. Chem. Soc.* **2009**, *131*, 16030-16032;

o) Chung, M.-K.; White, P. S.; Lee, S. J.; Gagné, M. R. *Angew. Chem., Int. Ed.* **2009**, *48*, 8683-8686;

p) Klivansky, L. M.; Koshkakaryan, G.; Cao, D.; Liu, Y. *Angew. Chem., Int. Ed.* **2009**, *48*, 4185-4189;

q) Au-Yeung, H. Y.; Pantos, G. D.; Sanders, J. K. M. *Angew. Chem., Int. Ed.* **2010**, *49*, 5331-5334.

r) Cougnon, F. B. L.; Au-Yeung, H. Y.; Pantos, G. D.; Sanders, J. K. M. *J. Am. Chem. Soc.* **2012**, *133*, 3198-3207.

8. *Selected examples of the use of DCC in systems chemistry:*

a) Corbett, P. T.; Sanders, J. K. M. *Angew. Chem., Int. Ed.* **2007**, *46*, 8858-8861;

b) Ludlow, R. F.; Otto, S. *J. Am. Chem. Soc.* **2008**, *130*, 12218-12219;

c) Ludlow, R. F.; Otto, S. *Chem. Soc. Rev.* **2008**, *37*, 101-108;

d) Sarma, R. J.; Nitschke, J. R. *Angew. Chem., Int. Ed.* **2008**, *47*, 377-380;

e) Nguyen, R.; Allouche, L.; Buhler, E.; Giuseppone, N. *Angew. Chem., Int. Ed.* **2009**, *48*, 1093-1096;

f) Nitschke, J. R. *Nature* **2009**, *462*, 736-738;

g) Wagner, N.; Ashkenasy, G. *Chem. -Eur. J.* **2009**, *15*, 1765-1775;

h) Campbell, V. E.; de Hatten, X.; Delsuc, N.; Kauffmann, B.; Huc, I.; Nitschke, J. R. *Nature Chem.* **2010**, *2*, 684-687;

i) Ludlow, R. F.; Otto, S. *J. Am. Chem. Soc.* **2010**, *132*, 5984-5986;

j) Mal, P.; Nitschke, J. R. *Chem. Commun.* **2010**, *46*, 2417-2419.

k) Breiner, B.; Clegg, J. K.; Nitschke, J. R. *Chem. Sci.* **2011**, *2*, 51-56.

9. Leclaire, J.; Vial, L.; Otto, S.; Sanders, J. K. M. *Chem. Commun.* **2005**, 1959-1961.

10. a) Goral, V.; Nelen, M. I.; Eliseev, A. V.; Lehn, J.-M. *Proc. Natl. Acad. Sci. U. S. A.* **2001**, *98*, 1347-1352;

b) von Delius, M.; Geertsema, E. M.; Leigh, D. A.; Slawin, A. M. Z. *Org. Biomol. Chem.* **2010**, *8*, 4617-4624.

11. a) von Delius, M.; Geertsema, E. M.; Leigh, D. A. *Nature Chem.* **2010**, *2*, 96-101;

b) von Delius, M.; Geertsema, E. R.; Leigh, D. A.; Tang, T. D. *J. Am. Chem. Soc.* **2010**, *132*, 16134-16145;

c) von Delius, M.; Barrell, M. J.; Campaña, A. G.; Geertzema, E. M.; Leigh, D. A. *Angew. Chem., Int. Ed.* **2011**, *50*, 285-290.

12. Kay, E. R.; Leigh, D. A.; Zerbetto, F. *Angew. Chem., Int. Ed.* **2007**, *46*, 72-191.

13. The term "double-level" system denotes a system whose building blocks are interconnected by two different types of exchange processes.

14. The term "constitutionally dynamic" is used to include both reversible metal coordination and dynamic covalent processes.

15. *Selected examples of the dynamic covalent chemistry of imines:*

a) Oh, K.; Jeong, K.-S.; Moore, J. S. *Nature* **2001**, *414*, 889-893;

b) Hochgurtel, M.; Kroth, H.; Piecha, D.; Hofmann, M. W.; Nicolaou, C.; Krause, S.; Schaaf, O.; Sonnenmoser, G.; Eliseev, A. V. *Proc. Natl. Acad. Sci. U. S. A.* **2002**, *99*, 3382-3387;

c) Hochgurtel, M.; Biesinger, R.; Kroth, H.; Piecha, D.; Hofmann, M. W.; Krause, S.; Schaaf, O.; Nicolau, C.; Eliseev, A. V. *J. Med. Chem.* **2003**, *46*, 356-358;

d) Nitschke, J. R.; Lehn, J.-M. *Proc. Natl. Acad. Sci. U. S. A.* **2003**, *100*, 11970-11974;

e) Giuseppone, N.; Lehn, J.-M. *J. Am. Chem. Soc.* **2004**, *126*, 11448-11449;

f) Nitschke, J. R. *Angew. Chem., Int. Ed.* **2004**, *43*, 3073-3075;

g) Giuseppone, N.; Schmitt, J. L.; Schwartz, E.; Lehn, J.-M. *J. Am. Chem. Soc.* **2005**, *127*, 5528-5539;

h) Hutin, M.; Frantz, R.; Nitschke, J. R. *Chem. -Eur. J.* **2006**, *12*, 4077-4082;

i) Hutin, M.; Schalley, C. A.; Bernardinelli, G.; Nitschke, J. R. *Chem. -Eur. J.* **2006**, *12*, 4069-4076;

j) Hartley, C. S.; Moore, J. S. *J. Am. Chem. Soc.* **2007**, *129*, 11682-11683;

k) Xu, S.; Giuseppone, N. *J. Am. Chem. Soc.* **2008**, *130*, 1826-1827;

l) Ziach, K.; Jurczak, J. *Org. Lett.* **2008**, *10*, 5159-5162;

m) Vongvilai, P.; Ramström, O. *J. Am. Chem. Soc.* **2009**, *131*, 14419-14425.

n) Campaña, A. G.; Carlone, A.; Chen, K.; Dryden, D. T. F.; Leigh, D. A.; Lewandowska, U.; Mullen, K. M. *Angew. Chem., Int. Ed.* **2012**, *51*, 5480-5483;

o) Kovaříček, P.; Lehn, J.-M. *J. Am. Chem. Soc.* **2012**, *134*, 9446-9455.

16. Nguyen, R.; Huc, I. *Chem. Commun.* **2003**, 942-943.

17. Dirksen, A.; Dirksen, S.; Hackeng, T. M.; Dawson, P. E. *J. Am. Chem. Soc.* **2006**, *128*, 15602-15603.

18. *Selected examples of hydrazone exchange in organic solvents:*

a) Cousins, G. R. L.; Furlan, R. L. E.; Ng, Y.-F.; Redman, J. E.; Sanders, J. K. M. *Angew. Chem., Int. Ed.* **2001**, *40*, 423-428;

b) Furlan, R. L. E.; Ng, Y.-F.; Otto, S.; Sanders, J. K. M. *J. Am. Chem. Soc.* **2001**, *123*, 8876-8877;

c) Choudhary, S.; Morrow, J. R. *Angew. Chem., Int. Ed.* **2002**, *41*, 4096-4098;

d) Furlan, R. L. E.; Ng, Y.-F.; Cousins, G. R. L.; Redman, J. E.; Sanders, J. K. M. *Tetrahedron* **2002**, *58*, 771-778;

e) Chung, M.-K.; Hebling, C. M.; Jorgenson, J. W.; Severin, K.; Lee, S. J.; Gagné, M. R. *J. Am. Chem. Soc.* **2008**, *130*, 11819-11827;

f) Gasparini, G.; Bettin, F.; Scrimin, P.; Prins, L. J. *Angew. Chem., Int. Ed.* **2009**, *48*, 4546-4550;

g) Ingerman, L. A.; Waters, M. L. *J. Org. Chem.* **2009**, *74*, 111-117;

h) Lao, L. L.; Schmitt, J.-L.; Lehn, J.-M. *Chem. -Eur. J.* **2010**, *16*, 4903-4910;

i) Simpson, M. G.; Pittelkow, M.; Watson, S. P.; Sanders, J. K. M. *Org. Biomol. Chem.* **2010**, *8*, 1181-1187;

j) Simpson, M. G.; Pittelkow, M.; Watson, S. P.; Sanders, J. K. M. *Org. Biomol. Chem.* **2010**, *8*, 1173-1180.

19. *Selected examples of hydrazone exchange in aqueous media:*

a) Bunyapaiboonsri, T.; Ramström, O.; Lohmann, S.; Lehn, J.-M.; Peng, L.; Goeldner, M. *Chem. Bio. Chem* **2001**, *2*, 438-444;

b) Eckardt, L. H.; Naumann, K.; Pankau, W. M.; Rein, M.; Schweitzer, M.; Windhab, N.; von Kiedrowski, G. *Nature* **2002**, *420*, 286;

c) Bunyapaiboonsri, T.; Ramström, H.; Ramström, O.; Haiech, J.; Lehn, J.-M. *J. Med. Chem.* **2003**, *46*, 5803-5811;

d) Congreve, M. S.; Davis, D. J.; Devine, L.; Granata, C.; O'Reilly, M.; Wyatt, P. G.; Jhoti, H. *Angew. Chem., Int. Ed.* **2003**, *42*, 4479-4482;

e) Bornaghi, L. F.; Wilkinson, B. L.; Kiefel, M. J.; Poulsen, S. A. *Tetrahedron Lett.* **2004**, *45*, 9281-9284;

f) Ramström, O.; Lohmann, S.; Bunyapaiboonsri, T.; Lehn, J.-M. *Chem. -Eur. J.* **2004**, *10*, 1711-1715;

g) Levrand, B.; Ruff, Y.; Lehn, J.-M.; Herrmann, A. *Chem. Commun.* **2006**, 2965-2967.

h) Mahon, C. S.; Jacson, A. W.; Murray, B. S.; Fulton, D. A. *Chem. Commun.* **2011**, *47*, 7209-7211.

20. J. R. Dimmock, S. C. Vashishtha, J. P. Stables, *Eur. J. Med. Chem.* **2000**, *35*, 241-243.

21. Pettit, G. R.; Grealish, M. P.; Jung, M. K.; Hamel, E.; Pettit, R. K.; Chapuis, J.-C.; Schmidt, J. M. *J. Med. Chem.* **2002**, *45*, 2534-2542.

22. Bradshaw, J. S.; Huszthy, P.; McDaniel, C. W.; Zhu, C. Y.; Dalley, K.; Izatt, R. M.; Lifson, S. *J. Org. Chem.* **1990**, *55*, 3129-3137.